UNIVERSITY OF LIVERPOOL

The adipocyte plasma membrane proteome and its role in drug-induced metabolic toxicity

Thesis submitted in accordance with the requirements of
The University of Liverpool for the degree of
Doctor of Philosophy

By

Carmen Arasti Rezola

Department of Molecular and Clinical Pharmacology

November 2019

Declaration

I hereby declare that the research presented in this thesis is my own work generated at the Wolfson centre for Personalised Medicine, Department of Molecular and Clinical Pharmacology, University of Liverpool, UK. The materials presented in this thesis are not part of any other degree or qualification.

Carmen Arasti

November 2019

Acknowledgements

I would like to thank my supervisors Dr Sudeep Pushpakom, Dr Parveen Sharma and Professor Sir Munir Pirmohamed for their guidance and support during this thesis, and the MRC Centre for Drug Safety Science for funding my PhD.

I would also like to thank my friends and colleagues at the Wolfson Centre, and everybody who contributed to this thesis. Especial thanks to Alex Penrose, Rosalind Jenkins, Eva Caamaño, Pedro Ayuso, Stephanie French, Soban Sadiq, Gurpreet Ghattaoraya and Carol Jolly for all their help and advice. I would also like to thank Dr Rocío Gómez Lencero and Dr Claire Terry for encouraging me to undertake this PhD and for their mentorship.

Finally, I thank my lovely family who have supported me every step of the way.

Thank you. Gracias.

TABLE OF CONTENTS

Publications and communications xv
Abstract xvi
Abbreviations xvii
CHAPTER 1 GENERAL INTRODUCTION 1
1.1. HIV disease 2
1.1.1. Symptoms 4
1.1.2. Transmission and risk factors 4
1.1.3. Diagnosis 5
1.1.4. Mortality 5
1.1.5. Pathogenesis 5
1.1.6. Pharmacological treatment 7
1.2. Antiretroviral drugs 10
1.2.1. History 10
1.2.2. Nucleoside/nucleotide reverse transcriptase inhibitors (NRTIs) 11
1.2.3. Non-nucleoside reverse transcriptase inhibitors (NNRTIs) 13
1.2.4. Protease inhibitors (PIs) 13
1.2.4.1. Lopinavir 14
1.2.4.2. Atazanavir 15
1.2.5. Integrase inhibitors 16
1.2.6. Entry inhibitors 17
1.3. ART-induced cardiometabolic disease 17
1.4. The adipose tissue as a regulator of metabolic homeostasis 21
1.4.1. Function and formation of the adipose tissue 23
1.4.2. Adipogenesis 27
1.4.3. Insulin signalling and glucose homeostasis in the adipocyte 31
1.4.4. Adipokines 33
1.4.4.1. Leptin 34
1.4.4.2. Adiponectin 35
1.4.4.3. Tumour necrosis factor alpha 36
1.4.4.4. Interleukin-6 36
1.4.4.5. Resistin 37
1.4.4.6. Visfatin 37
1.5. Effect of ART on adipose tissue and adipogenesis 39
1.6. ART-induced Obesity and inflammation 40

1.7. ART-induced Dyslipidaemia 42
1.8. ART-induced insulin resistance and diabetes 44
1.9. ART-induced cardiovascular disease 47
1.10. Adipocyte proteomics and relevance to metabolic disease 49
1.11. Mass spectrometry 50
1.12. Proteomic differences between VAT and SAT 52
1.12.1. Proteomics of murine adipocytes 53
1.12.2. Proteomics of human adipocytes 56
1.12.3. Adipokine proteomics 57
1.13. The importance of plasma membrane in drug transport and metabolic disease 58
1.13.1. Challenges of the study of the PM proteome 60
1.14. Adipocyte plasma membrane proteomics 61
1.15. Aims of the thesis 62
CHAPTER 2 OPTIMISATION AND VALIDATION OF AN ISOLATION METHOD FOR ENRICHMENT OF PLASMA MEMBRANE PROTEINS IN ADIPOCYTES 65
2.1. INTRODUCTION 66
2.1.1. Plasma membrane proteomics 66
2.1.2. Colloidal Silica Bead Isolation 67
2.1.3. Aims and objectives 68
2.2. METHODS 68
2.2.1. Cell culture and differentiation 68
2.2.1.1. Adipocyte subculture 69
2.2.1.2. Plating of cells 69
2.2.1.3. Adipocyte differentiation 70
2.2.2. Characterisation of differentiation using Oil red O staining 70
2.2.3. Colloidal silica bead isolation 71
2.2.3.1. Optimisation of lysis method for sample preparation 71
2.2.3.2. Optimisation of method of purification of the PM-enriched fraction 72
2.2.4. Determination of protein concentration (Bradford Assay) 72
2.2.5. Protein expression by Western blot 73
2.2.6. Colloidal Coomassie Blue staining of proteins 74
2.2.7. LC-MS/MS 75
2.2.7.1. Sample preparation for LC-MS/MS 75
2.2.7.2. Ziptip purification 75
2.2.7.3. Mass spectrometry 76

2.2.8. Bioinformatic analysis 77
2.2.8.1. Gene Ontology Cellular Component protein classification 77
2.2.9. Statistical analysis 78
2.3. RESULTS 78
2.3.1. Characterisation of adipocyte differentiation 78
2.3.2. Validation of Colloidal Silica Bead isolation method for the enrichment of plasma membrane proteins of the 3T3-F442A preadipocyte cell line 79
2.3.3. Optimisation of sample preparation for mass spectrometry after silica bead isolation 81
2.3.4. Purification of the plasma membrane fraction 83
2.3.5. Detection of proteins in membrane and cytosolic fractions using Coomassie blue 85
2.3.6. Comparison of total protein yield obtained by optimised colloidal silica bead isolation between this study and Prior et al´s study 87
2.3.7. Comparison of PM protein yield obtained by optimised colloidal silica bead isolation between this study and Prior et al´s study 88
2.4. DISCUSSION 89
CHAPTER 3 CHANGES IN THE ADIPOCYTE PLASMA MEMBRANE PROTEOME DURING ADIPOGENESIS AND FOLLOWING INSULIN STIMULATION 94
3.1. INTRODUCTION 95
3.1.1. Adipogenesis and plasma membrane proteomics 95
3.1.2. Proteomics and insulin signalling 98
3.1.3. Aims and objectives 100
3.2. METHODS 100
3.2.1. Adipocyte cell culture and differentiation 101
3.2.2. Starvation and insulin stimulation of mature adipocytes 101
3.2.3. Colloidal silica bead isolation 102
3.2.4. Determination of protein concentration (Bradford Assay) 102
3.2.5. Sample preparation for LC-MS/MS 102
3.2.5.1. Ziptip 102
3.2.6. LC-MS/MS analysis 102
3.2.7. Bioinformatic analysis 102
3.2.7.1. Protein identification and label-free relative quantitation of differentially regulated proteins 102
3.2.7.2. Protein classification and data curation 104
3.2.7.3. Protein pathway and network analysis 104
3.2.8. Statistical analysis 105
3.3. RESULTS 105

3.3.1. Differential regulation of the adipocyte proteome during adipogenesis 105
3.3.2. Differential regulation of the adipocyte proteome following insulin stimulation 109
3.3.3. Changes in the adipocyte plasma membrane proteome during adipogenesis and following acute insulin stimulation 112
3.3.4. Pathway analysis of significantly differentially regulated plasma membrane proteins during adipogenesis and following insulin stimulation 119
3.3.5. Network analysis of plasma membrane proteins significantly differentially regulated during adipogenesis and following insulin stimulation 121
3.3.6. Comparison of total proteins detected between this study and Prior et al´s study following insulin stimulation 125
3.3.7. Comparison of PM proteins detected between this study and Prior et al´s study following insulin stimulation 126
3.4. DISCUSSION 127
CHAPTER 4 EFFECT OF HIV PROTEASE INHIBITORS ON THE ADIPOCYTE PLASMA MEMBRANE PROTEOME 137
4.1. INTRODUCTION 138
4.1.1. HIV protease inhibitors and metabolic toxicity 138
4.1.2. Metabolic effects of lopinavir and atazanavir on the adipocyte 139
4.1.3. Metabolic effects of telmisartan on adipocytes 140
4.1.4. HIV PIs and adipocyte proteomics 141
4.1.5. Transport of lopinavir and atazanavir across the plasma membrane 142
4.1.6. Aims and objectives 143
4.2. METHODS 143
4.2.1. Drug addition 145
4.2.2. Silica bead isolation 145
4.2.3. Mass spectrometry 146
4.2.4. Bioinformatic analysis 146
4.2.4.1. Protein identification and label-free relative quantification of differentially regulated proteins 146
4.2.4.2. Protein classification and data curation 146
4.2.4.3. Protein pathway and network analysis 146
4.2.5. Colloidal Coomassie Blue staining of proteins 146
4.2.6. Validation of NKCC1 and NCAM by western blot 146
4.2.7. Statistical analysis 147
4.3. RESULTS 147

4.3.1. Differentially regulated proteins following drug treatment 147
4.3.2. Changes in the adipocyte plasma membrane proteome following exposure to PIs 156
4.3.3. Pathway analysis of plasma membrane proteins significantly differentially regulated following drug treatment 160
4.3.4. Network analysis of plasma membrane proteins significantly differentially regulated following drug treatment 162
4.3.5. Validation of target protein NKCC1 as a differentially regulated transporter following PIs exposure 164
4.3.6. Validation of target protein NCAM as a differentially regulated PM protein following PIs exposure 166
4.4. DISCUSSION 168
CHAPTER 5 FUNCTIONAL VALIDATION OF SELECTED PLASMA MEMBRANE PROTEINS IN THE ADIPOCYTE 173
5.1. INTRODUCTION 174
5.1.1. The role of NCAM and NKCC1 in cell biology 174
5.1.1.1. NCAM 174
5.1.1.2. NKCC1 175
5.1.2. Functional characterisation of the role of NCAM and NKCC1 in adipocyte metabolic toxicity 176
5.1.3. Aims and objectives 177
5.2. METHODS 178
5.2.1. Transfection and knockdown 178
On day 1 of differentiation, cells were washed twice with HBSS 178
5.2.2. Preparation of lysates from cell culture 178
5.2.3. BCA protein quantification assay 179
5.2.4. Determination of protein concentration (Bradford Assay) 179
5.2.5. Western blot 179
5.2.6. Oil red O Staining 179
5.2.7. Starvation and insulin stimulation of mature adipocytes 180
5.2.8. Immunofluorescence 180
5.2.9. Estimation of adiponectin by ELISA 181
5.2.10. Statistical analysis 182
5.3. RESULTS 182
5.3.1. Expression of NCAM during adipogenesis 182
5.3.2. Knockdown of NCAM 183
5.3.3. Effect of NCAM knockdown on adipocyte lipid accumulation 184
5.3.4. Effect of NCAM knockdown on basal GLUT4 expression 185

5.3.5. Effect of NCAM knockdown on adiponectin secretion 186
5.3.6. Expression of NKCC1 during adipogenesis 187
5.3.7. Knockdown of NKCC1 187
5.3.8. Knockdown of NKCC1 did not affect lipid droplet accumulation during adipogenesis of 3T3-F442A adipocytes 188
5.3.9. Effect of acute insulin stimulation on NKCC1 and NKCC2 189
5.3.10. Localisation of NKCC1 and NKCC2 in the plasma membrane of 3T3-F442A adipocytes 190
5.3.11. Effect of NKCC1 knockdown on basal GLUT4 expression 192
5.3.12. Effect of NKCC1 knockdown on adiponectin secretion 193
5.4. DISCUSSION 194
CHAPTER 6 FINAL DISCUSSION 201
6.1. Thesis Overview 202
6.2. Perspectives for future work 209
6.3. Conclusions 212
7. APPENDICES 214
APPENDICES CHAPTER 2 214
Appendix 1. List of adipocyte proteins detected by ProteinPilot-no sonication method.. 214
Appendix 2. List of adipocyte plasma membrane proteins-no sonication method 214
Appendix 3. List of adipocyte proteins detected by ProteinPilot-probe sonication method.. 214
Appendix 4. List of adipocyte plasma membrane proteins-probe sonication method 214
Appendix 5. Comparison total protein yield obtained by optimised colloidal silica bead isolation to Prior *et al.*, (2011) 214
APPENDICES CHAPTER 3 214
Appendix 1. List of proteins detected during adipogenesis. 214
Appendix 2. List of plasma membrane proteins detected during adipogenesis. 214
Appendix 3. List of significantly differentially regulated plasma membrane proteins detected during adipogenesis. 215
Appendix 4. Progenesis QI report of proteins detected during adipogenesis 215
Appendix 5. List of proteins detected following insulin stimulation. 215
Appendix 6. List of plasma membrane proteins detected following insulin stimulation. 215
Appendix 7. Progenesis QI report of proteins detected following insulin stimulation. 215

Appendix 8. Pathway analysis for significantly differentially regulated PM proteins detected during adipogenesis. 215
Appendix 9. Pathway analysis for significantly differentially regulated PM proteins detected following insulin stimulation. 215
Appendix 10. Comparison of proteins detected following insulin stimulation to Prior *et al.*, (2011). 216
APPENDICES CHAPTER 4 216
Appendix 1. List of proteins detected following drug treatments. 216
Appendix 2. List of plasma membrane proteins detected following drug treatments. 216
Appendix 3. Tukey's post hoc corrected p-values for pair-wise comparisons 216
Appendix 4. Plasma membrane proteins after Tukey's post hoc corrected p-values for pair-wise comparisons. 216
Appendix 5. Plasma membrane proteins significantly differentially regulated following drug treatments. 216
Appendix 6. Ranking of significantly differentially regulated PM proteins following drug treatments 216
Appendix 7. Progenesis QI report of proteins detected following drug treatments. 217
Appendix 8. Pathway analysis for significantly differentially regulated PM proteins detected following drug treatments. 217
Appendix 9. Expression of GLUT4 in the plasma membrane fraction of adipocytes following drug treatments. 217
8. REFERENCES 217

Table of Figures

Figure 1.1: Schematic diagram of the HIV virion structure 3
Figure 1.2: Mechanisms of action of antiretroviral drugs 9
Figure 1.3: Lopinavir 15
Figure 1.4: Atazanavir 16
Figure 1.5: Pathophysiology of the metabolic syndrome 18
Figure 1.6: Crosstalk between the adipose tissue and other tissues and organs for the regulation of metabolic homeostasis. 23
Figure 1.7. Metabolic role of the adipose tissue. 25
Figure 1.8: Stages of adipogenesis for the 3T3-F44A2 murine immortalised cell line 30
Figure 1.9: GLUT4 translocation process to the PM of adipocytes 33

Figure 1.10: Components of tandem mass spectrometry. 50
Figure 2.1: Sample preparation and LC-MS/MS analysis. 77
Figure 2.2: Characterisation of adipocyte differentiation using Oil red O staining. 79
Figure 2.3: Validation of colloidal silica bead isolation by western blotting. 80
Figure 2.4: Comparison of sample lysis methods. 82
Figure 2.5: Comparison of cytosolic and membrane fraction before and after washing. 84
Figure 2.6: Optimised colloidal silica bead isolation method for the 3T3-F442A cell line. 84
Figure 2.7: SDS-PAGE gels stained with Colloidal Coomassie blue for the detection of proteins in the PM-enriched fraction and cytosolic fraction prior to LC-MS/MS analysis. 86
Figure 2.8. Comparison of total detected proteins in the PM-enriched fraction by Prior *et al.*, (2011) and the current study. 88
Figure 2.9. Comparison of detected PM proteins by Prior et al., (2011) and the current study. 89
Figure 3.1: Flow diagram of methodology 101
Figure 3.2: Volcano plot showing differentially regulated proteins during adipogenesis. 106
Figure 3.3: Principal component analysis (PCA) distinguishes the silica bead isolated-plasma membrane fraction of undifferentiated preadipocytes and mature adipocytes. 108
Figure 3.4: Volcano plot showing differentially regulated proteins following insulin stimulation. 110
Figure 3.5: Principal component analysis (PCA) distinguishes the silica bead isolated-plasma membrane fraction of insulin stimulated adipocytes and unstimulated adipocytes. 111
Figure 3.6: Cellular Component Gene Ontology classification of the plasma membrane-enriched fraction isolated by colloidal silica bead isolation during adipogenesis. 113
Figure 3.7: Cellular Component Gene Ontology classification of the plasma membrane-enriched fraction isolated by colloidal silica bead isolation following insulin stimulation 113
Figure 3.8: Functional classification of the total of detected plasma membrane proteins during adipogenesis based on A) GO "Biological Process" (BP) annotations and B) GO "Molecular Function" (MF) annotations. 115
Figure 3.9: Functional classification of plasma membrane proteins significantly differentially regulated during adipogenesis based on A) GO "Biological Process" (BP) and B) GO "Molecular Function" (MF) annotations. 116
Figure 3.10: Functional classification of the total of detected plasma membrane proteins following insulin stimulation based on A) GO "Biological Process" (BP) annotations and B) GO "Molecular Function" (MF) annotations. 118

Figure 3.11: Overrepresented pathways involving significantly differentially regulated plasma membrane proteins during adipogenesis of the 3T3-F442A preadipocyte cell line. 120
Figure 3.12: Overrepresented pathways involving significantly differentially regulated plasma membrane proteins detected following insulin stimulation of mature 3T3-F442A adipocytes....121
Figure 3.13: Crosstalk between significantly differentially regulated plasma membrane proteins during adipogenesis and their predicted interactions with PPARγ and mTOR. 122
Figure 3.14: Crosstalk between significantly differentially regulated plasma membrane proteins identified following insulin stimulation and their predicted interactions with PPARγ and mTOR. 124
Figure 3.15. Comparison of total detected proteins in the PM-enriched fraction following insulin stimulation by Prior *et al*., (2011) and the current study.....126
Figure 3.16. Comparison of detected PM proteins following insulin stimulation by Prior et al., (2011) and the current study. 127
Figure 4.1: Chemical structure of telmisartan. 141
Figure 4.2: Flow diagram of methodology for experimental chapter 4 including target selection and validation. 144
Figure 4.3: Drug addition timeline following a chronic toxicity model. 145
Figure 4.4: Coomassie blue staining of proteins present in lysates of adipocytes dosed with lopinavir (±telmisartan), atazanavir (±telmisartan), and controls (vehicle) 148
Figure 4.5: Principal component analysis (PCA) distinguishes the silica bead isolated-plasma membrane fraction of adipocytes treated with different drug conditions. 150
Figure 4.6: Volcano plots showing differentially regulated proteins of the membrane-enriched fraction following exposure of adipocytes to A) Lopinavir (LOP), B) Lopinavir combined with telmisartan (LOP+TEL), C) Atazanavir (ATZ) and D) Atazanavir combined with telmisartan (ATZ+TEL), compared to control (vehicle: VEH) 152
Figure 4.7: Volcano plots showing differentially regulated proteins of the membrane-enriched fraction following exposure of adipocytes to lopinavir (LOP) compared to atazanavir (ATZ) 153
Figure 4.8: Volcano plots showing differentially regulated proteins of the membrane-enriched fraction following exposure of adipocytes to A) Lopinavir combined with telmisartan (LOP+TEL), compared to lopinavir (LOP), and B) Atazanavir combined with telmisartan (ATZ+TEL) compared to atazanavir (ATZ). 154
Figure 4.9: Cellular Component Gene Ontology classification of the plasma membrane-enriched fraction isolated by colloidal silica bead isolation after exposure to PIs 156

Figure 4.10: GO SLIM analysis for Biological Process (BP) and Molecular Function (MF) annotations were applied to the total number of detected PM proteins..156
Figure 4.11: Functional classification of significantly differentially regulated plasma membrane proteins based on A) GO "Biological Process" (BP) annotations and B) GO "Molecular Function" (MF) annotations. 160
Figure 4.12: Overrepresented pathways involving significantly differentially regulated plasma membrane proteins following exposure of the 3T3-F442A adipocytes to PIs. 161
Figure 4.13: Crosstalk between significantly differentially regulated plasma membrane proteins following exposure to PIs and PPARγ and mTOR.....163
Figure 4.14: Differential expression of NKCC1 and NKCC2 following lopinavir (±telmisartan) exposure in the adipocyte plasma membrane.....165
Figure 4.15: Differential expression of NKCC1 and NKCC2 following exposure to lopinavir (+/-telmisartan) and atazanavir in the adipocyte plasma membrane. 166
Figure 4.16: Differential expression of NCAM following exposure to lopinavir (+/-telmisartan) compared to control in the adipocyte plasma membrane. 167
Figure 4.17: Differential expression of NCAM following exposure to atazanavir (+/-telmisartan) compared to control in the adipocyte plasma membrane. 167
Figure 5.1: Expression of NCAM during adipogenesis. 182
Figure 5.2: Efficient knockdown of NCAM in 3T3-F442A adipocytes. 183
Figure 5.3: NCAM knockdown interfered with adipogenesis of 3T3-F442A cells reducing lipid droplet accumulation.....184
Figure 5.4: Effect of NCAM knockdown on basal GLUT4 expression of 3T3-F442A mature adipocytes.....185
Figure 5.5: Effect of NCAM knockdown on adiponectin secretion by mature 3T3-F442A adipocytes 186
Figure 5.6: Expression of NKCC1 during adipogenesis.....187
Figure 5.7: Efficient knockdown of NKCC1 in 3T3-F442A adipocytes.....188
Figure 5.8: Role of NKCC1 on lipid accumulation in differentiating 3T3-F442A adipocytes 189
Figure 5.9: Expression of NKCC1 and NKCC2 in the PM fraction of 3T3-F442A adipocytes following acute insulin stimulation 190
Figure 5.10: Localisation of NKCC1 and NKCC2 in the plasma membrane of 3T3-F442A adipocytes under basal conditions (control). 191
Figure 5.11: Localisation of NKCC1 and NKCC2 in the plasma membrane of 3T3-F442A adipocytes after acute insulin stimulation.. 192
Figure 5.12: Effect of NKCC1 knockdown on GLUT4 expression of 3T3-F442A mature adipocytes.....193
Figure 5.13: Effect of NKCC1 knockdown on adiponectin secretion by mature 3T3-F442A adipocytes. 194

Table of Tables

Table 1.1. Clinical parameters for the diagnosis of metabolic syndrome. 19
Table 1.2: Adipokines and their associated metabolic conditions. 38
Table 2.1. Cellular Component GO annotations considered for the classification of proteins as plasma membrane-associated proteins. 78
Table 4.1. Significantly differentially regulated proteins and PM proteins following the different drug conditions. 155

Publications and communications

Manuscripts in preparation

Arasti C., Sharma P., Jenkins R., Jones A., Caamano-Gutierrez E., Pirmohamed M., Pushpakom S. (2019). **Effect of HIV protease inhibitors on the adipocyte plasma membrane proteome and its role in antiretroviral-induced metabolic toxicity.**

Presentations

Arasti C., Sharma P., Jenkins R., Pirmohamed M., Pushpakom S. (2017). Role of adipocyte plasma membrane proteome in adipocyte differentiation and adipose function. Human Proteome Organization (HUPO) world congress (Dublin, Ireland).

Abstract

Although antiretroviral therapy (ART) has increased the life expectancy of HIV patients, chronic administration of antiretroviral drugs has also led to the development of metabolic and cardiovascular complications in these patients. Metabolic syndrome is a major public health burden worldwide and is a risk factor for cardiovascular disease (CVD). The risk of CVD in HIV-patients has doubled in comparison to the general population with 10% of the CVD-related deaths reported in HIV-infected patients. Certain antiretrovirals have a direct effect on the adipose tissue, a key regulator of metabolic homeostasis, inducing metabolic toxicity. However, there is little information on how antiretrovirals affect the adipose tissue to cause metabolic disease. The plasma membrane proteins play a key role in drug transport and cell signalling but they are often overlooked for their role in disease pathogenesis due to the complexity of studying the plasma membrane proteome. The aims of the present study were to investigate changes in the plasma membrane proteome of 3T3-F442A adipocytes during i) adipogenesis; ii) acute insulin stimulation; and, iii) following exposure to HIV protease inhibitors (PIs), to understand how it contributes to metabolic homeostasis and disease development.

This study was able to optimise and validate a protocol for the enrichment of adipocyte plasma membrane proteins using colloidal silica bead isolation method. Proteomic analysis was conducted by LC-MS/MS followed by label-free relative protein quantitation and bioinformatic analysis which led to the detection of 419 PM proteins (35% of the total detected proteins). Using this methodology, previously reported and novel plasma membrane proteins which showed differential regulation during adipogenesis and following insulin stimulation were identified. This study identified changes in the adipocyte plasma proteome following chronic exposure to PIs for the first time. Plasma membrane proteins NKCC1 and NCAM were then selected for functional validation to understand their role in PI-induced metabolic toxicity. NKCC1 showed significant upregulation when adipocytes were chronically exposed to lopinavir; however, this effect was lesser with atazanavir and was reversed by telmisartan. SiRNA-based knockdown of NKCC1 did not show any effect on adipocyte lipid accumulation, GLUT4 expression or adiponectin secretion. An opposite trend was observed regarding the expression of NKCC2, an isoform of NKCC1, following acute insulin stimulation and lopinavir treatment. A possible compensatory mechanism based on translocation of NKCC2 to the plasma membrane when NKCC1 is compromised may be taking place in the adipocyte, but this requires further investigation. Knockdown of NCAM on the other hand reduced lipid accumulation with no effects observed on GLUT4 or adiponectin.

In conclusion, this thesis presents a comprehensive analysis of the plasma membrane proteome of the adipocyte and provides with numerous plasma membrane protein candidates with potential implications in metabolic homeostasis with the aim of improving understanding of the mechanisms behind drug-induced metabolic toxicity.

Abbreviations

ABC	ATP-bindings cassette
ART	Antiretroviral therapy
BAT	Brown adipose tissue
BMI	Body mass index
BP	Biological Process
BSA	Bovine serum albumin
C/EBPs	CCAAT/enhancer-binding proteins
CC	Cellular Component
CVD	Cardiovascular disease
DMEM	Dulbecco's Modified Eagle's medium
ECM	Extracellular matrix
ER	Endoplasmic reticulum
ESI	Electrospray ionisation
FBS	Foetal Bovine Serum
FDR	False discovery rate
FFAs	Free fatty acids
GLUT4	Glucose transporter 4
GO	Gene Ontology
GSVs	GLUT4 storage vesicles
HDL	High-density lipoprotein
IDF	International Diabetes Federation
IL-6	Interleukin-6
IR	Insulin receptor
iTRAQ	Isobaric tags for relative and absolute quantitation
LC-MS/MS	Liquid chromatography tandem mass spectrometry
LDL	Low-density lipoprotein
MALDI	Matrix-assisted Laser Desorption/Ionization
MAPK	Mitogen-activated protein kinase

MCP-1	Monocyte chemo attractive protein 1
MF	Molecular Function
MI	Myocardial infarction
MSCs	Mesenchymal stem cells
NCAM	Neural cell adhesion molecule
NHS	National Health Service
NNRTIs	Non-nucleoside reverse transcriptase inhibitors
NRTIs	Nucleoside/nucleotide reverse transcriptase inhibitors
PAI-1	Plasminogen activator inhibitor-1
PIs	Protease inhibitors
PM	Plasma membrane
PPARγ	Peroxisome proliferator-activated receptor gamma
QTOF	Quadrupole time-of-flight mass analyser
ROS	Reactive oxygen species
SAT	Subcutaneous adipose tissue
SILAC	Stable Isotope Labeling with Amino acids in Cell culture
SLC	Solute carriers
SVF	Stromal vascular fraction
T2DM	Type 2 Diabetes Mellitus
TAGs	Triacylglycerols
TNFα	Tumour necrosis factor alpha
VAT	Visceral adipose tissue
VLDL	Very Low-density lipoprotein
WAT	White adipose tissue
WHO	World Health Organisation

CHAPTER 1
GENERAL INTRODUCTION

1.1. HIV disease

Infection by the Human Immunodeficiency Virus (HIV) was first observed in the clinic in 1981 in the United States, and the virus was first isolated at the Institut Pasteur at Paris in 1983 (Barré-Sinoussi *et al.*, 2013). According to the World Health Organization (WHO) there were 36.9 million people living with HIV in the world by the end of 2017, with a total of 940,000 people dying of HIV-related causes globally during that year, and only 59% of adults and 52% of children living with HIV were on antiretroviral therapy (World Health Organization, 2018).

HIV causes immunodeficiency, affecting the immune system's ability to fight infection, and it is characterised by a CD4 T cell count reduction (Parekh *et al.*, 2019). Although there is currently no cure for HIV infection, Highly Active Antiretroviral Therapy (HAART) has significantly decreased the number of deaths caused by HIV and increased the life expectancy of HIV-infected individuals, making HIV infection a manageable chronic condition (World Health Organization, 2016; Panel on Antiretroviral Guidelines for Adults and Adolescents, 2018).

There are two types of HIV: HIV-1 and HIV-2; both cause AIDS and show a genetic homology of 30% to 60%. However, HIV-2, which is mainly found in West Africa, is less transmissible and less pathogenic than HIV-1, whereas HIV-1 is considered a global pandemic (Marchant *et al.*, 2006). The structure of the virus comprises a lipid bilayer spherical membrane, which contains a cylindrical centre called the capsid. The virus membrane contains two proteins which enable the attachment of the virus to CD4 T lymphocytes: gp120 and gp41. Within the viral capsid, there are two single-stranded copies of viral RNA, and key proteins for viral replication:

reverse transcriptase, HIV integrase, HIV protease, the capsid protein p24, the matrix protein p17 and the nucleocapsid protein p7/p9 (Barré-Sinoussi, 1996; Maartens *et al.*, 2014).

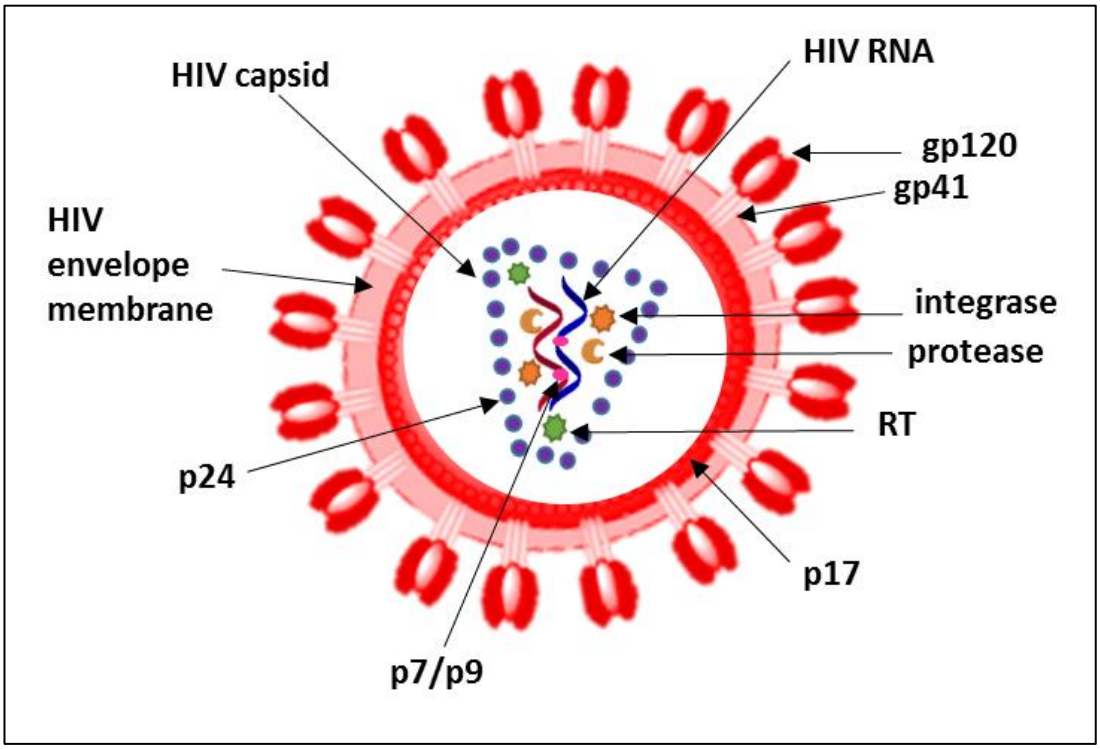

Figure 1.1: Schematic diagram of the HIV virion structure. The membrane of the virus is a lipid bilayer in which two proteins are located: the "outer envelope protein" gp120 and the transmembrane protein gp41. The HIV capsid contains the two single-stranded viral RNA copies and the viral proteins: integrase, protease and reverse transcriptase, p7/p9. p24 is a capsid protein, whereas p17 is a matrix protein. Adapted from: (Barré-Sinoussi, 1996; Maartens *et al.*, 2014). RT: reverse transcriptase.

There are three stages of infection: the initial stage known as the "acute phase" is characterised by a rapid spread and multiplication of the virus in the body, an exacerbated replication of the virus, and a peak in the levels of p24 antigen (p24 Ag) (Centers for Disease Control and Prevention (CDC), 2019; Parekh *et al.*, 2019). This phase usually arises from 2 to 4 weeks from the time of infection. The second stage is known as the "chronic phase" or "asymptomatic phase", in which antibodies against p24 Ag start being produced by the host immune system, leading to a decrease in viral load and in p24 Ag levels; the virus continues to multiply at a lower rate during this phase. The interval between the time of

infection and the start of antibody production by the host immune system is known as the "window period". If after the second stage, the patients remain untreated, the third stage begins and CD4 cells (also known as T-cells or helper cells) begin to be destroyed. The third stage is characterised by the onset of AIDS, and a reduction of CD4 cell levels, leading to a weakened immune system. In the final stage, opportunistic infections arise due to the inability of the patient's immune system to respond to infections (World Health Organization, 2018; Parekh *et al.*, 2019).

1.1.1. Symptoms

Symptoms are dependent on the infection stage. Some initial symptoms include: fever, rash, sore throat and headaches. The second "chronic" stage is asymptomatic. At later stages of infection when the immunosuppression caused by the virus has progressed, symptoms include: swollen lymph nodes, reduced body weight, fever and diarrhoea (World Health Organization, 2018; Parekh *et al.*, 2019). HIV-positive patients are more prone to opportunistic infections such as meningitis, tuberculosis and specific types of cancers such as Kaposi's sarcoma and lymphomas (World Health Organization, 2016).

1.1.2. Transmission and risk factors

The HIV virus can be transmitted via contact with infected body fluids (blood, breast milk, semen and vaginal secretions). The risk of transmission is proportional to the plasma viral load, which is very high in the first few months of infection (Maartens *et al.*, 2014).

Risk factors include: unprotected sex, sharing contaminated needles for the injection of drugs, unsafe blood transfusions or transplants and accidental

injuries among health workers; transmission can also occur from mother to child (World Health Organization, 2016; Centers for Disease Control and Prevention (CDC), 2019).

1.1.3. Diagnosis

The diagnosis of HIV depends on the stage of infection of the untreated individual, and it is based on the detection of various biomarkers such as: p24 Ag, T-helper cells, HIV RNA, and HIV antibodies (Parekh *et al.*, 2019). The detection of these biomarkers allows for the determination of a patient's serological status, their viral load, the progression of the disease, and the treatment effectiveness (Fearon, 2005). Enzyme immunoassays are able to detect HIV-specific antibodies after one to two weeks from the time of infection, and are the most commonly used assays for HIV diagnosis (Parekh *et al.*, 2019).

1.1.4. Mortality

Since the introduction of antiretroviral therapy (ART) the number of deaths caused by HIV has been considerably reduced. However, there is still an increased mortality of HIV-positive individuals compared to the general population; and non-AIDS related conditions, such as opportunistic infections, cancer and cardiovascular disease account for approximately 42% of these deaths (Croxford *et al.*, 2017).

1.1.5. Pathogenesis

HIV attacks activated CD4 T lymphocytes and replicates itself within these host cells (Kis *et al.*, 2010; Maartens *et al.*, 2014).

Figure 1.2 shows the virus cycle, which includes six phases: binding and entry, reverse transcription, integration, replication, budding and maturation (Kis *et al.*, (2010); Maartens, Celum and Lewin, (2014)). The virus binds to the CD4+ immune cell via the chemokine coreceptors CCR5 and CXCR4. The virus can also infect other cells such as monocytes, dendritic cells and macrophages (Maartens *et al.*, 2014). After attachment, the virus inserts viral RNA and viral proteins into the host cell. The next step involves reverse transcription of viral RNA into viral DNA by the viral reverse transcriptase. In the nucleus, integration of viral DNA into the host's DNA is carried out by the HIV integrase enzyme. Viral DNA is transcribed into viral mRNA which is translated to produce polypeptides. Polypeptides are cleaved into active viral proteins by the HIV protease. Viral proteins, together with viral mRNA are incorporated into new immature virions which are released from the host cell to infect other cells once matured (Figure 1.2) (Kis *et al.*, 2010; Maartens *et al.*, 2014).

Once transmission occurs, viral replication increases dramatically as well as the production of inflammatory cytokines and chemokines during the acute phase (Maartens *et al.*, 2014). During the chronic phase, the viral load decreases due to the host's immune response by CD8+ lymphocytes-mediated killing of infected cells. Production of neutralising antibodies starts approximately after three months after infection (Richman *et al.*, 2003); however, mutated forms of the HIV virus arise and cannot be recognised by the antibodies generated by the patient's immune system (Johnson *et al.*, 2002).

The virus' main action is the depletion of CD4+ T cells, by destruction and by reducing their production, leading to dysfunction of the immune system.

However, HIV infection is also characterised by immune activation; immune activation is triggered by activation of the Toll-like receptor in dendritic cells by the HIV virus, and this leads to increased production of interferon-α (activator of immune cells) (Maartens *et al.*, 2014).

Despite the advances of ART for HIV treatment, there is still not a cure for HIV. This is due to the ability of the virus to survive even in patients undergoing ART; the virus survives in a latent state inside the resting T cells, allowing residual replication of the virus in some patients (Siliciano *et al.*, 2011). Latency is the phenomenon by which HIV DNA is integrated into the host's DNA (being the host a resting T cell or an activated T-cell reverted to a resting stage) but no new virions are produced (Dahabieh *et al.*, 2015). The latent virus can also rest in reservoirs such as the lymphoid tissue, the gastrointestinal tract and the central nervous system (Maartens *et al.*, 2014). Elimination of latently infected T cells as an approach to potentially cure HIV is currently under investigation (Maartens *et al.*, 2014; Dahabieh *et al.*, 2015; Schwartz *et al.*, 2017).

1.1.6. Pharmacological treatment

The purpose of ART is to supress viral load, to prevent transmission and resistance, to restore immunity and to improve the quality of life of HIV patients (Margolis *et al.*, 2014). There are six classes of antiretroviral drugs: nucleoside/nucleotide reverse transcriptase inhibitors (NRTIs), non-nucleoside reverse transcriptase inhibitors (NNRTIs), protease inhibitors (PIs), integrase inhibitors, and entry inhibitors (these can be fusion inhibitors or CCR5 antagonists). The mechanisms of action of these drugs are described in Figure 1.2.

The British HIV Association guidelines recommend a starting choice of treatment of two NRTIs (tenofovir plus emtricitabine or abacavir plus lamivudine) combined with one of these six drugs (third agent): dolutegravir (integrase inhibitor), elvitegravir (integrase inhibitor) boosted with cobicistat, raltegravir (integrase inhibitor), atazanavir (PI) boosted with ritonavir (PI), darunavir (PI) boosted with ritonavir, and rilpivirine (NNRTI); alternatively the third agent can be efavirenz (NNRTI) (The British HIV Association, 2016). However, in reality, the patient will need to be switched to different classes of drugs including older drugs from time to time in order to avoid the development of viral resistance.

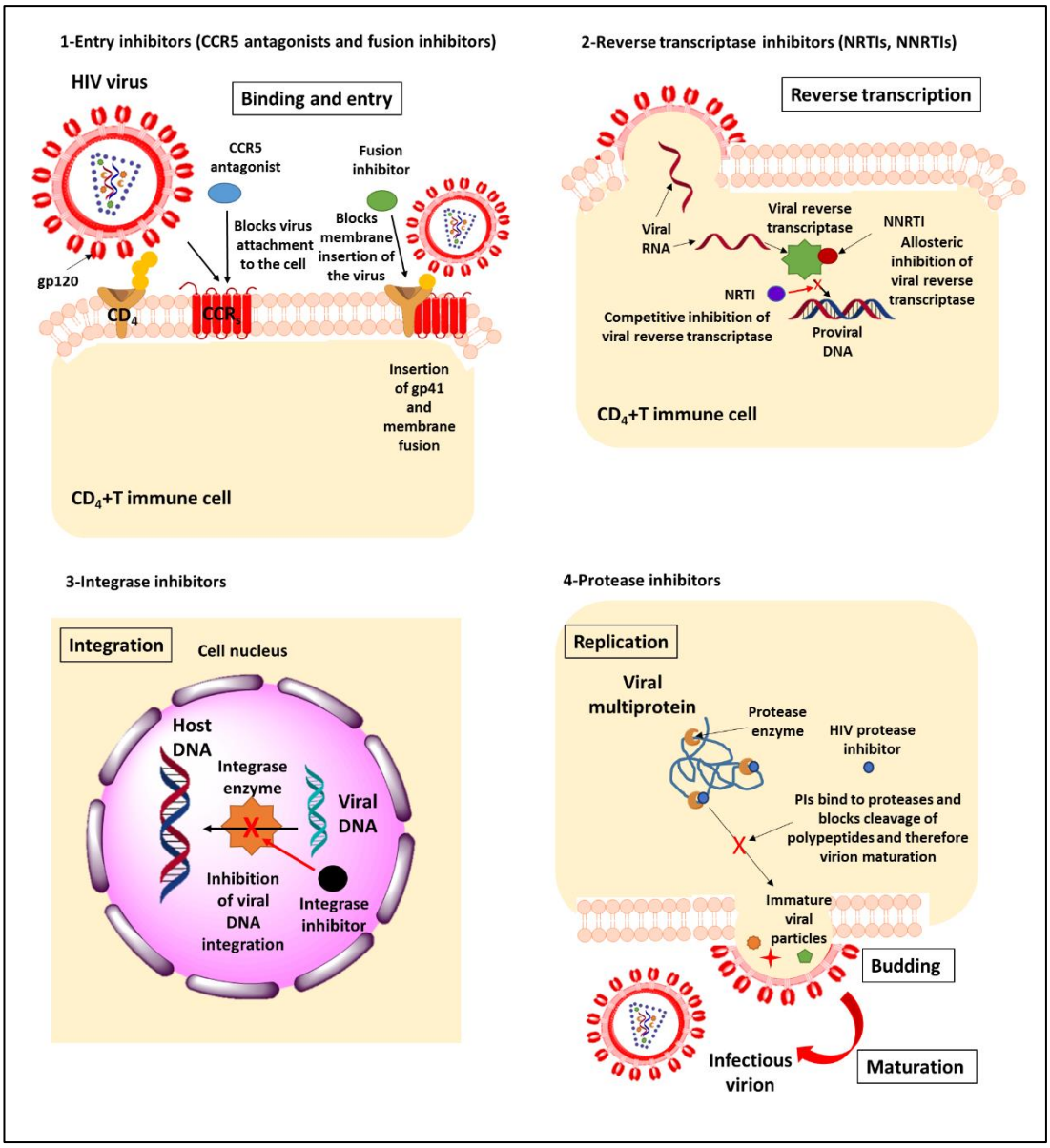

Figure 1.2: Mechanisms of action of antiretroviral drugs. 1) Infection and entrance of the virus into the host CD4+ immune cell by interaction of viral gp120 with the CD4 receptor and to CCR5 (C-C chemokine receptor type 5), or CXCR4 (C-X-C chemokine receptor type 4) coreceptors. CCR5 antagonists block the binding of the receptors to the virus and fusion inhibitors block the membrane insertion of the virus. 2) Once the virus has entered the cell it releases viral RNA which is converted to viral DNA by the viral reverse transcriptase. NRTIs block the action of reverse transcriptase by being incorporated into the viral DNA because they mimic nucleotides. NNRTIs bind to a non-active site of the reverse transcriptase and disrupt its shape, therefore blocking its attachment to the DNA by non-competitive inhibition. 3) The viral DNA enters the nucleus and it is inserted into the host DNA by the enzyme HIV integrase; integrase inhibitors stop the action of this enzyme by non-competitive inhibition. 4) Viral DNA is transcribed into mRNA and this starts the production of viral polypeptides; these polypeptides are cleaved into immature viral proteins by the HIV enzyme protease and reorganized at the cell membrane leading to the formation of new infectious virions. Protease inhibitors bind to the HIV protease in a non-competitive manner and block the cleavage of viral polypeptides into active viral molecules; this leads to the formation on

non-infectious virions. Adapted from: Kis et al., (2010) and Maartens, Celum and Lewin, (2014).

1.2. Antiretroviral drugs

1.2.1. History

The first HIV drug to be used in clinical trials was azidothymidine (AZT) (later named zidovudine) in 1985, and it was shown to increase survival by 24-weeks, but this effect disappeared after a short time (Fischl *et al.*, 1987). After zidovudine was approved for use in the clinic in 1987, the following drugs to be approved were: zalcitabine (ddC), didanosine (ddI) and stavudine (d4T); all of them are NRTIs and none of them are currently used (Vella *et al.*, 2012).

In the early 1990s monotherapy was associated to the onset of resistance and lack of effectiveness, and combination therapy became the standard for antiretroviral therapy by the end of the 1990s. A key finding was the reduction in mother-to-child transmission by NRTIs (Vella *et al.*, 2012).

It was in 1995 when new drug families, other than NRTIs appeared, such as NNRTIs and PIs. The first NNRTI was nevirapine, and the first PI was saquinavir (Vella *et al.*, 2012). The first combination therapy between drugs from different families was a triple combination of: indinavir, zidovudine and lamivudine, resulting in a sustained HIV suppression (Gulick *et al.*, 2000). Despite this promising result, the use of indinavir was reduced due to its toxicity (Vella *et al.*, 2012).

Following the Vacouver AIDS conference, and the publication of "International AIDS Society-USA recommendations for antiretroviral therapy" (Carpenter *et al.*,

1996), both in 1996, the use of protease inhibitors in triple drug combination antiretroviral therapy (cART) was established, and the mortality and morbidity associated with HIV was reduced dramatically. However, due to the toxicity associated with cART at that time, the quality of life of patients was still poor (Vella *et al.*, 2012).

Currently, a single tablet with established dose and once daily administration regime is available, which increases adherence and treatment success. The treatment is tailored individually based on the patients' viral load, disease status and virus genotype and mutations (The British HIV Association, 2016). Furthermore, the benefit of starting treatment immediately after diagnosis became evident, as well as the reduction of HIV transmission as a consequence of treatment. Nevertheless, and due to the increased life expectancy of patients, non-AIDS comorbidities emerged, including cardiovascular disease, metabolic toxicity, and cancer (Flexner, 2019). The search for a cure for HIV is focusing on investigation of the virus latency (Schwartz *et al.*, 2017) and vaccine development (Hsu *et al.*, 2017).

1.2.2. Nucleoside/nucleotide reverse transcriptase inhibitors (NRTIs)

NRTIs comprise the nucleoside reverse transcriptase inhibitors: zidovudine, lamivudine, abacavir, emtricitabine, didanosine (withdrawn) and stavudine (withdrawn); and the nucleotide reverse transcriptase inhibitors: tenofovir disoproxil fumarate, and tenofovir alafenamide (De Clercq, 2010; Holec *et al.*, 2017).

NRTIs are prodrugs, and they are converted, upon phosphorylation, into active metabolites of longer half-life. Their mechanism of action is the inhibition of HIV-1 reverse transcriptase by competitive inhibition with natural nucleosides (Figure 1.2) (Holec *et al.*, 2017).

The conversion of NRTI pro-drugs into active metabolites via phosphorylation takes place intracellularly; the active drug blocks the action of reverse transcriptase, acting as a functional nucleoside analogue and this leads to termination of synthesis of viral DNA (Holec *et al.*, 2017). Transport of NRTIs into the cell occurs by simple diffusion (if the drug is lipophilic like tenofovir, abacavir, zidovudine and stavudine) or via transporters. These transporters often belong to the solute carrier transporter SLC family: organic cation transporters (OCT) (Jung *et al.*, 2008), organic anion transporters (OAT) (Jafari *et al.*, 2014), concentrative nucleoside transporters (CNTs), and equilibrate nucleoside transporters (ENTs)(Varatharajan *et al.*, 2009; Holec *et al.*, 2017).

Chronic treatment with NRTIs leads to toxicity and drug resistance. NRTIs cause mitochondrial toxicity (especially older NRTIs), which leads to oxidative damage and cellular apoptosis (Margolis *et al.*, 2014). Mitochondrial dysfunction has been reported to be the cause underlying the side effects of NRTIs, such as renal toxicity, cardiomyopathy, myopathy, pancreatitis, hepatic steatosis, lactic acidosis and peripheral neuropathy. Another toxic effect associated to NRTIs and PIs is lipodystrophy (described in section 1.6) (Margolis *et al.*, 2014; Holec *et al.*, 2017).

1.2.3. Non-nucleoside reverse transcriptase inhibitors (NNRTIs)

NNRTIs bind to the active site of the reverse transcriptase causing a conformational change of the protein, which inhibits the addition of nucleosides to the viral DNA chain (Figure 1.2)(Kis *et al.*, 2010). NNRTIs are associated with less adverse drug reactions than NRTIs, but they show an early onset of drug resistance when used as a single agent; due to this, they are normally used in combination with other antiretrovirals. Adverse drug reactions include rash, and very rarely, Stevens-Johnson syndrome and toxic epidermal necrolysis (Margolis *et al.*, 2014). NNRTIs include: nevirapine, efavirenz, etravirine and rilpivirine; delavirdine is not currently recommended (De Clercq, 2010).

1.2.4. Protease inhibitors (PIs)

The HIV protease breaks down the viral precursor polypeptides into active viral proteins that are necessary for virion maturation. Protease inhibitors bind to the HIV protease and block its action, leading to the production of immature non-infectious virions (Figure 1.2) (Kis *et al.*, 2010). PIs include: saquinavir, ritonavir, nelfinavir, lopinavir, atazanavir, fosamprenavir, tipranavir, darunavir; indinavir is no longer recommended (De Clercq, 2010; Margolis *et al.*, 2014).

Common adverse effects of PIs are gastrointestinal problems, abdominal pain, nausea, vomiting and diarrhoea; but, most importantly, chronic use of PIs is associated to metabolic abnormalities such as dyslipidaemia, insulin resistance, type 2 diabetes mellitus (T2DM), lipodystrophy and an increased risk of myocardial infarction. Drug-induced metabolic disruption is especially relevant in first-generation PIs such as lopinavir (Margolis *et al.*, 2014). This is further explained in section 1.5.

PIs, in particular lopinavir and atazanavir, are the drugs of choice for experimental investigations in this thesis due to their metabolic effects.

1.2.4.1. Lopinavir

Lopinavir (Figure 1.3), a first-generation PI, shows highly specific binding capacity to the HIV-1 protease (Hurst *et al.*, 2000). In humans, lopinavir is rapidly metabolised by CYP3A4 and the metabolites formed are a lot less active than the parent drug. Ritonavir inhibits the metabolism of lopinavir by CYP3A4, increasing its half-life and its plasma concentration; therefore they are usually co-administered (Chandwani *et al.*, 2008; Margolis *et al.*, 2014).

The standard dose of lopinavir/ritonavir for adults is 800mg/200mg once daily or 400mg/100m twice daily (Food and Drug Administration (FDA), 2017). The once daily dosing is not recommended to paediatric patients, and a twice daily dose should be calculated based on body weight and body surface area. Its use in pregnancy is only applicable if the benefit justifies the potential risk to the foetus (Category C under FDA Pregnancy Risk Categories) (Chandwani *et al.*, 2008; Food and Drug Administration (FDA), 2017).

Lopinavir is no longer recommended for first-line therapy for HIV, and boosted atazanavir is the preferred PI for treatment, especially for patients with high risk of cardiovascular disease (The British HIV Association, 2016). Lopinavir use in PI monotherapy (boosted with ritonavir) in the MONARK randomised 96-week clinical study showed lower virological suppression compared to a combined regime of lopinavir/ritonavir plus zidovudine and lamivudine (Delfraissy *et al.*, 2008). The use of PI monotherapy is not recommended for routine ART (The British HIV Association, 2016).

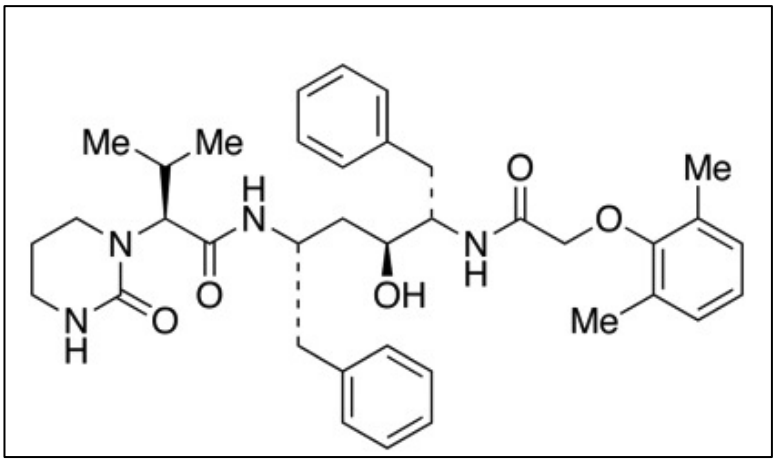

Figure 1.3: Lopinavir

1.2.4.2. Atazanavir

Atazanavir (Figure 1.4) is a well-tolerated, HIV-1-specific PI, and it is metabolised by CYP3A4 in the liver into inactive metabolites. Co-administration with drugs that induce or inhibit CYP3A4, such as efavirenz and nevirapine, are not recommended as they affect plasma concentrations of atazanavir (Croom *et al.*, 2009). The standard dose of atazanavir for adults is 300 mg together with 100 mg of ritonavir once daily for both treatment-naïve or treatment-experienced adults (Food and Drug Administration (FDA), 2018).

Paediatric use of atazanavir is based on body weight and should not be used in children of less than 5 kg of weight. In pregnancy, human and animal data have not reported an increased risk of teratogenicity (Food and Drug Administration (FDA), 2018).

Common adverse drug reactions of atazanavir are unconjugated hyperbilirubinemia and nausea, and chronic exposure causes renal toxicity. Nevertheless, the metabolic profile of atazanavir is a lot more favourable compared to that of lopinavir (Margolis *et al.*, 2014; Menshawy *et al.*, 2017). A recent meta-analysis (Menshawy *et al.*, 2017) compared the safety and efficacy of

atazanavir compared to lopinavir and darunavir taking data from nine randomised controlled clinical trials. They found no difference between the efficacy of lopinavir and atazanavir regimes in terms of virological failure and plasma concentrations of HIV RNA copies. However, regarding safety, lopinavir showed higher incidence of dyslipidaemia and gastrointestinal adverse effects. There were no differences in the incidence of metabolic adverse effects between atazanavir and darunavir (Menshawy *et al.*, 2017).

Atazanavir (Figure 1.4) is administered with ritonavir (boosted) to prolong the half-life and to increase systemic exposure, and this combination is one of the preferred ones for initial ART (The British HIV Association, 2016).

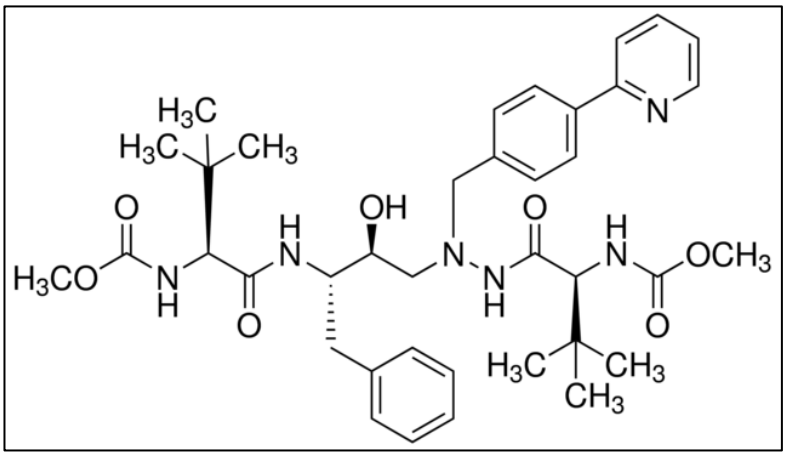

Figure 1.4: Atazanavir

1.2.5. Integrase inhibitors

The enzyme HIV integrase incorporates the viral DNA insertion into the host DNA; and integrase inhibitors prevent this (Kis *et al.*, 2010). Integrase inhibitors include: raltegravir, elvitegravir and dolutegravir (De Clercq, 2010). Raltegravir was the first integrase inhibitor to be approved by the FDA in 2007. It is metabolised by hepatic glucuronidation (uridine diphosphate glycuronosyltransferase-mediated) (Margolis *et al.*, 2014). Common adverse

drug reactions to raltegravir are nausea, headache, dizziness, insomnia and fatigue; less common and serious adverse effects are Steven-Johnson syndrome, hypersensitivity, toxic epidermal necrolysis, rhabdomyolysis and renal failure, but these are very rare and only occur in 2% of the patients (Margolis *et al.*, 2014).

1.2.6. Entry inhibitors

Entry inhibitors block the binding of the HIV virions to human CD4 cells, thus preventing their entry, and they are classified into two groups: CCR5 antagonists (maraviroc), and fusion inhibitors (enfuvirtide) (Figure 1.2). Maraviroc should only be used in patients infected with a HIV strain that binds to the CCR5 coreceptor, and it is not recommended for strains that bind to the CXCR4 coreceptor (Margolis *et al.*, 2014). Enfuvirtide is degraded into smaller peptides by hepatic peptidases, and maraviroc is metabolised by CYP3A4 (Dando *et al.*, 2003). Common adverse effects of enfuvirtide include local reactions such as erythema, pruritis and localised pain (Dando *et al.*, 2003); and common adverse effects of maraviroc are nausea, fatigue, headache and diarrhoea (Margolis *et al.*, 2014).

1.3. ART-induced cardiometabolic disease

Metabolic syndrome is defined as a cluster of different conditions, such as obesity, insulin resistance, hyperglycaemia, atherogenic dyslipidaemia, hypertension and pro-thrombotic and pro-inflammatory states (International Diabetes Federation, 2006; Huang, 2009). Metabolic syndrome is heavily associated with type 2 diabetes mellitus and cardiovascular disease (CVD) (Miranda *et al.*, 2005; Laclaustra *et al.*, 2007).

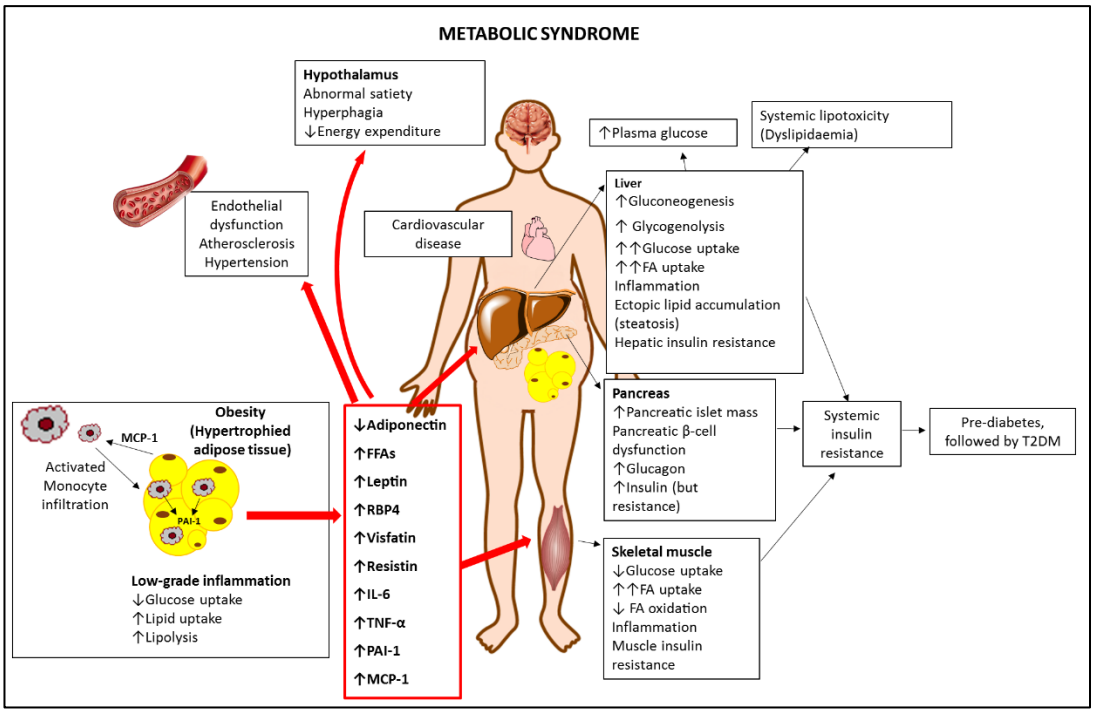

Figure 1.5: Pathophysiology of the metabolic syndrome. In obesity, adipose tissue expansion causes malfunction and inflammation characterised by increased lipolysis and secretion of pro-inflammatory cytokines by the adipose tissue. Increased release of FFAs to the circulation causes lipid deposition in other organs and tissues. In the liver, FFAs increase glucose production (increased gluconeogenesis and glycogenolysis). In the muscle, FFAs reduce insulin sensitivity and inhibit glucose uptake. Increased plasma glucose and increased plasma FFAs levels increase insulin secretion by the pancreas, leading to hyperinsulinemia and, ultimately, insulin resistance. Enhanced secretion of pro-inflammatory cytokines (TNFα and IL-6) further promotes insulin resistance, adipose tissue lipolysis, and increased hepatic glucose output. Increased production of PAI-1 by the adipose tissue results in a pro-thrombotic state, and reduction of adiponectin further contributes to the onset of metabolic syndrome. Hypertrophied adipocytes secrete higher amounts of leptin, but the brain does not respond with a correct satiety response (leptin resistance). Adapted from: Nature Medicine, (2012); Rezaee and Dashty, (2013); Eckel, Grundy and Zimmet, (2005). MCP-1: monocyte chemoattractant protein-1; TNF-α: tumor necrosis factor-α; PAI-1: plasminogen activator inhibitor-1; RBP4: retinol-binding protein-4; IL-6: interleukin-6; FFAs: free fatty acids.

The International Diabetes Federation estimates that around 25% of the adult world population have metabolic syndrome, and it establishes a definition for the diagnosis of metabolic syndrome in clinical practice (Table 1.1) (International Diabetes Federation, 2006).

Table 1.1. Clinical parameters for the diagnosis of metabolic syndrome.

Central obesity	BMI> 30 kg/m^2 or Waist circumference: ≥94 cm (male, European)(IDF); >102 cm (WHO) ≥80 cm (female, European) (IDF); >88 cm (WHO)
Plus any of the following:	
Increased triglycerides levels	≥150 mg/dL (1.7 mmol/L) (IDF, WHO)
Reduced HDL cholesterol	<40 mg/dL (1.03 mmol/L) in males (IDF); <35 mg/dL (WHO) <50 mg/dL (1.29 mmol/L) in females (IDF); <39 mg/dL (WHO)
High blood pressure (BP)	Systolic BP≥130 (IDF); ≥140 (NHS, WHO) or diastolic BP≥85 mmHg (IDF); ≥90 (NHS, WHO)
Raised fasting plasma glucose (FPG)	FPG≥100 mg/dL (5.6 mmol/L) or previously diagnosed with T2DM (IDF); >110 mg/dL (WHO)

WHO, World Health Organisation; IDF, International Diabetes Federation; NHS, National Health Service. Adapted from: International Diabetes Federation, (2006); Guo, (2014); NHS, (2016).

Metabolic syndrome can arise as an adverse drug reaction produced by the chronic use of certain drugs. The World Health Organisation (WHO) defines an adverse drug reaction as "a response to a drug which is noxious and unintended, and which occurs at doses normally used in man for the prophylaxis, diagnosis or therapy of disease or for the modification of physiological function" (World Health Organization, 2002).

Some examples of drugs that increase the risk of metabolic syndrome are antiretrovirals (Wand *et al.*, 2007; Magkos *et al.*, 2011), antipsychotics (Philippe *et al.*, 2005; Young *et al.*, 2015), antiepileptics (Wofford *et al.*, 2006; Olesen *et al.*, 2011; Verrotti *et al.*, 2011), immunosuppressants (Wofford *et al.*, 2006; Johnston

et al., 2008), steroids (Curtis *et al.*, 2006; Racil *et al.*, 2013) and anticancer drugs (Racil *et al.*, 2013). This thesis, focused on HIV antiretrovirals and, amongst these, on PIs.

HAART has significantly reduced the number of deaths caused by HIV, considerably increasing life expectancy for HIV-infected patients. However, this has led to an aging cohort of HIV patients dying from non-AIDS-related chronic conditions such as cancer, liver disease and CVD (Croxford *et al.*, 2017; Panel on Antiretroviral Guidelines for Adults and Adolescents, 2018). Antiretroviral-induced metabolic disease arises as a consequence of chronic exposure to antiretrovirals (particularly protease inhibitors) and it increases the risk of CVD (Barbaro *et al.*, 2006). For HIV-infected individuals on ART, the risk of CVD is 2-fold compared to the general population, and 1.5-fold higher compared to treatment-naïve HIV infected patients (Triant, 2013). CVD has been reported to be responsible for 10% of deaths of HIV patients (Martin *et al.*, 2013), and the burden of HIV-related CVD has been reported to be three times higher in the past two decades, being stroke and myocardial infarction the most prevalent causes. The most affected areas are sub-Saharan Africa and Asia Pacific (Shah *et al.*, 2018).

The link between ART and the development of T2DM has been clearly established (Wand *et al.*, 2007; Samaras, 2009; Araujo *et al.*, 2014). The prevalence of diabetes amongst a cohort of 352 patients under long-term treatment with PIs was 11%, and the prevalence of dyslipidaemia (LDL-related) was 28% (Bastard *et al.*, 2019).

A recent meta-analysis revealed that the odds of developing diabetes were 4 times higher for patients undergoing ART compared to treatment-naïve individuals (Nduka *et al.*, 2017). An increased risk of T2DM has been associated to PIs and certain NRTIs such as zidovudine (Blümer *et al.*, 2008) and stavudine (Brambilla *et al.*, 2003); whereas lower risk has been associated with efavirenz, nevirapine, tenofovir, abacavir, lamivudine and newer PIs like atazanavir and darunavir (Shlay *et al.*, 2005; Bernal *et al.*, 2007; Blümer *et al.*, 2008; Randell *et al.*, 2010; Karamchand *et al.*, 2016).

Insulin resistance precedes the development of T2DM in patients treated with ART. A recent study on HIV-infected African children on ART revealed that at least 40% of the subjects presented insulin resistance or lipid abnormalities (Innes *et al.*, 2016). ART may contribute to insulin resistance by causing β-cell dysfunction and loss of secretory capacity, but the mechanism behind ART-induced insulin resistance is thought to be multifactorial (Samaras, 2009).

ART-induced cardiometabolic disease is a multifactorial condition amongst HIV patients, and it is closely related to the adipose tissue. The combined deleterious effects of antiretrovirals on lipid metabolism (dyslipidaemias), insulin sensitivity (insulin resistance) and fat storage (lipodystrophy) all contribute to the development of cardiometabolic disease (van Wijk *et al.*, 2012; Hemkens *et al.*, 2014), and the mechanisms behind its onset are described in sections 1.5 to 1.9.

1.4. The adipose tissue as a regulator of metabolic homeostasis

The regulation of metabolic homeostasis is a combined effort between the endocrine system and organs exerting a metabolic role like the adipose tissue, the

liver, and the skeletal muscle (Figure 1.6). Disturbances in the adipose tissue metabolism may lead to cardiometabolic disease (Rezaee *et al.*, 2013).

Initially, the adipose tissue was regarded as an inert fat storage; however, the endocrine role of the adipose tissue and its function as a regulator of metabolic homeostasis are currently widely recognised (Guilherme *et al.*, 2008; Halberg *et al.*, 2008; Peinado *et al.*, 2012; Coelho *et al.*, 2013; Renes *et al.*, 2013; Lim *et al.*, 2014; Musi *et al.*, 2014).

The adipose tissue is a metabolically dynamic organ; it protects the body from lipotoxicity, controls insulin sensitivity and allows organ crosstalk through the secretion of adipocyte-specific cytokines known as adipokines (Coelho *et al.*, 2013). It can also undergo changes in size, phenotype and function, and it regulates energy expenditure and nutritional intake (Rosen and Spiegelman, 2006; Musi *et al.*, 2014; Kahn, 2019).

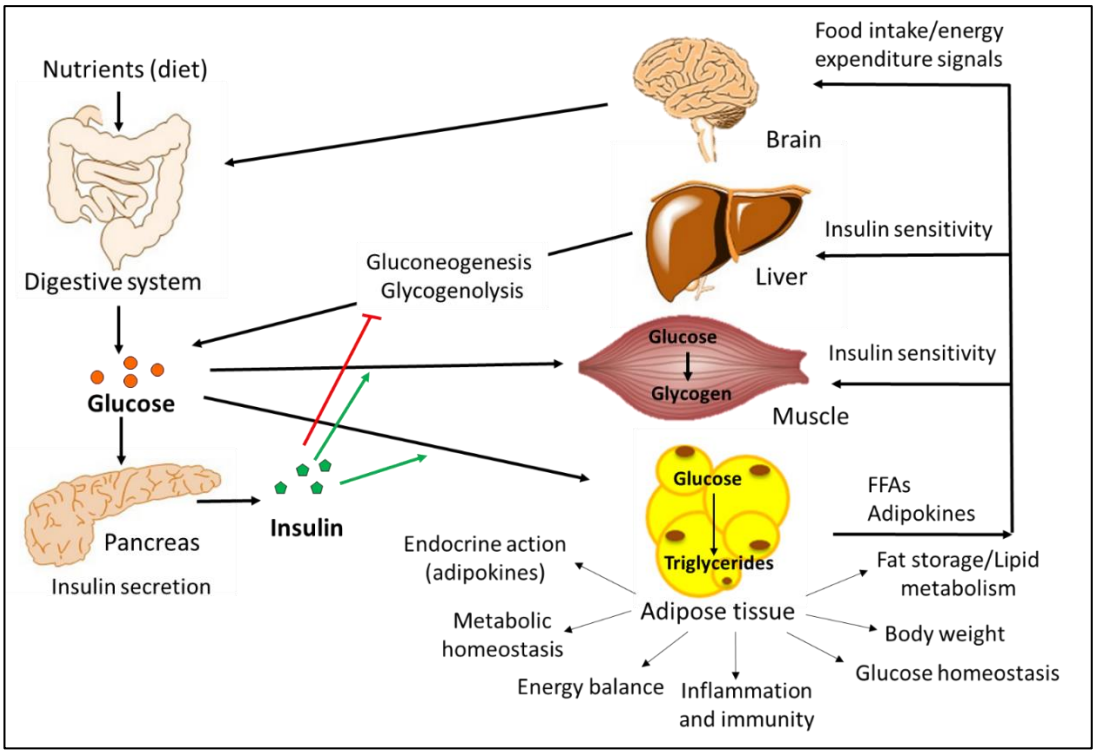

Figure 1.6: Crosstalk between the adipose tissue and other tissues and organs for the regulation of metabolic homeostasis. The brain sends signals of satiety and energy expenditure to regulate food intake. After food consumption, blood glucose levels increase, and the pancreas releases insulin in response. Insulin promotes glucose conversion into glycogen by the muscle and the liver, and into triglycerides by the adipose tissue. Insulin blocks glucose production by the liver via gluconeogenesis or glycogenolysis. Insulin inhibits lipolysis, by which triglycerides are mobilised into FFAs. The diet is a source of fat, and FFAs are released from the digestive system in the form of chylomicrons. Chylomicrons transport fatty acids to the adipose tissue, the liver and the muscle. During fasting, the triglycerides can be broken intro FFAs via lipolysis, and fatty acids are taken up by the liver and the muscle. The adipose tissue secretes adipokines to regulate a wide variety of biological processes such as body weight homeostasis, inflammation, and glucose and lipid homeostasis. Adapted from: (Rosen and Spiegelman, 2006; Coelho *et al.*, 2013; Kahn, 2019). FFAs: free fatty acids.

1.4.1. Function and formation of the adipose tissue

The adipose tissue comprises not only adipocytes, but also fibroblasts, preadipocytes, endothelial cells, macrophages, blood cells, and pericytes (Gimeno *et al.*, 2005; Coelho *et al.*, 2013). This highlights the impact of adipose tissue not only in metabolism, but also in immunity, osteogenesis and inflammation (Rezaee *et al.*, 2013).

A key metabolic role of the adipose tissue is the regulation of lipid storage via the processes of lipogenesis and lipolysis (Coelho *et al.*, 2013). Lipogenesis mainly occurs in the adipose tissue, but it also takes place in the liver and it involves the generation of fatty acids. Fatty acids are esterified together with glycerol-3-phosphate (glycerol-3-P) into triacylglycerols (TAGs), which are stored within lipid droplets (Luo *et al.*, 2016). Lipogenesis responds to changes in the diet and is mediated by hormones such as leptin, which inhibits lipogenesis, or angiotensin, which stimulates lipogenesis. Lipogenesis is stimulated by high plasma triglyceride levels (consequence of a diet rich in carbohydrates) and inhibited by fasting and polyunsaturated fatty acids; glucose is a substrate for lipogenesis and it stimulates lipogenesis by induction of insulin release and inhibition of glucagon release by the pancreas. Lipolysis on the other hand, involves the breakdown of TGAs into glycerol and FFAs during fasting or metabolic stress conditions, so they can be used as an energy source by other tissues (Figure 1.7) (Coelho *et al.*, 2013).

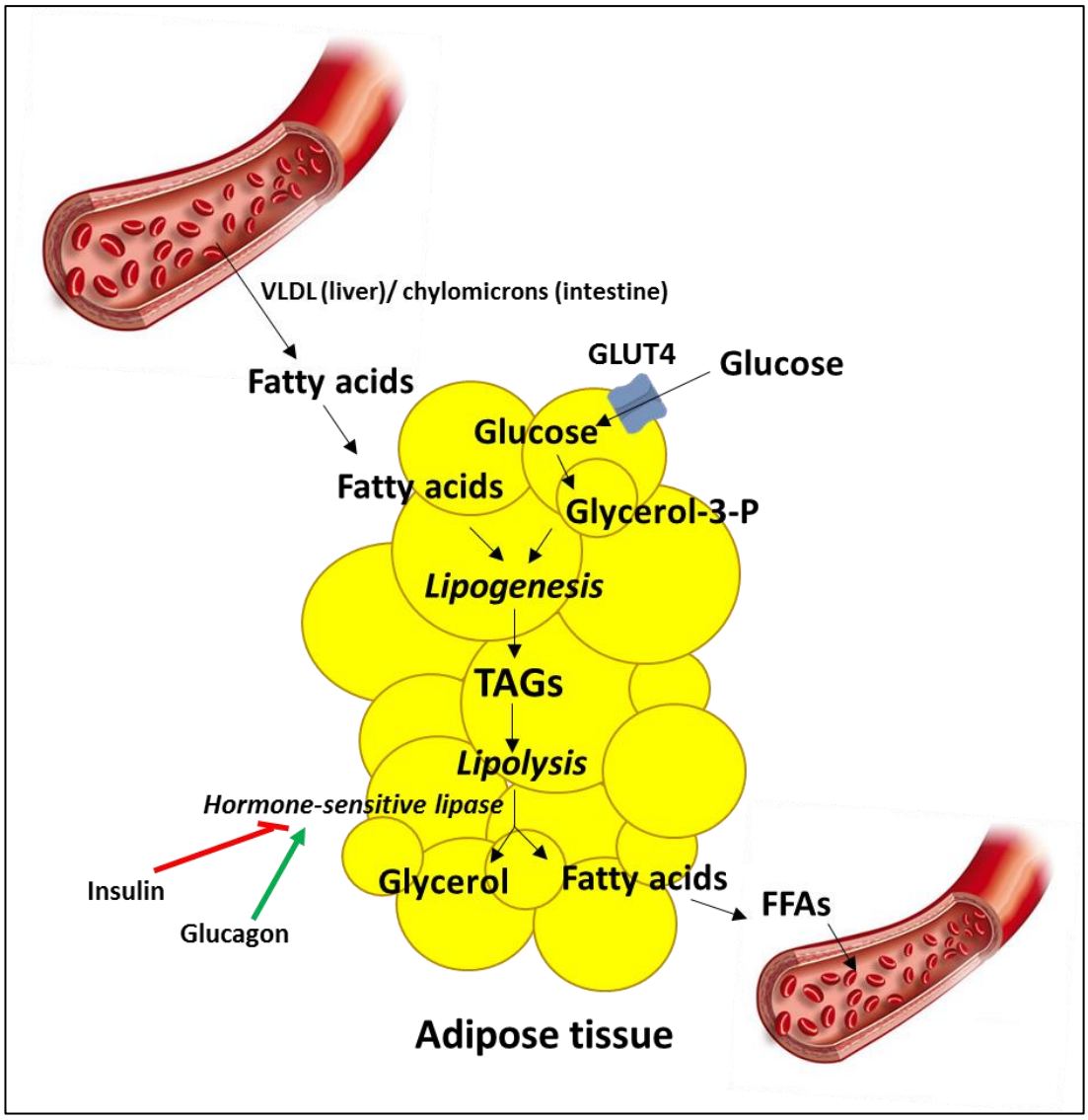

Figure 1.7. Metabolic role of the adipose tissue. After food has been consumed ("feeding state") insulin is released from the pancreas and it stimulates glucose transport into adipocytes via the GLUT4 transporter. Glucose breakdown into glycerol-3-phosphate (glycolysis) is a necessary step for lipogenesis. VLDL carries fatty acids from the liver, and chylomicrons carry TAGs from the intestine and release FFAs into the adipose tissue by action of lipoprotein lipase. Fatty acids are then esterified together with glycerol-3-phosphate to form TAGs, which are stored in lipid droplets. During fasting or metabolic stress, lipolysis takes place, and TAGs are broken down into glycerol and fatty acids by the enzymes hormone-sensitive lipase, and monoacylglycerol lipase. Hormone-sensitive lipase is inhibited by insulin and induced by glucagon and epinephrine. Glycerol is transported out of the adipocyte via aquaporin-like transporters and travels to the liver, where it will be used for gluconeogenesis. Albumin transports fatty acids in the bloodstream to the liver, the muscle and other organs where they will be oxidised. Adapted from Coelho *et al.*, (2013) and Luo *et al.*, (2016). TAGs: triacylglycerols; FFAs: free fatty acids; GLUT4: glucose transporter 4, VLDL: very-low-density lipoprotein.

The adipose tissue is subdivided into two different types: brown adipose tissue (BAT) and white adipose tissue (WAT), and they differ not only in colour, but also in morphology and functionality (Okita *et al.*, 2012; Kim *et al.*, 2015). WAT is also divided into two different categories: visceral adipose tissue (VAT) and subcutaneous adipose tissue (SAT) (Ota *et al.*, 2015). VAT is differentiated into different depots: omental, mesenteric, peritoneal and gonadal (Bjørndal *et al.*, 2011).

A key aspect of the adipose tissue is its secretory capacity, which varies depending on the type of adipose tissue (BAT or WAT) and its location in the body. Depending on their anatomical distribution (subcutaneous, visceral, omental), different adipose tissues contribute differently to energy balance and metabolic homeostasis (Wang *et al.*, 2013). WAT works as an energy reservoir whereas BAT contributes to energy expenditure (Stern *et al.*, 2015). BAT is mainly present in rodents and new-borns but it has also been reported to be present in adults, especially in the anterior neck and thoracic areas (Nedergaard *et al.*, 2007). Its brown colour is due to its high mitochondrial content within the adipocytes. Brown adipocytes express high levels of Uncoupling protein 1 (UCP1) (Stern *et al.*, 2015). UCP1 is responsible for energy expenditure and heat production, and it interferes with the electron transport chain (Okita *et al.*, 2012; Musi *et al.*, 2014). BAT regulates cold- and diet-induced thermogenesis, therefore regulating body temperature. Recent studies support that BAT activity is inversely proportional to the Body Mass Index (BMI) (Saely *et al.*, 2011).

VAT and SAT are different on a molecular, cellular, physiological and clinical level. Under obesity conditions, visceral adipocytes generate larger amounts of FFAs

than subcutaneous adipocytes (Brockman *et al.*, 2012; Murri *et al.*, 2014). In addition, VAT has a higher lipid metabolic activity, it is more sensitive to lipolysis and more prone to insulin resistance than SAT (Fang *et al.*, 2015).

Differences regarding the secretion of adipokines by VAT and SAT have been identified (Insenser *et al.*, 2012). VAT secretes high amounts of the pro-inflammatory adipokine resistin, IL-6 and PAI-1 (plasminogen activator inhibitor 1); in contrast, SAT secretes a high amount of adiponectin (which decreases inflammatory response, has an anti-atherosclerotic effect and improves insulin sensitivity) and leptin (Kershaw *et al.*, 2004; Peinado *et al.*, 2012; Coelho *et al.*, 2013).

In obesity, VAT recruits large amounts of macrophages, natural killer cells, and T lymphocytes, and it secretes higher levels of inflammatory cytokines compared to SAT. Excess of VAT has been strongly linked with heart disease, insulin resistance, and other obesity-related co-morbidities; increased SAT on the other hand, is thought to have a protective role (Peinado *et al.*, 2012; Ota *et al.*, 2015).

1.4.2. Adipogenesis

The process during which fibroblast-like preadipocytes differentiate into mature adipocytes is known as adipogenesis (Rosen and MacDougald, 2006). Adipogenesis is divided into two stages: determination, the process in which pluripotent mesenchymal stem cells (MSCs) are converted into committed preadipocytes, and terminal differentiation, the process in which committed preadipocytes differentiate into mature adipocytes (Rosen and MacDougald, 2006; Ali *et al.*, 2013).

During adipogenesis, preadipocytes undergo morphological changes and they start accumulating fat within lipid droplets (Sarjeant *et al.*, 2012); they also start taking on the characteristics of a mature adipocyte, such as insulin sensitivity, capacity to secrete adipokines, and lipid transport and synthesis mechanisms (Rosen and MacDougald, 2006).

Figure 1.8 represents the adipogenesis process for the murine immortalised cell line 3T3-F442A, the cell line of choice for this thesis, which is explained in section 1.12.1.

Adipogenesis is not only associated with morphological or secretory changes but also transcriptional and proteomic changes with downstream implications. Transcription factors such as peroxisome proliferator-activated receptor gamma (PPARγ) and CCAAT/enhancer-binding proteins (C/EBPs) function as inducers of adipogenesis (MacDougald *et al.*, 2002). PPARγ is the most critical of pro-adipogenic transcription factors, and it is the main regulator of adipogenesis both *in vitro* and *in vivo*. In fact, many suppressors of adipogenesis reduce PPARγ expression (Rosen and MacDougald, 2006). There are two isoforms of PPARγ: PPARγ1, expressed in most tissues, and PPARγ2, highly expressed in adipocytes; out of the two isoforms, PPARγ2 exhibits the most adipogenic potential. PPARγ also has an impact on insulin sensitivity, and its knockout has been shown to induce insulin resistance in mice (He *et al.*, 2003).

C/EBPs are a family of leucine zipper transcription factors; C/EBPβ, and C/EBPδ promote adipogenesis in the earlier stages, and then work in combination to activate C/EBPα, which promotes adipogenesis at a later stage (Sarjeant *et al.*, 2012; Ali *et al.*, 2013). Additional pro-adipogenic factors are: the AP-1 family of

transcription factors, Krupel-like factors (KLF4, KLF5, KLF6 and KLF15), sterol-regulatory-element-binding-protein-1 (SREBP1), and single transducers and activators of transcription (STATs) (Sarjeant *et al.*, 2012; Ali *et al.*, 2013).

Negative effectors of adipogenesis comprise the Wingless and INT-1 protein family (Wnts), GATA factors, Pref-1, and certain members of the KLF family such as KLF2 and KLF7 (Sarjeant *et al.*, 2012).

The MAPK (mitogen-activated protein kinase) pathway responds to metabolic changes in the cell and it also participates in adipogenesis (Rosen and MacDougald, 2006). MAPKs are subdivided into families: Extracellular signal-regulated kinases (ERK1/2), ERK5, Jun amino-terminal kinases (JNK1-3) and p38 kinases. In early adipogenesis, ERK1 induces preadipocyte proliferation and differentiation; however, in the later stages of adipogenesis, the action of ERK has to be inhibited for adipogenesis to progress, as ERK inactivates the action of PPARγ (Bost *et al.*, 2005; Rosen and MacDougald, 2006; Gehart *et al.*, 2010).

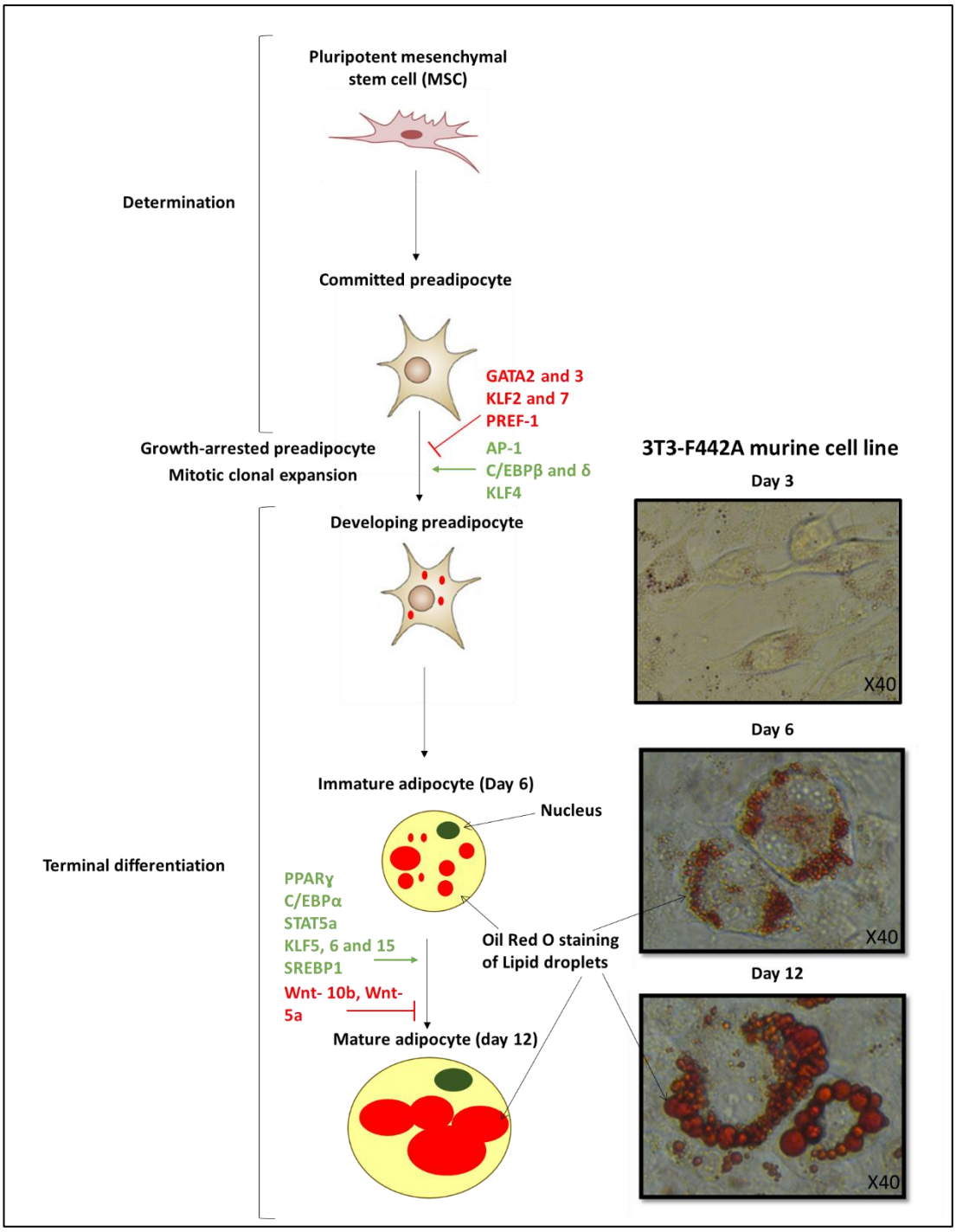

Figure 1.8: Stages of adipogenesis for the 3T3-F44A2 murine immortalised cell line. The first stage of adipogenesis is the determination from mesenchymal precursors to committed preadipocytes, followed by terminal differentiation in which preadipocytes go through morphological and functional changes to finally transform into mature and insulin-responsive adipocytes, able to accumulate triglycerides within lipid droplets (red spheres). Positive effectors of adipogenesis include: PPARγ, C/EBPα, β, and δ, AP-1, KLF4, 5, 6 and 15, STAT5a, and SREBP1. Negative effectors of adipogenesis include: GATA2 and 3, KLF2 and 7, PREF-1, and the Wnt-family proteins. Photomicrographs (40x magnification) showing lipid accumulation by Oil Red O staining of 3T3-F442A adipocytes. Differentiation is triggered by insulin and full differentiation is achieved at day 12. Time points: day 3, day 6 and day 12. Adapted from: Ali *et al.*, (2013), Lefterova *et al.*, (2009) and Sarjeant *et al.*, (2012). KLF: Krupel-like factors;

C/EBP: CCAAT/enhancer-binding proteins; PPARγ: peroxisome proliferator-activated receptor gamma; STAT: single transducers and activators of transcription; SREBP1: sterol-regulatory-element-binding-protein-1.

1.4.3. Insulin signalling and glucose homeostasis in the adipocyte

The actions of insulin in the adipose tissue include promotion adipocyte growth, differentiation, inhibition of lipolysis, stimulation of lipid synthesis, and regulation of glucose uptake for storage (Laviola *et al.*, 2006). Insulin receptor (IR) autophosphorylation and activation initiates two main signalling pathways: the Akt pathway and the MAPK (mitogen-activated protein kinases)/ERK (extracellular signal-regulated kinases) pathway. The Akt pathway mediates glucose uptake and inhibits lipolysis, whereas the ERK pathway induces preadipocyte proliferation and in induces early adipogenesis (Laviola *et al.*, 2006; Gehart *et al.*, 2010).

Glucose is transported into the adipocyte via the glucose transporter 4 (GLUT4). Under basal conditions, GLUT4 is slowly recycled between the plasma membrane (PM) and endosomes through a cycle of endo- and exocytosis (Dugani *et al.*, 2005). Within minutes of insulin binding to its receptor in the adipocyte plasma membrane, GLUT4 is translocated from cytoplasmic GLUT4 storage vesicles (GSVs) to the PM. This increases the number of GLUT4 transporters in the PM and therefore glucose uptake (Tokarz *et al.*, 2018). The mechanism of GLUT4 translocation and interplay of different proteins and can be visualised in Figure 1.9.

Once insulin binds to the insulin receptor, the latter is activated by auto-phosphorylation, triggering a cascade of phosphorylation events mediated by insulin receptor substrate 1 (IRS1) (Riehle *et al.*, 2016; Jaldin-Fincati *et al.*, 2017;

Tokarz *et al.*, 2018). IRS-1 promotes the conversion of phosphatidylinositol 3,4, bisphosphate (PIP2) into phosphatidylinositol (3,4,5)-triphosphate (PIP3) by the action of phosphatidylinositol-3-kinase (PI3K). PIP3 activates AKT Serine/Threonine Kinase 2 (Akt2) by the action of phosphatidylinositol-dependent protein kinase 1 (PDK1) and mTOR2. mTOR promotes protein synthesis, mRNA translation, blocks autophagy and induces cell growth (Riehle *et al.*, 2016). Akt then phosphorylates the Rab GTPase-activating proteins (GAPs) AS160 (Akt substrate of 160 kDa)/TBC1D4 (TBC1 Domain Family Member 4) and TBC1D1 (TBC1 Domain Family Member 1), blocking their inhibitory effect on Rab GTPases (Rab10 is the main Rab GTPase for GLUT4 translocation in adipocytes). Activated Rab10 binds to its effector Sec16A mobilising the GLUT4-containing vesicles to the PM. When the vesicles reach the PM, Rab10 binds to RalA, Myo1c and Exocyst components (Exoc6) needed for GLUT4 to be embedded in the PM (Riehle *et al.*, 2016; Jaldin-Fincati *et al.*, 2017; Tokarz *et al.*, 2018).

Insulin also induces actin remodelling by activation of small Rho GTPase Rac1; actin cytoskeleton remodelling is a key process for GLUT4-containing vesicle fusion to the PM (Tokarz *et al.*, 2018). GLUT4 vesicle fusion to the PM requires the action of proteins VAMP2, Syntaxin4 and SNAP23, forming what is known as a SNARE complex, which interacts with the protein Munc18c for effective fusion of GSVs to the PM (Jaldin-Fincati *et al.*, 2017; Tokarz *et al.*, 2018).

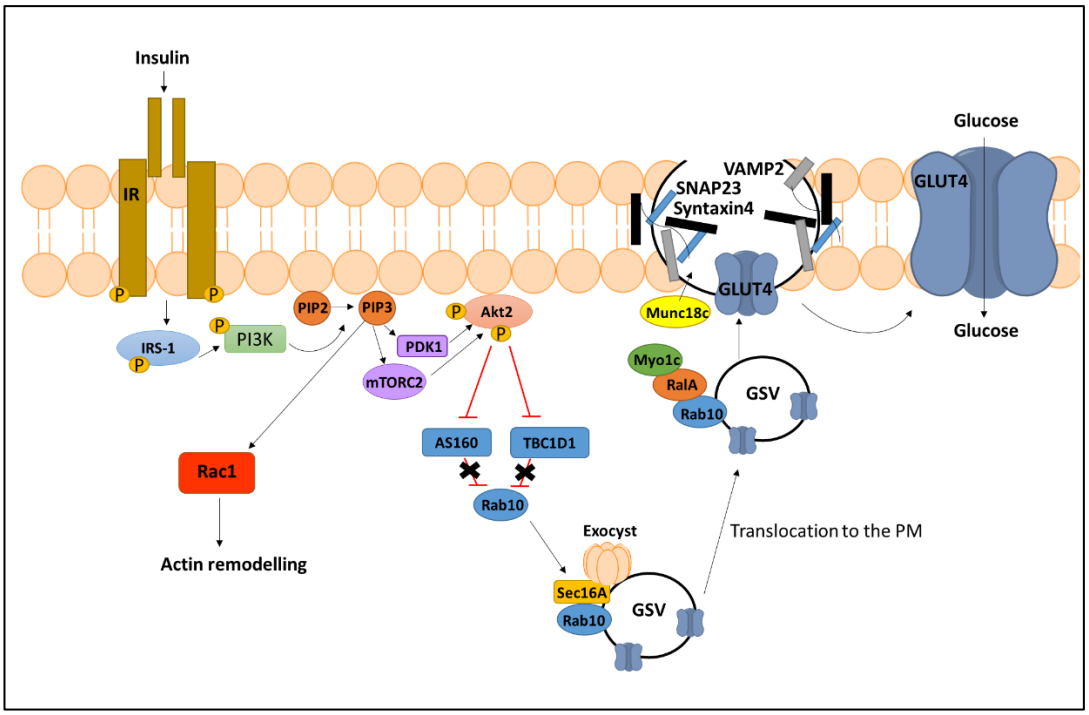

Figure 1.9: GLUT4 translocation process to the PM of adipocytes. Under basal conditions, GLUT4 is recycled through endocytosis and exocytosis from the PM to early endosomes, and from there to recycling endosomes back to the PM. When insulin binds to the insulin receptor, it triggers a cascade of phosphorylation events that lead to increased GLUT4 translocation to the PM. IRS-1 activates PI3K, which in turn leads to phosphorylation of Akt2. Phosphorylation and activation of Akt phophorylates AS160 and TBC1D1, which activates Rab10. Rab10 binds to its effector, Sec16A, and promotes vesicle trafficking. Once the GSVs reach the PM, Rab10 binds to RalA, the exocyst components and Myo1c, which facilitate the fusion of GSVs to the PM. Proteins participating in the insertion of GLUT4 into the PM are VAMP2, SNAP23, Syntaxin4 (SNARE complex), and Munc18c. Simultaneously to Akt phosphorylation, PI3K activates Rac1, which triggers actin remodelling, which is a key process for the fusion of GSVs to the PM. Adapted from Laviola *et al.*, (2006), Riehle and Abel, (2016), Jaldin-Fincati *et al.*, (2017), and Tokarz, MacDonald and Klip, (2018). IR: insulin receptor; GLUT4: glucose transporter 4; IRS-1: insulin receptor substrate 1; PI3K: phosphatidylinositol-3-kinase; PIP2: phosphatidylinositol 3,4, bisphosphate;PIP3: phosphatidylinositol (3,4,5)-triphosphate; PDK1: phosphatidylinositol-dependent protein kinase 1; mTORC2: mTOR Complex 2; Akt2: AKT Serine/Threonine Kinase 2; AS160:; TBC1D1: (TBC1 Domain Family Member 1); GSV: GLUT4 storage vesicles; RalA: RAS like proto-oncogene A; Myo1c: Myosin IC; SNAP23: Synaptosome associated protein 23; VAMP2: Vesicle associated membrane protein 2.

1.4.4. Adipokines

The adipose tissue is a secretory organ and acts in an autocrine or a paracrine manner to maintain metabolic homeostasis via the secretion of signalling molecules called adipokines, such as leptin and adiponectin; but it also secretes

cytokines such as TNF-α and interleukin 6 (IL-6), which have an action in other tissues and organs (Laviola *et al.*, 2006). Leptin and adiponectin are mainly secreted by adipocytes, whereas TNF-α and IL-6 are secreted by stromal vascular fraction (SVF) cells (Lehr *et al.*, 2012; Coelho *et al.*, 2013; Musi *et al.*, 2014).

Adipokines were first studied in 1994 when Dr Friedman´s group at the New York´s Rockefeller University discovered leptin (Zhang *et al.*, 1994). Alterations in adipokine secretion may lead to disruptions in metabolic homeostasis causing important complications, such as obesity-related conditions (Table 1.2). Regulation of beneficial adipokines such as adiponectin has been contemplated as a potential therapeutic practice for metabolic disease (Coelho *et al.*, 2013).

1.4.4.1. Leptin

Leptin, the product of the *ob* gene, is an adipokine mainly produced by the adipose tissue; it acts on the hypothalamus and regulates satiety, reducing appetite and promoting energy expenditure (Bi *et al.*, 2019). Leptin plasma levels depend on the amount of energy stored as fat, being higher in obese individuals and lower in lean individuals. Insulin regulates leptin levels and, during fasting, leptin plasma levels are low and increase after food consumption as a response to insulin (Rosen and Spiegelman, 2006; Coelho *et al.*, 2013).

Mice lacking the leptin encoding gene (*ob/ob*) presented with obesity, insulin resistance, impairment of glucose homeostasis and increased food intake (Genuth *et al.*, 1971). Leptin also plays a role in immunity and inflammation, acting as a pro-inflammatory cytokine (Liu *et al.*, 2018); hypertrophic adipocytes have been reported to secrete higher levels of leptin and less adiponectin. The higher levels of leptin observed in obesity states are likely to be a consequence of

leptin resistance, due to high concentrations of leptin in plasma not leading to a proper anorexic response by the brain (Liu *et al.*, 2018).

Leptin was also reported to improve glucose homeostasis in lipodystrophic mice and humans (Shimomura *et al.*, 1999; Oral *et al.*, 2002; Mantzoros, 2012), however the mechanisms behind the regulation of metabolic homeostasis by leptin are not fully understood (D'souza *et al.*, 2017). The therapeutic potential of leptin for the treatment of obesity has already been tested in the clinic, but the majority of patients developed a resistance to leptin (Luo *et al.*, 2016).

1.4.4.2. Adiponectin

Adiponectin is the adipokine most abundantly produced by the adipose tissue, and it exerts many metabolically beneficial effects (Coelho *et al.*, 2013). It enhances insulin sensitivity, regulates energy homeostasis, reduces inflammation and protects against atherosclerosis. Adiponectin acts as an insulin sensitiser and stimulates fatty acid oxidation and glucose uptake in the muscle, liver and adipose tissue via the AMP-activated protein kinase (AMPK) signalling pathway. But it exerts its insulin-sensitising effect role mainly in the liver, were it suppresses gluconeogenesis (Achari *et al.*, 2017). Decreased adiponectin levels have been associated with metabolic disease (Gimeno *et al.*, 2005; Lihn *et al.*, 2005; Mojiminiyi *et al.*, 2007). Adiponectin has been shown to promote adipogenesis of 3T3-L1 preadipocytes (Fu *et al.*, 2005).

Chronic overexpression of adiponectin increased subcutaneous fat accumulation but protected against insulin resistance in mice, and insulin-resistant rats showed a decreased expression of the adiponectin receptor (Bauer *et al.*, 2010; Achari *et al.*, 2017). Human visceral fat also presented low amounts of

adiponectin receptor, suggesting that disruption of adiponectin action is linked to a decreased response by the adiponectin receptor (Achari *et al.*, 2017).

1.4.4.3. Tumour necrosis factor alpha

TNF-α is a pro-inflammatory cytokine secreted mainly from macrophages from the SVF, but also produced by adipocytes in lesser amounts. In animal models, it has been shown to be upregulated in obesity states; this has been suggested to be caused by increased infiltration of macrophages in obese adipose tissue (Lehr *et al.*, 2012; Coelho *et al.*, 2013). TNF-α has been linked to obesity, diabetes and inflammation (Kershaw *et al.*, 2004; Coelho *et al.*, 2013). TNF-α promotes insulin resistance by decreasing the expression of proteins that are essential for insulin signalling and adipogenesis (such as PPARγ and C/EBPα), and it also enhances lipolysis (Guilherme *et al.*, 2008).

1.4.4.4. Interleukin-6

Almost 30% of all circulating IL-6 is produced by the adipose tissue, but the majority is produced by cells from the SVF (Musi *et al.*, 2014). IL-6 levels are higher in VAT than in SAT. IL-6 is a pro-inflammatory cytokine, and increased levels of this protein are associated with obesity, heart disease, impaired glucose tolerance, and T2DM (Kershaw *et al.*, 2004; Coelho *et al.*, 2013).

In adipocytes and hepatocytes, IL-6 interferes with the insulin signalling cascade by inhibition of the autophosphorylation capacity of the IR and impairment of phosphorylation of IRS-1. However, in skeletal muscle, it promotes glucose uptake and increases fatty acid oxidation. There is still controversy about the role of IL-6 in glucose homeostasis (Coelho *et al.*, 2013; Musi *et al.*, 2014).

In T2DM, increased levels of IL-6 in plasma have been associated with increased body weight and elevated FFAs concentrations, as well as with insulin resistance. Furthermore, IL-6 impairs adipogenesis and decreases adiponectin secretion (Kershaw *et al.*, 2004).

1.4.4.5. Resistin

Increased levels of resistin have been associated with obesity and insulin resistance in rodents (Steppan *et al.*, 2001). McTernan *et al.*, (2002) found higher mRNA expression levels of this pro-inflammatory adipokine in human abdominal adipose tissue compared to adipose tissue from the thigh. However, the production of resistin by human adipocytes is a lot lower than that of mice, being mainly produced by macrophages and monocytes in humans, and there is still controversy about the association between resistin and human obesity (Luo *et al.*, 2016).

Nevertheless, resistin has been recently proposed as a factor for prognosis in T2DM, and higher levels of this protein have been associated with reduced survival in diabetic patients (Kapłon-Cieślicka *et al.*, 2018).

1.4.4.6. Visfatin

Visfatin is mainly secreted by VAT, and in smaller amounts by SAT and macrophages, exerting different metabolic effects depending on the depot of production (Musi *et al.*, 2014). VAT-produced visfatin has been associated with insulin resistance, whereas visfatin produced by SAT has been linked to improved insulin sensitivity (Lee *et al.*, 2009). In VAT, it acts as a pro-inflammatory cytokine, stimulating the production of TNF-α and IL-6 (Lee *et al.*, 2009; Coelho *et al.*, 2013; Musi *et al.*, 2014).

Additional adipokines and their impact in metabolic toxicity are presented in Table 1.2.

Table 1.2: Adipokines and their associated metabolic conditions.

Adipokine	**Related condition**	**Reference**
Decreased levels of adiponectin	Insulin resistance, metabolic syndrome and atherosclerosis.	(Gimeno *et al.*, 2005; Lihn *et al.*, 2005; Mojiminiyi *et al.*, 2007)
Monocyte chemo attractive protein 1 (MCP-1)	Insulin resistance and type 2 diabetes (in humans) and atherosclerosis.	(Kershaw *et al.*, 2004; Lehr *et al.*, 2012; Lim *et al.*, 2014)
TNFα	Insulin resistance in obese mice (still controversial in obese humans).	(Hotamisligil, 1999; Guilherme *et al.*, 2008; Lehr *et al.*, 2012)
Increased resistin and decreased adiponectin levels	Cardiovascular disease	(Frankel *et al.*, 2009; Lehr *et al.*, 2012)
Plasminogen activator inhibitor-1 (PAI-1)	Fibrosis. Link between abdominal fat, insulin resistance and cardiovascular disease.	(Frankel *et al.*, 2009; Coelho *et al.*, 2013)
Angiotensinogen	Increased levels in obesity, may lead to hypertension.	(Kotsis *et al.*, 2010; Coelho *et al.*, 2013; Musi *et al.*, 2014)
Dipeptidyl peptidase 4 (DPP4)	Increased risk of metabolic syndrome.	(Lamers *et al.*, 2011)
Increased IL-6 levels	Obesity, insulin resistance, atherosclerosis, coronary artery disease and unstable angina.	(Kershaw *et al.*, 2004; Coelho *et al.*, 2013)
Retinol binding protein 4 (RBP4)	Insulin resistance. Increased plasma levels are a biomarker of metabolic syndrome, prediabetes and cardiovascular disease.	(Brockman *et al.*, 2012; Tabak *et al.*, 2017)
Adipsin	Increased levels ssociated with adiposity and higher BMI.	(Schrover *et al.*, 2018)

1.5. Effect of ART on adipose tissue and adipogenesis

Adipogenesis is strongly affected by the different classes of antiretroviral drugs, but ART also interferes in adipokine secretion, insulin signalling, mitochondrial function and apoptosis (Koethe, 2017).

Amongst antiretroviral drugs, the first-generation PIs such as lopinavir and nelfinavir particularly result in dysregulation of adipogenesis. First-generation PIs have been associated with visceral fat accumulation, dyslipidaemias, release of pro-inflammatory cytokines, and adipogenesis inhibition by downregulation of PPARγ (Minami *et al.*, 2011; Koethe, 2017). Lopinavir is known not only to heavily disrupt adipogenesis (Pacenti *et al.*, 2006; Minami *et al.*, 2011; Zha *et al.*, 2013; Pushpakom *et al.*, 2018), but also to tamper with insulin signalling and to interfere with GLUT4 translocation (Kitazawa *et al.*, 2014). Lopinavir toxicity on adipose tissue is discussed in more depth in chapter 4. The metabolic toxic effects observed with lopinavir are not seen with newer protease inhibitors such as atazanavir and darunavir (Jones *et al.*, 2008; Minami *et al.*, 2011).

The NNRTI Efavirenz strongly disrupts adipogenesis by down-regulation of key adipogenic factors such as PPARγ, SREBP-1 and C/EBPα, leptin, adiponectin and lipoprotein lipase; this was observed *in vitro* as a dose-dependent effect (Díaz-Delfín *et al.*, 2011). Efavirenz also enhanced the release of pro-inflammatory cytokines (IL-6, IL-8 and MCP-1) (Koethe, 2017).

Maraviroc, a CCR5 receptor antagonist and entry inhibitor, was found to exert beneficial metabolic effects in human adipocytes *in vitro*. It decreased the release of pro-inflammatory cytokines, and it did not alter adipogenesis or lipid

accumulation. It also did not interfere with PPARγ or SREBP-1 expression (Díaz-Delfín *et al.*, 2013).

Disruption of adipogenesis seems to vary between different integrase inhibitors; raltegravir did not alter adipogenesis *in vitro* and had no effect on adipokine or cytokine secretion either (Minami *et al.*, 2011; Pérez-Matute *et al.*, 2011); on the other hand, elvitegravir did impair adipogenesis and lipid accumulation *in vitro* in human Simpson-Golabi-Behmel syndrome (SGBS) preadipocytes showing a dose-dependent inhibitory effect (Moure *et al.*, 2016).

1.6. ART-induced Obesity and inflammation

Obesity is characterised by hyperplasia and hypertrophy of the adipose tissue, as well as chronic low-grade inflammation (Gimeno *et al.*, 2005; Coelho *et al.*, 2013). Obese adipose tissue is exposed to hypoxia, inflammation and endoplasmic reticulum stress. However, an acute local inflammation is necessary for correct expansion of adipose tissue and for the prevention of lipotoxicity; problems arise when the inflammation becomes chronic (Stern *et al.*, 2015). Hypertrophied adipocytes recruit macrophages into the adipose tissue via secretion of MCP-1; macrophages then secrete pro-inflammatory cytokines such as TNF-α and IL-6 (Figure 1.5).

The secretion of MCP-1 and TNFα during obesity-induced inflammatory states leads to an increased lipolysis rate and decreased synthesis of triglycerides, this causes an increase in the levels of FFA released into the circulation (Guilherme *et al.*, 2008). TNFα is a key trigger for low-grade inflammation in metabolic syndrome. TNFα enhances lipolysis via reduction of the antilipolytic action of insulin; it also increases the levels of cAMP (cyclic AMP) and reduces the

expression of perilipin, a lipid droplet protein that regulates lipolysis (Langin *et al.*, 2006).

Hypertrophied adipocytes secrete decreased levels of adiponectin and increased levels of leptin and resistin; together with increased release of FFAs, this decreases insulin sensitivity in skeletal muscle and the liver (through increased lipid deposition in liver and muscle and increased inflammation) (Mihai *et al.*, 2015). ART stimulates the secretion of pro-inflammatory cytokines, which increase the expression of the enzyme 11β-hydroxysteroid dehydrogenase type 1 (11β-HSD1); overexpression of this enzyme in adipose tissue leads to increased lipolysis and ectopic deposition of FFAs (Anuurad *et al.*, 2010).

Antiretroviral drugs affect the distribution and metabolic homeostasis of the adipose tissue; patients under ART experience body weight gain and abnormal distribution of fat depots known as lipodystrophy. Increases in BMI were apparent after 1-year treatment with integrase inhibitors raltegravir, dolutegravir, elvitegravir, the PI darunavir and the NNRTI rilpivirine (Taramasso *et al.*, 2017).

Lipodystrophy is characterised by lipoatrophy of the limbs, face, and buttocks, alone or in combination with lipohypertrophy of visceral, cervical and dorsocervical areas known as the "buffalo hump" (Koethe, 2017). Therapeutic regimes including NRTIs and PIs are highly associated with lipodystrophy (Anuurad *et al.*, 2010).

PIs exert different actions in lipid metabolism, which combined may account for the onset of lipodystrophy: inhibition of apolipoprotein B degradation, disruption of the insulin signalling pathway by inhibition of IRS-1 phosphorylation,

downregulation of PPARγ and disruption of adipogenesis, reduction of glucose uptake by blockage of GLUT4 translocation to the PM, and finally release of reactive oxygen species (ROS) (Anuurad *et al.*, 2010). However, a regression of lipodystrophy in HIV patients under atazanavir treatment has been reported, suggesting that it is mainly the first-generation PIs that are responsible for lipodystrophy (Haerter *et al.*, 2004). This may be explained by the minimal effects of atazanavir on adipogenesis and lipid homeostasis compared to lopinavir (Minami *et al.*, 2011).

1.7. ART-induced Dyslipidaemia

Dyslipidaemia is a metabolic disorder characterised by altered concentrations of lipids in the blood. It is usually associated with diabetes, lipodystrophy and insulin resistance, but it can also arise without these conditions (Oh *et al.*, 2007). In patients undergoing ART, the most common dyslipidaemias are hypertriglyceridaemia with reduced HDL-cholesterol concentrations, followed by increased total cholesterol and LDL-cholesterol levels (Calza *et al.*, 2016).

Hypertriglyceridaemia, increased total cholesterol, and reduced HDL-cholesterol have been reported after treatment with the NRTIs, particularly stavudine, and didanosine (Crane *et al.*, 2011; van Oosterhout *et al.*, 2012). Efavirenz is the NNRTI most associated with dyslipidaemia; patients treated with efavirenz showed hypertriglyceridaemia and increased total cholesterol (Young *et al.*, 2005). However, the incidence rate of dyslipidemia induced by NNRTIs was smaller than the one induced by ritonavir-boosted PIs (Sension *et al.*, 2015; Calza *et al.*, 2016).

Amongst PIs, the prevalence of dyslipidaemia is higher for tipranavir, indinavir, lopinavir and fosamprenavir (all of them boosted with ritonavir), compared to the intermediate prevalence showed by saquinavir/ritonavir, darunavir/ritonavir and the low effect on lipid metabolism showed by atazanavir (boosted and non-boosted with ritonavir) (van Wijk *et al.*, 2012; Calza *et al.*, 2016). One of the newer PIs: tipranavir has been reported to induce a marked increase in the levels of triglycerides; atazanavir on the other hand, showed a favourable effect on lipid metabolism (Oh *et al.*, 2007; Calza *et al.*, 2016).

Integrase inhibitors (raltegravir, elvitegravir and dolutegravir) and the CCR5 antagonist maraviroc have generally a low impact on lipid metabolism (Quercia *et al.*, 2015; Sension *et al.*, 2015).

The mechanism behind ART-induced dyslipidaemia is complex, multifactorial and still not fully elucidated, but there seems to be a strong link to lipodystrophy (van Wijk *et al.*, 2012). A proposed mechanism consists in the increase hepatic de novo lipogenesis by PIs; this is triggered by accumulation of SREBP-1 (a transcription factor involved in cholesterol synthesis) in the liver. PIs also stimulate hepatic synthesis of triglycerides. A second mechanism is the PI-induced suppression of Apolipoprotein B (ApoB) breakdown in the liver, causing an increased production of VLDL and increased amounts of circulating triglycerides. Increased levels of ApoB has been previously correlated with insulin resistance and metabolic syndrome (van Wijk *et al.*, 2012; Lim *et al.*, 2015; Calza *et al.*, 2016).

An additional mechanism is based on structural similarity of the catalytic region of HIV protease and proteins cytoplasmic retinoic acid-binding protein type 1

(CRABP-1) and low-density lipoprotein-receptor-related protein (LRP), both involved in lipid metabolism. CRABP-1 stimulates adipogenesis by converting retinoic acid into cis-9-retinic acid, which binds to the retinoic X receptor (RXR)-PPARγ dimer. If PIs bind to CRABP-1, the action of PPARγ may be inhibited and so would adipogenesis, leading to lipoatrophy, increased levels of circulating FFAs and hyperlipidaemia (van Wijk *et al.*, 2012).

Binding of PIs to LRP would block the hydrolysis of triglycerides into FFAs by lipoprotein lipase, leading to a decreased storage of FFAs by adipocytes and contributing to the development of lipodystrophy.

In PI-induced lipodystrophy, there is a decreased expression of LDL receptors, resulting in increased LDL plasma concentrations (Calza *et al.*, 2016). Mitochondrial damage exerted by some NRTIs (stavudine, zidovudine and didanosine) may also contribute to ART-induced dyslipidaemia and lipodystrophy (van Wijk *et al.*, 2012; Calza *et al.*, 2016).

Dyslipidaemia is associated with an increased risk of CVD; therefore, it is important to manage dyslipidaemia in patients under ART, as they are a population with high risk of CVD. Management of ART-dyslipidaemia involves changes in lifestyle and diet, but also switching to antiretroviral drugs with a better lipid metabolic profile and, if this is not effective, treatment with statins or fibrates is applied (Calza *et al.*, 2016).

1.8. ART-induced insulin resistance and diabetes

Insulin resistance is a major contributor to the onset of metabolic syndrome and it emerges at the initial stages of T2DM. It is characterised by excessive levels of

insulin required to maintain normoglycaemia, and a decreased insulin sensitivity in both skeletal muscle and adipose tissue (Guo, 2014).

Disruption of adipokine secretion by the adipose tissue plays a crucial role in the development of insulin resistance and the impairment of glucose metabolism (Coelho, Oliveira and Fernandes, 2013; Murri et al., 2014).

Insulin resistance in adipocytes is characterised by increased lipolysis and increased release of FFAs, leading to dyslipidaemia (Guilherme *et al.*, 2008). It has been established that the onset of systemic insulin resistance is associated with high levels of circulating fatty acids in the bloodstream (Nordstrom *et al.*, 2005; Guilherme *et al.*, 2008). Under healthy, insulin-sensitive conditions, fatty acids are turned into triglycerides and accumulated within lipid droplets in adipocytes; failure to accumulate triglycerides within adipocytes increases the release of FFAs into the blood stream, therefore disrupting insulin signalling leading to insulin resistance in skeletal muscle and in the liver (Figure 1.5)(Guilherme *et al.*, 2008).

Dysregulation of systemic adipokine secretion decreases insulin sensitivity and induces lipid deposition and inflammation in the liver and muscle. This triggers an increased gluconeogenesis and glycogenolysis by the liver, and decreased glucose uptake and decreased fatty acid oxidation by the muscle; all of these events lead to increased glycaemia and an exacerbation of insulin resistance (Figure 1.5) (Rosen and Spiegelman, 2006; Lee *et al.*, 2009; Coelho *et al.*, 2013; Klöting *et al.*, 2014). As the muscle and adipose tissue are less sensitive to the effects of insulin, the pancreas is forced to increase insulin production to keep

normoglycaemia and, overtime this leads to β-cell dysfunction and the onset of T2DM (Wilcox, 2005).

Insulin resistance was one of the first reported metabolic adverse drug reactions of chronic HIV ART. The incidence of insulin resistance varies between different antiretroviral drugs, and differences exist even within classes (Feeney *et al.*, 2011).

HIV antiretroviral drugs cause insulin resistance via two mechanisms: some directly affect the insulin signalling pathway causing an acute decrease in insulin sensitivity; others tamper with mitochondrial function of the adipose tissue or skeletal muscle (Feeney *et al.*, 2011).

First-generation PIs are strongly associated with insulin resistance, and the mechanism behind this is thought to be the reduction of glucose uptake via inhibition of GLUT4 translocation (Feeney *et al.*, 2011; Giralt *et al.*, 2011). Lopinavir/ritonavir combination has been shown to reduce insulin sensitivity by 25% (measured by euglycemic clamps) after 10-day exposure in healthy individuals (Noor *et al.*, 2006). On the other hand, atazanavir and darunavir have been reported to have a minimal impact in insulin signalling (Noor *et al.*, 2006; Araujo *et al.*, 2014).

NNRTIs have only been associated with small changes in insulin sensitivity, with efavirenz being deleterious and nevirapine beneficial for insulin sensitivity; however, these effects on insulin sensitivity were too small to be considered of clinical significance (Feeney *et al.*, 2011).

Switching treatment to an alternative antiretroviral less likely to cause insulin resistance (e.g. from lopinavir to atazanavir) seems to be the most applied

strategy to prevent the development of insulin resistance; but management of this condition in HIV-infected patients under ART also comprises exercise and pharmacotherapy with metformin and thiazolidinediones (Feeney *et al.*, 2011).

1.9. ART-induced cardiovascular disease

As previously discussed, ART strongly increases the risk of CVD in HIV patients (Barbaro *et al.*, 2006; Wand *et al.*, 2007; Hemkens *et al.*, 2014). HIV infection itself increases the risk of CVD caused by low-grade inflammation and endothelial dysfunction, but this risk is lower in ART-naïve HIV positive patients compared to those receiving ART (Triant, 2013; Laurence *et al.*, 2018).

It is important to remark that the risk of ART-induced CVD increases with chronic exposure to ART and age. The conflicting data regarding ART-induced CVD may be explained by the cohorts of the studies which found no association between ART and increased risk of CVD including only young subjects (Kaplan-Lewis *et al.*, 2016).

First-generation PIs such as ritonavir, lopinavir and indinavir, and the NRTIs abacavir and didanosine have been particularly associated with high risk of myocardial infarction (MI) (Barbaro *et al.*, 2006; van Wijk *et al.*, 2012; Bavinger *et al.*, 2013; Hemkens *et al.*, 2014; Laurence *et al.*, 2018). Newer PIs like atazanavir presented a reduced risk for MI compared to other PIs (lopinavir and darunavir mainly) and NNRTIs (efavirenz mainly) (Kaplan-Lewis *et al.*, 2016; LaFleur *et al.*, 2017). Despite the use of NNRTIs being preferred to first-generation PIs, there is also a pro-atherogenic effect regarding this drug class, particularly under efavirenz treatment (Gleason *et al.*, 2016; Kaplan-Lewis *et al.*, 2016).

Regarding integrase inhibitors and fusion inhibitors, there is not a lot of data to reach a definite conclusion; generally, integrase inhibitors and fusion inhibitors (enfuviritide and maraviroc) are regarded as lipid neutral and not associated with CVD (with the exception of elvitegravir, which causes lipid metabolism disruption similar to that of efavirenz) (Kaplan-Lewis *et al.*, 2016).

A recent study has proposed an additional mechanism behind ART-induced CVD involving platelet activation and generation of ROS leading to induction of fibrosis, and inhibition of extracellular matrix (ECM) autophagy and macrophage polarisation, which increases inflammation (Laurence *et al.*, 2018). Hypercholesterolemia and hypertriglycerideamia increase platelet activation and, in their systematic review, Laurence, *et al.* (2018) found that first-generation PIs (ritonavir, lopinavir and darunavir) induced platelet activation, blocked ECM autophagy and increased the production of ROS. Atazanavir also induced platelet activation, but it induced ECM autophagy and it did not increase ROS production.

Raltegravir, an integrase inhibitor which has not been associated to CVD, was used as a comparator and it did not have any effects on platelet activation or ROS production (Laurence *et al.*, 2018).

The role of adipokines in the development of CVD has also been thoroughly studied (Lehr *et al.*, 2012; Leal *et al.*, 2013; Fisman *et al.*, 2014). ART has been associated with reduced levels of adiponectin in the circulation thereby reducing its cardioprotective action (Lehr *et al.*, 2012). Contrary, increased levels of resistin have been found in patients undergoing ART, and this is thought to be a consequence of low-grade inflammation, as this adipokine is mostly secreted by macrophages rather than by adipocytes. Additionally, after ART initiation, increased circulating levels of visfatin were reported, and this was consistent with patients with coronary disease (Palios *et al.*, 2012).

Changes in the diet and lifestyle, treatment with statins and fibrates, and ART switch to drugs associated with lower risk of CVD when possible, are the current strategies for the management of ART-induced CVD (Maggi *et al.*, 2017).

1.10. Adipocyte proteomics and relevance to metabolic disease

The term "proteomics" was first defined in 1995 as the "large-scale characterization of the entire protein complement of a cell line, tissue, or organism" (Wilkins *et al.*, 1996; Graves *et al.*, 2002, p.40).

An important quality of the proteome is that it is dynamic; this means that the proteome of a cell or organism changes depending on internal and external influences, and it may undergo changes in synthesis, degradation, post-translational modifications and translocation. Consequently, any given genome

has the potential to encode for an infinite number of proteomes (Graves *et al.*, 2002).

Significant advances in the methodologies for the isolation, detection and characterisation of proteins on a global scale have made it possible to interrogate the proteome of an organism or tissue, or even subcellular organelles, in pursuit for association with disease mechanisms. Indeed, mass spectrometry-based proteomic methodologies have allowed for thorough investigation of the mechanisms behind metabolic disease in the past few years, and it has led to the detection of a considerable amount of protein biomarkers for metabolic disease in the adipocyte (Renes *et al.*, 2013; Kim *et al.*, 2015).

1.11. Mass spectrometry

Mass spectrometry is a highly sensitive analytical technique by which the sample of interest is ionized, and the generated gaseous ions are then separated based on their mass-to-charge (*m/z*) ratio. It consists of an ionization source, a mass analyser (two in tandem MS), a detector, and a computer for data analysis (Figure 1.10) (Aebersold *et al.*, 2003; Lane, 2005).

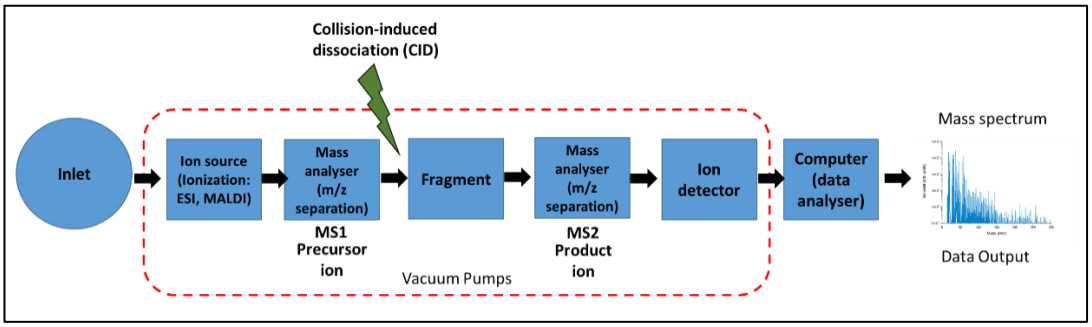

Figure 1.10: Components of tandem mass spectrometry. Adapted from: Aebersold and Mann, (2003); Lane, (2005).

For mass spectrometry analysis, the sample is reduced, alkylated and subjected to proteolytic digestion into peptides (usually by trypsin), and then injected into

the mass spectrometer by the inlet from atmospheric pressure into a vacuum. Then, the ionization source turns the analytes into gaseous ions. Matrix-assisted Laser Desorption/Ionization (MALDI), together with Electrospray Ionisation (ESI) are the two most commonly applied ionization methods for mass spectrometry (Karas *et al.*, 1990). ESI ionizes the analytes from a liquid sample, whereas MALDI uses a laser to ionize samples that are in the shape of a crystalline matrix. ESI is used for mass spectrometry coupled with liquid chromatography (LC) (ESI-LC-MS) and is used for the analysis of complex samples, whereas MALDI-MS is used to analyse large, non-volatile biopolymers (Aebersold *et al.*, 2003; Lane, 2005).

There are four kinds of mass analysers: quadrupole, ion trap, time of flight and Fourier transform ion cyclotron (FT-MS) analysers (Lane, 2005). They can be used individually or in combination as a tandem. The mass analyser separates the analyte ions based on their *m/z* ratio (MS1) and, in tandem mass analysers, the precursor ions get fragmented into product ions in a collision cell and separated based on their *m/z* ratio by a second mass analyser (MS2); this offers higher sensitivity than LC-MS. The detector registers the number of ions and their *m/z* values (Aebersold *et al.*, 2003; Savaryn *et al.*, 2016).

Software is used to analyse the resulting mass spectra and match the spectrum to a peptide using a reference dataset, this is known as the peptide-spectrum match (PSM). However, this matching could be false, and the False Discovery Rate (FDR) is applied to avoid false positives. FDR is the proportion of false positives out of the total amount of identified matches. FDR is applied both for matching spectra

to peptides and peptides to proteins, making identifications more stringent (Aggarwal *et al.*, 2016).

Tandem mass spectrometry provides with a sequence of peptide fragments from each precursor peptide (MS2). For protein identification, this sequence is matched to a specific protein by a software against a protein reference sequence database (Aebersold *et al.*, 2003; Aggarwal *et al.*, 2016).

The mass spectrometer used in this thesis was a TripleTOF™ 6600 (ABSCIEX, Warrington, UK), and included a capillary nano-HPLC trap column, (ekspert™ nanoLC 415, SCIEX, Warrington, UK), the use of ESI and a hybrid quadrupole time-of-flight mass analyser (QTOF).

1.12. Proteomic differences between VAT and SAT

The association of VAT (particularly omental adipose tissue) to metabolic disease is greater than that of SAT (Bjørndal *et al.*, 2011; Murri *et al.*, 2014). A number of studies have addressed the proteomic differences between these two types of adipose tissue (Perez-Perez *et al.*, 2009; Peinado *et al.*, 2010; Insenser *et al.*, 2012; Lingling Fang *et al.*, 2015). Perez-Perez *et al.*, (2009) addressed the proteomic differences between human subcutaneous and omental adipose tissue extracted from obese individuals. They found differences in the expression of proteins involved in inflammation, stress and glucose and lipid metabolism. An example was the detection of epithelial cytokeratins (CK-7, CK-8, CK-18 and CK-19) exclusively in omental adipose tissue , as well as overexpression of inflammatory proteins such as complement component C4-A, fibrinogen and ceruloplasmin. They also found an increased abundance of metabolic enzymes (GAPDH, ALDH1, DHL) in omental adipose tissue , as well as upregulation of heat shock proteins

(HSP90, HSP70 and HSP27), and FABP5 (Perez-Perez *et al.*, 2009). HSP70 and FABP5 have been previously associated with obesity and type 2 diabetes (Cangeri Di Naso *et al.*, 2015; Xie *et al.*, 2016).

1.12.1. Proteomics of murine adipocytes

One of the problems of studying human adipocytes is the inherent variability of the samples collected from individuals who have very different lifestyles and genetic backgrounds; especially regarding the pathogenesis of the adipose tissue. The use of animal models helps reducing this genetic variability, as they are breed in the same conditions (Kim *et al.*, 2015).

Proteomics has been used by several researchers to characterise the function of proteins in murine adipocytes and link to the disease phenotype. Peinado *et al.*, (2011) used the *Zmpste24*$^{-/-}$ mice as a model of lipodystrophy. This model is deficient in the proteins Zmpste24 (a metalloproteinase) and lamin A (a nuclear envelope protein); mutations in the genes encoding for these proteins have been linked to increased aging and lipodystrophy. They studied the proteome of WAT as well as the metabolome in serum of this murine model. They found a downregulation of vimentin and they also identified a novel protein: High-Mobility Group Box-1 protein, which is dysregulated in lipodystrophy. In addition, they observed *Zmpste24*$^{-/-}$ adipocytes were smaller than wild type murine adipocytes; this confirmed a reduced fat accumulation capacity and a lipodystrophic phenotype of *Zmpste24*$^{-/-}$ adipocytes (Peinado *et al.*, 2011).

In vivo mouse models were used to investigate the role of the protein STRA6 (stimulated by retinoic acid 6) in obesity and insulin resistance (Zemany *et al.*, 2014). STRA6 is a receptor for RBP4, and elevated levels of RBP4 have been

associated to insulin resistance. Adipose-STRA6 knockout mice (Adipose-Stra6$^{-/-}$) were generated and fed with normal (chow) or high-fat diet. Adipose-Stra6$^{-/-}$ mice fed with chow diet presented decreased body weight and reduced fat mass and the levels of insulin and leptin were also decreased; whereas Adipose-Stra6$^{-/-}$ mice fed with high-fat diet showed a mild improvement on insulin sensitivity but unchanged body weight. This study concluded that reduced STRA6 expression by adipocytes reduced body weight and improved insulin sensitivity (Zemany *et al.*, 2014).

Adipogenesis disruption may lead to metabolic toxicity (Sarjeant *et al.*, 2012; Gustafson *et al.*, 2013, 2015). Therefore, the application of proteomics to the discovery of new proteins interfering with adipogenesis is key to understand the mechanisms behind metabolic toxicity.

The use of cell lines for adipocyte and adipogenesis research poses advantages and disadvantages. The advantages are that a cell line provides with a homogenous population of cells at the same stage of differentiation, and a stable source of cells by passage; the disadvantages are that the molecular changes observed in cell lines may not correlate to human cells. Furthermore, the adipogenic capacity of a preadipocyte cell line diminishes as the passage number increases (Ali *et al.*, 2013).

There are three types of cellular models used to investigate adipocytes and adipogenesis *in vitro*. The first type includes pluripotent fibroblasts, which are able to differentiate not only into adipocytes, but into a variety of cells such as chondrocytes or myocytes; this includes cell lines such as BALB/c-3T3, RCJ3.1, 10T1/2 and CHEF/18 (Sarjeant *et al.*, 2012). The second type are cell lines in

which fibroblast-like cells, also known as preadipocytes, differentiate only into adipocytes (committed differentiation). The cell lines committed to differentiate into adipocytes are: 3T3-L1, 3T3-F442A, 1246, TA1, 30A5 and Ob1771 (Rosen, Eguchi and Xu, 2009; Sarjeant and Stephens, 2012). The third cellular model includes primary adipocytes isolated and cultured from murine or human adipose tissue biopsies (Rosen and MacDougald, 2006; Carswell *et al.*, 2012).

The murine immortalised cell lines 3T3-L1 and 3T3-F442A are fibroblast-like cells, also known as preadipocytes, which differentiate only into adipocytes. 3T3-L1 and 3T3-F442A are the most frequently used murine cell lines for the study of adipogenesis and they are extensively characterised (Sarjeant *et al.*, 2012; Ali *et al.*, 2013; Ruiz-Ojeda *et al.*, 2016). They are both derived from 17- to 19-day-old NIH Swiss 3T3 mouse embryos and they both produce mature adipocytes that are morphologically and biochemically similar to adipocytes from fat tissue (Sarjeant *et al.*, 2012). Differently to 3T3-L1, 3T3-F442A preadipocytes are relatively easier to culture and to handle because they do not need a glucocorticoid-supplemented differentiation cocktail to differentiate. Furthermore, the 3T3-F442A cell line was reported to exhibit a higher commitment to differentiation and higher lipid droplet accumulation than 3T3-L1 when implanted into athymic mice to produce ectopic fat. In addition, the ectopic fat generated by implantation of 3T3-F442A preadipocytes was more biochemically and histologically similar to adipose tissue *in situ,* than the ectopic fat generated from 3T3-L1 preadipocytes (Rosen and MacDougald, 2006; Sarjeant *et al.*, 2012; Ruiz-Ojeda *et al.*, 2016). For the above-mentioned reasons, the murine immortalised cell line 3T3-F44A2 was used in this thesis.

Back in 1979, the protein changes during adipogenesis of the murine immortalised cell line 3T3-L1 were studied for the first time by using 2-DE (Sidhu, 1979). This study identified actin as one of the proteins showing altered biosynthesis during adipogenesis (Sidhu, 1979; Renes *et al.*, 2013). Decreased actin expression contributes to cytoskeletal remodelling, which is a key step for adipogenesis (Renes *et al.*, 2013). To date, there are a vast amount of publications using the 3T3-L1 and 3T3-F442A cell lines for the study of adipogenesis (Choi *et al.*, 2004; Welsh *et al.*, 2004; Perez-Diaz *et al.*, 2014; Peláez-García *et al.*, 2015; Ojima *et al.*, 2016).

1.12.2. Proteomics of human adipocytes

The first proteome map for human adipose tissue was achieved in 1999, using adipose tissue extracted from morbidly obese women who suffered from polycystic ovary syndrome (Solomon, 1999). A more recent study also used VAT extracted from morbidly obese polycystic ovary syndrome patients, and analysed it using 2-DE and mass spectrometry (Corton *et al.*, 2008). They identified an increased expression of glutathione S-transferase M3 (GSTM3) and Annexin V both in response to inflammation, as well as increased production of ROS characteristic of obesity (Corton *et al.*, 2008).

Label-free proteomics was applied to the investigation of differences in the proteome of SAT of lean, overweight, and morbidly obese patients (Benabdelkamel *et al.*, 2015). The differentially regulated proteins detected in this study were involved in lipid and glucose metabolism, cytoskeleton remodelling, energy homeostasis and redox balance. Pathway analysis of the differentially expressed proteins revealed differences between the overweight

SAT and morbidly obese SAT proteomes. Cell-to-cell signalling and interaction pathways were overrepresented in overweight SAT; whereas lipid metabolism, small molecule biochemistry and cancer pathways were overrepresented in morbidly obese SAT. Differential protein expression was confirmed by immunoblotting, which showed downregulation of AFABP (Adipocyte Fatty Acid Binding Protein), FAA (fumaryl aceto acetase) and GPD1 (glycerol 3 phosphate dehydrogenase), and up-regulation of CRYAB (alpha crystallin B) and CES1 (liver carboxylesterase 1) in morbidly obese SAT compared to lean SAT (Benabdelkamel *et al.*, 2015).

CRYAB was previously found to be upregulated during adipogenesis in a proteomic study of human adipose-derived stem cells; the results of this study coincided in the finding of differentially regulated proteins involved in cytoskeleton remodelling and redox homeostasis (DeLany *et al.*, 2005). Interestingly, the differentially expressed proteins identified in a proteomic study comparing VAT of healthy and unhealthy obese patients, were also proteins involved in lipid metabolism and cytoskeleton structure maintenance; this may suggest that these two processes are altered during obesity independently of the type of adipose tissue (VAT or SAT) (Alfadda *et al.*, 2017).

1.12.3. Adipokine proteomics

Proteomics has helped to identify more than 600 different adipokines in both human and murine adipocytes, as well as to observe differences in adipokine secretion between humans and mice (Lehr *et al.*, 2012; Renes *et al.*, 2013). Some examples are the adipokine adipsin, which expression was found increased in obese humans but decreased in obese mice; and TNFα, which follows endocrine

secretion in mice and is released to the blood stream whereas in humans, it acts as a paracrine adipokine acting locally in the adipose tissue (Arner, 2005; Renes *et al.*, 2013).

Recently, novel adipokines involved in obesity were identified in a proteomic study on 3T3-L1 adipocytes (Laria *et al.*, 2018). During obesity, hypertrophied adipocytes are subjected to hypoxia, therefore 3T3-L1 adipocytes were cultured in hypoxic conditions for 24 hours and were then analysed via LC-MS/MS. Amongst the differentially regulated proteins, some proteins were downregulated upon hypoxia, including adiponectin, matrix metalloproteinase-11 and thrombospondin-1 and -2; differential regulation of these four protein targets upon hypoxia compared to normoxia was confirmed by western blotting (Laria *et al.*, 2018).

Adipokinome changes during adipogenesis have been the focus of proteomic studies due to the relevance of this process to metabolic homeostasis. In a study by Ojima *et al.*, (2016), 3T3-L1 adipocytes were differentiated for 10 days and analysed by iTRAQ (isobaric tags for relative and absolute quantitation) labelling and LC-MS/MS; this study identified different types of collagen at different stages of differentiation; and varying levels of adipokines (adiponectin, retinoic acid receptor responder 2 (Rarres2) and adipsin depending on the stage of differentiation (Ojima *et al.*, 2016).

1.13. The importance of plasma membrane in drug transport and metabolic disease

The PM is a semipermeable phospholipid bilayer that separates the cell from the extracellular environment, and acts as a filter for exchange of micronutrients and

cell signals between the extracellular and the intracellular compartments (Savas *et al.*, 2011).

Proteins are an important component of the PM and they can be integral, peripheral or lipid-anchored. Integral membrane proteins are embedded within the phospholipid bilayer; peripheral membrane proteins are associated to the lipid bilayer by non-covalent bonds (hydrophobic/ionic interactions), and lipid-anchored membrane proteins are attached by covalent bonds to either the internal or the external side of the membrane (Cordwell *et al.*, 2010; Savas *et al.*, 2011; Lai, 2013).

PM proteins are involved in trafficking, transport, signalling and disease; they are also the target for a vast number of drugs and therefore they are the focus of extensive research for the discovery of potential therapeutic targets (Cordwell *et al.*, 2010; Prior *et al.*, 2011; Lai, 2013; Hörmann *et al.*, 2016).

Approximately 70% of drug targets are proteins located in the PM, these include receptors, adhesion molecules and transporters (Zhao *et al.*, 2004). Transporters can be carriers, channels, or voltage/ligand-gated ion channels; there are two superfamilies of carriers: the ATP-bindings cassette (ABC) and solute carriers (SLC) (Tan *et al.*, 2008).

Drug transport of small hydrophobic molecules normally takes place via simple diffusion, but larger molecules require to be transported into the cell. Carriers are important for drug disposition, and polymorphisms in SLCs have been associated with different conditions (e.g. Alzheimer's disease) (Hediger *et al.*, 2013). ABC transporters, and more specifically P-glycoprotein (P-gp), are involved in drug resistance, as many drugs are substrates for P-gp. Drug disposition is influenced

by transporters and therefore is important for a successful therapy (Kulbacka *et al.*, 2017).

The contribution of the PM to metabolic syndrome has been recently highlighted, and several publications reported a link between PM and diet-induced insulin resistance and inflammation; these studies point towards a relationship between the PM lipid composition and the onset of insulin resistance in the liver and the adipose tissue (Wei *et al.*, 2016; Holmes, 2017; Perona, 2017). It has been suggested that changes in the phospholipid composition of the PM alter its fluidity and flexibility, and this disrupts the insulin signalling pathway. The presence of high amounts of saturated fatty acids in the PM have been shown to decrease its fluidity; reduce the number of IRs; decrease insulin affinity to its receptor; and impede GLUT4 insertion into the PM. However, polyunsaturated fatty acids increased the fluidity of the PM and improved insulin sensitivity (Perona, 2017).

More importantly, the PM comprises key proteins for adipocyte metabolic homeostasis, such as GLUT4 and IR, and any alterations in the function of these proteins may lead to changes in the insulin sensitivity (Fröjdö *et al.*, 2009; Riehle *et al.*, 2016). In fact, this is one of the mechanisms underlying the metabolic toxicity of first-generation PIs (Feeney *et al.*, 2011; Giralt *et al.*, 2011).

1.13.1. Challenges of the study of the PM proteome

The study of PM proteomics faces several difficulties due to the heterogeneity, poor solubility, complex post-translational modifications (PTMs) and relatively small abundance of PM proteins; the latter makes their detection challenging because they are usually masked by highly abundant proteins. Furthermore,

standard proteomic procedures like 2-DE gels are not suitable for the detection of integral membrane domains because of their poor water solubility (they tend to aggregate and precipitate in aqueous solutions) (Tan *et al.*, 2008; Cordwell *et al.*, 2010; Barrera *et al.*, 2011; Renes *et al.*, 2013).

1.14. Adipocyte plasma membrane proteomics

Due to the challenges of adipocyte PM proteomics, only a few studies have been conducted to date (Aboulaich *et al.*, 2004; Xie *et al.*, 2010; Prior *et al.*, 2011; Renes *et al.*, 2013). The first in-depth global proteomic analysis of the adipocyte was performed by Adachi *et al.*, (2007) using 3T3-L1 adipocytes; this study involved subfractionation of the different cellular components of the adipocyte (nuclei, mitochondria, membrane and cytosol) to analyse their proteome separately and reduce the complexity of the adipocyte proteome. They combined in-gel digestion of proteins followed by LC-MS/MS and bioinformatic analysis, and detected a total of 3,287 proteins, which were recorded in the Max-Planck Unified Proteome database. Proteins involved in insulin signalling and GLUT4 translocation (VAMP-8, syntaxin-12, Rab-10, -14 and -2) were identified (Adachi *et al.*, 2007). Nevertheless, this study did not differentiate between the PM proteome and other organelle membranes such as mitochondria and ER.

Xie *et al.*, (2010) applied SDS-PAGE and HPLC-ESI-MS/MS to SAT samples from healthy lean individuals, and identified a total of 1493 proteins; out of these, 202 (13.5%) were PM proteins. This highlighted the low amount of PM proteins compared to that of the whole cell. They detected 433 proteins which were not detected by Adachi *et al.*, (2007) in their murine adipocyte study; hence, these proteins may be exclusive of human adipocytes. They classified the adipocyte

proteome by molecular function, which included annotations such as lipid metabolism, transport, activation and oxidation of FFAs, synthesis of TAG and de-novo lipogenesis, adipocyte lipolysis and lipid droplet maintenance, all key for adipocyte metabolic homeostasis (Xie *et al.*, 2010).

It was not until recently that the first quantitative proteomic analysis of the adipocyte PM was published (Prior *et al.*, 2011); this was performed using 3T3-L1 adipocytes and combining the techniques of colloidal silica bead isolation, stable isotope labelling with amino acids in cell culture (SILAC), vesicle immunoadsorption and LC-MS/MS. Out of a total of 486 *bona fide* adipocyte PM proteins identified in this study, 52 were novel adipocyte PM proteins. An interesting observation from this study was the high concentration of hydrolases of unknown function; these hydrolases are thought to participate on the modulation of the ECM, which is characteristic of differentiation into mature adipocytes (Renes *et al.*, 2013). In addition, sodium/hydrogen exchanger (NHE6), a novel PM protein in 3T3-L1 adipocytes, was identified and found to be involved in insulin signalling. Moreover, this study revealed a functional association between the ER and the PM of the adipocyte, that may influence lipid metabolism (Prior *et al.*, 2011).

1.15. Aims of the thesis

Antiretroviral-induced metabolic toxicity increases the risk of CVD amongst HIV patients, resulting in a higher mortality rate compared to the general population (Barbaro *et al.*, 2006; Wand *et al.*, 2007; Hemkens *et al.*, 2014). Antiretroviral drugs, and PIs in particular, are known to cause metabolic disruptions in the adipose tissue, a key regulator of metabolic homeostasis (Minami *et al.*, 2011;

Koethe, 2017). The mechanisms behind antiretroviral-induced metabolic disease include alterations in adipogenesis and adipokine secretion, and development of insulin resistance, but they have not been completely elucidated.

Unveiling the molecular mechanisms underlying metabolic syndrome and its comorbidities has become the focus of extensive research in the field of proteomics.

Proteomics is a powerful tool to help revealing the molecular events that take place within the adipose tissue and identifying how these changes may lead to metabolic disease, as well as identifying potential therapeutic targets. Despite being challenging, PM proteomics has helped to identify the role of PM proteins in important events of adipocyte biology such as adipogenesis and insulin signalling (Prior *et al.*, 2011). However, a lot remains to be understood, and developments on proteomic techniques (e.g. enrichment and purification) may help identify new PM targets with therapeutic implications.

The specific aims of this project were:

1) To develop a methodology protocol for the enrichment and isolation of the adipocyte PM proteome using the murine immortalised cell line 3T3-F442A and validate this method.

2) To investigate the changes in the adipocyte PM proteome during adipogenesis and following acute insulin stimulation.

3) To investigate the changes in the adipocyte PM proteome following exposure to protease inhibitors.

4) To select PM proteins targets for validation and to characterise their potential role in drug-induced adipocyte toxicity.

CHAPTER 2
OPTIMISATION AND VALIDATION OF AN ISOLATION METHOD FOR ENRICHMENT OF PLASMA MEMBRANE PROTEINS IN ADIPOCYTES

2.1. INTRODUCTION

2.1.1. Plasma membrane proteomics

Due to the complexity and the dynamic nature of the proteome, proteomics cannot be studied by using only one specific technique, but a combination of mass spectrometry and protein separation techniques (Renes *et al.*, 2013).

Tandem mass spectrometry in the form of LC-MS/MS, a highly accurate and sensitive technique, is currently the preferred technique for proteomic analysis, and it is especially suitable for complex samples. Initially the protein samples are digested into peptides and injected into the mass spectrometer. The ion source, in this case ESI, will then form the ions that are first separated by the *m/z* ratio (MS1) and then fragmented (MS2) into product ions for detection against databases (Aebersold *et al.*, 2003; Lane, 2005).

In this way, mass spectrometry is a powerful technique for the study of PM proteomics with a single analysis able to identify thousands of proteins (Savas *et al.*, 2011). However, PM proteins are low in relative abundance and are often masked by highly abundant cytoplasmic proteins in mass spectrometry analyses (Renes *et al.*, 2013).

The underrepresentation of PM proteins in large-scale proteomic datasets makes it necessary to separate the proteins of interest from biological contaminants; effective sample preparation involving enrichment and purification of PM proteins prior to analysis is therefore essential to overcome the challenge in their detection (Tan *et al.*, 2008; Cordwell *et al.*, 2010; Barrera *et al.*, 2011; Savas *et al.*, 2011; Lai, 2013; Renes *et al.*, 2013). Enrichment of PM proteins has been demonstrated by different techniques such as centrifugation and

subfractionation (Adachi *et al.*, 2007; Lai, 2013), biotinylation (Zhao *et al.*, 2004; Hörmann *et al.*, 2016), aqueous/polymer two-phase partitioning (Cao *et al.*, 2006; Schindler *et al.*, 2006) and colloidal silica bead-isolation (Kim *et al.* 2011; Prior *et al.* 2011; Sharma *et al*. 2015).

Due to its high lipid content and complexity, sample preparation is a very important step for mass spectrometry analysis of adipose tissue. Fractionation and enrichment techniques are extremely useful to increase the detection of PM proteins and to facilitate mass spectrometry analysis (Savas *et al.*, 2011).

2.1.2. Colloidal Silica Bead Isolation

Colloidal silica bead isolation was selected as the enrichment technique in the current study because it had been previously applied to 3T3-L1 adipocytes for the study of the PM proteome (Prior *et al.*, 2011). However, it has not been yet applied for the 3T3-F442A adipocyte cell line, and this required optimisation, which was the objective of this chapter.

Colloidal silica bead isolation was first introduced in the 1980s by Chaney and Jacobson for the isolation of cellular plasma membranes (Chaney and Jacobson 1983; Kim et al. 2011). The principle of this method is that the monolayer of cells is exposed to a solution of colloidal silica beads which are positively charged and in turn bind to the negatively charged PM by electrostatic interactions. Polyacrylic acid (anionic polymer) cross-links the beads to the PM proteins and helps maintain their native conformation. Following cell lysis, the samples are subjected to ultracentrifugation through a Nycodenz density gradient to achieve further purification. The pellet containing the PM proteins attached to the beads is separated from the supernatant (which contains the cytoplasmic proteins), and

is then exposed to detergents to detach the beads from the PM proteins (Sharma et al. 2015; Kim et al. 2011).

It is important to highlight that generating a completely purified pure PM fraction is difficult as the membrane-enriched fraction almost always is contaminated with the highly abundant cytoplasmic proteins that cannot be completely removed (Lai, 2013). Furthermore, the PM is interconnected to other organelles such as mitochondria, cytoplasmic vesicles and endoplasmic reticulum (ER) (Prior *et al.*, 2011); this may explain the presence of proteins from other organelles in the PM. Nevertheless, enrichment techniques have proven to be extremely useful for the study of PM proteins, and to facilitate mass spectrometry analysis by reducing peptide complexity (Zhao *et al.*, 2004; Savas *et al.*, 2011).

2.1.3. Aims and objectives

The aims of this chapter were:

1) To optimise colloidal silica bead isolation of PM proteins for the 3T3-F442A preadipocyte cell line and analyse the PM-enriched fraction using LC-MS/MS.
2) To assess PM protein yield and confirm the efficiency of enrichment of PM proteins to facilitate the detection of the adipocyte PM proteome.

2.2. METHODS

2.2.1. Cell culture and differentiation

The immortalised murine 3T3-F442A preadipocytes (available in-house at the Wolfson Centre for Personalised medicine) were cultured in T75 vented cell culture flasks (Thermo Fisher Scientific, Runcorn, UK) in Dulbecco's Modified

Eagle's medium (DMEM) (Sigma-Aldrich, Dorset, UK), containing glucose with L-glutamine, sodium pyruvate and sodium bicarbonate supplemented with 10% Foetal Bovine Serum (FBS) (Thermo Fisher Scientific, Runcorn, UK) and incubated under standard conditions (5% CO_2 and 37°C atmosphere). Flasks are passaged every other day after reaching approximately 70% confluency. Confluency higher than 70% was avoided in order to prevent contact differentiation.

2.2.1.1. Adipocyte subculture

Once the cells reached 70% confluency, media was discarded and cells were washed with Hanks Balanced Salt Solution (HBSS) (Sigma-Aldrich, Dorset, UK) and detached using trypsin-edta solution 0.25% (Sigma-Aldrich, Dorset, UK). Cells were observed under the microscope to confirm detachment. Cell numbers and viability were determined using trypan blue stain in a Countess™ automated cell counter (Thermo Fisher Scientific, Runcorn, UK). A cell viability >90% was ensured. The obtained number of cells/ml was used to calculate the volume of the cell suspension to be added into a new flask or plates in order to seed the desired number of cells.

2.2.1.2. Plating of cells

Rat tail collagen (Thermo Fisher Scientific, Runcorn, UK) was diluted (1:30) in distilled water and each well of the 6-well plate (Greiner Bio-One, Gloucestershire, UK) was coated with the diluted collagen solution and incubated for 1 hour prior to the addition of cells. Wells were then washed with HBSS to wash off the excess of collagen. The cells were passaged and counted using a trypan blue cell viability method in the cell counter. Cells were seeded at a density

of 10,000-15,000 cells/well. The cells were kept in the incubator and the media was changed every 48 hours.

2.2.1.3. Adipocyte differentiation

A period of 48 hours after plating was allowed for preadipocytes to grow before triggering differentiation (day 0). Old media was removed and a 1/2000 dilution of insulin (stock 10 mg/mL insulin solution from bovine pancreas (Sigma-Aldrich, Dorset, UK)) in DMEM was mixed and filtered through a 0.22 μm syringe filter (Thermo Fisher Scientific, Runcorn, UK) and added to the cells to get a final insulin concentration of 5 μg/mL, except for the preadipocytes intended to be kept undifferentiated. Differentiation medium was changed every 48 hours and cells were differentiated for 10 to 12 days.

2.2.2. Characterisation of differentiation using Oil red O staining

Cells were washed with HBSS and fixed with 4% Formaldehyde in PBS (Santa Cruz Biotechnology, Texas, USA) for one hour inside a cell culture hood. Cells were washed again with HBSS. Then, a filtered Oil red O solution (2 parts of Oil red O stock in 3 parts of distilled water) was added to the cells. Plates were placed on a plate shaker for one hour. Excess of Oil red O dye was removed with water and cells were observed under the microscope. Images were taken under the microscope at x20 and x40 magnification. A 70% isopropyl alcohol (IPA)/water solution was added to the cells and plates were placed on the plate shaker for 45 minutes. The 70% IPA solution extracts the dye from lipid droplets. The IPA solution containing the dye was pippetted in triplicate into a 96-well plate. Lipid accumulation was quantified by reading the absorbance at 450 nm.

2.2.3. Colloidal silica bead isolation

Figure 2.6 shows the optimised colloidal silica bead isolation method for the 3T3-F442A cell line. On day 12 of differentiation, plates were placed on an ice bed and the cells were washed three times with cold MBS-buffered saline (20 mM 2-(N-morpholino)ethanesulfonic acid (MES) hydrate (Sigma Aldrich, Dorset, UK) + 135 mM NaCl, pH 6.0). After washing, the cells were exposed to 1% ice-cold silica beads solution (LUDOX® colloidal silica 30% suspension in water, Sigma Aldrich, Dorset, UK) in MBS and incubated for 10 minutes on ice. Cells were washed three times with MBS to remove unbound beads and then exposed to 0.1% Polyacrylic acid (pH 6.0) (Sigma Aldrich, Dorset, UK) solution in MBS for 10 minutes to block the free cationic groups on the silica beads. Cells were lysed by scraping into phosphate buffer (13.08 mM KH2PO4, 62.27 mM Na2HPO4, 500 mL ddH_2O, pH 7.4).

2.2.3.1. Optimisation of lysis method for sample preparation

In order to decide which method of sample preparation would yield the highest amount of total proteins and PM proteins, two methods were compared: lysis of the cells by scraping them out of the plate (no sonication), or harsher lysis by probe sonicator. These two methods were performed separately and compared. The final lysate was centrifuged at 10,000 rpm for 10 minutes at 4°C. The supernatant containing the cytosolic fraction was placed into a new eppendorf tube and the pellet containing the PM proteins bound to the silica beads was resuspended in phosphate buffer.

2.2.3.2. Optimisation of method of purification of the PM-enriched fraction

An additional stage in the original silica bead isolation protocol (Kim et al. 2011) was purification of the PM-enriched fraction by ultracentrifugation through a Nycodenz® density gradient, but this was found incompatible with the use of phosphate buffer, and a pellet containing the PM-enriched fraction could not be formed. This was therefore removed from the protocol and an alternative purification method was optimised.

A washing stage was added to the sample preparation protocol in order to remove as many cytosolic contaminants as possible from the cell pellet containing the PM-enriched fraction. The pellet was washed (resuspended and centrifuged) 3 times and finally resuspended in 500 µL of phosphate buffer. Samples were stored at -20°C until used.

2.2.4. Determination of protein concentration (Bradford Assay)

The total protein concentration of the silica-bead isolated samples was determined using a Bradford protein assay (Bradford, 1976). Bovine serum albumin (BSA) (Thermo Fisher Scientific, Runcorn, UK) was used as a protein standard. In a 96 well plate, 10 µL each of the standard and the sample were added in duplicate, followed by 10 µL of diluent (phosphate buffer). A 1:4 Bradford reagent (Bio Rad, Deeside, UK) dilution in phosphate buffer was prepared and 200 µL of this solution were added to each well. The plate was left to set for 2 minutes and absorbance was measured on a plate reader (DTX 880 Multimode Detector, Beckman Coulter, High Wycombe, UK) at a wavelength of 570 nm. Absorbance values were plotted against the standards concentrations and linear regression was applied to calculate the concentration of the samples.

2.2.5. Protein expression by Western blot

Proteins were separated upon molecular weight and according to their electrophoretic mobility by SDS-polyacrylamide gel electrophoresis (SDS-PAGE) depending on the gel pore size. Gels containing 4-12% polyacrylamide gradient were used for this thesis.

A total of 5% β-mercaptoethanol (Sigma-Aldrich, Dorset, UK) diluted 1:10 in NuPAGE® LDS Sample Buffer (Invitrogen, Runcorn, UK) containing lithium dodecyl sulfate (LDS) loading buffer was added to samples containing 20 µg of protein at a pH of 8.4 to denature the samples for gel electrophoresis. Samples were mixed and centrifuged at 1000 rpm for 30 seconds.

A total of 8 µL of the molecular weight marker (10–250 kD, Precision Plus Protein Kaleidoscope™ Prestained Protein Standards (BioRad, Deeside, UK) and 20 µg of protein per sample were loaded in each well of a NUPAGE 4-12% Bis-Tris GEL 1.5MM 15W (Life Technologies, Warrington, UK) in a gel tank (Invitrogen, Runcorn, UK) filled with running buffer (50 mM MOPS (NuPAGE® MOPS SDS Running Buffer (20X), ThermoFisher, Runcorn, UK), 50 mM Tris Base, 0.1% SDS, 1 mM EDTA, pH 7.7, ddH_2O to 1L). Samples were then subjected to electrophoresis for 1 hour using a voltage of 180V. After electrophoresis, the gel was placed into transfer buffer (100 mL of 10xTransfer buffer (192 mM glycine, 25 mM Tris base, 10% methanol, ddH_2O to 1L) and transferred onto a nitrocellulose membrane (Geneflow, Lichfield, UK). The transfer was run for 1 hour at 100V.

The membrane was then blocked with a milk-TBS-T solution (5% non-fat dried milk in TBS-T: 100 mL of 10xTBS (250 mM Tris-Base, 1500 mM NaCl, 20 mM KCl,

pH 7.4),1 mL of Tween 20, ddH_2O to 1L) on a rocker for 30 minutes at room temperature. After blocking, the membrane was incubated overnight at 4°C with the primary antibodies (Na^+/K^+-ATPase antibody (1:100 dilution, Developmental Studies Hybridoma Bank (DSHB), Iowa city, USA); Insulin Receptor antibody, (1:250 dilution, BD Biosciences (Oxford,UK)), GAPDH antibody, (1:5,000 dilution, Cell Signalling Technology (London,UK)) and β-actin antibody (1:1,000 dilution, Santa Cruz Biotechnology (Texas, US)).

Following incubation with the primary antibodies, the membrane was washed with TBS-T (3 washes of 10 minutes each) and then incubated with the secondary antibody labelled with horseradish peroxidase (anti-rabbit and anti-mouse; 1:5000 dilution; Jackson ImmunoResearch, Cambridgeshire, UK), for 2 hours on a rocker at 4^0C and then washed again with TBS-T (3 washes of 10 minutes each). Chemiluminescence was performed by incubating the membrane with Pierce™ ECL Western Blotting Substrate (ThermoFisher, Runcorn, UK) in a 1:1 solution for 4 minutes and placed into a ChemiDoc™ imaging system (Bio Rad, Deeside, UK) for imaging.

2.2.6. Colloidal Coomassie Blue staining of proteins

A total of 20 μg of protein lysate was loaded into each well and proteins were separated by molecular weight by SDS PAGE. Gels were then fixed in a solution of 7% glacial acetic acid in 40% (v/v) methanol in ddH_2O for 1 hour at room temperature on a rocker. After fixing, gels were incubated in a 4:1 solution of Coomassie Brilliant Blue stain (Sigma-Aldrich, Dorset, UK) in methanol on a rocker for 1 hour. Gels were washed with a destaining solution (10% acetic acid, 25% (v/v) methanol in ddH_2O) for 60 seconds on a rocker, and then rinsed in

25% methanol in ddH_2O and destained overnight at room temperature in 25% methanol in ddH_2O on a rocker. Gels were then visualised in a ChemiDoc™ imaging system.

2.2.7. LC-MS/MS

2.2.7.1. Sample preparation for LC-MS/MS

Samples containing 100 µg of protein were treated with a 10 mM solution of the reducing agent dithiothreitol (DTT) (Sigma-Aldrich, Dorset, UK) in LC-MS water (ThermoFisher, Runcorn, UK) for 15 minutes at room temperature. The samples were then alkylated with a 5.5 mM solution of iodoacetamide (Sigma-Aldrich, Dorset, UK) in LC-MS water and incubated in the dark for 15 minutes at room temperature. After this, the samples were treated with 1.54 µg of trypsin from a 0.8 µg/µLTrypsin Gold-Mass Spec Grade (Promega, Southampton, UK) solution in 15 mM ammonium bicarbonate (Sigma-Aldrich, Dorset, UK) and incubated overnight at 37°C. Trypsin is a proteolytic enzyme which cleaves proteins into peptides on the C-terminal side of arginine and lysine residues (except when there is a proline on the C-terminal side). The next day, the membrane samples containing silica beads were centrifuged in order to discard the silica beads and the supernatant was separated into a new eppendorf. The samples were stored at -20°C until use.

2.2.7.2. Ziptip purification

Ziptips are 10µL pipette tips with a bed of chromatography membrane and they are used for concentrating, desalting and purification of peptide and protein samples. An aliquot containing 1 µL of 1% trifluoroacetic acid (TFA) and 10µL of sample was prepared in high quality eppendorfs and vortexed. A total of 10µL of

100% Acetonitrile (ACT) was pipetted twice through the Ziptip® (Merk Millipore, Watford, UK) column priming the chromatography membrane to allow peptides from the sample to bind. The column was then washed three times with 10µL of 0.1% TFA. The sample (10µL) was then applied to the Ziptip column and passed 10-12 times; this allowed the analyte to be trapped inside the column. The column was then washed five times with 10µL of 0.1% TFA to remove the excess of sample. The sample was eluted into a new eppendorf tube using 10µL of 75% ACT. Purified samples were dried in a centrifugal eppendorf sample concentrator 5301 (Stevenage, UK) at 30 ºC for 15 minutes and stored at -4°C until LC-MS/MS analysis.

2.2.7.3. Mass spectrometry

The purified and dried samples containing the digested peptides were re-hydrated in 10 µL of 0.1% formic acid, vortexed and centrifuged for 30 seconds. Samples were diluted 1:10 in 0.1% formic acid and 3 µg of digested peptide mixture were loaded into the mass spectrometer.

Mass spectrometry was performed using reverse-phase LC-MS/MS. The samples were injected into a capillary nano-HPLC trap column and then passed through an analytical column (ekspert™ nanoLC 415, SCIEX, Warrington, UK). Analytes were ionised using electrospray ionisation (ESI) and sprayed into the mass spectrometer (TripleTOF™ 6600, ABSCIEX, Warrington, UK) using a 10 µm diameter needle. Analyte positively charged ions entered the mass spectrometer via voltage and vacuum gradient into a hybrid quadrupole time-of-flight mass analyser (QTOF). The resulting mass spectra was analysed using ProteinPilot™ software (SCIEX, Warrington, UK) and a FDR of 5% was applied for protein

identification. Figure 2.1 represents the complete process of sample preparation and analysis by mass spectrometry.

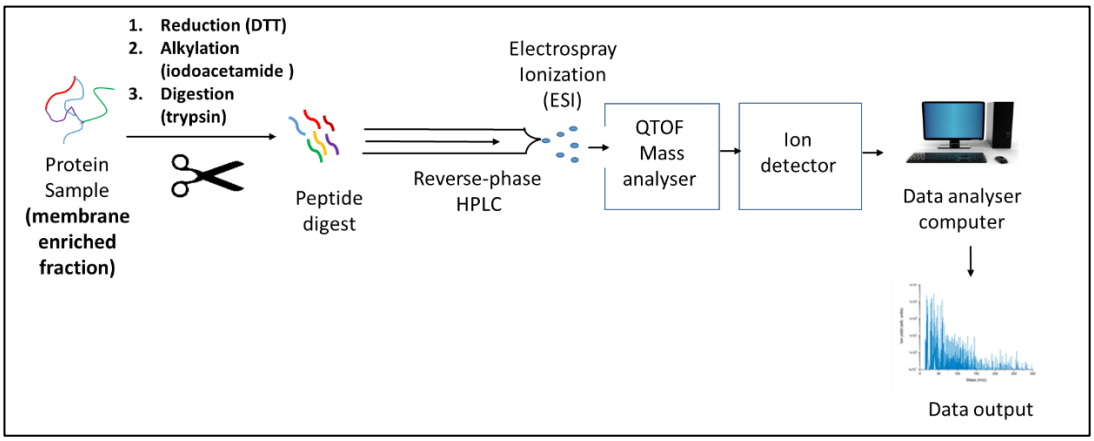

Figure 2.1: Sample preparation and LC-MS/MS analysis. Protein lysates were reduced via addition of DTT, alkylated using iodoacetamide and finally trypsinised into peptides. The silica beads were separated by centrifugation and the supernatant was purified using a Ziptip column and analysed by ESI-LC-MS/MS. ProteinPilot™ was used for protein identification using a 5%FDR.

2.2.8. Bioinformatic analysis

2.2.8.1. Gene Ontology Cellular Component protein classification

Proteins were classified under the Gene Ontology (GO) annotations obtained from the GO database (http://www.geneontology.org). Searches were made for the Cellular Component (CC) GO term "plasma membrane" but also for the annotations presented in Table 2.1 under which plasma membrane-associated proteins were classified. The subcellular location obtained from ProteinPilot (column K in both Appendix 2 and 4 of chapter 2) was not considered, and only GO CC terms were used to classify PM proteins. Venny 2.1 (Oliveros, 2015) was used to compare different protein lists and identify matches and differences.

The accession codes from Prior *et al.*, (2011) were International Protein Index (IPI) codes, which are no longer in use. To allow comparison to the current

study´sprotein list, IPI codes were converted to Uniprot accession codes using the DAVID gene ID conversion tool (https://david.ncifcrf.gov/conversion.jsp).

Table 2.1. Cellular Component GO annotations considered for the classification of proteins as plasma membrane-associated proteins.

Plasma membrane-associated proteins GO term: Cellular Component	Cell-cell adherens junction
	Focal adhesion
	Cell surface
	Cell projection
	Cell junction
	Membrane raft
	Plasma membrane raft
	Basolateral plasma membrane
	Extrinsic component of cytoplasmic side of membrane
	Extrinsic component of cytoplasmic side of plasma membrane
	Intercalated Disc
	T-Tubule
	Caveola
	Extrinsic component of the plasma membrane
	External side of the plasma membrane
	Apical plasma membrane
	Lateral plasma membrane
	Basal plasma membrane
	Cell-cell junction

2.2.9. Statistical analysis

For statistical analysis of absorbance values obtained from Oil red O staining, a 1-way ANOVA followed by Dunnett's correction for multiple testing was applied. All expriments were done in triplicate to ensure reproducibility (n=3). A p-value of <0.05 was considered significant.

2.3. RESULTS

2.3.1. Characterisation of adipocyte differentiation

Differentiation of adipocytes was confirmed using Oil Red O staining (Figure 2.2). Lipid droplets were stained in a red colour and were observed to increase in size

and number during adipogenesis. Measurement of absorbance of the extracted dye was proportional to the lipid droplet content of adipocytes and showed an increasing trend from day 3 to day 12 of adipogenesis.

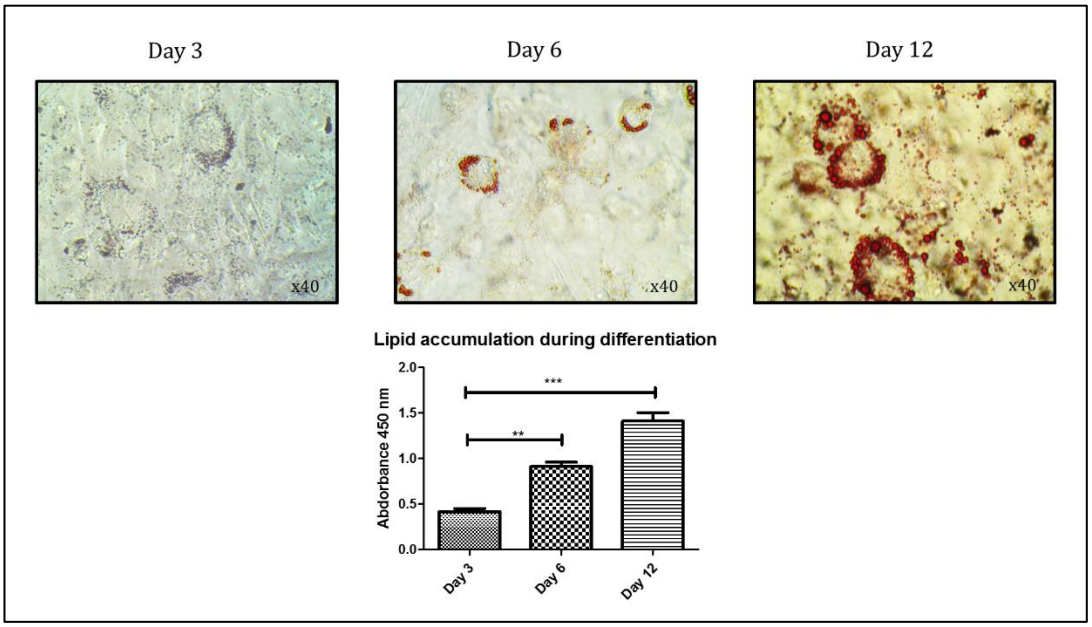

Figure 2.2: Characterisation of adipocyte differentiation using Oil red O staining. Photomicrographs (40x magnification) showing lipid accumulation by Oil Red O staining of 3T3-F442A murine adipocytes on days 3, 6 and 12 of differentiation. Full differentiation was achieved by day 12. Absorbance of extracted lipid-bound Oil Red O within the adipocytes and preadipocytes was measured at 450 nm. Analysis was conducted by 1-way ANOVA followed by Dunnett's correction for multiple testing (n=3).

2.3.2. Validation of Colloidal Silica Bead isolation method for the enrichment of plasma membrane proteins of the 3T3-F442A preadipocyte cell line

Colloidal silica bead isolation was carried out and validated for both undifferentiated (preadipocytes) and differentiated adipocytes. Na^+/K^+-ATPase and insulin receptor (IR) were selected as representative control proteins expressed in the PM and therefore detected in the PM fraction; β-actin and GAPDH were selected as representative proteins expressed in the cytoplasm and therefore used as cytosolic controls. Western blotting revealed the presence of

Na^+/K^+-ATPase and insulin receptor in the PM fraction but not in the cytosolic fraction. β-actin and GAPDH were enriched and present in the cytosolic fraction, but absent or depleted in the PM fraction (Figure 2.3). This confirms that the colloidal silica bead isolation method was able to achieve an effective enrichment of PM proteins.

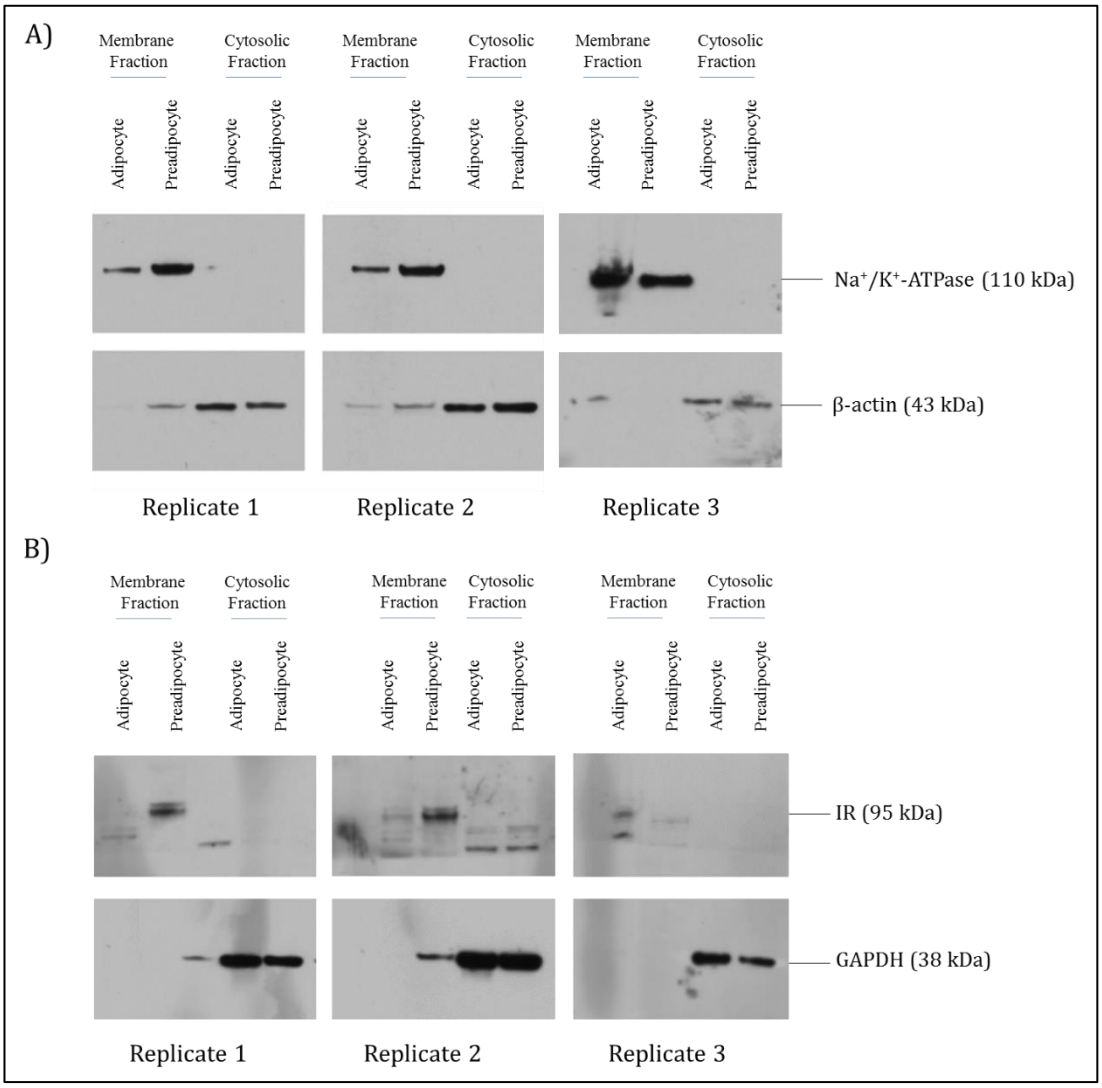

Figure 2.3: Validation of colloidal silica bead isolation by western blotting. Western blots for validation of colloidal silica bead isolation targeting A) Na^+/K^+-ATPase and β-actin, and B) targeting Insulin receptor (IR) and GAPDH to ensure correct separation of plasma membrane proteins from cytosolic proteins. A total of 10 µg of protein were loaded per well. Experiments were run in triplicate for both preadipocytes and mature adipocytes.

2.3.3. Optimisation of sample preparation for mass spectrometry after silica bead isolation

Due to their low abundance, PM proteins are easily masked in mass spectrometry analysis by higher abundant cytosolic proteins. Therefore, enrichment techniques like colloidal silica bead isolation are a good approach for detection of PM proteins. An optimal method which yielded the highest PM protein content with the lowest cytosolic protein component was needed. Two different lysis methods were performed: the first in which the cells were scraped using a cell scraper and collected from the plate as the only method of lysis ("no sonication"), and the second in which a more harsh lysis method was performed using a probe sonicator ("probe sonication"). Comparison of the two lysis methods is presented in Figure 2.4.

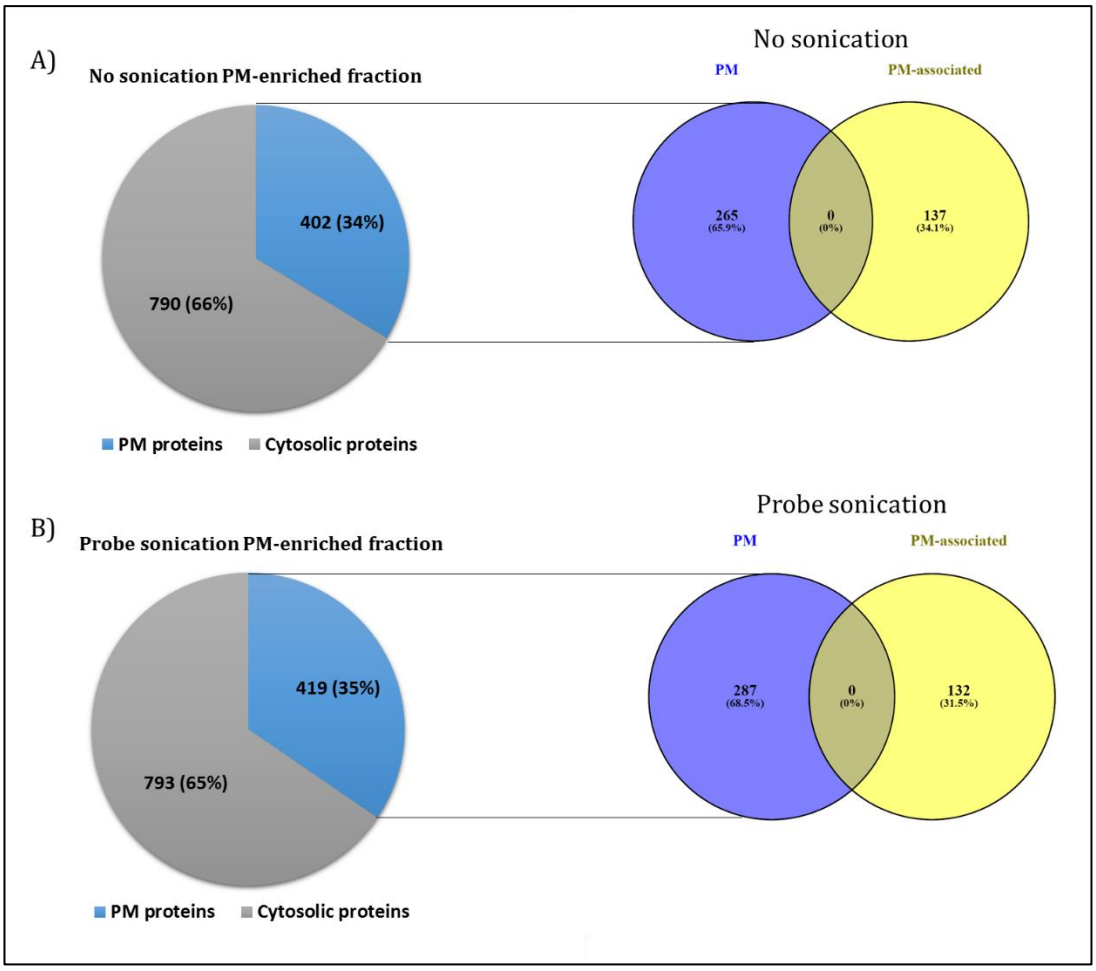

Figure 2.4: Comparison of sample lysis methods. Venn diagram showing the number of detected PM proteins after A) no sonication and B) probe sonication. Percentage of PM proteins is shown in blue (no sonication: 402, 34%, probe sonication: 419, 35%) and the percentage of cytosolic proteins present in the silica bead-isolated membrane fraction is shown in grey (no sonication: 790, 66%, probe sonication: 793, 65%). Venny 2.1 (Oliveros, 2015) was used to compare the number of unique PM proteins (purple; no sonication: 265, 65.9%, probe sonication: 287, 68.5%) and unique PM-associated proteins (yellow; no sonication: 137, 34.1%, probe sonication: 132, 31.5%) detected for the two methods. PM: plasma membrane, (n=3).

"Probe sonication" provided a larger number of total proteins (1212 proteins compared to 1192), a higher number of PM proteins (419 compared to 402), and the lowest percentage of cytosolic contaminants (65%). Lists of the total of proteins detected and PM proteins can be found in the accompanying USB as "Appendix 1-4. Chapter 2".

2.3.4. Purification of the plasma membrane fraction

After performing silica bead isolation and probe sonicator lysis ("harsh sonication"), western blot confirmed optimal enrichment of PM proteins (only present in the membrane fraction). However, it also revealed the presence of cytosolic proteins in the plasma membrane fraction. This could be a consequence of the omission of Nycodenz® density gradient step from the optimised protocol which is based on the original protocol (Kim *et al.*, 2011). Nycodenz® was found incompatible with the use of phosphate buffer instead of HEPES buffer; it was observed that the sample could not go through the density gradient and a pellet containing the purified PM-enriched fraction could not be formed.

In order to further purify the PM-enriched fraction from cytosolic proteins, the pellet containing the PM-enriched fraction was washed in fresh phosphate buffer. This additional step applied to the silica bead bound pellet was carried out to remove cytosolic contaminants before LC-MS/MS analysis (Zhao *et al.*, 2004; Lai, 2013). Washing resulted in a reduction in the cytosolic protein β-actin in the PM-enriched fraction. PM protein content (Na+/K+-ATPase) did not seem to be altered by washing. This was compared for both preadipocytes and differentiated adipocytes (Figure 2.5).

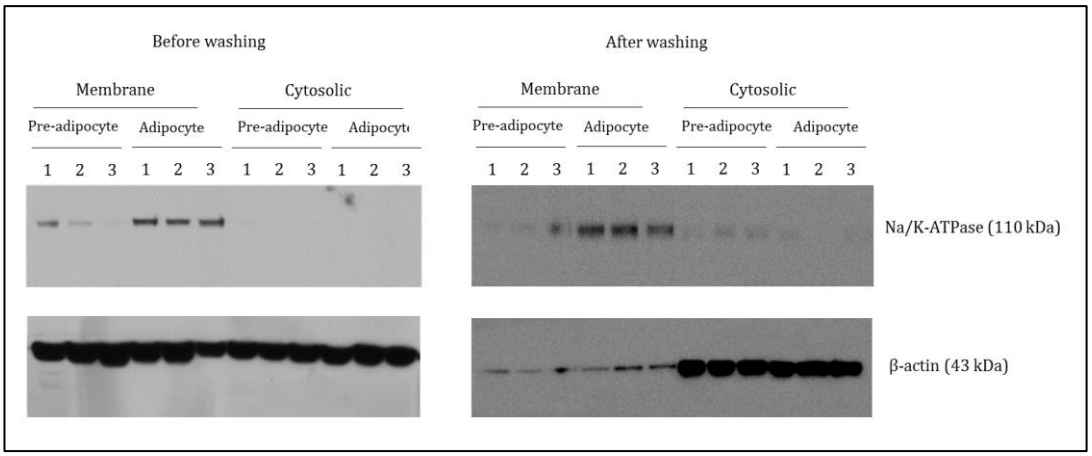

Figure 2.5: Comparison of cytosolic and membrane fraction before and after washing. Washing reduced the presence of cytosolic proteins (β-actin) from the PM fraction leaving the content of PM proteins (Na^+/K^+-ATPase) unaltered. A total of 10 µg of protein were loaded per well. Experiments were run in triplicate for both preadipocytes and mature adipocytes.

The final optimised protocol for enrichment and analysis of adipocyte PM proteins is presented in Figure 2.6.

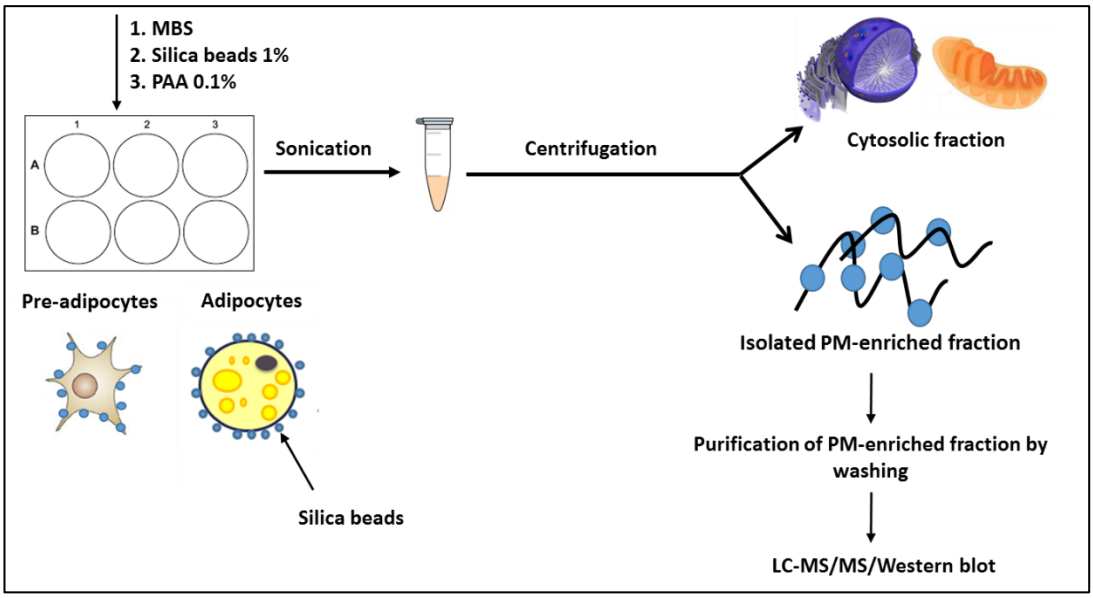

Figure 2.6: Optimised colloidal silica bead isolation method for the 3T3-F442A cell line. The silica beads (blue spheres) bind to the PM of the cell by electrostatic interactions. Cells were scraped out of the plate, lysed by sonication and separated via centrifugation: the supernatant contains the cytosolic components of the cell (cytosolic fraction) and the pellet is formed by the PM proteins bound to the silica beads (PM-

enriched fraction). The PM-enriched fraction was washed to remove remaining cytosolic contaminants prior to use for western blot or LC-MS/MS.

2.3.5. Detection of proteins in membrane and cytosolic fractions using Coomassie blue

Before performing mass spectrometry there was a need of ensure protein content in the samples. The presence of proteins in cell lysates was observed using SDS-PAGE gels stained with Coomassie blue. As expected, more protein bands were observed in the cytosolic fraction compared to the PM-enriched fraction. The PM-enriched fractions before and after washing were also stained to observe presence of protein bands as a checkpoint prior analysis by LC-MS/MS (Figure 2.7).

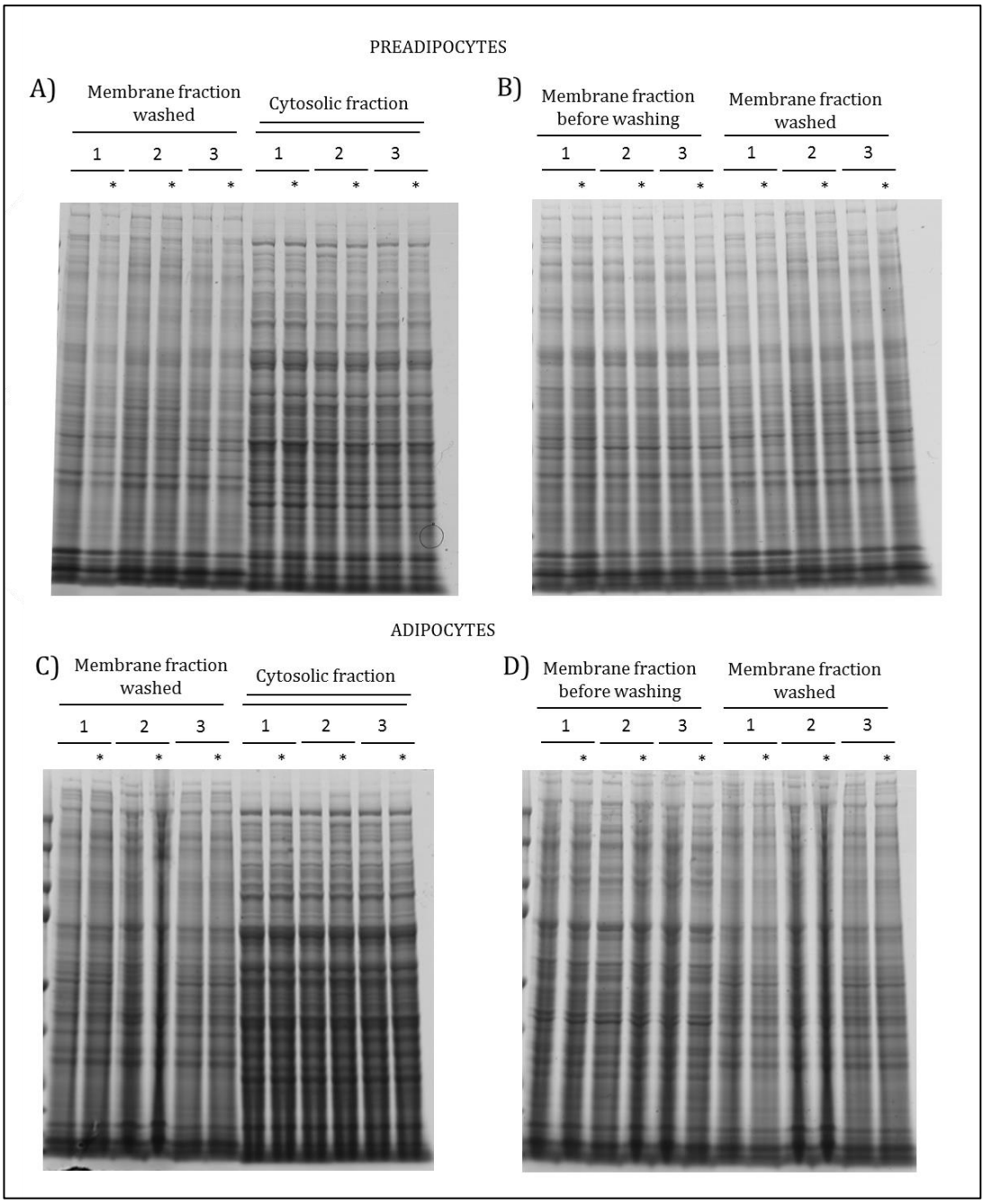

Figure 2.7: SDS-PAGE gels stained with Colloidal Coomassie blue for the detection of proteins in the PM-enriched fraction and cytosolic fraction prior to LC-MS/MS analysis. A total of 20 µg of protein determined by Bradford assay were loaded per lane. A) Comparison of the PM fraction (after washing) to the cytosolic fraction of preadipocytes. B) Comparison of the PM fraction lysates of preadipocytes before and after washing. C) Comparison of the PM fraction (after washing) to the cytosolic fraction of mature adipocytes. D) Comparison of the PM fraction lysates of mature adipocytes before and after washing. Every experiment was performed in triplicate; * represents technical replicate.

2.3.6. Comparison of total protein yield obtained by optimised colloidal silica bead isolation between this study and Prior et al´s study

To our knowledge, the only study that has applied colloidal silica bead isolation for the enrichment of PM proteins from adipocytes to date was Prior *et al.*, (2011).

The total protein yield obtained by the colloidal silica bead isolation optimised method (probe sonication) was compared to the yield obtained by Prior *et al*., (2011). A total of 950 protein matches were identified between the two studies, but with the current study detecting 262 proteins which were not reported by Prior *et al.*, (2011) in the adipocyte PM-enriched fraction (Figure 2.8). A complete list of proteins can be found in the accompanying USB as "Appendix 5 Chapter 2. Comparison total protein yield obtained by optimised colloidal silica bead isolation to Prior *et al*., (2011)". Although Prior *et al.*, (2011) obtained a higher yield of proteins, it needs to be noted that their list of proteins is a result of a combination of various techniques including colloidal silica bead isolation, SILAC, subcellular fractionation, and GLUT4 vesicle immunoadsorption, whereas out study only used silica bead isolation as enrichment technique.

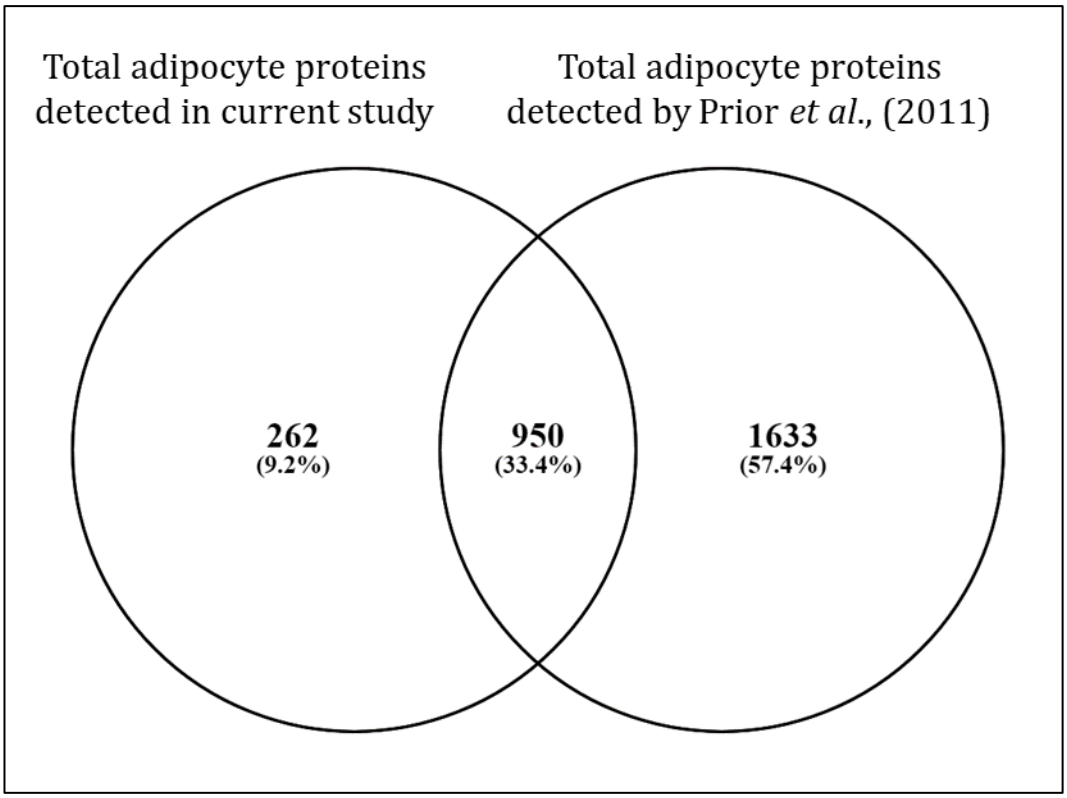

Figure 2.8. Comparison of total detected proteins in the PM-enriched fraction by Prior *et al.*, (2011) and the current study.

2.3.7. Comparison of PM protein yield obtained by optimised colloidal silica bead isolation between this study and Prior et al´s study

The number of PM proteins detected by Prior *et al.*, (2011) in the adipocyte PM-enriched fraction was compared to the number of PM proteins detected in this thesis in the PM-enriched fraction. A total of 142 proteins were common between the two studies, but the current study provided 277 PM proteins that had not been detected by Prior *et al.*, (2011) (Figure 2.9). A complete list of proteins can be found in the accompanying USB as "Appendix 5 Chapter 2. Comparison to Prior et al., (2011)"

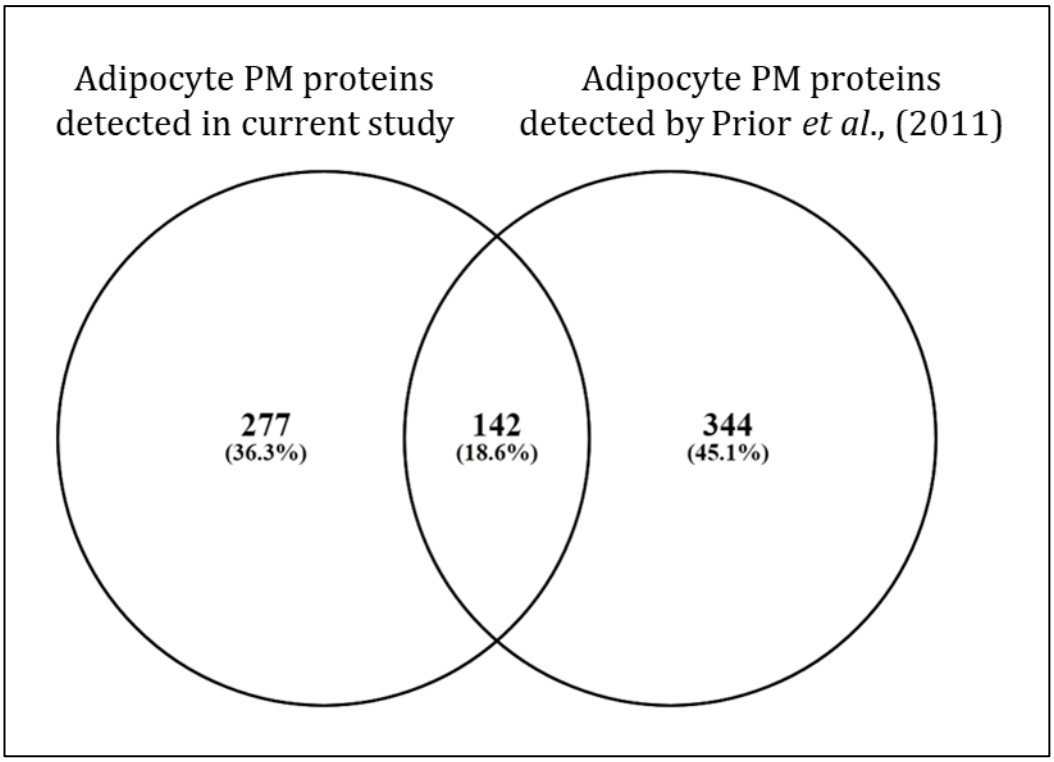

Figure 2.9. Comparison of detected PM proteins by Prior *et al.*, (2011) and the current study.

2.4. DISCUSSION

The detection and study of PM proteins is challenging due to the heterogeneity, poor solubility, low abundance and post-translational modifications characteristic of this class of proteins. Their low abundance makes them easily masked by more abundant cytoplasmic proteins when performing mass spectrometry. Furthermore, it is important to consider the dynamic nature of the proteome, which changes in response to stimuli (Renes *et al.*, 2013); an example of this are the changes in the composition of the PM proteome due to the translocation of proteins from cytoplasmic vesicles to the PM in response to certain triggers (e.g. insulin stimulation). Mass spectrometry runs may identify or miss different proteins depending on their sensitivity as well as time point of

analysis; this means that some of the proteins of interest are either missed during analysis or not present in the sample.

Due to the reasons mentioned above, published work on adipocyte PM proteomics is limited (Prior *et al.*, 2011). Protein enrichment techniques are needed to provide a good starting point of for mass spectrometry analysis of PM proteins. For this thesis, the technique of choice for enrichment was colloidal silica bead isolation because previous publications have applied this technique for cardiomyocytes (Sharma *et al.*, 2015) and 3T3-L1 adipocytes (Prior *et al.*, 2011). However, this technique has not been previously applied to the 3T3-F442A preadipocyte cell line.

In order to optimise colloidal silica bead isolation for the 3T3-F442A cell line and adapt it for mass spectrometry analysis, modifications from the original protocol were performed. First, there was a need to achieve the highest possible yield of PM proteins. For this, two different lysis techniques (lysis by a cell scraper and lysis by probe sonication) were applied and the total number of PM proteins detected by the ProteinPilot software was compared and classified based on GO Cellular Component annotations. Probe sonication was the lysis method rendering the highest yield of PM proteins and was selected the lysis method of choice. Another modification to the original protocol was the change from a Sucrose/HEPES buffer to a phosphate buffer for the lysate to be produced in. Phosphate buffer was the buffer of choice for mass spectrometry analysis, but it was incompatible with the Nycodenz® density gradient, and therefore was taken out of the protocol and replaced by centrifugation at 10,000 rpm for 10 minutes. As a consequence of not applying the density gradient, the PM enriched fraction

required further purification; and this was shown by western blot revealing high amounts of cytosolic proteins in the PM fraction (Figure 2.5).

Therefore, an additional purification step was required to lower the presence of cytosolic proteins in the PM-enriched fraction as much as possible, but without losing PM proteins in the process. This was achieved by washing the silica bead isolated fraction pellet with phosphate buffer. Washing of the PM-enriched fraction has been previously used in membrane proteomics studies (Zhao *et al.*, 2004; Cordwell *et al.*, 2010; Lai, 2013) and it was proven to effectively reduce the amount of cytosolic proteins from the PM fraction (Figure 2.5). It should be noted that it is not feasible to completely remove all the cytosolic protein content from the PM fraction. Even after enrichment and separation techniques are applied, mass spectrometry analysis will detect cytosolic proteins in the PM fraction due to its high sensitivity and the high abundance of cytosolic proteins. In fact, previous studies on adipocyte PM proteomics identified a large number of cytosolic proteins even after enrichment; Prior *et al.*, (2011) found that out of the total of proteins identified after colloidal silica bead isolation, 22.8% were mitochondrial proteins, 12.3% belonged to the ER, and 6% were Golgi proteins (Prior *et al.*, 2011; Renes *et al.*, 2013).

Based on the results of various optimisation methods conducted as explained, a final optimisation procedure was selected, which incorporated the following steps: a) probe sonication of cells; b) phosphate buffer as the buffer of choice; and c) purification of PM fraction by washing (3 times wash using phosphate buffer).

This final optimised method for the study of the adipocyte PM proteome effectively enriched and led to the detection of a high amount of PM proteins

during mass spectrometry (419 proteins, 35% of total detected proteins); a previous study on human adipocytes (Xie *et al.*, 2010) identified 202 (13.5% of total detected proteins) PM proteins upon subcellular fractionation.

It is important to note the dynamic nature of the PM proteome, and its connection with other cell organelles (e.g. ER, vesicles); many PM proteins are translocated to the PM from other cellular compartments to exert their action. For this reason, a previous study by Prior *et al.*, (2011) employed not only silica bead isolation, but also vesicle immunoadsorption techniques, subcellular fractionation and SILAC, to obtain a higher yield of PM proteins (486 PM proteins, 18.9% of total detected proteins). The optimised methodology presented in the current study provided with 277 PM proteins not previously reported by Prior *et al.*, (2011) in the PM-enriched fraction (Figure 2.9); there were also 142 PM proteins which showed an overlap between the two studies. It is important to highlight that the current study used the 3T3-F442A preadipocyte cell line and in Prior *et al.*, (2011) they used the 3T3-L1 cell line, therefore differences in proteins detected may be a consequence of the differences between these two cell lines. Furthermore, cells were differentiated for 12 days and Prior *et al.*, (2011) differentiated adipocytes until day 10 of adipogenesis.

Results from the current study concluded that the protocol developed in this thesis was efficient for the analysis of the adipocyte PM proteome. Although the use of silica bead isolation combined with additional enrichment techniques (e.g. vesicle immunoadsorption, SILAC or iTRAQ) may increase the yield of PM proteins for the current study, limitations regarding time and costs needed to be

considered, and this method was developed as a platform that could be improved in following studies.

In conclusion, this chapter establishes a method which will be applied for the experiments performed in experimental chapters 3 and 4 for the study of changes in the adipocyte PM proteome during adipogenesis and following exposure to antiretrovirals respectively.

CHAPTER 3
CHANGES IN THE ADIPOCYTE PLASMA MEMBRANE PROTEOME DURING ADIPOGENESIS AND FOLLOWING INSULIN STIMULATION

3.1.INTRODUCTION

3.1.1. Adipogenesis and plasma membrane proteomics

Adipogenesis, the process in which preadipocytes differentiate and mature into adipocytes, has been extensively studied in the field of proteomics (Welsh *et al.*, 2004; Molina *et al.*, 2009; Borkowski *et al.*, 2014). The adipose tissue is an endocrine organ and a key regulator of metabolic homeostasis (Kershaw *et al.*, 2004). Adipogenic differentiation is key for the functionality of adipose tissue (Rosen and MacDougald, 2006). Mature adipocytes not only store lipids, but they also secrete adipokines, which play an important role in insulin sensitivity and adipogenic differentiation. Dysregulation of adipogenesis affects adipocyte function resulting in conditions such as lipodystrophy, insulin resistance (Sarjeant *et al.*, 2012; Gustafson *et al.*, 2015) and obesity (Gustafson *et al.*, 2013; Klöting *et al.*, 2014).

The first large scale proteomic analysis of the adipocyte was performed by Adachi et al. (2007) by dividing the cell into different compartments using subcellular fractionation. The first study focusing on the PM proteome of adipocytes was not published until recently (Prior *et al.*, 2011), this may be due to the challenges in studying PM proteins discussed in sections 1.13.1 and 2.1.1. In their study, they detected a new PM protein in 3T3-L1 adipocytes, the sodium/hydrogen exchanger NHE6, which increased during adipogenesis and was shown to be insulin-responsive and to translocate to the PM in GLUT4 storage vesicles (GSVs) following insulin stimulation (Prior *et al.*, 2011).

Despite the scarcity of publications focusing on the adipocyte PM proteome, adipogenesis has been thoroughly studied in the field of proteomics, leading to

the detection of important PM proteins playing a role in adipocyte differentiation (Kratchmarova *et al.*, 2002; Choi *et al.*, 2004; Welsh *et al.*, 2004; DeLany *et al.*, 2005; Lee *et al.*, 2006; Kamal *et al.*, 2013).

A recent study focused on the role of NCAM (Neural Cell Adhesion Molecule), a protein important in adipogenesis, using NCAM knockout mice and the 3T3-L1 preadipocyte cell line (Yang *et al.*, 2011). They discovered a key role of this protein in adipogenesis and insulin signalling. Silencing of this cell adhesion protein in 3T3-L1 preadipocytes inhibited differentiation and led to insulin resistance. Expression of proteins involved in the insulin signalling cascade such as PI3K-akt and IGF-1 was impaired in *Ncam*$^{-/-}$ mesenchymal stem cells. Furthermore, NCAM knockout induced the expression of TNFα, and contributed to insulin resistance.

APMAP (Adipocyte Plasma Membrane Associated Protein), a novel adipocyte integral PM protein participating in adipogenesis of 3T3-L1 preadipocyte cell line, was found by Albrektsen et al. (2001) in a differential mRNA expression study in adipogenesis. Using mRNA differential display analysis, they found a novel mRNA (DD16) induced during adipogenesis and detected the DD16 protein expression by western blotting in membrane fractions (isolated by subcellular fractionation). They gave the DD16 protein the name of APMAP. APMAP was found to be translocated to the PM from the endoplasmic reticulum during adipogenesis (Albrektsen *et al.*, 2001; Bogner-Strauss *et al.*, 2010) and it was reported to interfere with PPARγ, a key regulator of adipogenesis. In fact, knockdown of this protein resulted in inhibition of adipogenesis (Bogner-Strauss *et al.*, 2010).

Hong *et al.*, (2005) focused on the investigation of a specific gene of unknown function which expression was particularly high in adipose tissue according to the Genome Institute of Novartis Research Foundation (GNF) SymAtlas v0.8.0 database (http://symatlas.gnf.org/SymAtlas/). They named the product of this gene adipogenin. The levels of adipogenin mRNA were found to substantially increase during adipogenesis of 3T3-L1 adipocytes, and they were also higher in obese mice compared to controls. Adipogenin was located in the adipocyte PM by transfection with green fluorescent protein (GFP)-adipogenin constructs. Knockdown of adipogenin reduced lipid droplet accumulation in 3T3-L1 adipocytes and reduced the expression of PPARγ, revealing its involvement in adipogenesis (Hong *et al.*, 2005).

Lipid rafts are membrane microdomains responsible for essential functions of the PM, such as trafficking, signalling, transport and maintenance of cell structure. They comprise several therapeutic targets, and their relevance in proteomics has been highlighted (Tan *et al.*, 2008). Kim *et al*. (2009) used 2-DE and LC-MS/MS (ESI) analysis to observe changes in the proteome of the 3T3-L1 cell line in order to identify novel lipid raft proteins involved in adipogenesis. They found the expression of globular C1q receptor (gC1qR) to be increased gradually during adipogenesis. Immunoblotting identified considerable amounts of this protein in lipid rafts of mature adipocytes but not in those of preadipocytes. Furthermore, they determined that silencing of this protein decreased lipid accumulation by disrupting adipogenesis and blocked insulin receptor activation. Expression levels of PPARγ and other adipogenic proteins were largely decreased in the gC1qR knockdown cells compared to controls (Kim *et al.*, 2009).

3.1.2. Proteomics and insulin signalling

Insulin regulates glucose uptake by adipocytes so it can be stored in the form of triglycerides. Most of the glucose uptake in adipocytes is carried out by GLUT4; in fact, GLUT4 is only expressed in insulin responsive tissues such as adipose tissue, myocardium and skeletal muscle (Kawaguchi *et al.*, 2010). As previously mentioned, GLUT4 is stored inside vesicles (GSVs) in the cytoplasm of adipocytes, and it translocates to the PM after insulin stimulation while undergoing several post-translational modifications in the process (Sadler *et al.*, 2013). GLUT4 translocation to the PM of adipocytes following insulin stimulation is a thoroughly studied pathway due to its involvement in insulin sensitivity and glucose homeostasis (Kawaguchi *et al.*, 2010; Tokarz *et al.*, 2018).

But for GLUT4 translocation to occur, insulin needs to bind to the IR in the PM of adipocytes, triggering a cascade of phosphorylation events (Figure 1.9). The study of these phosphorylation events through mass spectrometry is known as phosphoproteomics. Various studies have applied proteomics for the identification of novel proteins implicated in the insulin signalling pathway as well as in GLUT4 translocation, aiming to identify new proteins playing a role in insulin resistance and diabetes (Guilherme *et al.*, 2000; Schmelzle *et al.*, 2006; Krüger *et al.*, 2008; Jedrychowski *et al.*, 2010).

Schmelzle *et al*. (2006) studied tyrosine phosphorylation triggered by insulin on 3T3-L1 adipocytes using LC-MS/MS and iTRAQ, and identified known phosphotyrosine proteins (caveolin 1 and 2, PTRF and fatty acid binding protein 4), and proteins involved in GLUT4 translocation to the PM (Syntaxin 4, Munc18c, Annexin II and EH domain-containing protein 2). They also found two

transporters involved in the insulin signalling pathway; SLC12A4, a K^+-Cl^- transporter, and SLC38A2, an aminoacid transporter, both of which were phosphorylated following insulin stimulation (Schmelzle *et al*. 2006) .

Proteomics has been specifically applied to GSVs, as they are key for insulin sensitivity. A technique for the isolation of GLUT4-containing vesicles was developed by Guilherme *et al*. (2000), resulting in the identification of proteins involved in GLUT4 translocation such as VAMP2 and the transferrin receptor (TfR).

Three PM proteins have been recently found to participate in the fusion of GSVs to the PM of adipocytes: Cysteine-string protein 1 (Csp1), C2domain-containing phosphoprotein (CDP138) and low density lipoprotein receptor-related protein 1 (LRP1). Csp1, a protein involved in neurotransmission and exocytosis, was located in the PM but not in the GSVs of adipocytes by immunofluorescence. It was shown to interact with the SNARE protein Syntaxin 4 for vesicle fusion (Chamberlain *et al.*, 2001). CDP138 was found to be part of the protein kinase B β (Akt2) signalling cascade and was involved in the incorporation of GLUT4 in the PM (Xie *et al.*, 2011). LPR1 was detected in high amounts in GSVs, and its depletion was observed to reduce GLUT4 expression in adipocytes (Jedrychowski *et al.*, 2010).

The above-mentioned proteomic studies have identified numerous adipocyte PM proteins of metabolic relevance. This highlights the effectiveness of applying proteomics to the discovery of new therapeutic targets for metabolic disease. However, only one of these publications focused on the PM of adipocytes specifically, rather than the whole cell proteome, and none of them studied

changes in the PM proteome during adipogenesis. The PM comprises a large proportion of transporters, receptors and therapeutic targets and, in this chapter, performed a global proteomic analysis of the PM of 3T3-F442A adipocytes during the process of adipocyte differentiation and also following acute insulin stimulation was performed, with the aim of identifying new PM proteins involved glucose homeostasis.

3.1.3. Aims and objectives

The aims of this chapter were:

1) To undertake LC-MS/MS of PM-enriched lysates to identify known and novel PM proteins which are differentially regulated during adipogenesis and following acute insulin-stimulation.
2) To undertake bioinformatic analysis to locate differentially regulated PM proteins in their respective biological pathways.
3) To bioinformatically predict interactions between differentially regulated PM proteins identified and, PPARγ and mTOR (key cytosolic regulators of adipogenesis and insulin signalling respectively).
4) To select potential PM protein targets for validation.

3.2. METHODS

A flow diagram of the methodology is presented in Figure 3.1.

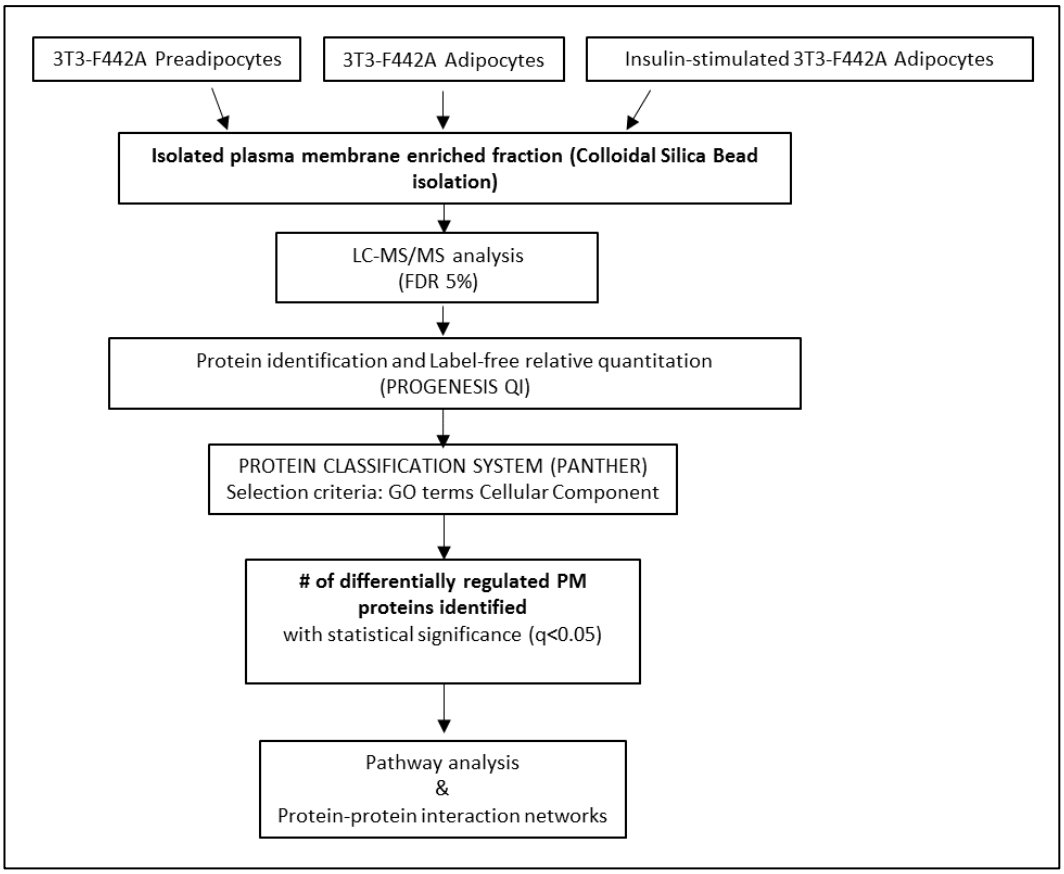

Figure 3.1: Flow diagram of methodology used. Optimised methodology for the study of the PM proteome of the 3T3-F442A preadipocyte cell line.

3.2.1. Adipocyte cell culture and differentiation

Cell culture and adipocyte differentiation were performed as described in section 2.2.1 of Chapter 2.

3.2.2. Starvation and insulin stimulation of mature adipocytes

On day 11 of differentiation, adipocytes were serum-starved overnight. On day 12, adipocytes were incubated with 200 nM of insulin for 20 minutes. A 20 minutes incubation time with insulin was applied as previously described in Prior *et al.*, (2011); in their study, they used a 100 nM insulin concentration, but a higher insulin concentration of 200 nM was used for this thesis to observe any changes in the PM proteome at a higher dose of insulin. Following insulin stimulation, lysates were prepared for colloidal silica bead isolation.

3.2.3. Colloidal silica bead isolation

Colloidal silica bead isolation was performed as described in section 2.2.3 of Chapter 2.

3.2.4. Determination of protein concentration (Bradford Assay)

Protein concentration was determined using a Bradford assay as described in section 2.2.4 of Chapter 2.

3.2.5. Sample preparation for LC-MS/MS

Samples were processed for LC-MS/MS analysis as described in section 2.2.7 of Chapter 2.

3.2.5.1. Ziptip

Samples were de-salted by Ziptip as described in section 2.2.7.2 of Chapter 2.

3.2.6. LC-MS/MS analysis

The purified and dried samples containing the digested peptides were re-hydrated in 10 µl of 0.1% formic acid, vortexed and centrifuged for 30 seconds. Samples were diluted 1:10 in 0.1% formic acid and 3 µg of digested peptide mixture were loaded into the mass spectrometer. Mass spectrometry analysis was performed as described in section 2.2.7.3 of Chapter 2.

3.2.7. Bioinformatic analysis

3.2.7.1. Protein identification and label-free relative quantitation of differentially regulated proteins

Mass spectrometry raw files (.wiff files) were analysed by Progenesis QI software (version 4.0, Nonlinear Dynamics, Newcastle, UK). This software calculates the relative abundance of proteins between the different conditions based on the

sum of peptide intensities. Alignment of ion intensity maps from each run to a reference sample run allows normalisation and comparison of protein abundances between runs and compensates between-run variation. The software applies a logarithmic (base 10) transformation to obtain a normal distribution.

The MS/MS spectra for the detected peptides ions were exported from Progenesis QI into MASCOT search engine for protein identification (http://www.matrixscience.com). The database used for protein identification was the UniProt murine protein database, the MS/MS tolerance used was 50 mmu (absolute milli-mass units), and peptide tolerance used was 10 ppm (parts per million). The significant threshold for protein identification was set for a 5% False Discovery Rate (FDR). Post-translational modification carbamidomethylation of cysteine (Carbamidomethyl (C)) was included in the MASCOT MS/MS Ion search (this post-translational modification was included because iodoacetamide was used as an alkylating agent and this produces carbamidomethylation of cysteine residues). The MASCOT protein identification results were then imported into Progenesis QI and the restricition of minimum of unique peptides was set to 1. Progenesis reports can be found in the accompanying USB within the chapter 3 folder as "Appendix 4 Chapter 3. Progenesis QI report of proteins detected during adipogenesis" and "Appendix 7 Chapter 3. Progenesis QI report of proteins detected following insulin stimulation". All differentially regulated proteins detected by Progenesis QI were presented as volcano plots plotting the $-\log_{10}q$-value against $\log_2$Fold change using Microsoft Excel (2016).

3.2.7.2. Protein classification and data curation

Proteins were classified under the Gene Ontology (GO) annotations obtained from the GO database (http://www.geneontology.org): "Cellular Component" (CC), "Biological Process" (BP) and "Molecular Function" (MF). Proteins were classified as plasma membrane proteins under the Cellular Component "plasma membrane" annotation, and as plasma membrane-associated proteins under the GO annotations listed in Table 2.1.

Proteins were further manually curated using literature searches performed in PubMed (https://www.ncbi.nlm.nih.gov/pubmed/), ISI Web of Science (http://www.webofknowledge.com/), Uniprot (https://www.uniprot.org/) and The Human Protein Atlas (http://www.proteinatlas.org/). PANTHER GO-Slim BP and MF were applied to classify proteins based on BP and MF GO terms. Fisher's exact test with FDR multiple test correction was applied (FDR-corrected p value<0.05 was considered significant).

3.2.7.3. Protein pathway and network analysis

Pathway analysis was carried out using PANTHER Overrepresentation test (annotation version 65). Fisher's exact test with FDR multiple test correction was applied (FDR-corrected p-value<0.05 was considered significant). Protein networks were created using the Search Tool for the Retrieval of INteracting Genes (STRING) database for functional protein association networks (https://string-db.org/) (version 10.5) (Szklarczyk *et al.*, 2017). PPARγ and mTOR were added to the network analysis to observe any links of the detected PM proteins to these key regulators of adipogenesis and insulin signalling respectively.

3.2.8. Statistical analysis

Progenesis QI compared the relative protein abundance between groups using a one-way analysis of variance (ANOVA, $p<0.05$) and post-hoc correction for multiple comparison based on the False Discovery Rate (FDR). A q-value (FDR-corrected p-value) of <0.05 was considered significant. Progenesis also calculated the maximum fold change (comparing protein relative abundances between any two conditions), statistical power values (probability of finding real differences for a specific protein between conditions), confidence score (confidence in identification of a specific protein), as well as the number of peptides and unique peptides identified for each protein. Principal component analysis (PCA) was performed in Progenesis QI to observe clusters of proteins and capture differences between conditions. All experiments were done in triplicate (n=3) to ensure reproducibility.

3.3. RESULTS

3.3.1. Differential regulation of the adipocyte proteome during adipogenesis

Analysis of differential protein expression was performed in Progenesis QI and a total of 562 proteins were identified when comparing mature adipocytes to preadipocytes. Out of these, 452 of these proteins were significantly differentially regulated ($q<0.05$) during adipogenesis. The p-values for each analysis were corrected for multiple testing with FDR and a q-value of <0.05 considered as significant. A threshold for fold changes (FC) was applied (FC<0.5 was considered as down-regulated and FC>1.5 was considered as upregulated). A total of 79 proteins were >50% up-regulated (green) and 102 were >50% down-

regulated (red). Fold changes were calculated based on the normalised abundances for a specific protein between the two conditions (differentiated vs undifferentiated). Figure 3.2 presents a volcano plot showing all differentially regulated proteins detected by the software. A list of these proteins can be found in the accompanying USB within the chapter 3 folder as "Appendix 1 Chapter 3". Progenesis QI report for adipogenesis can be found in within the chapter 3 folder as "Appendix 4 Chapter 3".

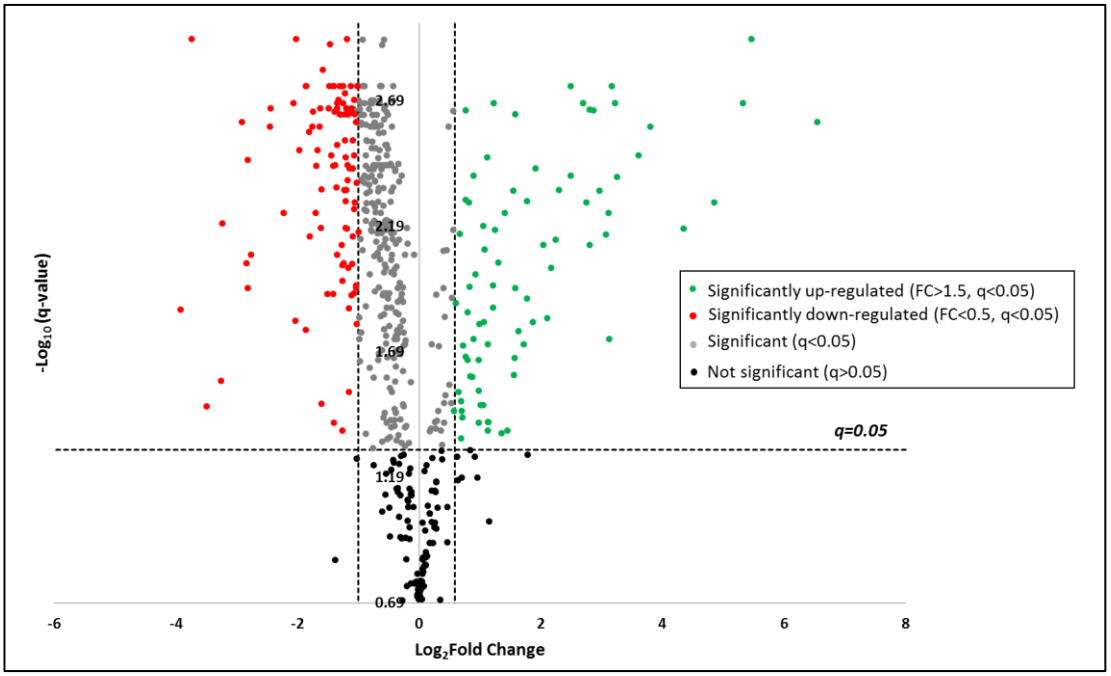

Figure 3.2: Volcano plot showing differentially regulated proteins during adipogenesis. Logarithmic ratios of fold change (FC) of differentiated adipocytes (n=3) vs undifferentiated preadipocytes (n=3) were plotted against the q-value (q<0.05 considered significant: dotted horizontal line). Positive fold change values indicate up-regulation (green) of protein expression in differentiated adipocytes relative to undifferentiated preadipocytes and negative FC values indicate down-regulation (red) of protein expression in differentiated adipocytes relative to undifferentiated preadipocytes. The vertical lines represent selected thresholds for FC: >50% up-regulation (FC>1.5) or >50% down-regulation (FC<0.5). Analysis was conducted by 1-way ANOVA followed by Tukey's correction for multiple testing. All differentially regulated proteins are listed in Appendix 1 of Chapter 3.

Principal component analysis (PCA) was performed in Progenesis QI (Figure 3.3.). PCA showed effective separation of the two clusters corresponding to the

two different types of cells (group 1-differentiated adipocytes; blue data points; group 2- un-differentiated preadipocytes; purple data points). The preadipocyte samples were not tighly clustered (group 2) suggesting higher variability between samples within the preadipocyte cluster (group 2), than within the adipocyte cluster (group 1).

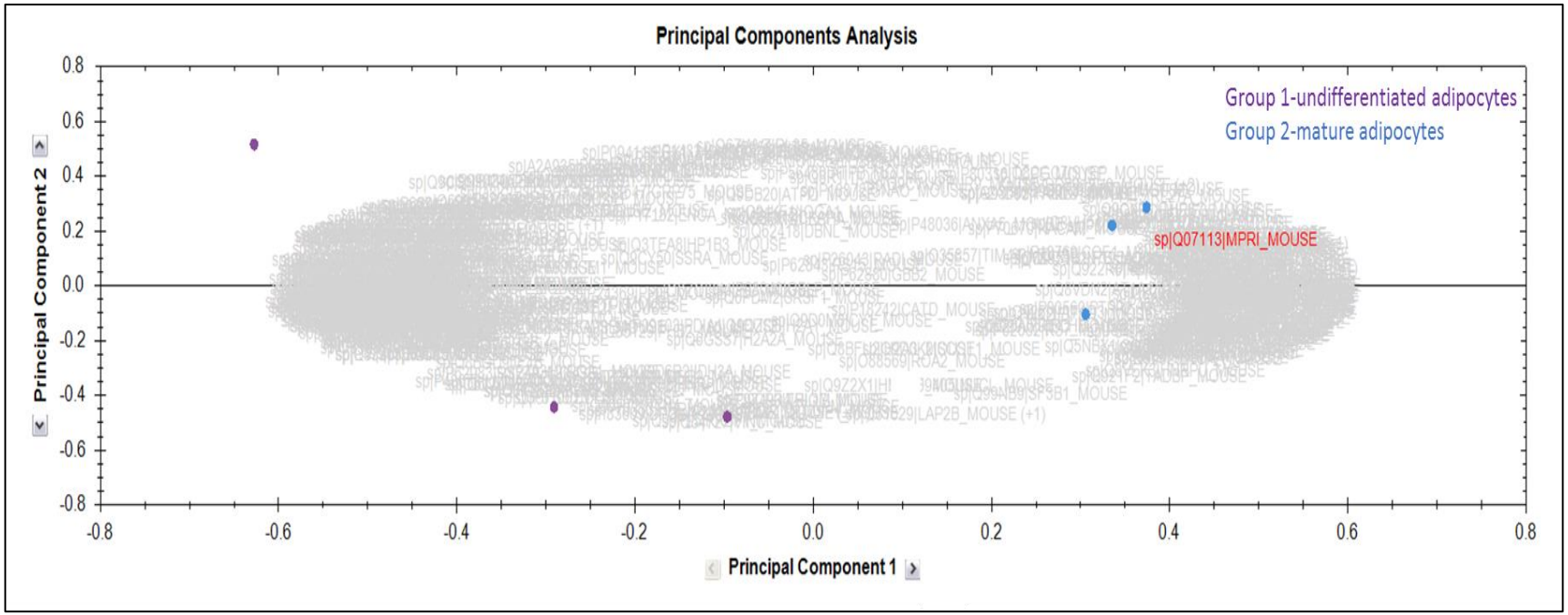

Figure 3.3: Principal component analysis (PCA) distinguishes the silica bead isolated-plasma membrane fraction of undifferentiated preadipocytes and mature adipocytes. Group 1-undifferentiated adipocytes: purple data points; group 2-mature adipocytes: blue data points.

3.3.2. Differential regulation of the adipocyte proteome following insulin stimulation

Progenesis QI data analysis identified a total of 534 proteins when comparing insulin stimulated mature adipocytes to control (unstimulated) mature adipocytes. The p-values for each analysis were corrected for multiple testing with FDR and a q-value of <0.05 which was considered as significant. A threshold for FC was applied (FC<0.5 was considered down-regulated and FC>1.5 was considered up-regulated). Fold changes were calculated based on the normalised abundances for a specific protein between the two conditions (insulin stimulated vs unstimulated).

Figure 3.4 presents a volcano plot showing all differentially regulated proteins detected by the software. A list of these proteins can be found in the accompanying USB within the chapter 3 folder as "Appendix 5 Chapter 3". Progenesis QI report for insulin stimulation can be found in within the chapter 3 folder as "Appendix 7 Chapter 3".

After correction for multiple testing, insulin stimulation of mature adipocytes rendered no statistically significant differentially regulated proteins (q>0.05). Before applying correction for multiple testing, 90 of these proteins were found significantly differentially regulated (p<0.05) following exposure to insulin (7 were >50% up-regulated (green) and 1 was >50% down-regulated (red)).

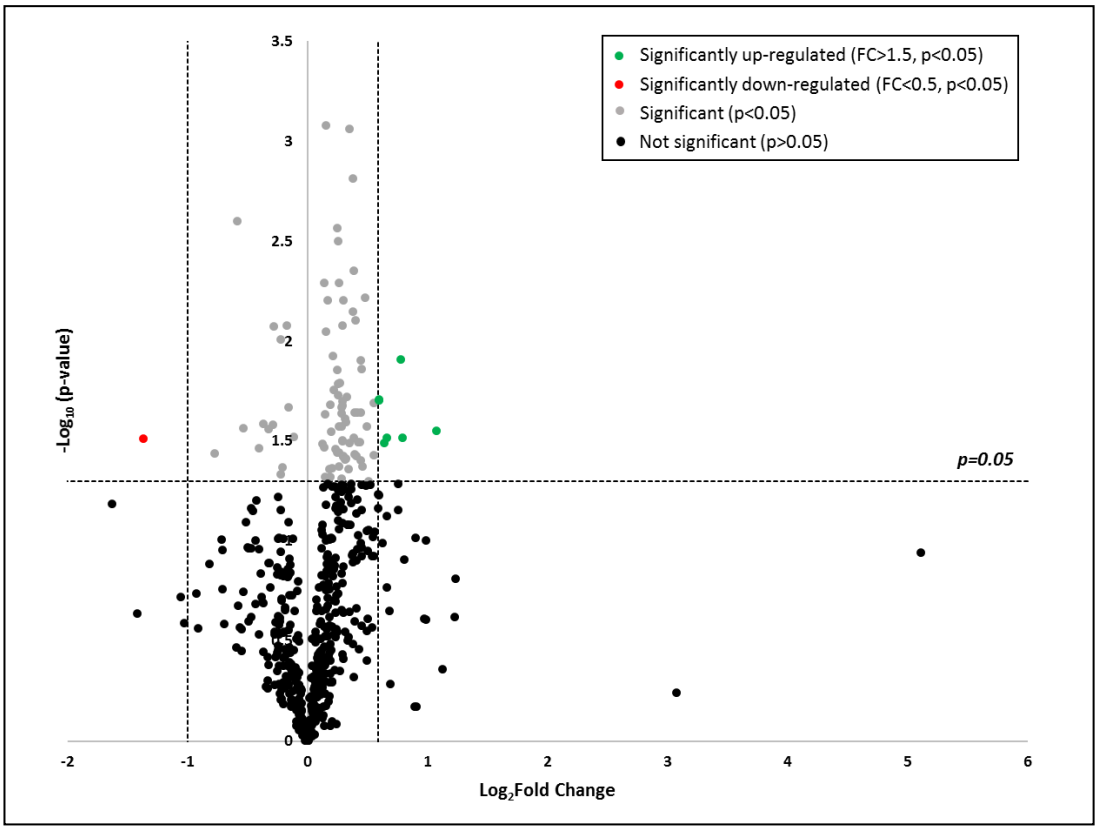

Figure 3.4: Volcano plot showing differentially regulated proteins following insulin stimulation. Logarithmic ratios of fold change (FC) of insulin stimulated adipocytes (n=3) vs unstimulated adipocytes (n=3) were plotted against the p-value (FDR correction for multiple testing was not applied and p<0.05 (not corrected for multipe testing) is considered significant: dotted horizontal line). Positive FC values indicate up-regulation (green) of protein expression in insulin-stimulated adipocytes relative to non-stimulated adipocytes and negative fold change values indicate down-regulation (red) of protein expression in insulin-stimulated adipocytes relative to non-stimulated adipocytes. The vertical lines represent selected thresholds for FC: >50% up-regulation (FC>1.5) or >50% down-regulation (FC<0.5). 1-way ANOVA followed by Tukey's correction for multiple testing. All differentially regulated proteins are listed in Appendix 5 of Chapter 3.

PCA (Figure 3.5.) showed separation of the two clusters corresponding to the two different types of cells (group 1-insulin stimulated adipocytes; blue data points; group 2- unstimulated adipocytes; purple data points). For insulin-stimulated adipocytes (group 1) samples were not tighly clustered suggesting higher variability between samples within this cluster (group 1), than within the unstimulated adipocyte cluster (group 2).

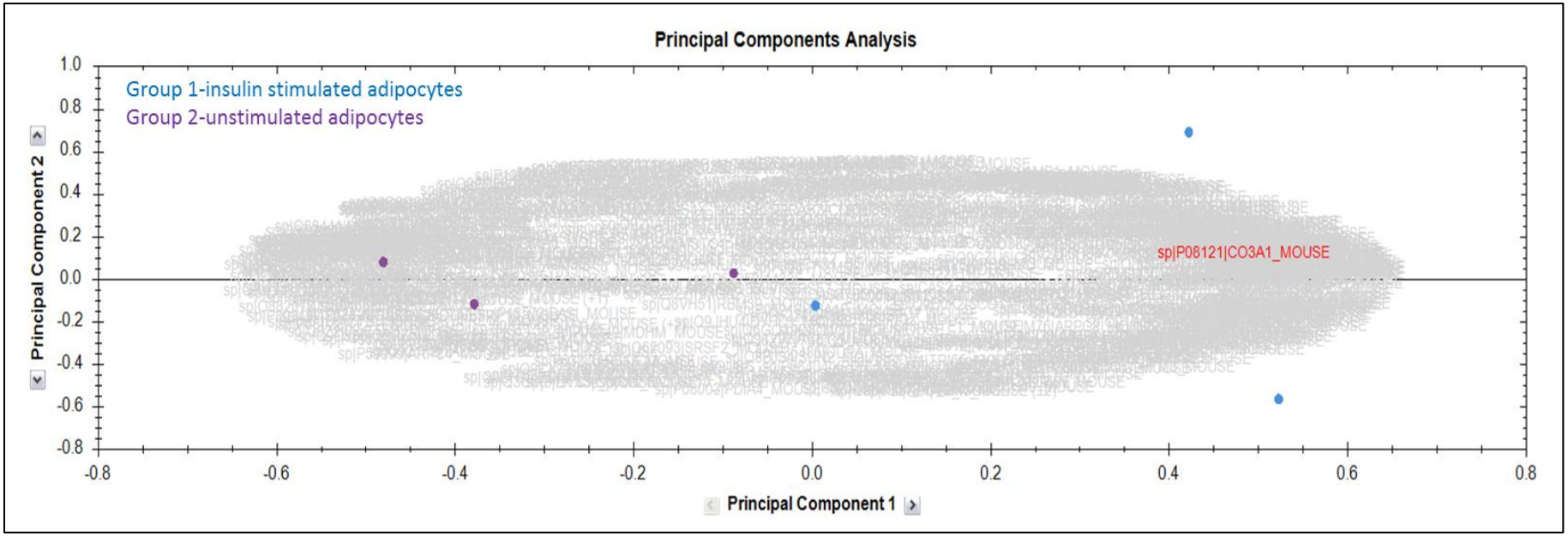

Figure 3.5: Principal component analysis (PCA) distinguishes the silica bead isolated-plasma membrane fraction of insulin stimulated adipocytes and unstimulated adipocytes. Group 1-insulin stimulated adipocytes: blue data points; group 2-unstimulated adipocytes: purple data points.

3.3.3. Changes in the adipocyte plasma membrane proteome during adipogenesis and following acute insulin stimulation

Adipogenesis

Out of the total 562 proteins identified by Progenesis QI, 159 were PM proteins; the rest (403) were classified as cytosolic proteins. A total of 452 proteins were found to be significantly differentially regulated ($q<0.05$) and that included 130 PM proteins, out of which 15 were transporters and 5 were receptors. Out of these 130 PM proteins, 23 were 50% up-regulated and 27 were 50% down-regulated (thresholds: FC>1.5 up-regulated, FC<0.5 down-regulated). A list of these proteins can be found in the accompanying USB as "Appendix 3 Chapter 3".

Insulin stimulation

Progenesis QI detected a total of 534 proteins, 146 were PM proteins; the rest (388) were classified as cytosolic proteins. A total of 90 proteins were found to be significantly differentially regulated ($p<0.05$) and that included 28 PM proteins, out of which 2 were transporters and 2 were receptors. Out of these 28 PM proteins, 4 were 50% up-regulated (thresholds: FC>1.5 up-regulated, FC<0.5 down-regulated). A list of these proteins can be found in the accompanying USB within the chapter 3 folder as "Appendix 6 Chapter 3".

PM proteins represented 28% (n=159) and 27% (n=146) of total proteins identified during adipogenesis and insulin stimulation respectively. The rest (72% (n=403) and 73% (n=388) respectively) were classified as cytosolic proteins. The Cellular Component Gene Ontology annotations for PM proteins detected during adipogenesis and following insulin stimulation are presented in Figure 3.6 and Figure 3.7 respectively.

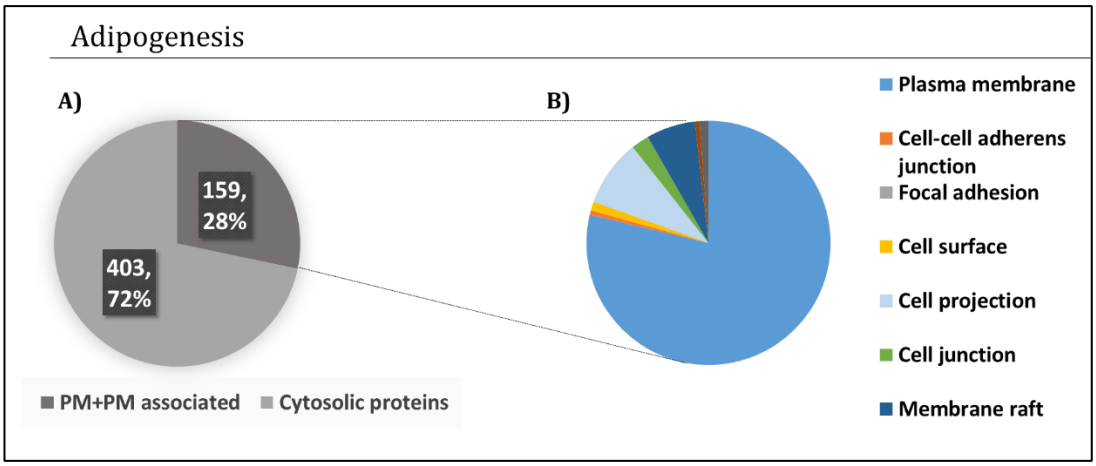

Figure 3.6: Cellular Component Gene Ontology classification of the plasma membrane-enriched fraction isolated by colloidal silica bead isolation during adipogenesis. A) LC-MS/MS analysis of the adipocyte plasma-membrane enriched fraction (enriched by colloidal silica bead isolation) identified 159 (28% of the total proteins identified) plasma membrane proteins during adipogenesis. The remaining 72% (403 proteins) were classified as cytosolic proteins. B) GO Cellular Component annotations performed using the PANTHER protein classification system. Proteins were classified as plasma membrane or plasma membrane-associated proteins based on Cellular Component GO terms.

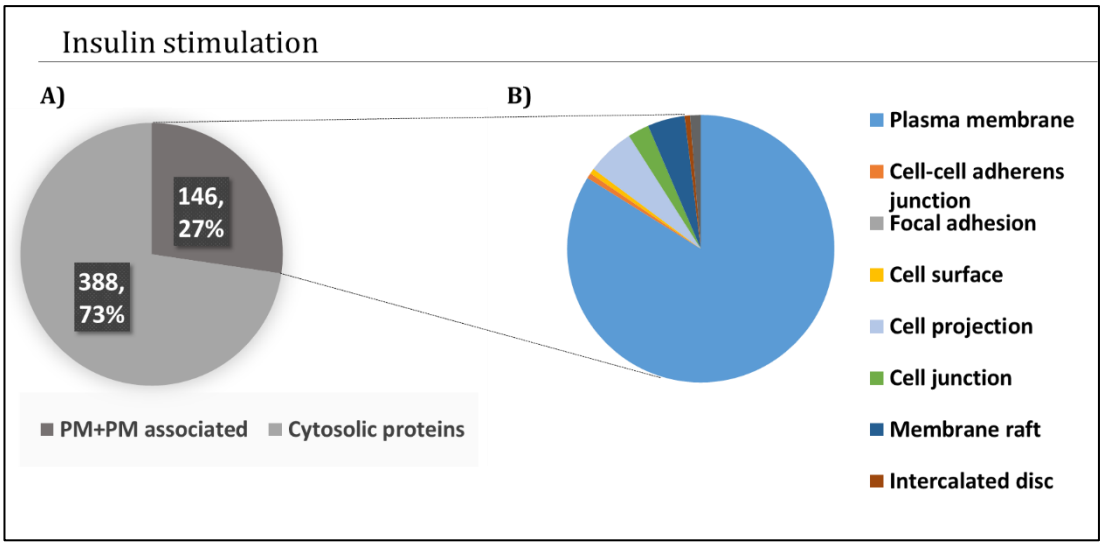

Figure 3.7: Cellular Component Gene Ontology classification of the plasma membrane-enriched fraction isolated by colloidal silica bead isolation following insulin stimulation. A) LC-MS/MS analysis of the adipocyte plasma-membrane enriched fraction (enriched by colloidal silica bead isolation) identified 146 (27% of the total proteins identified) plasma membrane proteins following insulin stimulation. The remaining 73% (388 proteins) were classified as cytosolic proteins. B) GO Cellular Component annotations performed using the PANTHER protein classification system. Proteins were classified as plasma membrane or plasma membrane-associated proteins based on Cellular component GO terms.

GO SLIM analysis for Biological Process (BP) and Molecular Function (MF) annotations were applied to the total number of detected PM proteins during adipogenesis (159 PM proteins) (Figure 3.8). This analysis compared all murine ("Mus Musculus") annotations recorded in the Gene Ontology Consortium database to the list of PM proteins presented in the current study. The most overrepresented BP annotations were: "metabolic process", "primary metabolic process", "localisation" and "transport". The most overrepresented MF annotations were: "catalytic activity" and "hydrolase activity".

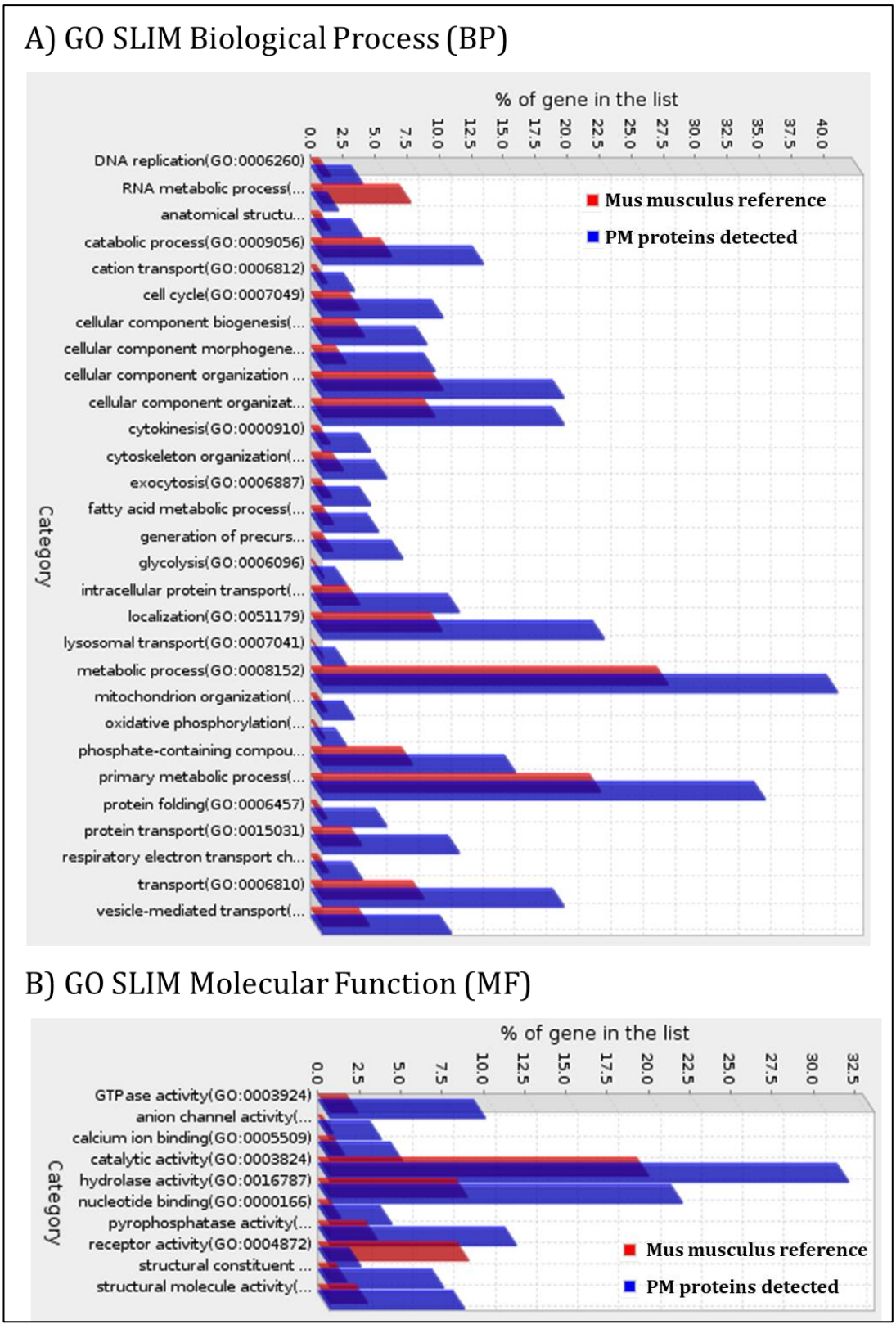

Figure 3.8: Functional classification of the total of detected plasma membrane proteins during adipogenesis based on A) GO "Biological Process" (BP) annotations and B) GO "Molecular Function" (MF) annotations. Significantly differentially regulated plasma membrane proteins detected were functionally characterised based on GOBP and GOMF annotations contained in the Gene Ontology Consortium database. The number of proteins involved in each GO annotation (blue) is

compared to the reference database (red) to observe over or under-representation. Fisher's exact test with FDR multiple test correction was applied and only results for P < 0.05 were considered.

Out of the total of detected PM proteins during adipogenesis, 130 PM proteins were significantly differentially regulated. GO SLIM analysis for “Biological Process” (BP) and “Molecular Function” (MF) analysis was also applied to the significantly differentially regulated PM proteins detected (Figure 3.9).

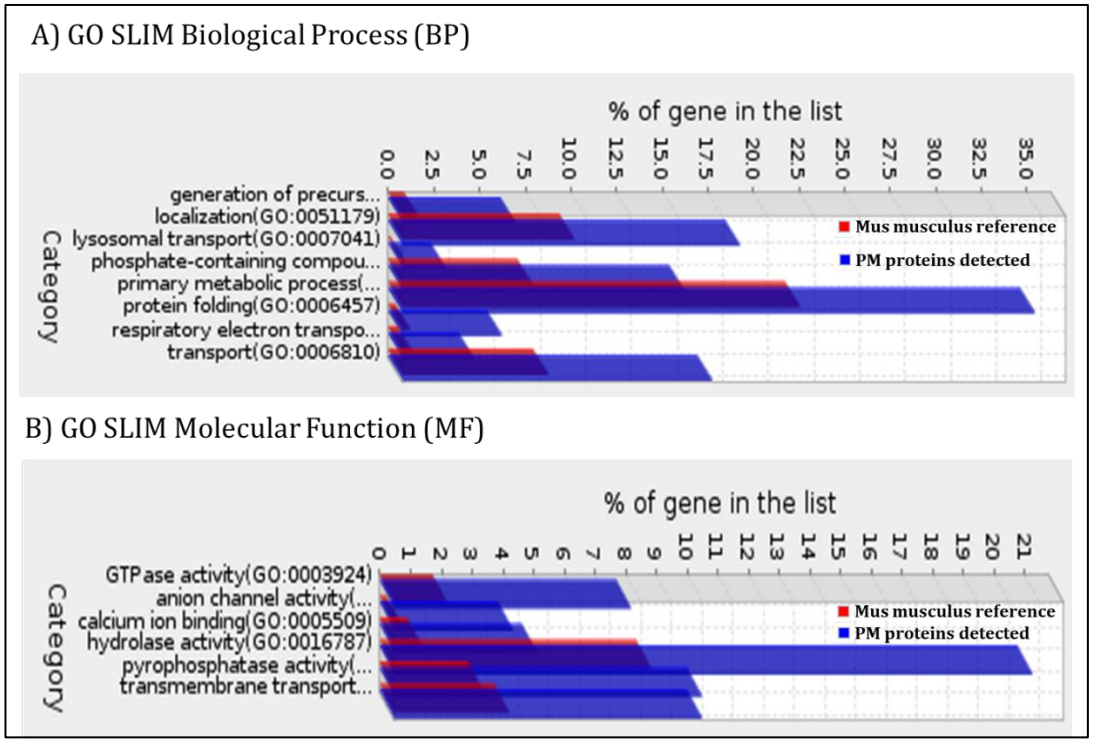

Figure 3.9: Functional classification of plasma membrane proteins significantly differentially regulated during adipogenesis based on A) GO "Biological Process" (BP) and B) GO "Molecular Function" (MF) annotations. Significantly differentially regulated plasma membrane proteins detected during adipogenesis were functionally characterised based on GO BP and GO MF annotations contained in the Gene Ontology Consortium database. The number of proteins involved in each GO annotation (blue) is compared to the reference database (red) to observe over or under-representation. Fisher's exact test with FDR multiple test correction was applied and only results for P < 0.05 were considered.

GO SLIM analysis for Biological Process (BP) and Molecular Function (MF) annotations were applied to the total number of detected PM proteins following insulin stimulation (146 PM proteins) (Figure 3.10). The most overrepresented BP annotations were: “cellular process”, “metabolic process” and “primary

metabolic process". The most overrepresented MF annotations were: "catalytic activity", "hydrolase activity" and "protein binding".

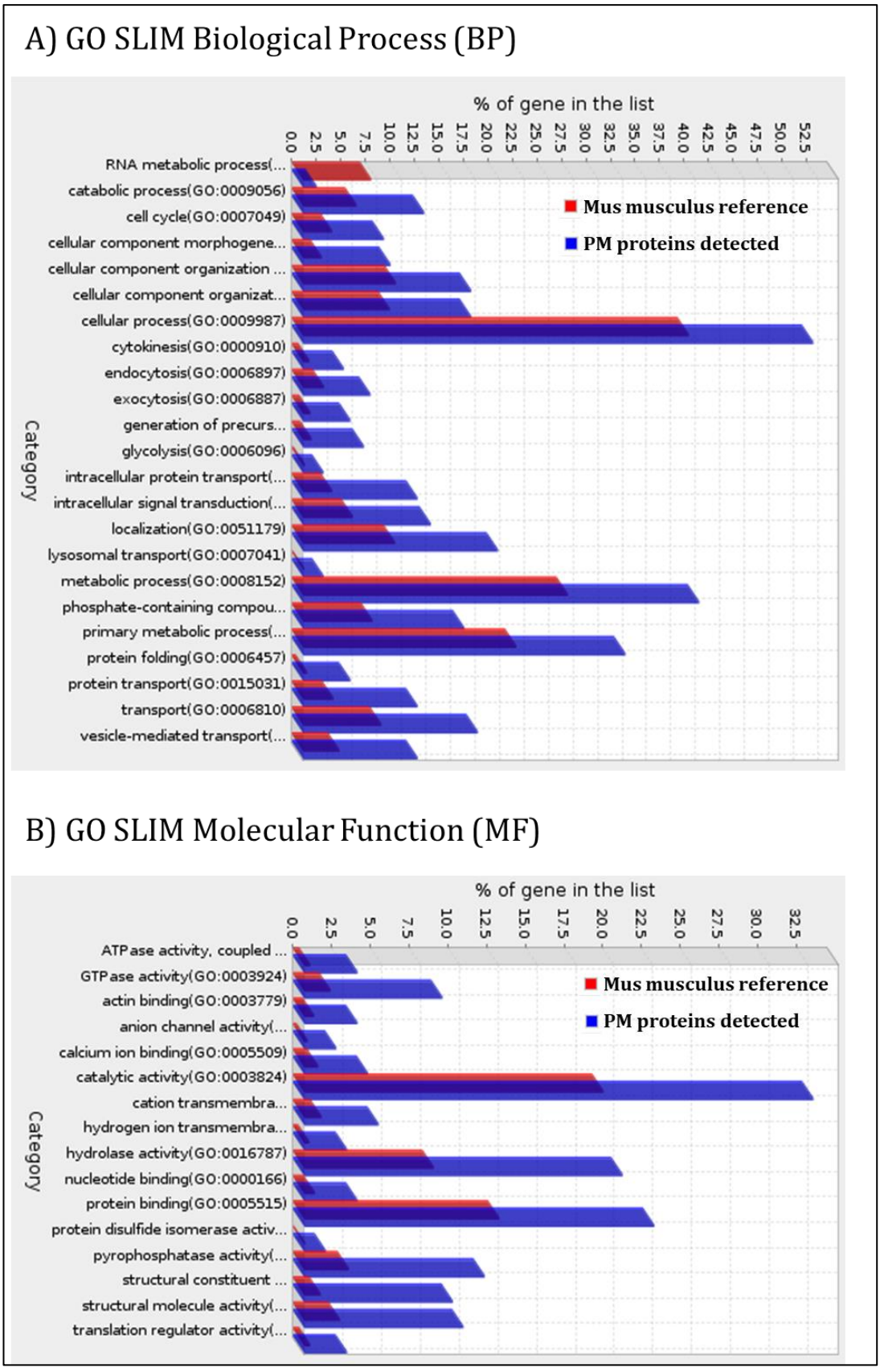

Figure 3.10: Functional classification of the total of detected plasma membrane proteins following insulin stimulation based on A) GO "Biological Process" (BP) annotations and B) GO "Molecular Function" (MF) annotations. Significantly differentially regulated plasma membrane proteins detected were functionally

characterised based on GOBP and GOMF annotations contained in the Gene Ontology Consortium database. The number of proteins involved in each GO annotation (blue) is compared to the reference database (red) to observe over or under-representation. Fisher's exact test with FDR multiple test correction was applied and only results for $P < 0.05$ were considered.

3.3.4. Pathway analysis of significantly differentially regulated plasma membrane proteins during adipogenesis and following insulin stimulation

Pathway analysis was carried out using PANTHER overrepresentation test (Croft *et al.*, 2014) in order to identify the biological pathways in which the significantly differentially regulated PM proteins were involved. Pathway analysis revealed a total of 123 overrepresented pathways for adipogenesis.

Figure 3.11 shows 10 selected pathways out of the 123; a complete list of pathways can be found in the accompanying USB as “Appendix 8 of Chapter 3”.

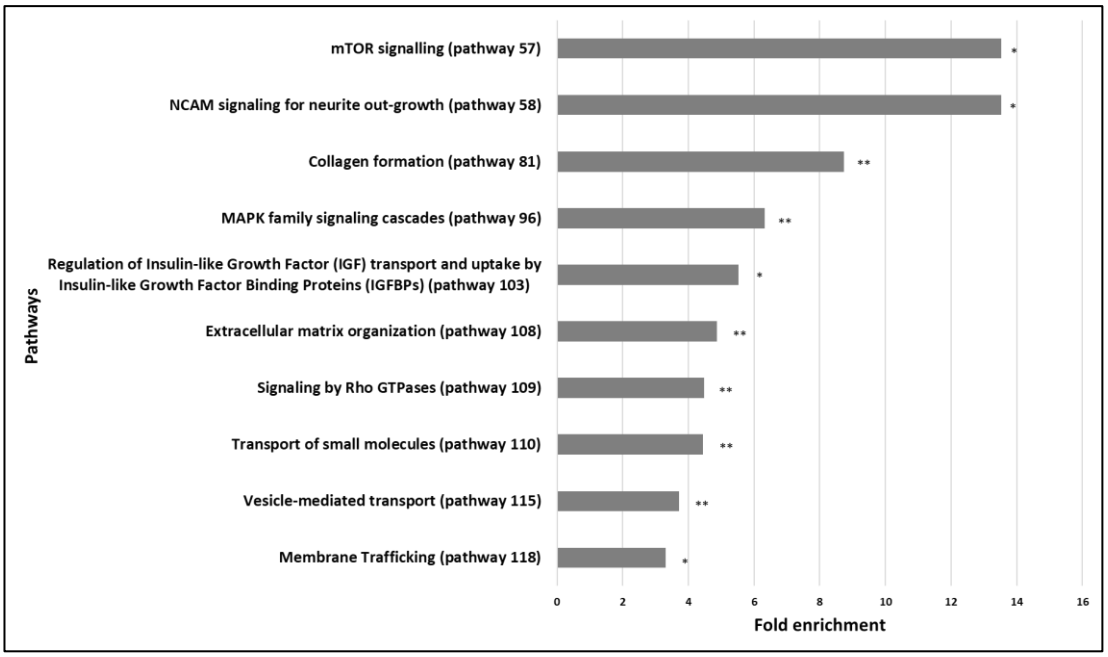

Figure 3.11: Overrepresented pathways involving significantly differentially regulated plasma membrane proteins during adipogenesis of the 3T3-F442A preadipocyte cell line. Fisher's exact test with FDR multiple test correction was applied, ** P ≤0.01 * P ≤0.05.; pathways are ordered by fold enrichment and pathway number is indicated; mTOR: Mechanistic target of rapamycin, NCAM: Neural cell adhesion molecule, MAPK: mitogen activated protein kinases.

For insulin stimulation, pathway analysis of significantly ($p<0.05$, no FDR corrected) differentially regulated PM proteins revealed 4 overrepresented pathways presented in Figure 3.12. A complete list of pathways can be found in the accompanying USB as “Appendix 9 of Chapter 3”.

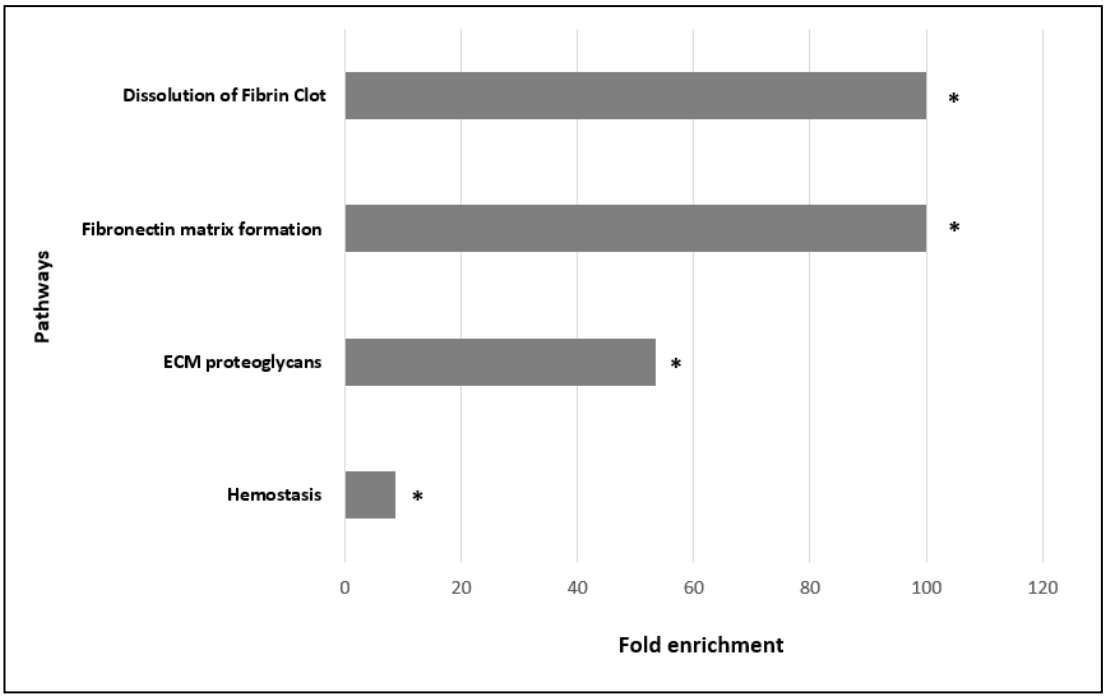

Figure 3.12: Overrepresented pathways involving significantly differentially regulated plasma membrane proteins detected following insulin stimulation of mature 3T3-F442A adipocytes. Fisher's exact test with FDR multiple test correction was applied, ** P ≤0.01 * P ≤0.05; ECM: Extracellular matrix. Network analysis of plasma membrane proteins significantly differentially regulated during adipogenesis and following insulin stimulation

3.3.5. Network analysis of plasma membrane proteins significantly differentially regulated during adipogenesis and following insulin stimulation

Protein-protein interaction networks were generated using STRING (Szklarczyk *et al.*, 2015), in order to observe connections between the differentially regulated PM proteins identified during adipogenesis (Figure 3.13) and following insulin stimulation (Figure 3.14). Additionally, network analysis was performed to observe any crosstalk between these PM proteins and PPARγ and mTOR, which are regulators of adipogenesis and insulin signalling respectively.

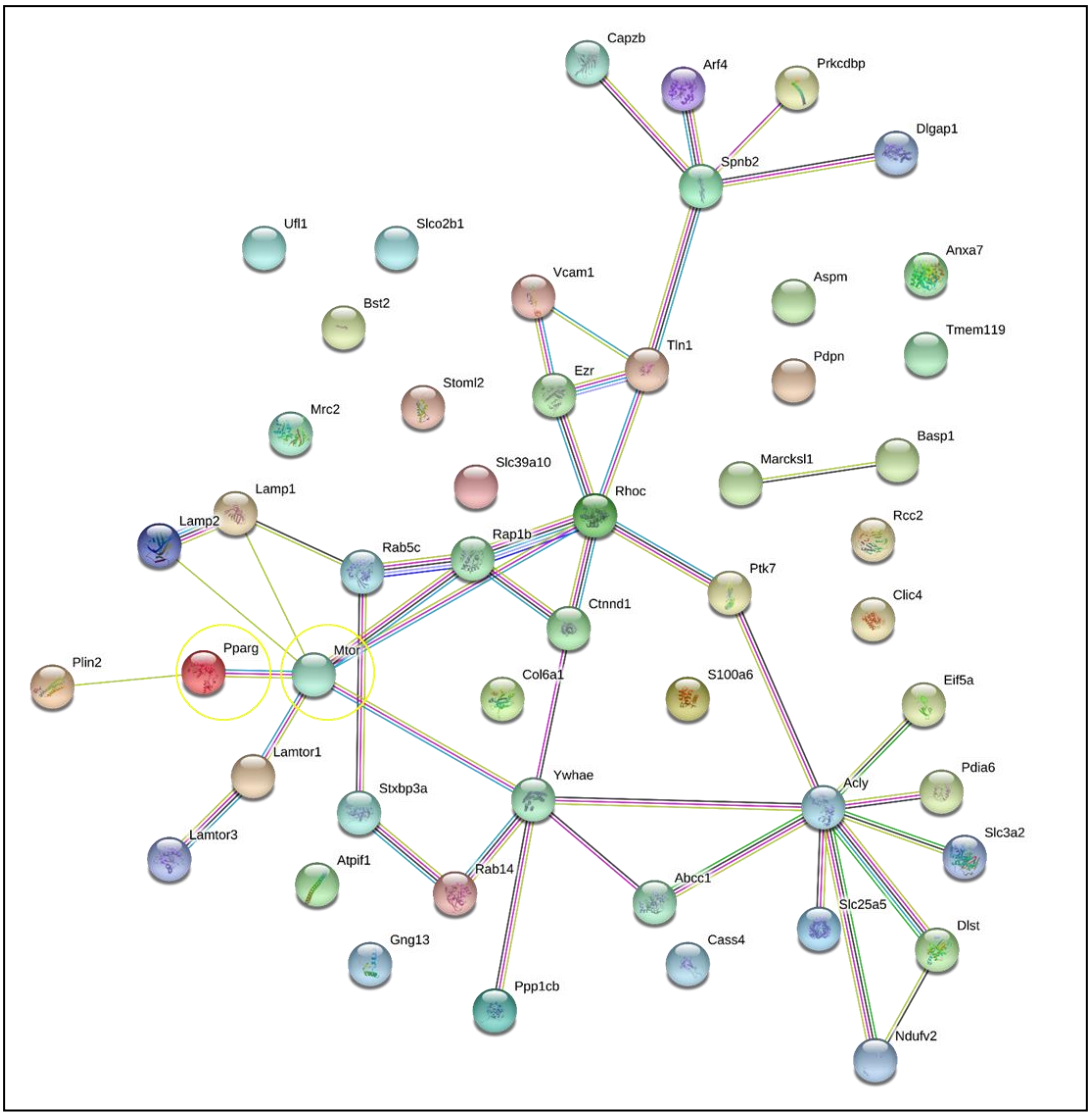

Figure 3.13: Crosstalk between significantly differentially regulated plasma membrane proteins during adipogenesis and their predicted interactions with PPARγ and mTOR. Proteins that showed statistically significant differential abundance and were 50% up- or down-regulated during adipogenesis were imported into the Search Tool for the Retrieval of Interacting Genes database (STRING) version 10.5 (Szklarczyk *et al.*, 2017). Nodes represent individual proteins (annotated by gene names): Capzb, F-actin-capping protein subunit beta; Ywhae, 14-3-3 protein epsilon; Arf4, ADP-ribosylation factor 4; Spnb2, Spectrin beta 2; Abcc1, ATP-binding cassette, sub-family C (CFTR/MRP), member 1; Rcc2, Regulator of chromosome condensation 2; Tln1, Talin 1; Ppp1cb, Protein phosphatase 1, catalytic subunit, beta isoform; Pdia6, Protein disulfide isomerase associated 6; Rhoc, Ras homolog gene family, member C; Vcam1, Vascular cell adhesion molecule 1; Ndufv2, NADH dehydrogenase (ubiquinone) flavoprotein 2; Cass4, Cas scaffolding protein family member 4; Aspm, Asp (abnormal spindle)-like, microcephaly associated; Ufl1, UFM1 specific ligase 1; Lamtor3, Late endosomal/lysosomal adaptor, MAPK and MTOR activator 3; Lamtor1, Ragulator complex protein LAMTOR1; Rab5c, Ras-related protein Rab-5C; Lamp1, Lysosomal-associated membrane protein 1; Ptk7, Inactive tyrosine-protein kinase 7; Eif5a, Eukaryotic translation initiation factor 5A-1; Tmem119, Transmembrane protein 119; Basp1, Brain acid soluble protein 1; Clic4, Chloride intracellular channel protein 4; Pdpn,

Podoplanin; Slco2b1, Solute carrier organic anion transporter family member 2B1; Prkcdbp, Protein kinase C delta-binding protein; Gng13, Guanine nucleotide binding protein (G protein), gamma 13; Col6a1, Collagen alpha-1(VI) chain; S100a6, Protein S100-A6; Lamp2, Lysosomal-associated membrane protein 2; Marcksl1, MARCKS-related protein; Anxa7, Annexin A7; Rab14, Ras-related protein Rab-14; Slc3a2, Solute carrier family 3; Plin2, Perilipin 2; Rap1b, Ras-related protein Rap-1b; Atpif1, ATPase inhibitory factor 1; Dlst, Dihydrolipoamide S-succinyltransferase (E2 component of 2-oxo-glutarate complex); Stoml2, Stomatin-like protein 2; Ezr, Ezrin; Dlgap1, Disks large-associated protein 1; Acly, ATP-citrate synthase; Stxbp3a, Syntaxin binding protein 3A; Slc25a5, ADP/ATP translocase 2; Slc39a10, Zinc transporter ZIP10; Bst2, Bone marrow stromal cell antigen 2; Mrc2, Mannose receptor, C type 2; Ctnnd1, Catenin delta 1; Pparg, Peroxisome proliferator activated receptor gamma; Mtor, Mechanistic target of rapamycin (serine/threonine kinase). Links between proteins are colour coded and provide different information: known interactions from curated databases (Light blue), known interactions experimentally determined (purple), predicted interactions based on gene neighborhood (green), predicted interactions based on gene fusions (red), predicted interactions based on gene co-occurrence (dark blue), textmining (light green), co-expression (black), protein homology (light purple). mTOR and PPARγ entries were added to the network to observe their interactions with differentially regulated proteins (highlighted in yellow). No additional interactions were added.

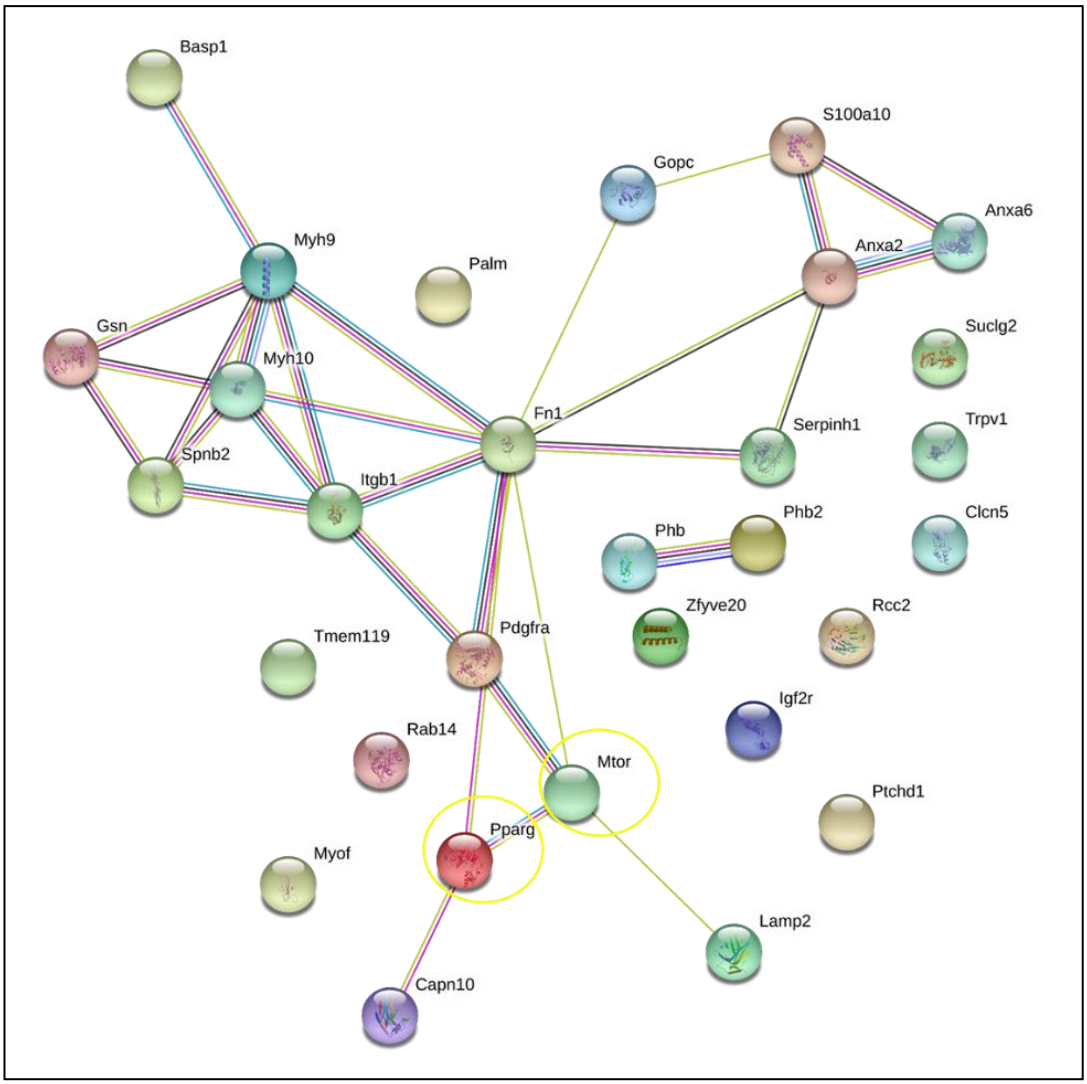

Figure 3.14: Crosstalk between significantly differentially regulated plasma membrane proteins identified following insulin stimulation and their predicted interactions with PPARγ and mTOR. Proteins that showed significant differential abundance (before applying correction for multiple testing) were imported into the Search Tool for the Retrieval of Interacting Genes database (STRING) version 10.5 (Szklarczyk *et al.*, 2017). Nodes represent individual proteins (annotated by gene names): Palm, Paralemmin-1; Basp1, Brain acid soluble protein 1; Transmembrane protein 119; Pdgfra, Platelet derived growth factor receptor, alpha polypeptide; Trpv1, Transient receptor potential cation channel, subfamily V, member 1; Ptchd1, Patched domain containing protein 1; Lamp2, Lysosomal-associated membrane protein 2; Gsn, Gelsolin; Rab14, Ras-related protein Rab-14; Anxa6, Annexin A6; Zfyve20, Zinc finger; Phb, Prohibitin; Anxa2, Annexin A2; Rcc2, Protein RCC2; Igf2r, Insulin-like growth factor 2 receptor; Clcn5, H(+)/Cl(-) exchange transporter 5; Capn10, Calpain-10; Suclg2, succinate-Coenzyme A ligase, GDP-forming, beta subunit; S100a10, Protein S100-A10; Myof, Myoferlin; Itgb1, Integrin beta 1; Gopc, Golgi associated PDZ and coiled-coil motif containing protein; Myh9, Myosin-9; Spnb2, Spectrin beta 2; Myh10, Myosin-10; Fn1, Fibronectin 1; Phb2, Prohibitin 2; Serpinh1, Serine (or cysteine) peptidase inhibitor, clade H, member 1; Mtor, Mechanistic target of rapamycin (serine/threonine kinase); Pparg, Peroxisome proliferator activated receptor gamma. Links between proteins are colour coded and provide different information: known interactions from curated databases (Light blue), known interactions experimentally determined (purple),

predicted interactions based on gene neighborhood (green), predicted interactions based on gene fusions (red), predicted interactions based on gene co-occurrence (dark blue), textmining (light green), co-expression (black), protein homology (light purple). mTOR and PPARγ entries were added to the network to observe their interactions with differentially regulated proteins (highlighted in yellow). No additional interactions were added.

3.3.6. Comparison of total proteins detected between this study and Prior et al´s study following insulin stimulation

In their study, Prior *et al.*, (2011) performed an analysis of the PM proteome of 3T3-L1 adipocytes following acute insulin stimulation using a concentration of 100 nM insulin for 20 minutes. For this thesis, 3T3-F442A adipocytes were stimulated with 200 nM insulin for 20 minutes and analysed the adipocyte PM proteome. Prior *et al*., (2011) reported a total yield of 413 proteins in the PM-enriched fraction; a total of 534 proteins were detected in the PM-enriched fraction obtained using colloidal silica bead isolation (Figure 3.15). Both studies shared 60 proteins in common; A total of 474 proteins not reported by Prior *et al.*, (2011) were detected. A complete list of proteins can be found in the accompanying USB as "Appendix 10 Chapter 3. Comparison of proteins detected following insulin stimulation to Prior *et al.,* (2011)"

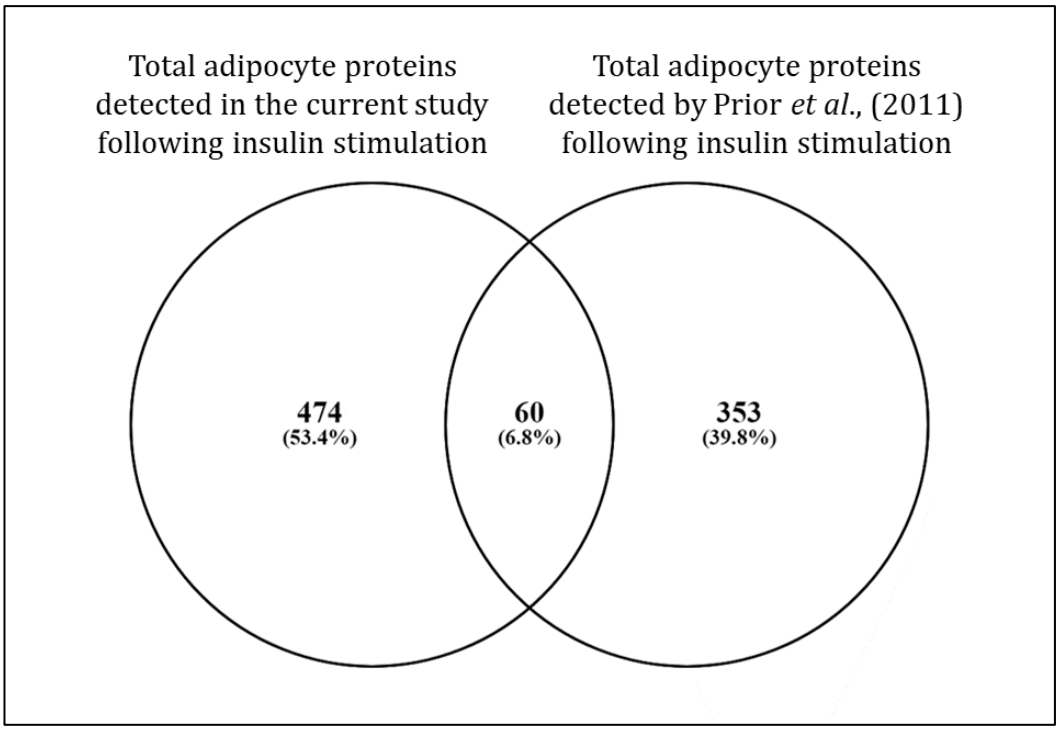

Figure 3.15. Comparison of total detected proteins in the PM-enriched fraction following insulin stimulation by Prior *et al.*, (2011) and the current study.

3.3.7. Comparison of PM proteins detected between this study and Prior et al´s study following insulin stimulation

The number of detected PM proteins by Prior *et al.*, (2011) in the PM-enriched fraction following acute insulin stimulation was 74, whereas our study detected a total of 146 PM proteins. The two studies had only 5 proteins with our study identifying 141 PM proteins that were not reported by Prior *et al.*, (2011) following acute insulin stimulation (Figure 3.16). A complete list of proteins can be found in the accompanying USB as "Appendix 10 Chapter 3. Comparison of proteins detected following insulin stimulation to Prior *et al.*, (2011)".

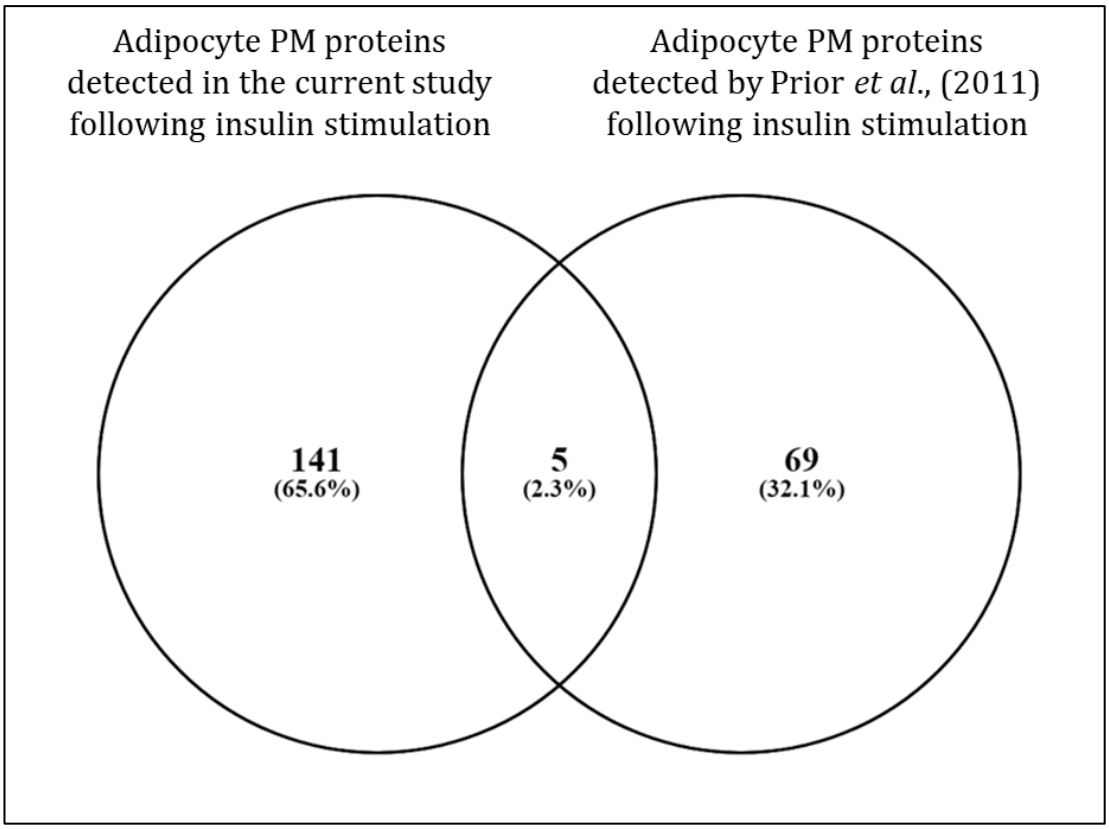

Figure 3.16. Comparison of detected PM proteins following insulin stimulation by Prior *et al.*, (2011) and the current study.

3.4. DISCUSSION

Various studies have applied proteomics to investigate adipogenesis (Kratchmarova *et al.*, 2002; Choi *et al.*, 2004; Welsh *et al.*, 2004; DeLany *et al.*, 2005; Lee *et al.*, 2006; Kamal *et al.*, 2013), but only a few of them have focused on changes in adipocyte PM proteins (Aboulaich *et al.*, 2004; Prior *et al.*, 2011). The present study examines the adipocyte PM proteome during: 1) adipogenesis and, 2) following acute insulin stimulation. This study has combined enrichment of PM proteins by colloidal silica bead isolation followed by detection of proteins using LC-MS/MS. The 3T3-F44A2 preadipocyte cell line was used as a murine *in vitro* model for the study of adipogenesis and insulin signalling.

Progenesis QI was the software of choice for label-free relative protein quantitation, as it has been used for this purpose in a number of publications on PM proteomics (Li *et al.*, 2012; Takahashi *et al.*, 2012, 2013; Bi *et al.*, 2015; Gutierrez-Carbonell *et al.*, 2016; Sidhu *et al.*, 2016).

In spite of the low abundance of PM proteins observed in proteomic experiments and the difficulty of their detection by mass spectrometry, the experimental design presented in the current study was able to detect 159 PM proteins for adipogenesis (28% of the total detected), and 146 PM proteins in mature adipocytes undergoing acute insulin stimulation (27% of the total proteins detected). 130 PM proteins were significantly differentially regulated during adipogenesis and out of these, 15 were transporters and ion channels and 5 were receptors. For mature adipocytes undergoing insulin stimulation, 28 significantly differentially regulated PM proteins were detected, and out of these, 2 were transporters and channels and 2 were receptors.

"Molecular function" GO analysis of the PM proteins significantly differentially regulated during adipogenesis revealed that the majority of these proteins were involved in catalytic and hydrolase activity; this was consistent with previous findings in other studies (Prior *et al.*, 2011; Renes *et al.*, 2013). In terms of "biological process" GO terms, most proteins were classified under metabolic processes, thus correlating with the role of adipose tissue in regulating metabolic homeostasis. PM proteins were also classified under the transport category, a key function of the PM, which comprises a high amount of transporter proteins.

Amongst the differentially regulated PM proteins detected during adipogenesis in the current study, key regulators of adipocyte differentiation were found, such

as RACK1 and ezrin, proteins with a role in adipogenesis identified by Kong *et al.*, (2016) and Titushkin *et al.*, (2013) respectively. In addition, some of these PM proteins were associated to metabolic disease, such as perilipin-2, ezrin and prohibitin-2. Prohibitin-2 has been associated with obesity (Ande *et al.*, 2014), ezrin dysfunction has been linked to diabetes and cardiovascular disease (Huang, 2012), and perilipin-2 has been linked to obesity, adipose tissue inflammation and fatty liver disease (McManaman *et al.*, 2013; Takahashi *et al.*, 2016). mRNA levels of perilipin-2 increase during adipogenesis, however, protein levels decrease during adipogenesis, and this was consistent with results presented in the current study (Brasaemle *et al.*, 1997; Takahashi *et al.*, 2016).

The current study also detected PM proteins that had not been previously reported in adipogenesis. An example was zinc transporter ZIP10 (Slc39a10); a 2-fold downregulation of this transporter was found in adipocytes when compared to preadipocytes. This particular transporter has been previously associated with breast cancer invasiveness but not with metabolic disease. However, zinc transporters have been previously associated with insulin resistance and T2DM (Fukunaka *et al.*, 2017; Norouzi *et al.*, 2017), and other members of this transporter family such as ZIP13 (SLC39A13) and zinc transporter 7 (SLC30A7) have been linked to metabolic toxicity. ZIP13 has been shown to inhibit biogenesis of beige adipocytes (Fukunaka *et al.*, 2017), whereas, increased expression of zinc transporter 7 led to disruption of insulin signalling, glucose uptake and lipid accumulation during adipogenesis of 3T3-L1 cells (Tepaamorndech *et al.*, 2016). Other examples of proteins not previously associated to adipogenesis were disks large-associated protein 1 and Podoplanin; the former has been associated with HIV-related lipoatrophy (Norouzi *et al.*,

2017), and the latter is known to participate in the hemostasis pathway and to play a role in platelet activation and aggregation. Podoplanin also regulates adherence to the ECM in fibroblast reticular cells, and this may explain the up-regulation of this protein in preadipocytes compared to mature adipocytes observed in the current study (Cueni *et al.*, 2009). A number of overrepresented pathways involving significantly differentially regulated PM proteins were identified; some of these pathways were characteristic of adipogenesis, such as pathways linked to ECM organization and degradation (Renes *et al.*, 2013), MAPK family signalling cascades, and Regulation of Insulin-like Growth Factor (IGF) transport (Bost *et al.*, 2005). ECM remodelling is triggered by insulin and is a key process for adipogenesis. Mature adipocytes invest a lot of energy in ECM maintenance and, in obesity states in which adipocytes are hypertrophic, ECM stability is compromised (Mariman *et al.*, 2010). MAPKs play a role in both normal and pathogenic adipogenesis (Bost *et al.*, 2005); in fact, prolonged activation of MAPKs leads to obesity and the knockout of MAPK3 improved insulin resistance in mice (Guo, 2014). IGF regulates insulin signalling in the first stages of adipogenesis because preadipocytes present more receptors for IGF than for insulin compared to differentiated adipocytes, and this is reverted as adipogenesis progresses (Rosen and MacDougald, 2006). The NCAM signalling pathway was also overrepresented, and NCAM has been recently found to be a key regulator of adipogenesis (Yang *et al.*, 2011).

Collagen VI was observed to be up-regulated in mature adipocytes compared to preadipocytes in the current study, and this was also reported by Renes *et al.* (2013). Previous studies identified collagens to be differentially regulated in adipocytes in response to insulin (Prior *et al.*, 2011) and during adipogenesis

(Ibrahimi *et al.*, 1992; Tseng *et al.*, 2005; Mariman *et al.*, 2010; Renes *et al.*, 2013); hence the overrepresentation of collagen formation pathway in the currentstudy makes sense.

Rho GTPases signalling pathway was found to be overrepresented; Rho GTPases are known to exhibit anti-adipogenic activity and they have to be inhibited in the early stages of adipogenesis for normal differentiation. Other pathways of interest identified in the current study were pathways related to transport (e.g. membrane trafficking, and transport of small molecules); insulin signalling pathways such as mTORC1-mediated signalling (mTOR is a key mediator of insulin signalling), and vesicle-mediated transport, which is key for insulin-mediated transport of GLUT4 to the PM (Adachi *et al.*, 2007).

PM proteins significantly differentially regulated during adipogenesis were also found to interact with PPARγ and mTOR, two key regulators of adipogenesis and insulin signalling respectively.Known associations were found, such as the one between Perilipin-2 and PPARγ (PPARγ is the key mediator in adipogenesis and expression of Perilipin-2 is one of the earliest events in adipogenesis) (McManaman *et al.*, 2013; Takahashi *et al.*, 2016), and similarly between mTOR and YWHAE (14-3-3 protein epsilon). 14-3-3 proteins have been previously linked to mTOR and they have been proposed as potential therapeutic targets for diabetes, obesity and cardiovascular disease (Kleppe *et al.*, 2011; Kim *et al.*, 2013). This further assures the validity of results presented in the current study.

Identification of PM proteins that are differentially regulated following insulin stimulation was attempted; however, none of the proteins stood correction for multiple testing ($q \leq 0.05$). This may be because innadecuate stimulation of

adipocytes with insulin (20 minutes, 200 nM), or the failute to collect the lysates at the optimal time point. Longer incubation times, or collection of lysate at a different time point (possibly within the first 10 minutes of stimulation) may be required to induce a significant change in PM protein expression levels and detect this. Even though none of the PM proteins identified satisfied statistical significance on correction for multiple testing, pathway and network analysis was performed for those identified.

Higher variability between samples from the same cluster was observed in the PCA analysis for the insulin stimulation experiment compared to PCA analysis of the adipogenesis experiment. The separation between the replicates was more evident for the adipogenesis experiment than for the insulin stimulation experiment. This may be due to the fact that for the adipogenesis experiment the software compared two different types of cells (preadipocytes vs adipocytes), whereas for the insulin stimulation experiment the same type of cells (mature adipocytes) were compared, relying only on acute insulin stimulation to cause a difference in protein expression.

Following insulin stimulation of mature adipocytes, it was observed that the main overrepresented pathways in which differentially regulated PM proteins participated involved ECM remodelling (Fibronectin matrix formation, ECM proteoglycans, dissolution of Fibrin clot and Hemostasis pathways). Within these pathways proteins such as fibronectin, a main component of the ECM together with elastin, laminin and different types of collagen, and integrin beta-1 (integrins are PM proteins serving as connectors of the ECM to the actin cytoskeleton) were found to be sigficantly differentially regulated. The density of

the ECM has been proven to regulate insulin sensitivity and adiponectin (insulin sensitising adipokine) secretion in adipocytes; the higher the density of the ECM the less responsive adipocytes were to insulin and less was the amount of adiponectin secreted by adipocytes (Li *et al.*, 2010).

Fibronectin and integrin beta-1 were linked in network analysis. A study by Alghadir *et al.*, (2016) observed increased levels of fibronectin in T2DM patients and reported a reduction in fibronectin levels and improved insulin sensitivity after aerobic exercise. The current study observed a slight decrease (less than 50% downregulation) in fibronectin levels upon acute insulin stimulation consistent with previous studies. Integrin beta-1 gene (*Itgb1*) was found to be significantly induced in white adipose tissue (WAT) of obese individuals (Henegar *et al.*, 2008). These results are consistent with previous studies and highlight the importance of ECM proteins in the insulin signalling pathway of adipocytes, as well as their role in obesity and insulin resistance (Wang *et al.*, 2006; Henegar *et al.*, 2008; Li *et al.*, 2009, 2010; Mariman *et al.*, 2010; Williams *et al.*, 2015).

Transport of GLUT4 to the PM following insulin stimulation is an important event for glucose transport into the adipocytes. Although GLUT4 itself was not detected during mass spectrometry analysis, PM proteins that are involved in GLUT4 translocation and glucose homeostasis were found in the current study. These included RAB14 (Dugani *et al.*, 2005; Reed *et al.*, 2013) and prohibitin-2, which was significantly upregulated in the current study; incidentally both these proteins have been previously associated with obesity and alteration of glucose homeostasis (Ande *et al.*, 2014).

Following acute insulin stimulation, A number of proteins that were previously not reported to play a role in insulin signalling were found (Figure 3.16) and 141 PM proteins that were not identified by Prior *et al.*, (2011) were detected. Interestingly, the two most significantly regulated PM proteins observed following insulin stimulation were: paralemmin-1 (PALM) and brain acid soluble protein 1 (BASP1); however, these were not found to be part of any overrepresented pathway. In addition, network connections linking PALM to mTOR, PPARγ or any other PM proteins identified to be differentially regulated were not observed. However, it is interesting to notice that BASP1 is known to be secreted from human adipocytes during adipogenesis (Zhong *et al.*, 2010), and its expression is thought to be a genetic predictor of obesity (Gibson *et al.*, 2016). PALM is a phosphoprotein involved in PM dynamics and cell shape control, particularly in the stabilization of PM. To date, no studies on the role of PALM in adipocytes or insulin signalling have been published; however, it has been observed to be upregulated in fibroblasts, neurons and other elongated cells, and is thought to participate in the maintenance of "extreme" plasma membrane shape and conferring protection from membrane blebbing (Kutzleb *et al.*, 2006; Albrecht *et al.*, 2013). Findings presented in the current study suggest that remodelling of cell shape and ECM re-organisation were relevant processes which take place during insulin stimulation of mature adipocytes. Future research is now required to understand the role of these proteins in this pathway.

The current study suffers some limitations: certain important PM proteins for adipogenesis and glucose homeostasis such as NHE6, adiponectin receptors (ADIPOR1 and ADIPOR2), GLUT4 and IR were not identified. Interestingly, expression of IR (Figure 2.3) and GLUT4 (Appendix 9 of Chapter 4) was detected

in the silica bead isolated PM fraction, as well as other PM proteins which will be presented in the next chapters (NCAM and NKCC1). However, these proteins were not detected when analysed by mass spectrometry. This may be due to the limitations of mass spectrometry in detecting low abundant PM proteins even after enrichment. Even though Prior *et al.*, (2011) detected GLUT4 and NHE6 in their PM fraction (also isolated by colloidal silica beads) after mass spectrometry analysis, it is important to note that their study not only used silica bead isolation, but also GLUT4 Vesicle Immunoadsorption and SILAC. The combination of various enrichment techniques may have led to a higher yield of PM proteins and to the detection of PM proteins that are vesicle-transported, such as GLUT4 and NHE6. Future studies may build on the presented methodology and incorporate other techniques such as employed by Prior *et al*., (2011) and further improve the detection of PM proteins.

In summary, this chapter presents a comprehensive proteomic analysis of the adipocyte PM during adipogenesis and following acute insulin stimulation. LC-MS/MS label-free relative quantitation analysis identified differentially regulated PM proteins known to play a role in adipogenesis and insulin signalling; novel PM proteins that may be important in these two processes were also identified. Amongst the overrepresented pathways, key biological pathways for adipocytes and insulin signalling were identified, which correlated with published literature. In addition, a number of interactions were predicted between the differentially regulated PM proteins and PPARγ and mTOR. Taken together, these findings highlight the importance of PM proteins in adipocyte biology and metabolic homeostasis; these proteins could also be associated with the development of metabolic disease sequelae, such as obesity, type 2 diabetes and insulin

resistance which arise as a result of a number of reasons including drug treatment and further discussed in subsequent chapters.

The next chapter will apply this chapter's experimental methodology for the investigation of the effect of antiretroviral drugs (protease inhibitors) on the adipocyte PM proteome.

CHAPTER 4
EFFECT OF HIV PROTEASE INHIBITORS ON THE ADIPOCYTE PLASMA MEMBRANE PROTEOME

4.1. INTRODUCTION

4.1.1. HIV protease inhibitors and metabolic toxicity

The association between HIV protease inhibitors and metabolic disease has been clearly established (Hruz *et al.*, 2001; Jericó *et al.*, 2005; Magkos *et al.*, 2011; Martin *et al.*, 2013; Zha *et al.*, 2013; Patel *et al.*, 2018; Tanaka *et al.*, 2018). Specifically, the lopinavir/ritonavir combination has been strongly linked to metabolic syndrome (Noor *et al.*, 2006; Tanaka *et al.*, 2018). Importantly, ART-induced comorbidities such has dyslipidaemia, insulin resistance, hypertension and abnormal fat distribution (lipodystrophy), are risk factors for CVD in the long term (Jericó *et al.*, 2005). The mechanism of action of PIs can be found in Figure 1.2 in section 1.1.6 of the general introduction.

Lopinavir is a first-generation PI and, when chronically administered, it leads to the onset of lipodystrophy, dyslipidaemia and contributes to the development of CVD (Worm *et al.*, 2010; Hemkens *et al.*, 2014; Tanaka *et al.*, 2018). HIV-associated lipodystrophy affects up to 50% of patients under HAART and it complicates the management of the disease due to its associated cardiovascular complications (Martin *et al.*, 2013). The metabolic profile of HIV-Infected African children on lopinavir/ritonavir treatment was compared to those who switched to a nevirapine antiretroviral therapy (Arpadi *et al.*, 2013); children treated with lopinavir/ritonavir had lower high-density lipoprotein (HDL), and higher total cholesterol, low-density lipoprotein (LDL) and triglycerides compared to the nevirapine-treated ones, with 8.4% of patients presenting with lipodystrophy (Arpadi *et al.*, 2013).

Atazanavir is a second generation protease inhibitor which exhibits a relatively favourable metabolic impact in HIV patients when compared to lopinavir under chronic usage (Minami *et al.*, 2011; Aberg *et al.*, 2012). It resulted in a lower risk of CVD (LaFleur *et al.*, 2017), and a lower impact on hyperglycaemia and glucose uptake compared to lopinavir (Noor *et al.*, 2006; Stanley *et al.*, 2009; Hemkens *et al.*, 2014). Patients treated with atazanavir presented with reduced risk of developing T2DM (Spagnuolo *et al.*, 2017). An improvement in lipodystrophy has also been associated with atazanavir regimens, showing a reduction of abdominal and dorsocervical fat accumulation in patients (Haerter *et al.*, 2004).

4.1.2. Metabolic effects of lopinavir and atazanavir on the adipocyte

Although the mechanisms by which PIs cause metabolic toxicity are not yet fully elucidated, disturbances in the adipocyte differentiation process (adipogenesis), adipokine secretion, cell survival, oxidative stress and other cellular abnormalities caused by these drugs have been reported (Pacenti *et al.*, 2006; Minami *et al.*, 2011; Pushpakom *et al.*, 2018).

In their study, Minami *et al.*, (2011) compared the effect of four different classes (integrase inhibitors, NRTIs, NNRTIs and PIs) of antiretrovirals on adipogenesis. By using an *in vitro* 3T3-L1 preadipocyte cell line, they found each of these drugs to be associated with different metabolic effects with each class having different impact on lipid accumulation and adipogenesis. Whilst atazanavir had no effect on adipocyte lipid accumulation during adipogenesis, lopinavir significantly reduced lipid accumulation. Moreover, lopinavir inhibited the expression of key adipogenic regulators such as the PPARγ, C/EBP-α, and SREBP-1c with minimal effect observed with atazanavir (Minami *et al.*, 2011).

Lopinavir is a known inhibitor of adipogenesis *in vitro* (Pacenti *et al.*, 2006; Minami *et al.*, 2011; Zha *et al.*, 2013; Pushpakom *et al.*, 2018). Exposure to lopinavir reduced the number of differentiating adipocytes and decreased the expression of adipogenic genes (*Mrap*, *Cd36* and *G0s2*) while increasing the expression of genes involved in the Wnt signalling pathway (which inhibits adipogenesis) (Rosen and MacDougald, 2006). Furthermore, lopinavir has been shown to induce ER stress and to impair autophagy in adipocytes (Zha *et al.*, 2013). It has also been shown to cause oxidative stress in both differentiated and undifferentiated adipocytes by inducing the expression of superoxide dismutase (SOD) and 8-hydroxy-2' -deoxyguanosine (8-OHdG), biomarkers of oxidative stress. Atazanavir on the other hand, did not increase the expression of any of these biomarkers in undifferentiated or differentiated 3T3-L1 adipocytes (Minami *et al.*, 2011).

4.1.3. Metabolic effects of telmisartan on adipocytes

Telmisartan (Figure 4.1) is an angiotensin receptor blocker and a partial agonist of PPARγ, and it is clinically used to treat hypertension. Telmisartan has been reported to have a beneficial effect on the metabolism of HIV patients, lowering blood pressure and improving both lipid and glucose metabolism. It also protected against insulin resistance and reduced the levels of cystatin C, a risk marker for CVD (Vecchiet *et al.*, 2011; Lake *et al.*, 2013). It has been proposed as a first-choice drug to treat hypertension for patients undergoing HAART (Vecchiet *et al.*, 2011). Some of the beneficial effects of telmisartan, such as improvement of glucose and lipid metabolism may be linked to PPARγ activation, but others such as cholesterol reduction have not been completely clarified

(Vecchiet *et al.*, 2011). The deleterious metabolic effects caused by lopinavir have been shown to be reversed by telmisartan in the *in vitro* 3T3-F442A adipocyte cell line (Pushpakom *et al.*, 2018). Therefore, it was included in this study to investigate how telmisartan will affect changes induced by lopinavir on the adipocyte proteome. Whether telmisartan does lead to reduction in insulin resistance in HIV patients treated with HAART is currently being tested in a phase II clinical trial (Pushpakom *et al.*, 2015).

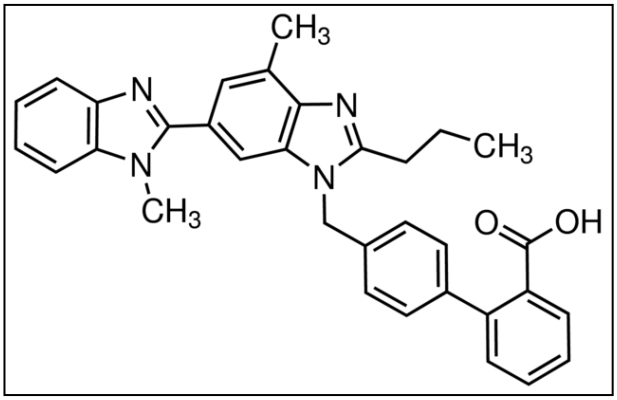

Figure 4.1: Chemical structure of telmisartan.

4.1.4. HIV PIs and adipocyte proteomics

HIV protease inhibitors have been shown to interact and modify the expression of key proteins involved in adipocyte biology, such as GLUT4 (Hresko *et al.*, 2011). As previously discussed, GLUT4 is translocated to the PM of adipocytes following exposure of adipocytes to insulin. The GLUT4 translocation process is explained in more detail in Figure 1.9. Lopinavir is known to disrupt insulin signalling, and several molecular mechanisms have been proposed, such as: 1) inhibition of GLUT4 translocation to the PM of adipocytes following insulin stimulation; 2) inhibition of tyrosine phosphorylation of IRS1; and, 3) up-regulation of protein tyrosine phosphatase 1B (PTP1B) expression (Kitazawa *et al.*, 2014; Wang *et al.*, 2015). Atazanavir has been shown not to affect the expression of GLUT4 at

therapeutic doses and it has been reported not to interfere with glucose uptake *in vitro* or *in vivo* (Noor *et al.*, 2004; Hresko *et al.*, 2011).

Another important protein for adipocyte biology is the secreted adipokine adiponectin, which is an insulin sensitiser (Kadowaki *et al.*, 2006). A recent study observed reductions in circulating adiponectin levels in wild type mice treated with lopinavir/ritonavir (Dasuri *et al.*, 2016). However, this reduction was not observed in mice treated with lopinavir/ritonavir which had been genetically modified to overexpress adiponectin. The metabolic adverse effects caused by lopinavir (lipodystrophy, hyperglycemia and hyperinsulinemia) were diminished in mice overexpressing adiponectin; this highlighted the crucial role of this protein in the maintenance of metabolic homeostasis (Dasuri *et al.*, 2016). Atazanavir did not interfere with adiponectin secretion in subcutaneous and omental human adipocytes (Jones *et al.*, 2008).

4.1.5. Transport of lopinavir and atazanavir across the plasma membrane

There is no defined mechanism for the transport of HIV PIs into the adipocyte, but PM proteins are essential for the transport of drugs into the cell. In the liver, OATP1B1 (*SLCO1B1*), a transporter located in the PM, has been suggested to mediate the uptake of both lopinavir and atazanavir (Hartkoorn *et al.*, 2010; Kis *et al.*, 2010). In addition, both lopinavir and atazanavir are known substrates of the PM transporters Pgp (P-glycoprotein), MRP1 (Multidrug resistance-associated protein 1) and MRP2 (Multidrug resistance-associated protein 2) (Kis *et al.*, 2010).

A number of studies have focused on the effect on PIs on both the adipocyte and adipogenesis, and largely focussed on cytoplasmic proteins (Pacenti *et al.*, 2006; Minami *et al.*, 2011; Zha *et al.*, 2013; Kitazawa *et al.*, 2014). However, to date there have been no previous reports on how HIV PIs affect the PM proteome of 3T3-F442A adipocytes. Since these drugs may modify the adipocyte PM and this might have a significant role in metabolic toxicity associated with PIs, this aspect is addressed by the current chapter.

4.1.6. Aims and objectives

The aims of this chapter were:

1) To assess changes in the PM proteome of 3T3-F442A adipocytes following treatment with lopinavir and atazanavir alone, and also assess how those changes are effected when treated in combination with telmisartan.
2) To select targets, amongst the significantly differentially regulated PM proteins, for functional validation based on pathway analysis, network analysis, and literature data curation.
3) To validate expression of differentially regulated proteins.

4.2. METHODS

A flow diagram of the methodology for this experimental chapter is presented in Figure 4.2.

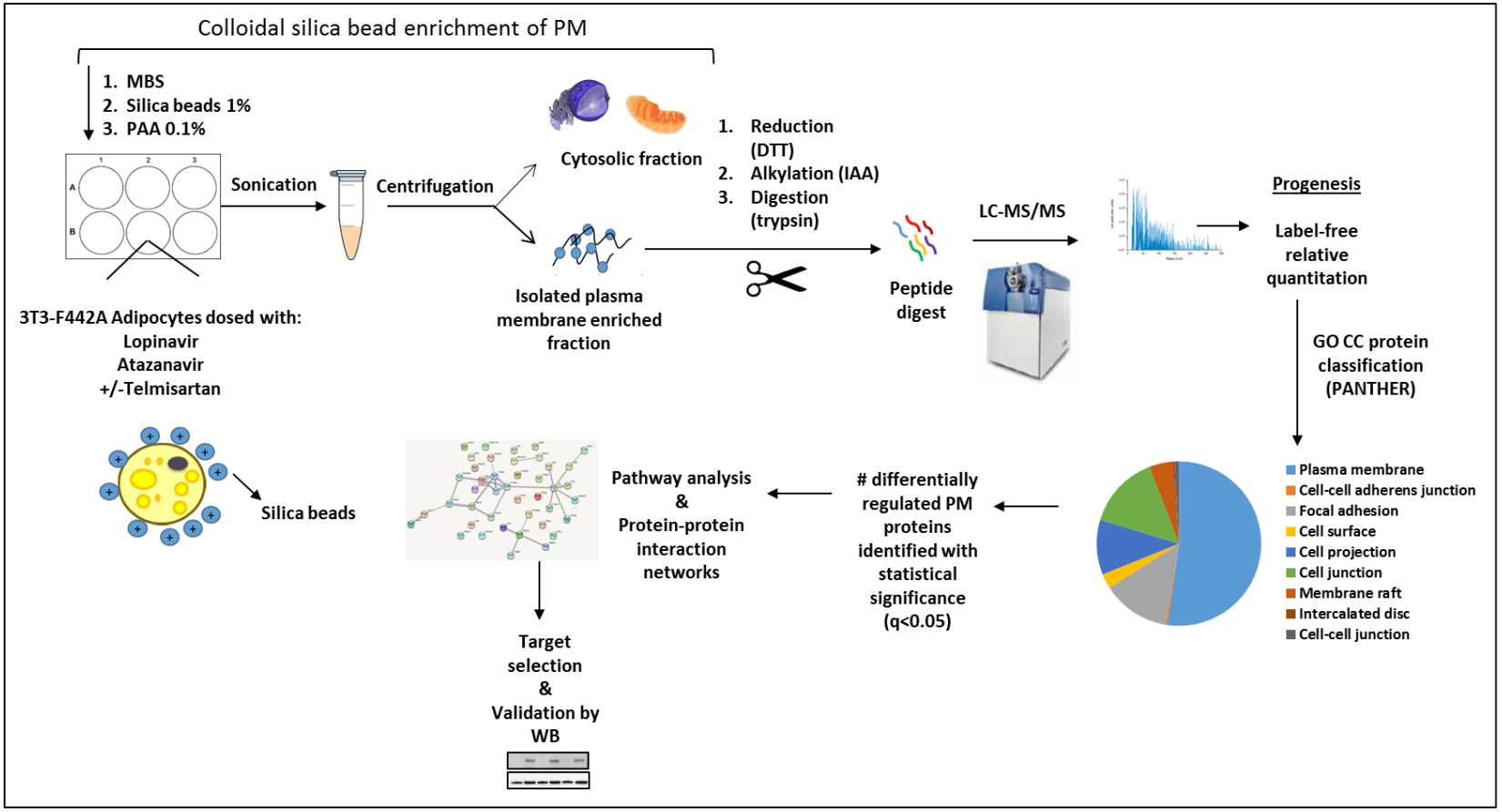

Figure 4.2: Flow diagram of methodology for experimental chapter 4 including target selection and validation. Mature 3T3-F442A adipocytes were dosed every 48 hours for 10 days with lopinavir (+/- telmisartan) and atazanavir (+/- telmisartan). The PM fraction was enriched by silica bead isolation. LC-MS/MS was performed and Progenesis QI software was used for label-free relative protein quantitation. Bioinformatic analysis was applied for the significantly differentially regulated PM proteins. Targets were validated by western blot. Experiments were carried out in triplicate.

4.2.1. Drug addition

Adipocytes were grown and differentiated into mature adipocytes as previously mentioned in section 2.2.1. On day 2 of adipogenesis, cells were treated with lopinavir (10 µM) or atazanavir (4.4 µM) alone and in combination with telmisartan (5 µM) (Santa Cruz Biotechnology, Texas, US); doses established by Pushpakom *et al.*, (2018)The vehicle (methanol) was added to the control cells in a 1:200 ratio (7.5 µL of methanol in 1.5 mL of differentiation media). Drug additions were carried out every 48 hours for a period of 10 days (4 drug additions in total) (Figure 4.3); this chronic *in vitro* toxicity model was previously optimised by our research team (Pushpakom *et al.*, 2018), and it was done to simulate a chronic exposure of patients to the drugs clinically. All experiments were done in triplicate to ensure reproducibility.

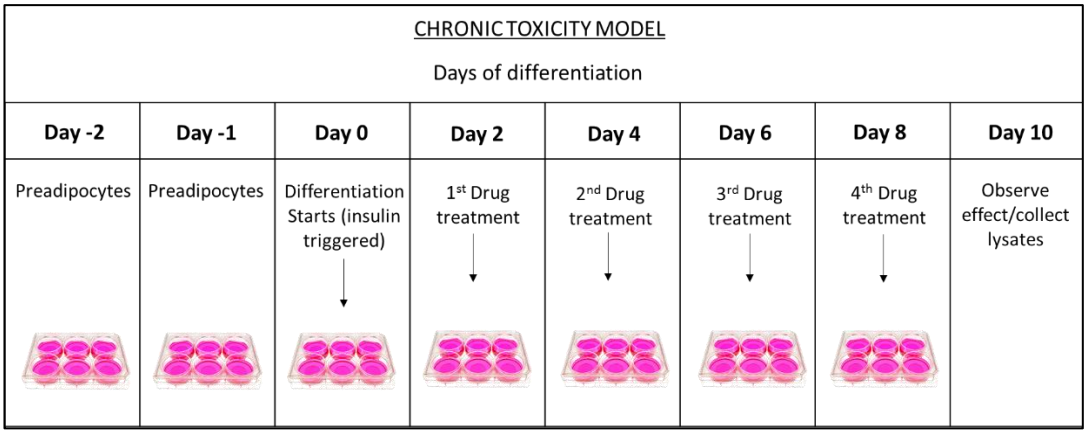

Figure 4.3: Drug addition timeline following a chronic toxicity model. Cells were plated and left to grow for 24 hours; on day 0, differentiation (from preadipocytes to adipocytes) was triggered by adding insulin to the medium. Drugs were added every 48 hours from day 2 to day 10 of adipogenesis (4 drug additions). On day 10 the effect of drugs on the cells was observed and lysates were collected.

4.2.2. Silica bead isolation

Colloidal silica bead isolation was performed as described in section 2.2.3 of Chapter 2.

4.2.3. Mass spectrometry

Mass spectrometry analysis was performed as described in section 2.2.7.3 of Chapter 2, with the exception that for this experiment, samples were not diluted 1:10 in 0.1% formic acid. A total of 100 µg of protein was reduced, alkylated and passed through a Ziptip column and dried. Samples were resuspended in 10 µl of 0.1% formic acid and 10 µg of digested peptide mixture were injected into the mass spectrometer.

4.2.4. Bioinformatic analysis

4.2.4.1. Protein identification and label-free relative quantification of differentially regulated proteins

Performed as described in section 3.2.7.1 of Chapter 3. The Progenesis report can be found in the accompanying USB within the Chapter 4 folder as "Appendix 7 Chapter 4. Progenesis QI report of proteins detected following drug treatments".

4.2.4.2. Protein classification and data curation

Performed as described in section 3.2.7.2 of Chapter 3.

4.2.4.3. Protein pathway and network analysis

Performed as described in section 3.2.7.3 of Chapter 3.

4.2.5. Colloidal Coomassie Blue staining of proteins

Performed as described in section 2.2.6 of Chapter 2.

4.2.6. Validation of NKCC1 and NCAM by western blot

Performed as described in section 2.2.5 of Chapter 2. The T4 antibody from Developmental Studies Hybridoma bank targeted both transporter isoforms NKCC1 (*slc12a2*) and NKCC2 (*slc12a1*). Band densitometry was performed in Image Lab Software (BioRad, Deeside, UK).

4.2.7. Statistical analysis

Statistical analysis of label-free relative quantitation data was performed as described in section 3.2.8 of Chapter 3. For pair-wise comparisons between drug conditions, an ANOVA and Tukey's multiple comparison post hoc test (based on FDR) were performed in the R studio statistical software environment (R core team, 2017) (https://www.R-project.org), using a script kindly provided by Dr Eva Caamaño from the Computational Biology Facility (University of Liverpool). A q-value (FDR-corrected p-value) of <0.05 was considered significant.

For western blot densitometry, data distribution was assumed to be normal, consistently with previous publications (Luo *et al.*, 2018; Schrank *et al.*, 2018) and 1-way ANOVA with Tukey's post hoc correction was applied for multiple comparisons. Unpaired two-tailed T-tests were applied for the comparison of two groups after performing an F-test to ensure equal variances. Statistic analysis of western blot densitometry data was performed in GraphPad Prism (Version 5.0, GraphPad Software, USA). Data are presented as means ± Standard deviation (SD). All expriments were done in triplicate to ensure reproducibility (n=3). A p-value of <0.05 was considered significant.

4.3. RESULTS

4.3.1. Differentially regulated proteins following drug treatment

Prior to LC-MS/MS analysis, the protein content of samples was assessed by Coomassie blue staining of gels (Figure 4.4). Differentiating adipocytes were treated with PIs, lopinavir and atazanavir alone and in combination with the PPARγ agonist, telmisartan. The PM fraction was isolated by colloidal silica bead

isolation and analysed by LC-MS/MS; the resulting mass spectra were imported into Progenesis QI software for label-free relative protein quantitation.

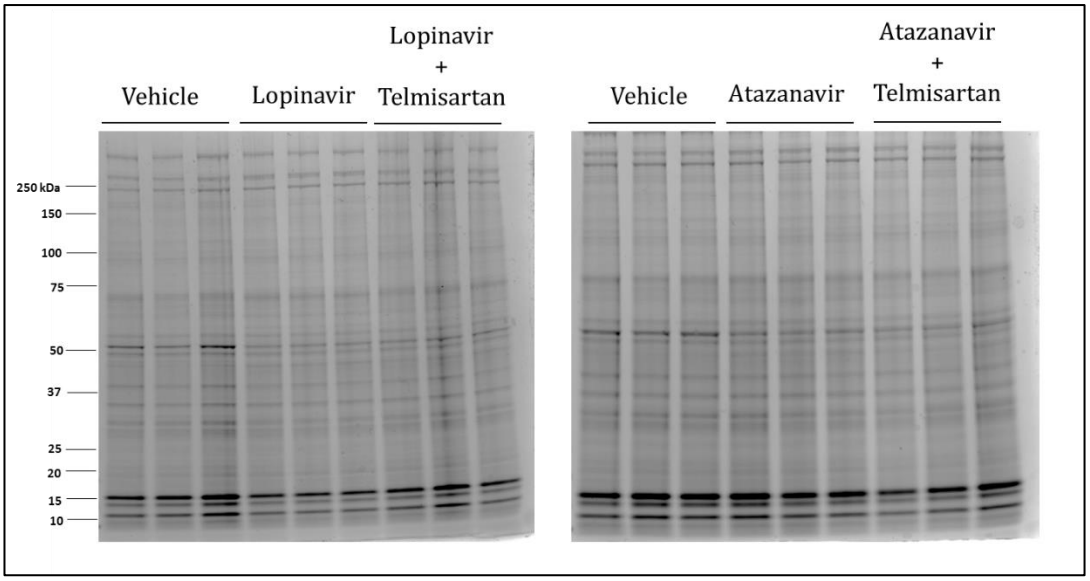

Figure 4.4: Coomassie blue staining of proteins present in lysates of adipocytes dosed with lopinavir (±telmisartan), atazanavir (±telmisartan), and controls (vehicle). A total of 20µg of protein were loaded per lane to ensure protein content previous to LC-MS/MS analysis; samples were run in triplicate.

Using Progenesis QI software, a list of detected proteins was obtained and changes in relative protein abundance under all the different drug conditions: 1) lopinavir, 2) lopinavir combined with telmisartan, 3) atazanavir, 4) atazanavir combined with telmisartan and 5) control (vehicle) were identified. A total of 824 proteins were identified at an FDR of 5%.

PCA was performed in the Progenesis QI (Figure 4.5). PCA showed effective separation of the 5 clusters corresponding to the 5 different drug conditions (group 1-atazanavir combined with telmisartan; group 2-atazanavir; group 3-lopinavir combined with telmisartan; group 4-lopinavir; group 5-vehicle). An outlier run was present in the lopinavir group, and a bigger separation was

observed between replicates from the same cluster in two different drug conditions (lopinavir combined with telmisartan; vehicle). This suggested higher variability between samples in groups 3, 4 and 5 as compared to groups 1 and 2.

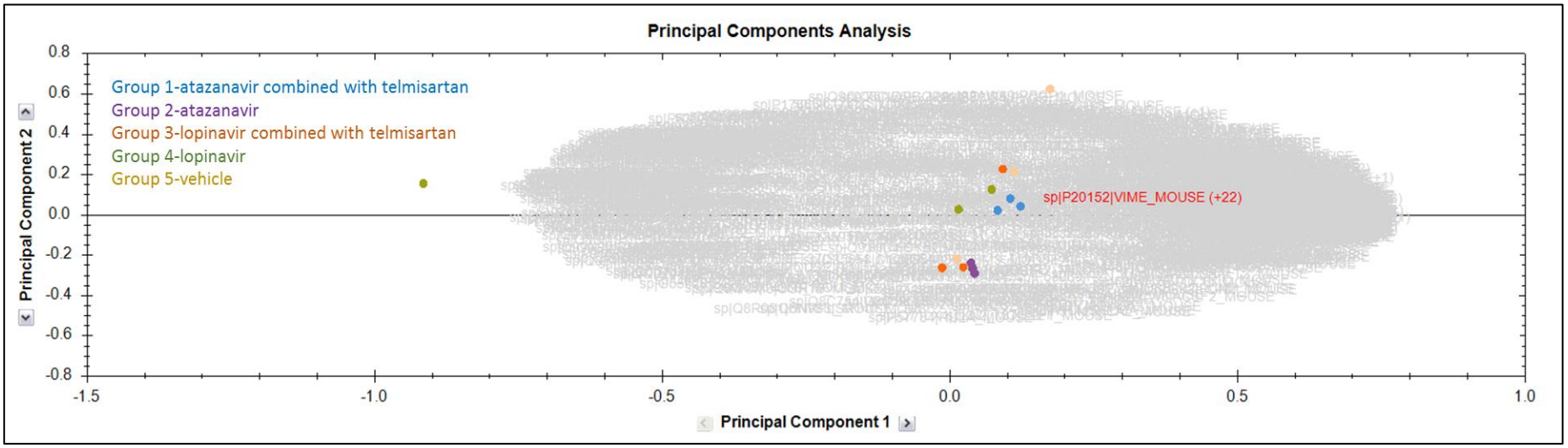

Figure 4.5: Principal component analysis (PCA) distinguishes the silica bead isolated-plasma membrane fraction of adipocytes treated with different drug conditions. Group 1-atazanavir combined with telmisartan: blue data points; group 2-atazanavir: purple data points; group 3-lopinavir combined with telmisartan: orange data points; group 4-lopinavir: green data points; group 5-vehicle: yellow data points.

The identified proteins were then classified based on Cellular Component GO terms (GOCC) in order to differentiate PM proteins from cytosolic proteins. Out of the total of 824 proteins identified, 283 were classified as PM proteins, of which 96 were found to be significantly differentially regulated (Appendix 5, Chapter 4); the rest of detected proteins (541) were classified as cytosolic proteins. Pairwise comparisons were performed using a 1-way ANOVA followed by Tukey's post hoc correction for multiple testing, and results were presented as volcano plots (Figure 4.6, Figure 4.7, Figure 4.8) and only significantly differentially regulated ($q < 0.05$ (p-value corrected for multiple testing)) proteins were considered. Tukey´s post hoc analysis and ANOVA data analysis of all the drug treatments revealed a total of 96 PM proteins that were significantly differentially regulated. This list of significantly differentially regulated PM proteins is presented in Appendix 5 Chapter 4 (in the accompanying USB).

A complete list of all the detected proteins and PM proteins following the different drug treatments can be found in the accompanying USB within the Chapter 4 folder as "Appendix 1 Chapter 4" and "Appendix 2 Chapter 4" respectively. The Progenesis QI report for the different drug treatments can be found within the Chapter 4 folder as "Appendix 7 Chapter 4".

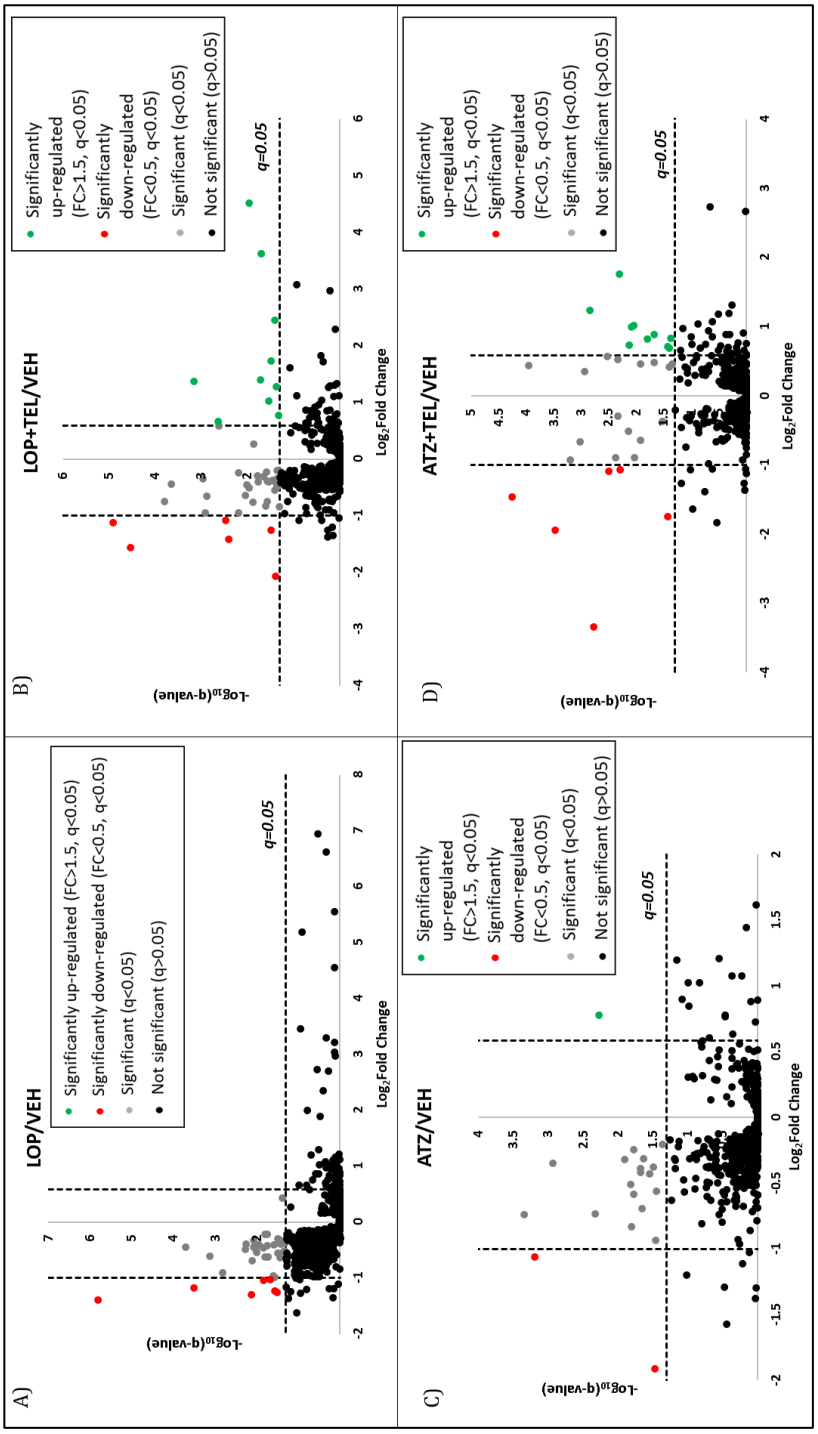

Figure 4.6: Volcano plots showing differentially regulated proteins of the membrane-enriched fraction following exposure of adipocytes to A) Lopinavir (LOP), B) Lopinavir combined with telmisartan (LOP+TEL), C) Atazanavir (ATZ) and D) Atazanavir combined with telmisartan (ATZ+TEL), compared to control (vehicle: VEH). Logarithmic ratios of FC (log2FC) were plotted against the q-value (–log10q-value). A q-value <0.05 is considered significant (dotted horizontal line). Positive FC values indicate up-regulation (green) of protein expression, and negative FC values indicate down-regulation (red). The vertical lines represent the selected thresholds for FC: >50% up-regulation (FC>1.5) or >50% down-regulation (FC<0.5); 1-way ANOVA followed by Tukey's correction for multiple testing. All differentially regulated proteins are listed in Appendix 3 of Chapter 4.

Figure 4.6 shows differential regulation of proteins after being treated with lopinavir and atazanavir, alone and in combination with telmisartan, compared to controls.

Figure 4.7 shows differential regulation of proteins when comparing lopinavir against atazanavir. In order to observe the changes in the PM of adipocytes when

PIs were coincubated with telmisartan, protein expression of individual drug treatments (lopinavir, atazanavir) was compared to those in combination with telmisartan (Figure 4.8).

Table 4.1 shows the amounts of significantly differentially regulated proteins and PM proteins following the different drug comparisons.

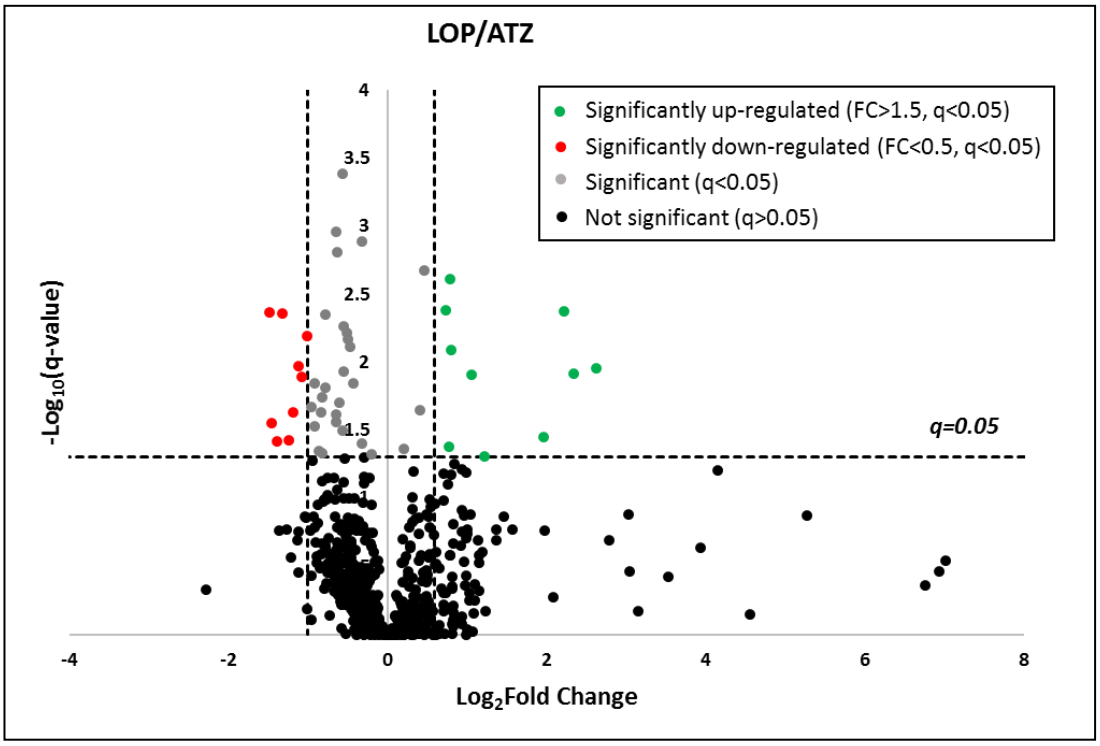

Figure 4.7: Volcano plots showing differentially regulated proteins of the membrane-enriched fraction following exposure of adipocytes to lopinavir (LOP) compared to atazanavir (ATZ). Logarithmic ratios of FC (log2FC) were plotted against the q-value **(**–log10q-value) plotted against. A q-value <0.05 is considered significant (dotted horizontal line). Positive FC values indicate up-regulation (green) of protein expression, and negative FC values indicate down-regulation (red). The vertical lines represent the selected thresholds for FC: >50% up-regulation (FC>1.5) or >50% down-regulation (FC<0.5); 1-way ANOVA followed by Tukey's correction for multiple testing. All differentially regulated proteins are listed in Appendix 3 of Chapter 4.

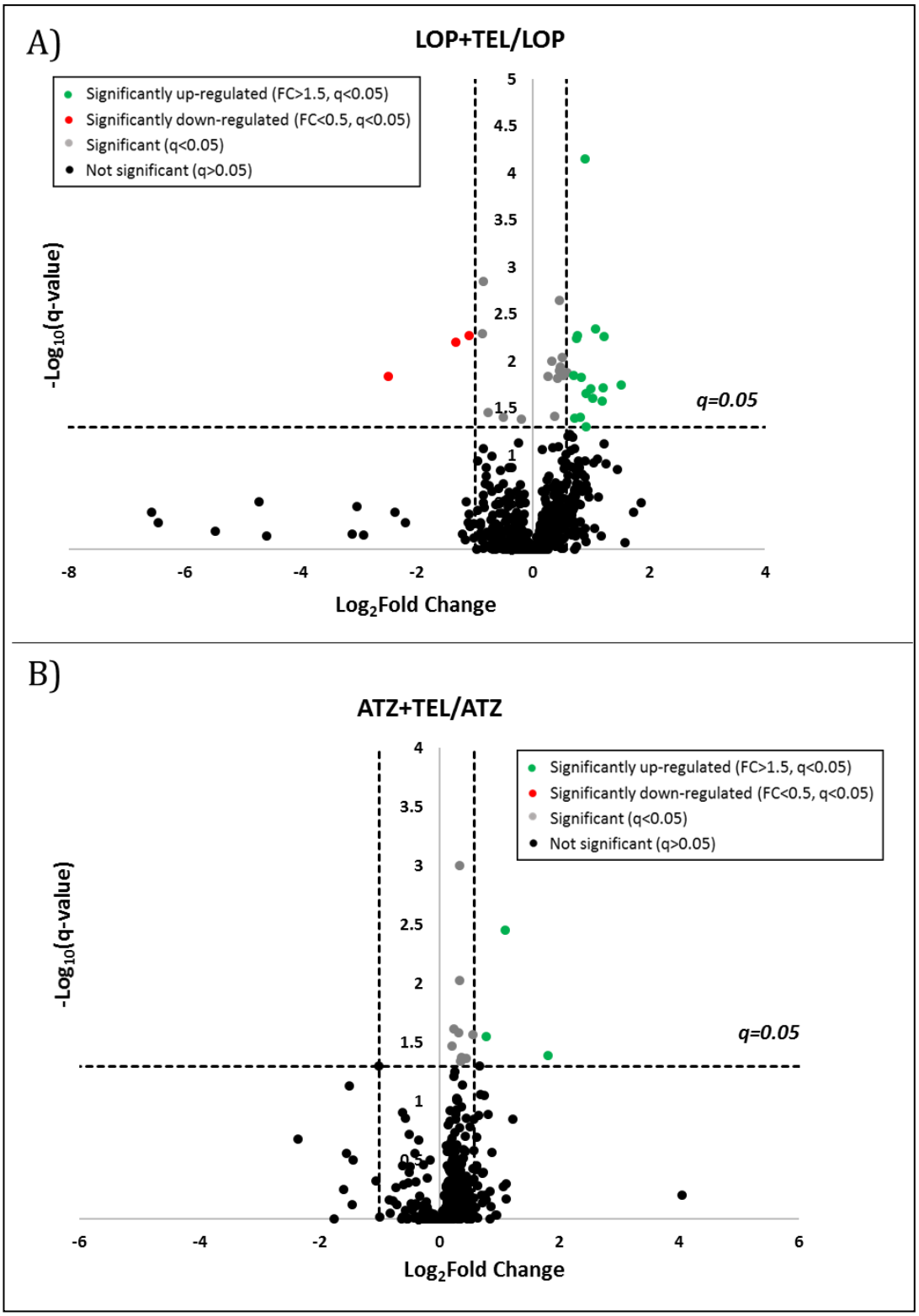

Figure 4.8: Volcano plots showing differentially regulated proteins of the membrane-enriched fraction following exposure of adipocytes to A) Lopinavir combined with telmisartan (LOP+TEL), compared to lopinavir (LOP), and B) Atazanavir combined with telmisartan (ATZ+TEL) compared to atazanavir (ATZ). Logarithmic ratios of FC (log2FC) were plotted against the q-value (–log10q-value) plotted against. A q-value <0.05 is considered significant (dotted horizontal line). Positive FC values indicate up-regulation (green) of protein expression, and negative FC

values indicate down-regulation (red). The vertical lines represent the selected thresholds for FC: >50% up-regulation (FC>1.5) or >50% down-regulation (FC<0.5); 1-way ANOVA followed by Tukey's correction for multiple testing. All differentially regulated proteins are listed in Appendix 3 of Chapter 4.

Table 4.1. Significantly differentially regulated proteins and PM proteins following the different drug conditions.

Drug treatment pair-wise comparisons	Significantly differentially regulated proteins	Proteins >50% up-regulated	Proteins >50% down-regulated	Significantly differentiall y regulated PM proteins	PM proteins >50% up-regulated	PM proteins >50% down-regulated
Lopinavir/Vehicle	39	0	7	19	0	2
Lopinavir+Telmisartan/ Vehicle	46	10	6	17	4	2
Atazanavir/Vehicle	20	1	2	10	0	1
Atazanavir+Telmisartan /Vehicle	32	10	6	9	1	1
Lopinavir/Atazanavir	47	10	9	22	4	3
Lopinavir+Telmisartan/ Lopinavir	34	16	3	11	5	1
Atazanavir+Telmisartan /Atazanavir	13	3	0	3	1	0

4.3.2. Changes in the adipocyte plasma membrane proteome following exposure to PIs

Out of the total of detected PM proteins (283 PM proteins detected), 96 were significantly differentially regulated following exposure to PIs. Of this, 4 of them were transporters or channels and 3 were receptors.

Proteins were classified as plasma membrane proteins based on Cellular Component GO terms (Figure 4.9).

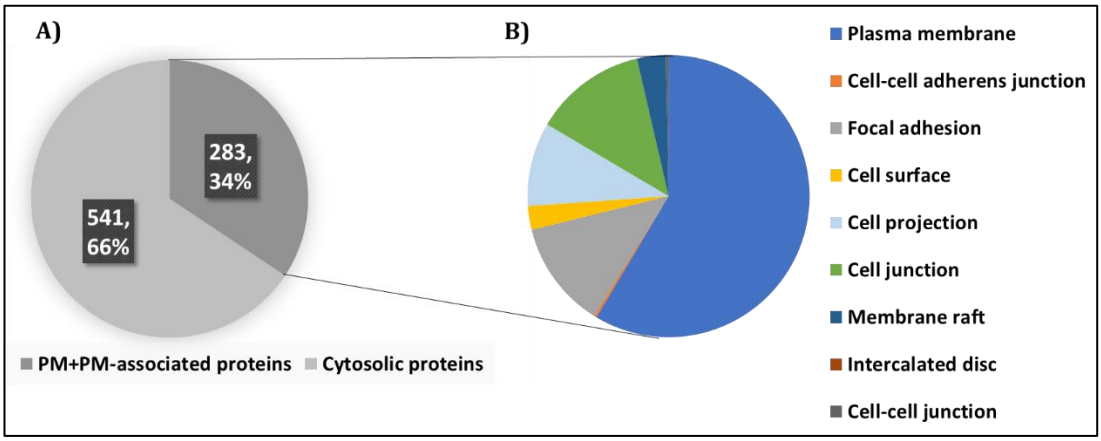

Figure 4.9: Cellular Component Gene Ontology classification of the plasma membrane-enriched fraction isolated by colloidal silica bead isolation after exposure to PIs. A) LC-MS/MS analysis of the adipocyte plasma-membrane enriched fraction (enriched by colloidal silica bead isolation) identified 283 (34%) plasma membrane proteins following exposure to PIs. The remaining 66% (541 proteins) were classified as cytosolic proteins. B) GO Cellular Component annotations performed using the PANTHER protein classification system. Proteins were classified as plasma membrane or plasma membrane-associated proteins based on Cellular Component GO terms.

GO SLIM analysis for Biological Process (BP) and Molecular Function (MF) annotations were applied to the total number of detected PM proteins (283 PM proteins) (Figure 4.10).

A) GO SLIM Biological Process (BP)

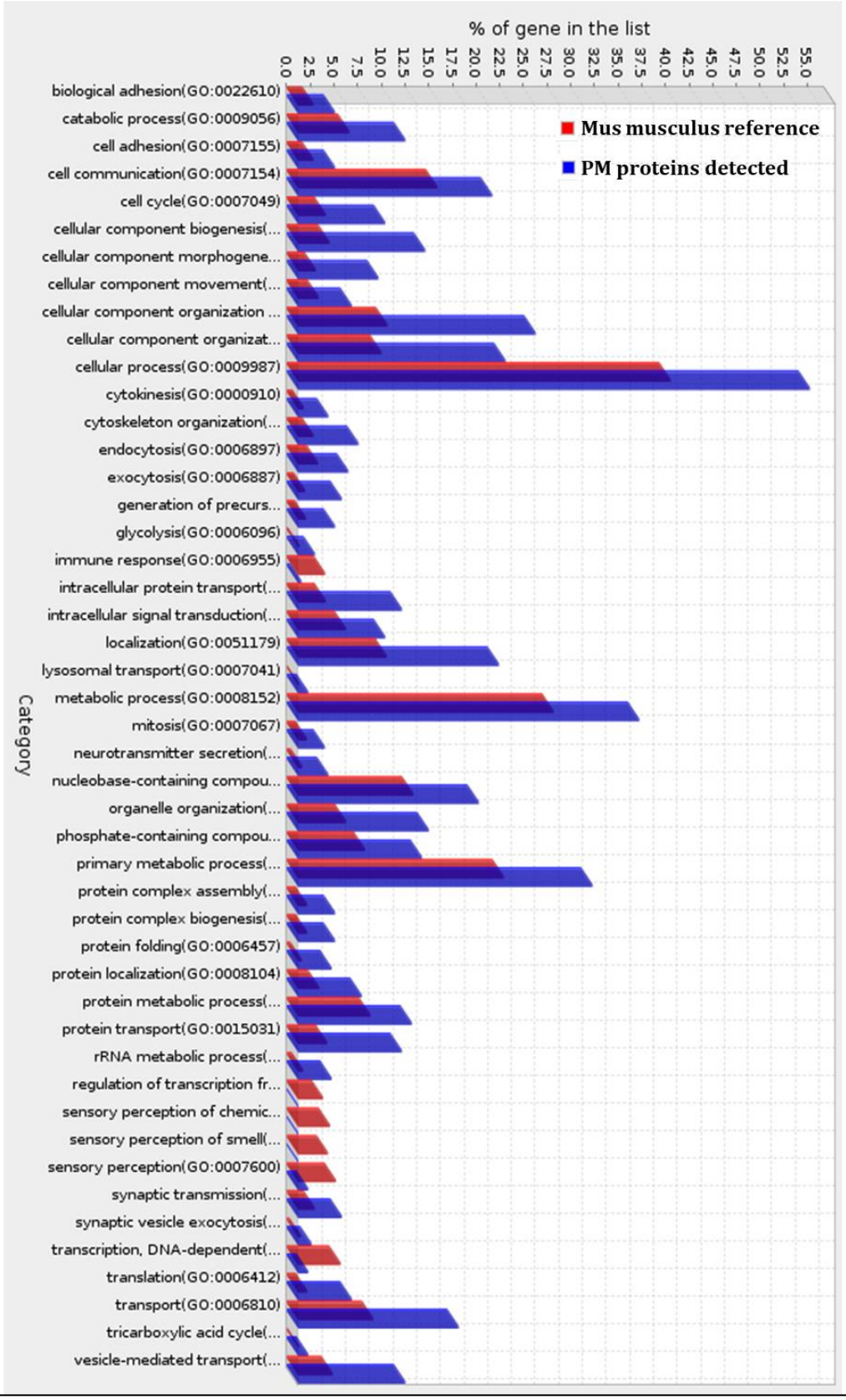

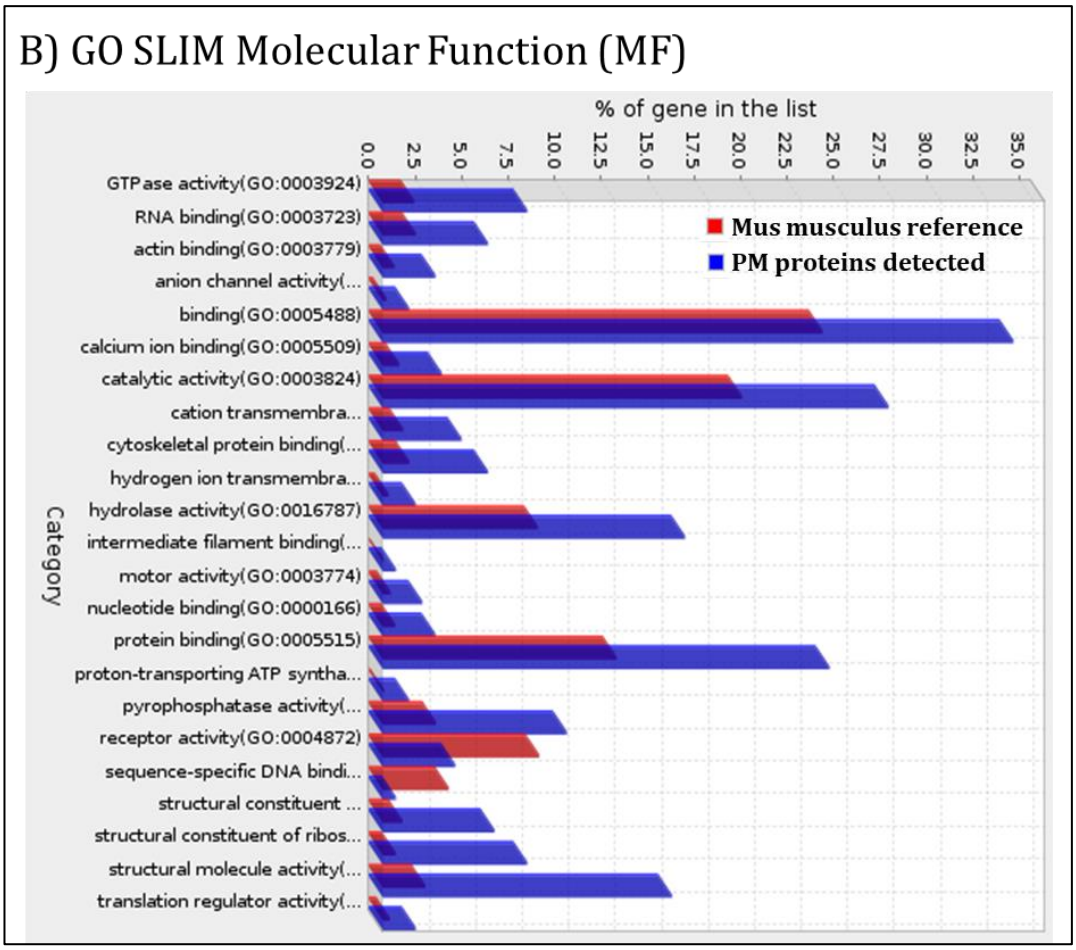

Figure 4.10: Functional classification of the total of detected plasma membrane proteins after exposure to PIs based on A) GO "Biological Process" (BP) annotations and B) GO "Molecular Function" (MF) annotations. Significantly differentially regulated plasma membrane proteins detected were functionally characterised based on GOBP and GOMF annotations contained in the Gene Ontology Consortium database. The number of proteins involved in each GO annotation (blue) is compared to the reference database (red) to observe over or under-representation. Fisher's exact test with FDR multiple test correction was applied and only results for $P < 0.05$ were considered.

The most overrepresented BP annotations were: “cellular process”, “metabolic process”, “primary metabolic process” and “cellular component organization”. Transport-related annotations such as: “intracellular protein transport”, “protein transport”, “transport” and “vesicle-mediated transport” were also overrepresented. The most overrepresented “Molecular Function” annotations were: “binding”, “catalytic activity”, “protein binding”, “hydrolase activity” and “structural molecule activity”; transport-related annotations: “anion channel activity”, “cation transmembrane transporter activity” “hydrogen ion

transmembrane transporter activity", "proton-transporting ATP synthase activity" were also overrepresented.

GO SLIM analysis for Biological Process (BP) and Molecular Function (MF) annotations were also applied to the significantly differentially regulated PM proteins detected in the current study. The most overrepresented BP annotations were: "cellular component organization or biogenesis", "cellular component organization" and "localization" Transport-related annotations such as: "transport", "vesicle-mediated transport", "protein transport" and "intracellular protein transport" were also overrepresented. Regarding MF, the most overrepresented annotations were: "structural molecule activity", and "GTPase activity" and "pyrophosphatase activity" (Figure 4.11).

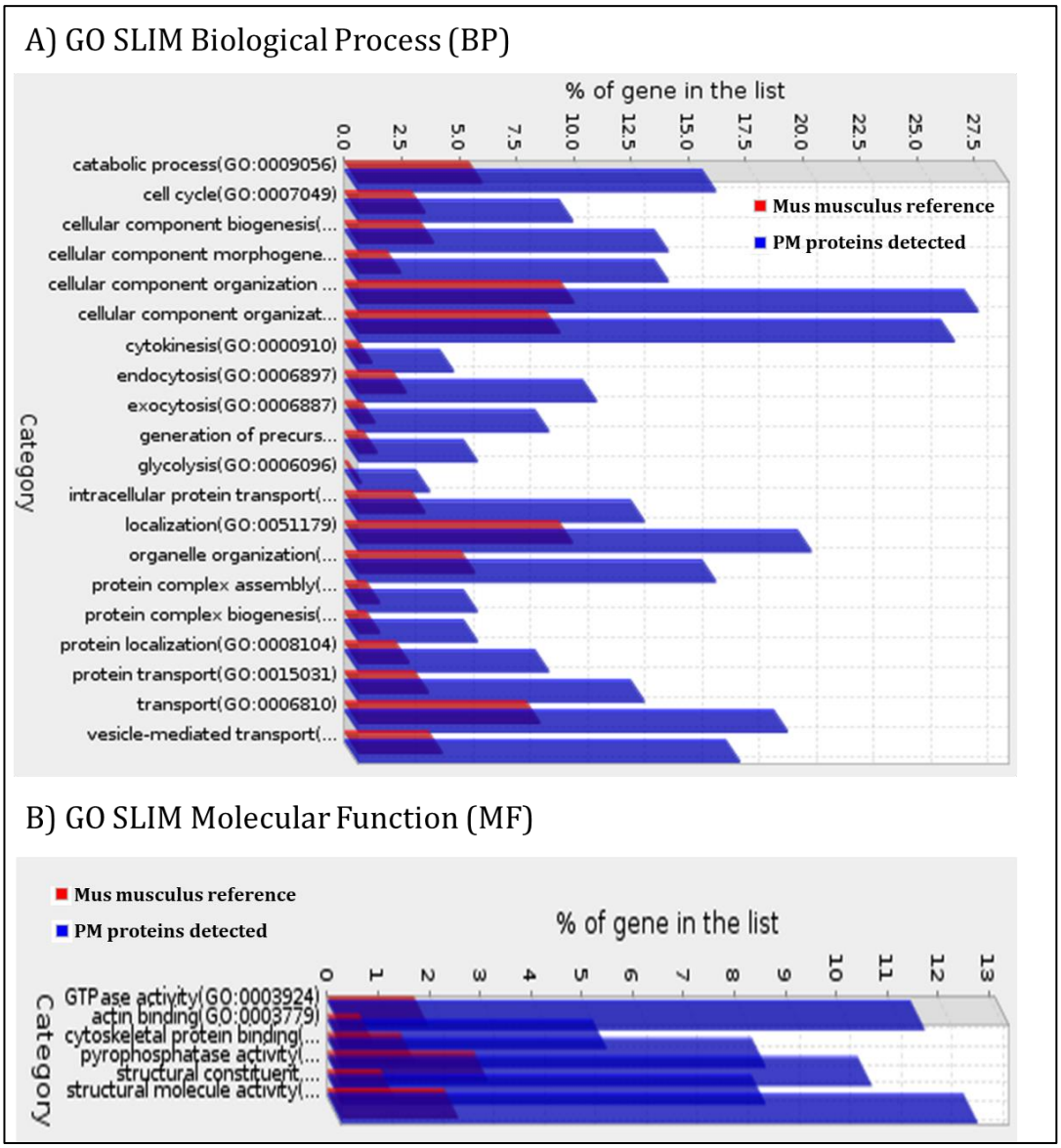

Figure 4.11: Functional classification of significantly differentially regulated plasma membrane proteins based on A) GO "Biological Process" (BP) annotations and B) GO "Molecular Function" (MF) annotations. Significantly differentially regulated plasma membrane proteins detected were functionally characterised based on GOBP and GOMF annotations contained in the Gene Ontology Consortium database. The number of proteins involved in each GO annotation (blue) is compared to the reference database (red) to observe over or under-representation. Fisher's exact test with FDR multiple test correction was applied and only results for $P < 0.05$ were considered.

4.3.3. Pathway analysis of plasma membrane proteins significantly differentially regulated following drug treatment

Pathway analysis was carried out using PANTHER Overrepresentation test (Croft *et al.*, 2014) in order to identify the biological pathways in which the significantly

differentially regulated PM proteins were involved (Figure 4.12). Pathway analysis revealed a total of 43 overrepresented pathways following exposure to PIs. Figure 4.12 shows 16 selected pathways out of the 43. A complete list of the pathways can be found in the accompanying USB as “Appendix 8 of Chapter 4”.

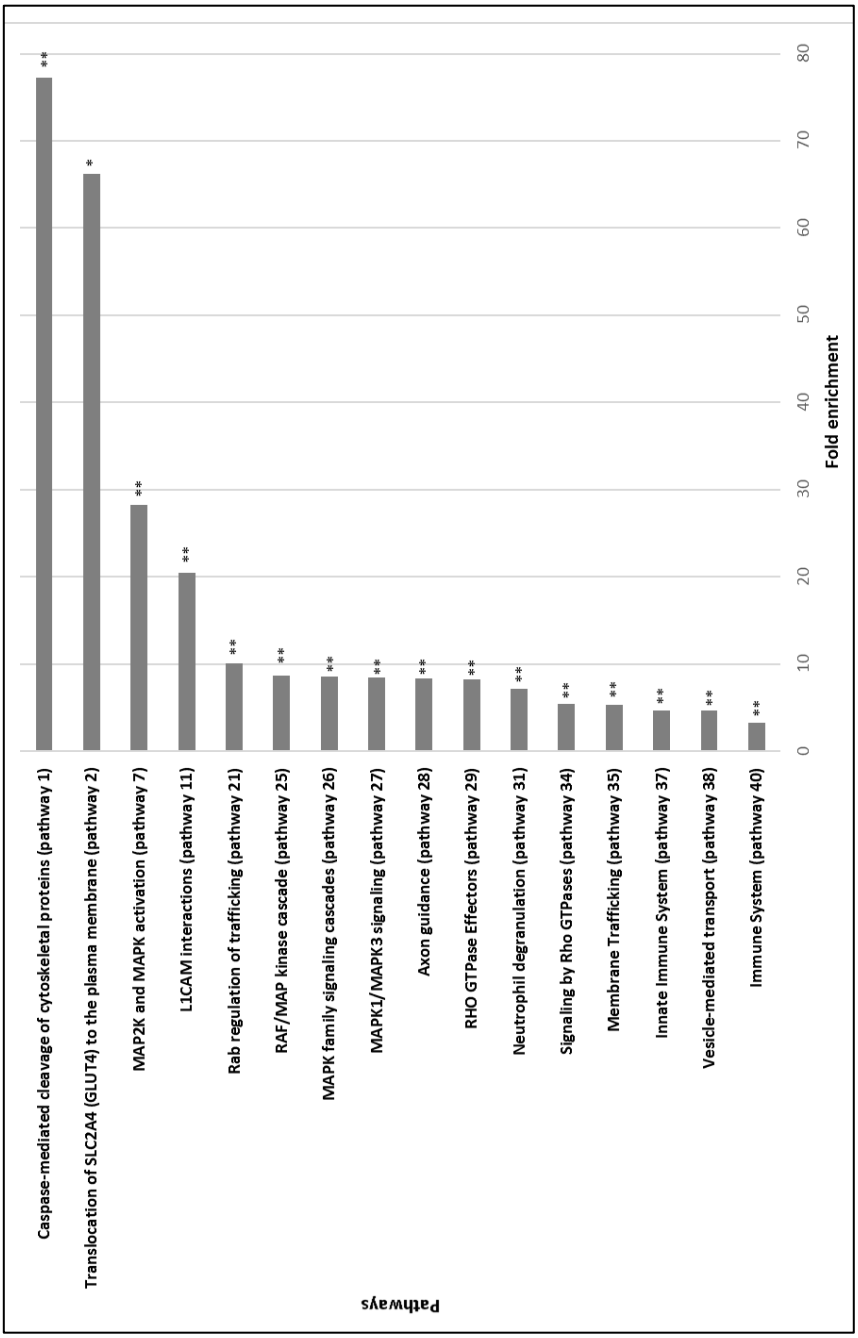

Figure 4.12: Overrepresented pathways involving significantly differentially regulated plasma membrane proteins following exposure of the 3T3-F442A adipocytes to PIs. Fisher’s exact test with FDR multiple test correction was applied ** P ≤0.01 * P ≤0.05; pathways are ordered by fold enrichment and pathway number is indicated; GLUT4: Glucose transporter 4; MAP: mitogen-activate protein; MAPK: mitogen activated protein kinases, MAPK1: Mitogen-activated protein kinase 1, MAPK3: Mitogen-activated protein kinase 3, MAP2K: Dual specificity mitogen-activated protein kinase kinase, L1CAM: Neural cell adhesion molecule L.

4.3.4. Network analysis of plasma membrane proteins significantly differentially regulated following drug treatment

Protein-protein interaction networks were generated using the Search Tool for the Retrieval of INteracting Genes database (STRING) (Szklarczyk *et al.*, 2015), in order to observe links between the significantly differentially regulated PM proteins (only 50% up- or down-regulated) following expsosure to PIs (Figure 4.13). PPARγ and mTOR (regulators of adipogenesis and insulin signalling respectively) were added to the network analysis to observe any predicted interactions with the PM proteins.

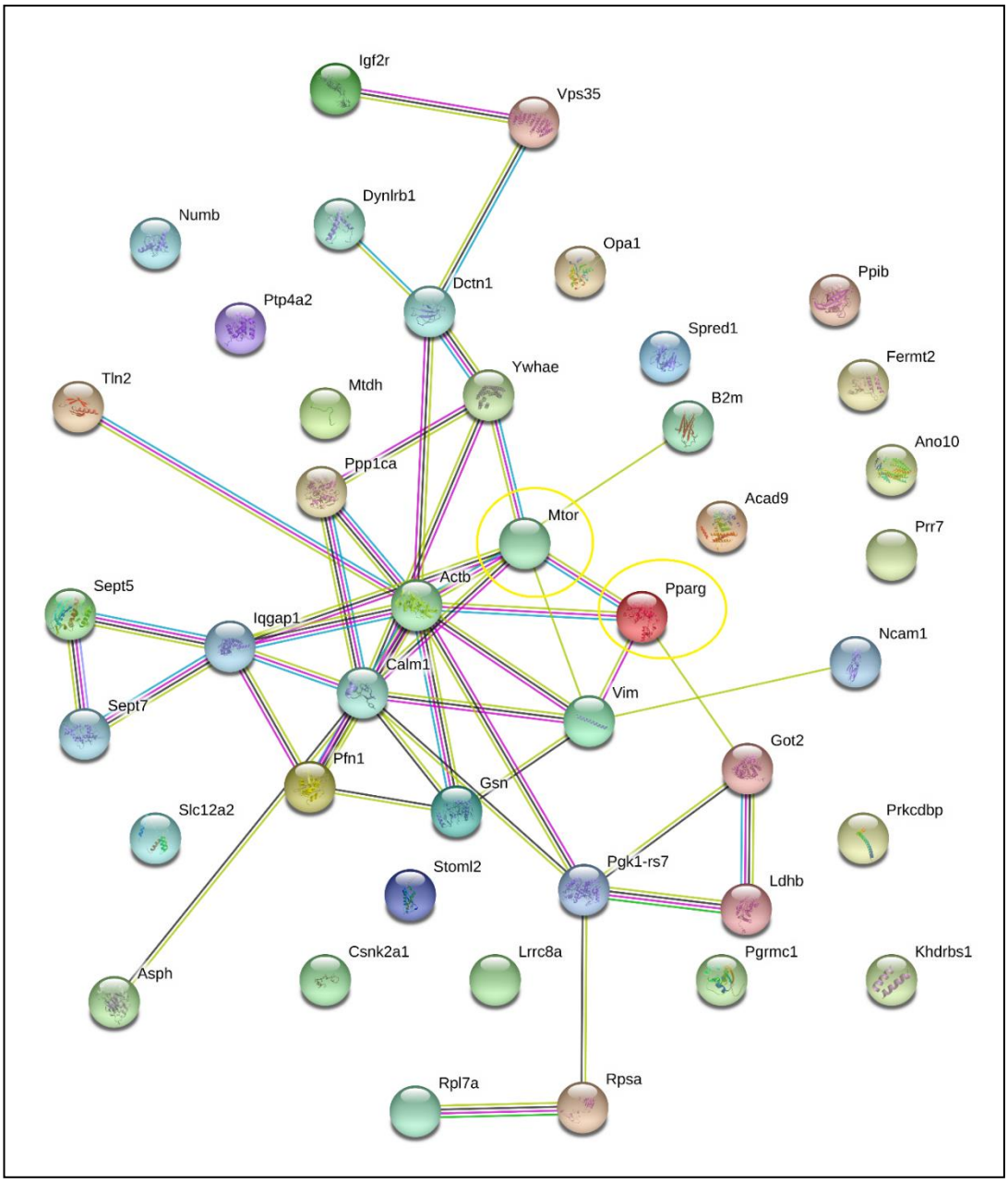

Figure 4.13: Crosstalk between significantly differentially regulated plasma membrane proteins following exposure to PIs and PPARγ and mTOR. Proteins that showed statistically significant differential abundance and were 50% up- or down-regulated following exposure to PIs were imported into the Search Tool for the Retrieval of Interacting Genes database (STRING) version 10.5 (Szklarczyk *et al.*, 2017). Nodes represent individual proteins (annotated by gene names): Slc12a2, Solute carrier family 12, member 2; Vps35, Vacuolar protein sorting-associated protein 35; Igf2r, Insulin-like growth factor 2 receptor; Tln2, Talin 2; Acad9, Acyl-CoA dehydrogenase family member 9; Dctn1,Dynactin 1; Pgk1-rs7, Phosphoglycerate kinase-1, related sequence-7; Ppp1ca, Protein phosphatase 1, catalytic subunit, alpha isoform; B2m,Beta-2 microglobulin; Pgrmc1,Progesterone receptor membrane component 1; Ppib, Peptidylprolyl isomerase B; Actb, Actin, beta; Rpl7a, Ribosomal protein L7A; Ywhae, Tyrosine 3-monooxygenase/tryptophan 5-monooxygenase activation protein, epsilon polypeptide; Gsn, Gelsolin; Sept7, Septin 7; Ptp4a2, Protein tyrosine phosphatase 4a2; Vim, Vimentin; Pfn1, Profilin 1; Dynlrb1, Dynein light chain roadblock-type 1;

Lrrc8a, Volume-regulated anion channel subunit LRRC8A; Prkcdbp, Protein kinase C, delta binding protein; Fermt2, Fermitin family homolog 2; Stoml2, Stomatin (Epb7.2)-like 2; Got2, Glutamate oxaloacetate transaminase 2, mitochondrial; Sept5, Septin 5; Calm1,Calmodulin 1; Khdrbs1, KH domain containing, RNA binding, signal transduction associated 1; Iqgap1, IQ motif containing GTPase activating protein 1; Ncam1, Neural cell adhesion molecule 1; Mtdh, Metadherin; Spred1, Sprouty protein with EVH-1 domain 1, related sequence; Ano10, Anoctamin 10; Csnk2a1, Casein kinase 2, alpha 1 polypeptide; Prr7, Proline rich 7; Numb, Protein numb homolog; Asph, Aspartate-beta-hydroxylase; Rpsa,Ribosomal protein SA; Ldhb, Lactate dehydrogenase B; Opa1, Optic atrophy 1; Mtor, Mechanistic target of rapamycin (serine/threonine kinase); Pparg, Peroxisome proliferator activated receptor gamma. Links between proteins are colour coded and provide different information: known interactions from curated databases (Light blue), known interactions experimentally determined (purple), predicted interactions based on gene neighbourhood (green), predicted interactions based on gene fusions (red), predicted interactions based on gene co-occurrence (dark blue), text mining (light green), co-expression (black), protein homology (light purple). mTOR and PPARγ entries were added to the network (highlighted in yellow). No additional interactions were added.

4.3.5. Validation of target protein NKCC1 as a differentially regulated transporter following PIs exposure

NKCC1 (*slc12a2*) was selected as a target for validation based on the fact that it was the most significantly differentially regulated transporter across various drug comparisons (Appendix 6 Chapter 4). Progenesis found NKCC1 to be 6.16-fold up-regulated when comparing LOP to ATZ; it was also up-regulated in other comparisons (3.5-fold up-regulated, ATZ+TEL vs ATZ; 8.4-fold up-regulated, LOP+TEL vs ATZ; 5.5-fold up-regulated, LOP+TEL vs VEH). All of these changes were significant after correction for multiple testing ($q<0.05$). This target was therefore chosen to be validated by western blotting. The antibody used to detect NKCC1 in this study was non-specific and was also able to detect its isoform, NKCC2 (Figure 4.14, Figure 4.15).

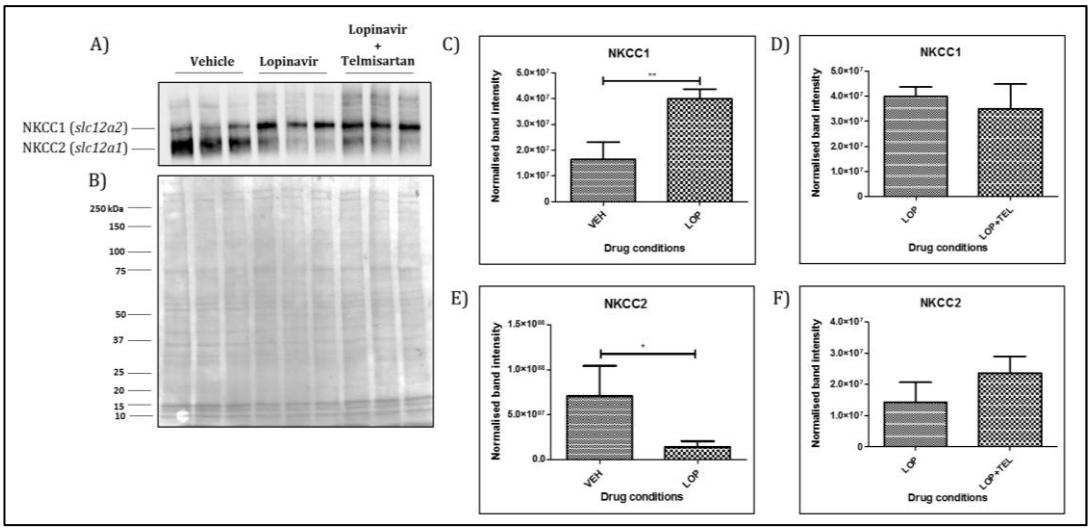

Figure 4.14: Differential expression of NKCC1 and NKCC2 following lopinavir (±telmisartan) exposure in the adipocyte plasma membrane. A) Western blot analysis of NKCC1 and NKCC2 expression in the silica bead-isolated plasma membrane fraction of 3T3-F442A adipocytes following treatment with lopinavir (LOP) and lopinavir combined with telmisartan (LOP+TEL). B) A total of 10 µg of protein were loaded per well and a Ponceau Red stain was used as a loading control to normalise the plasma membrane fraction. C) Band densitometry analysis of NKCC1 comparing LOP vs VEH (control). D) Band densitometry analysis of NKCC1 comparing LOP vs LOP+TEL. E) Band densitometry analysis of NKCC2 comparing LOP vs VEH (control). F) Band densitometry analysis of NKCC2 comparing LOP vs LOP+TEL. Densitometry performed in Image Lab. Data are presented as mean ± SD, n=3. * P <0.05 (unpaired T-test).

Western blot analysis showed significant up-regulation of NKCC1 after exposure to lopinavir compared to the control (Figure 4.14). A slight non-significant reversal trend of the lopinavir-induced NKCC1 upregulation was observed. NKCC2 on the other hand, was significantly down-regulated after adipocytes were chronically exposed to lopinavir; this was also reversed by telmisartan (Figure 4.14).

Western blot analysis of atazanavir-treated adipocyte samples (Figure 4.15) also showed a significant up-regulation in NKCC1 expression compared to the vehicle control; however, this up-regulation was lesser than what was induced by lopinavir.

There was no significant difference in NKCC2 expression after exposure to atazanavir compared to controls (Figure 4.15).

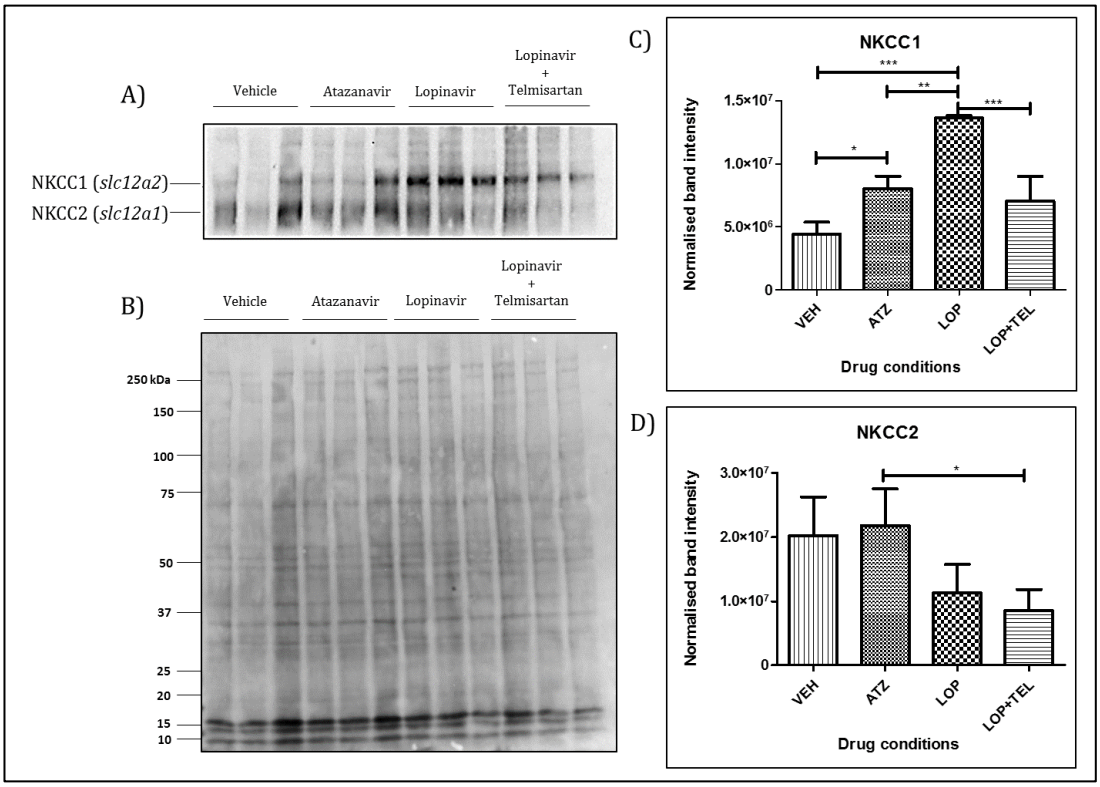

Figure 4.15: Differential expression of NKCC1 and NKCC2 following exposure to lopinavir (+/-telmisartan) and atazanavir in the adipocyte plasma membrane. A) Western blot analysis of NKCC1 and NKCC2 expression in the silica bead-isolated plasma membrane fraction of 3T3-F442A adipocytes following treatment with lopinavir (LOP), lopinavir combined with telmisartan (LOP+TEL), and atazanavir (ATZ) compared to control (VEH). B) A total of 10 µg of protein were loaded per well and a Ponceau Red stain was used as a loading control to normalise the plasma membrane fraction. C) Band densitometry analysis of NKCC1 and D) NKCC2 protein expression performed in Image Lab. Data are presented as mean ± SD, n=3. * P <0.05, ** P <0.01, *** P < 0.001 (One-way ANOVA followed by Tukey's Multiple Comparison Test).

4.3.6. Validation of target protein NCAM as a differentially regulated PM protein following PIs exposure

The PM protein NCAM is a key regulator of adipogenesis and modulates insulin signaling (Yang *et al.*, 2011); this protein was found to be significantly differentially regulated following treatment of adipocytes with the different drug conditions; the effect of PIs and PIs in combination with telmisartan on NCAM

expression has not been previously reported. Therefore, differential protein expression of NCAM observed by LC-MS/MS was investigated by western blot (Figure 4.16, Figure 4.17). Western blot analysis revealed no significant differences in NCAM protein expression following any of the drug treatments.

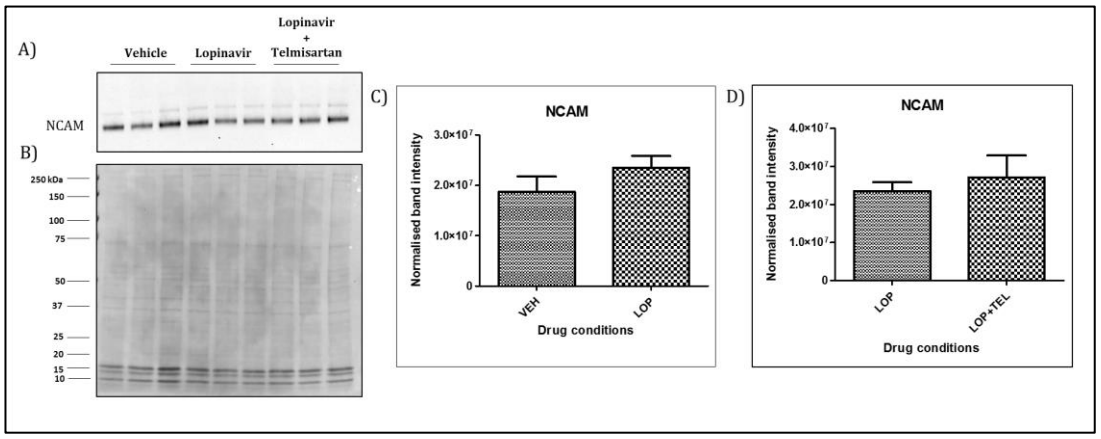

Figure 4.16: Differential expression of NCAM following exposure to lopinavir (+/- telmisartan) compared to control in the adipocyte plasma membrane. A)Western blot analysis of NCAM expression in the silica bead-isolated plasma membrane fraction of 3T3-F442A adipocytes following treatment with lopinavir (LOP) and lopinavir combined with telmisartan (LOP+TEL). B) A total of 10 µg of protein were loaded per well and a Ponceau Red stain was used as a loading control to normalise the plasma membrane fraction. C) Band densitometry analysis of NCAM comparing LOP vs VEH (control). D) Band densitometry analysis of NCAM comparing LOP vs LOP+TEL. Densitometry performed in Image Lab. Data are presented as mean ± SD, n=3. * P <0.05 (Unpaired T-test).

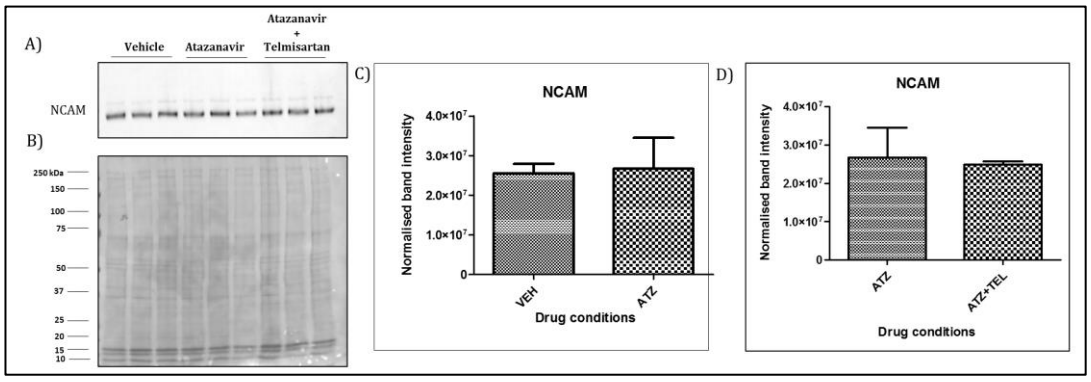

Figure 4.17: Differential expression of NCAM following exposure to atazanavir (+/- telmisartan) compared to control in the adipocyte plasma membrane. A) Western blot analysis of NCAM expression in the silica bead-isolated plasma membrane fraction of 3T3-F442A adipocytes following treatment with atazanavir (ATZ) and atazanavir combined with telmisartan (ATZ+TEL). B) A total of 10 µg of protein were loaded per well and a Ponceau Red stain was used as a loading control to normalise the plasma

membrane fraction. C) Band densitometry analysis of NCAM comparing ATZ vs VEH (control). D) Band densitometry analysis of NCAM comparing ATZ vs ATZ+TEL. Densitometry performed in Image Lab. Data are presented as mean ± SD, n=3. * P <0.05 (Unpaired T-test).

4.4. DISCUSSION

The PM mediates drug transport into and out of the cell; it is also a location vastly important for cell signalling including insulin signalling in response to a glucose stimuli. Therefore, changes in the PM proteome could play a role in the development of metabolic toxicity observed with PIs. Therefore, this chapter examined changes in the PM proteome of 3T3-F442A differentiating adipocytes after being treated with the PIs lopinavir and atazanavir. Lopinavir was selected as the drug of choice for the investigation of adipocyte metabolic toxicity due to its metabolic adverse drug reactions (Hruz *et al.*, 2001; Galescu *et al.*, 2013; Kitazawa *et al.*, 2014; Patel *et al.*, 2018). Atazanavir was selected as a comparator drug to lopinavir, as it has been shown to have more favourable metabolic effects (Haerter *et al.*, 2004; Noor *et al.*, 2006; Stanley *et al.*, 2009; Minami *et al.*, 2011; LaFleur *et al.*, 2017; Spagnuolo *et al.*, 2017). Telmisartan, an antihypertensive drug, was administered to the cells in combination with the two PIs, as it has been reported to reverse PI-induced metabolic toxicity (Pushpakom *et al.*, 2018).

Out of the total of 824 proteins detected by proteomic analysis, 283 (34%) were confirmed to be PM proteins with 96 of them significantly differentially regulated after exposure to PIs. Bioinformatic analysis based on Biological Process and Molecular Function GO annotations suggested that the most important processes in which PM proteins participated were: cell structure organisation and maintenance, and transport. PM proteins which are known to pay a role in metabolic disease were found showing significantly altered expression levels in the current study. Profilin-1, whose expression in WAT was increased by high fat

diet and has been proposed to modulate glucose tolerance (Pae and Romeo, 2014) was found significantly up-regulated following exposure to lopinavir. Cathepsin D, a PM protein reported to be activated and up-regulated in obese adipose tissue (Masson *et al.*, 2011) was found to be significantly down-regulated in telmisartan treated samples (coincubation of lopinavir with telmisartan). Key adipogenic proteins, such as NEDD4 (Li *et al.*, 2016) and NCAM (Yang *et al.*, 2011) were found in the current study.

Based on differential regulation data combined with bioinformatic analysis and literature data curation, two potential targets were selected for validation: the Na^+-K^+:$2Cl^-$- transporter NKCC1, and NCAM.

Lopinavir uptake in the liver has been shown to be mediated by SLC transporters, particularly organic anion and cation transporters (OATs, OCTs), organic anion-transporting polypeptides (OATPs). Lopinavir and atazanavir are both substrates of OATP1B1 (*SLCO1B1*), and lopinavir is also a substrate of OATP1A2 (*SLCO1A2*) and OATP1B3 (*SLCO1B3*) (Hartkoorn *et al.*, 2010; Kis *et al.*, 2010). Metabolic toxicity due to lopinavir has been suggested to be a result of accumulation of the drug in the adipose tissue; given NKCC1, a transporter present in the adipocyte, showed increased expression in the presence of lopinavir, this protein was selected for further validation. NKCC1 is inhibited by bumetanide and furosemide diuretics (Orlov *et al.*, 2015); however, there was no information about the effect of lopinavir or atazanavir on NKCC1 in the adipocyte PM.

NCAM is a key regulator of adipogenesis, and a modulator of insulin signalling (Yang *et al.*, 2011). Given how PIs affect adipogenesis and insulin signalling, NCAM was selected as a second target for further investigation. There is no previously published data on the effect of lopinavir and atazanavir on the

expression NCAM in the adipocyte. The expression of this protein was investigated by western blotting but no significant differences in protein expression under any of the different drug treatments were found. A non-significant increase in NCAM protein levels was observed by western blotting in the lopinavir condition compared to the control. As lopinavir is a disruptor of adipogenesis and NCAM promotes adipogenesis, a downregulation of NCAM by lopinavir was expected but the opposite effect was observed. This might suggest a lack of direct effect on lopinavir on NCAM; lopinavir may be disrupting adipogenesis through a pathway independent of NCAM, or may be modulating adipogenesis through the reduction of *PPARγ* expression.

Western blotting results showed detection of both isoforms of SLC12A: NKCC1 and NKCC2 by the T4 antibody; detection of both isoforms with this antibody has been previously observed for the murine MMDD1 (mouse macula densa-derived 1) cell line (Fraser *et al.*, 2015). NKCC2 was thought to be exclusively expressed in the kidney and to be localised in recycling endosomes in the cytoplasm; recently, Singh *et al.*, (2016) found that NKCC2 translocated from the ER to the PM of COS7 cells undergoing hyperosmotic stress (Singh *et al.*, 2016).

Interestingly, while expression of NKCC1 was up-regulated after lopinavir exposure compared to controls, NKCC2 followed the opposite trend and was down-regulated. A compensatory effect involving these two isoforms was already reported regarding glucose-induced insulin secretion in pancreatic β-cells (Alshahrani *et al.*, 2012). The authors showed NKCC2 to compensate for the inhibition or silencing of NKCC1 in β-cells by preserving the cells´ insulin secretory capacity and concluded that both isoforms contribute to insulin secretion by β-cells with the expression of NKCC2 increased upon NKCC1

inhibition (Alshahrani *et al.*, 2012, 2015). The role of NKCC1 and NKCC2 in insulin secretion and glucose homeostasis will be explained in more detail in chapter 5, and the role of these transporters in metabolic toxicity will be further investigated.

A key finding was that addition of telmisartan to lopinavir significantly reversed the lopinavir-induced downregulation of NKCC1 expression in the PM of adipocytes. Telmisartan has been previously reported to reverse metabolic toxicity caused by lopinavir in adipocytes *in vitro* (Pushpakom *et al.*, 2018). To the best of our knowledge, the relationship between NKCC1 and lopinavir has not been previously investigated, and the results presented in this study on NKCC1 with both lopinavir alone and in combination with telmisartan could suggest a role of NKCC1 in metabolic toxicity induced by lopinavir.

Another interesting point for discussion is the role of NKCC1 in the regulation of cell volume; this is activated by threonine phosphorylation and changes in cell shape (shrinking) (Arroyo *et al.*, 2013). One of the most overrepresented pathways in which the PM proteins detected in the current study participated was "caspase-mediated cleavage of cytoskeletal proteins"; this pathway involves regulation of cell shape and cytoskeleton remodelling. NKCC1 has been shown to serve as a scaffolding protein for Cofilin-1 in the process of actin cytoskeleton remodelling, a key process for adipogenesis (Ali *et al.*, 2013; Titushkin *et al.*, 2013). Cofilin-1 was detected in the current study and is known to play a role in GLUT4 translocation to the PM (Chiu *et al.*, 2010; Schiapparelli *et al.*, 2017). NKCC1 may be involved in the regulation of cell shape or act as a scaffolding protein in adipocytes, but this has not been reported before. NKCC2 has not been

linked to cell volume regulation and it is thought to have a different function than NKCC1 (Singh *et al.*, 2016).

Differential regulation of NKCC1 and NKCC2 transporters following exposure to protease inhibitors in the adipocyte PM has not been previously identified. There is a need to understand the disposition of PIs in adipocytes; as it may be possible that NKCC1 could be a contributor to lopinavir-induced metabolic toxicity. In the next chapter, functional assays for the study of the role of NKCC1 in lipid accumulation during adipogenesis and to investigate its potential role in insulin signaling and glucose homeostasis.

CHAPTER 5
FUNCTIONAL VALIDATION OF SELECTED PLASMA MEMBRANE PROTEINS IN THE ADIPOCYTE

5.1. INTRODUCTION

5.1.1. The role of NCAM and NKCC1 in cell biology

Based on the results presented in the previous chapter, two targets were selected for functional validation; these were NCAM and NKCC1.

5.1.1.1. NCAM

NCAM is a PM protein that belongs to the immunoglobulin superfamily and it is mainly expressed in the central and peripheral nervous system; however, it is a ubiquitous protein found to be expressed in epithelial cells, pancreatic β-cells, skeletal muscle cells, natural killer cells and adipocytes (Francavilla *et al.*, 2007). NCAM is an important cell-cell adhesion protein, and it has been linked to synaptic plasticity associated with memory and learning (Larsen *et al.*, 2000). There are three isoforms of this protein encoded by the same gene (*NCAM1*): NCAM-120, NCAM-140 and NCAM-180, where the numbers correspond to the molecular weight. Only NCAM-140 and NCAM-180 have transmembrane domains. NCAM-120 was not found to be expressed in the 3T3-L1 preadipocyte cell line (Yang *et al.*, 2011).

NCAM has previously been identified as a key regulator of adipogenesis for both bone-marrow-derived mesenchymal stem cells (MSCs) and 3T3-L1 adipocytes via the PI3K–Akt signalling cascade. Furthermore, NCAM deficiency induced insulin resistance in MSCs, the mechanism behind this was thought to be TNFα induction and reduction of insulin receptor activation (Yang *et al.*, 2011).

5.1.1.2. NKCC1

NKCC1, is an electroneutral transporter responsible for sodium and chlorine active transport in the cells. It maintains ionic balance and regulates cell volume (Hamann *et al.*, 2010). There are two isoforms of NKCC transporters encoded by *slc12a2* (NKCC1) and *slc12a1* (NKCC2), and there is approximately a 60% homology between these two isoforms (Hoffmann *et al.*, 2009). NKCC1 is mainly localised in the PM and it has been found to be expressed in most cell types (especially epithelial cells). On the other hand, NKCC2 was thought to be kidney-specific, and it is highly expressed in the thick ascending limb of the loop of Henle where it is involved in ion reabsorption. Both NKCC1 and NKCC2 are regulated by the actin cytoskeleton, and they are both activated in response to osmotic cell shrinkage (Hoffmann *et al.*, 2009). NKCC1 is activated by threonine phosphorylation, whereas the activation mechanism for NKCC2 remains unclear. NKCC1 has been suggested to serve as a scaffolding protein under osmotic stress conditions (Hoffmann *et al.*, 2009). NKCCs are inhibited by the loop diuretics bumetanide and furosemide, with NKCC2 being less sensitive to bumetanide than NKCC1 (Alshahrani *et al.*, 2012, 2015).

In pancreatic β-cells, NKCC transporters have been implicated in insulin secretion in response to glucose (Alshahrani *et al.*, 2012). A compensatory effect between NKCC1 and NKCC2 regarding insulin secretion by pancreatic β-cells was observed by Alshahrani *et al.*, (2015). For their study, Alshahrani *et al.*, (2015) silenced the expression of NKCC1 in COS7 cells and noticed an increased expression of NKCC2; they explained this to be a protective mechanism for insulin secretion from β-cells in the absence of NKCC1. It was also found that knockout of *Nkcc1* improved glucose tolerance in $NKCC1^{KO}$ mice compared to wild type

mice. This strong insulin secretion response to glucose in NKCC1^{KO} mice was suggested to be a result of the compensatory action of NKCC2 expressed by pancreatic β-cells (Alshahrani *et al.*, 2012).

5.1.2. Functional characterisation of the role of NCAM and NKCC1 in adipocyte metabolic toxicity

Several researchers have studied the role of specific proteins of interest in adipocyte metabolism (Albrektsen *et al.*, 2001; Lamers *et al.*, 2011; Li *et al.*, 2016; Takahashi *et al.*, 2016). When trying to elucidate the role of a protein in adipocyte biology, the impact of the protein in adipogenesis is usually investigated (Hong *et al.*, 2005; Kim *et al.*, 2009); followed by their effect on insulin signalling (Krüger *et al.*, 2008; Xie *et al.*, 2016), GLUT4 translocation (Sano *et al.*, 2007; Jedrychowski *et al.*, 2010), adipokine secretion (Wu *et al.*, 2014), and lipid metabolism (Tepaamorndech *et al.*, 2016). Many of these studies apply knockdown of the protein of interest, followed by Oil red O staining to observe the effects of silencing of the gene encoding for this protein on lipid accumulation (Hong *et al.*, 2005; Kim *et al.*, 2009; Li *et al.*, 2016).

The role of NCAM in adipogenesis was already published by Yang *et al.*, (2011), and this publication was used as guide for the optimisation of the functional validation protocol presented in this study. In their study, Yang *et al.*, (2011) assessed the influence of NCAM on adipogenesis by silencing its gene (using siRNA) followed by Oil Red O staining to observe lipid droplet accumulation in the NCAM-knockdown adipocytes compared to controls. They found that adipogenesis was disrupted and lipid accumulation was markedly reduced following NCAM knockdown. Reduced expression of adipogenic markers such as

PPARγ and fatty acid-binding protein (αP2) in NCAM-knockdown adipocytes was also observed when compared to controls. In addition, silencing of *Ncam* impaired the insulin signalling cascade, which led to the suggestion that NCAM was a modulator of insulin signalling. However, the effect of knockdown of NCAM on events such as GLUT4 translocation and secretion of adiponectin, that are important for insulin sensitivity has not been investigated.

Expression of NKCC1 has been previously found in NIH3T3 fibroblasts (fibroblast cell line obtained from NIH Swiss mouse embryo fibroblasts), in which, overexpression of this transporter induced cell proliferation and phenotypic transformation (Panet *et al.*, 2000; Schliess *et al.*, 2000). To the best of our knowledge, the role of NKCC1 in adipogenesis and adipocyte metabolism has not been previously studied. A combination of functional assays were employed; such as knockdown assays, lipid accumulation assays, estimation of adiponectin secretion by ELISA, and GLUT4 protein expression by western blot to study the role of NKCC1 and NCAM in adipogenesis and insulin signalling.

5.1.3. Aims and objectives

The aims of this chapter were:

1) To optimise a method for functional validation of proteins of interest, using NCAM as a model, and to apply this method to the 3T3-F442A preadipocyte cell line.

2) To investigate the role of NKCC1, in adipocyte metabolic toxicity using the optimised functional assays.

5.2. METHODS

5.2.1. Transfection and knockdown

On day 1 of differentiation, cells were washed twice with HBSS (Sigma-Aldrich, Dorset, UK) and incubated with trypsin-EDTA solution (Sigma-Aldrich, Dorset, UK) for 2 minutes until complete detachment. Cells were counted and re-plated in 24-well plates at a density of 10,000 cells/well in DMEM suplemented with 10% FBS. Cells were then transfected in suspension with Lipofectamine RNA iMAX transfection reagent (Fisher Scientific, Loughborough, UK) following manufacturer's instructions, reaching a concentration of small interfering RNA (siRNA) and scrambled RNA (scRNA) of 25 nM per well. Expression of the gene of interest was silenced by siRNA, which is a synthetic RNA designed to target a specific mRNA to cause its degradation.The scRNA is a control which nucleotide sequence is that of the siRNA rearranged. FlexiTube siRNA or scRNA were purchased from QIAGEN (Manchester, UK); siRNA (Mm_Ncam1_3) target sequence: CCGGTTCATAGTCCTGTCCAA; siRNA (Mm_Slc12a2_7) target sequence: TCCATTCAGAATATTAAGAAA; scRNA target sequence: AATTCTCCGAACGTGTCACGT. 72 hours after knockdown (day 4 of adipogenesis), the differentiation medium was changed, and from then it was changed every 48 hours. The cells were maintained until day 10 of differentiation and lysates were collected on days 4, 7 and 10 of differentiation. Efficient knockdown was confirmed by western blotting.

5.2.2. Preparation of lysates from cell culture

Cells were washed twice with cold HBSS and lysed by scraping into 50 µL of cold RIPA buffer. Lysates were maintained on ice for 30 minutes and vortexed every

10 minutes. Lysates were centrifuged at 14,000 rpm for 30 minutes at 4 ºC, and the resulting supernatant was collected into a fresh tube. The pellet was discarded and samples were stored at -20 ºC until use.

5.2.3. BCA protein quantification assay

Total protein quantification of whole lysates was performed using a Pierce™ BCA Protein Assay Kit by Thermo Fisher Scientific (Runcorn, UK). In a 96-well plate, 25 µL of each diluted albumin standard and sample (diluted 1:4), were loaded into each well in duplicate. A total of 200 µL of working reagent (WR) was loaded into each well and the plate was mixed on a plate shaker for 30 seconds. The plate was incubated in the dark for 30 minutes at 37°C. The plate was cooled to room temperature and absorbance was measured at 595 nm in a plate reader (DTX 880 Multimode Detector, Beckman Coulter, High Wycombe, UK).

5.2.4. Determination of protein concentration (Bradford Assay)

Protein content of the silica bead-isolated PM fraction samples was determined using a Bradford assay as described in section 2.2.4 of Chapter 2.

5.2.5. Western blot

Western blot was performed as reported in section 2.2.5. A total of 20 µg (for PM-enriched samples) or 10 µg (for whole lysate samples) of protein were loaded per well. Band densitometry was performed in Image Lab Software (BioRad, Deeside, UK).

5.2.6. Oil red O Staining

Oil red O staining was performed as described in section 2.2.2 of Chapter 2.

5.2.7. Starvation and insulin stimulation of mature adipocytes

Insulin stimulation was performed as described in section 3.2.2 of Chapter 3. A 100 nM insulin concentration was used.

5.2.8. Immunofluorescence

Cells were grown and differentiated on coverslips for 10 days, washed with cold PBS and fixed in 4% paraformaldehyde in PBS for 30 minutes at 4 ºC. After fixation, cells were washed with cold PBS and permeabilised with permeabilisation buffer (0.2% tween-20, 0.5% Triton X-100 in PBS) for 30 minutes at 4 ºC. Cells were blocked for 30 minutes at room temperature in blocking buffer (permeabilisation Buffer +5% BSA). The cells were then incubated with the NKCC1 primary antibody (1:1000 dilution in blocking buffer) overnight at 4 ºC, cells were washed 3 times (15 minutes each) with permeabilisation buffer at room temperature. Cells were then incubated with the Alexa Fluor 488 secondary antibody (1:1000) (Thermo Fisher Scientific, Runcorn, UK) at room temperature for one hour and protected from the light. Cells were then washed in PBS-T (0.2% tween-20 in PBS) for 10 minutes and incubated with Alexa Fluor™ 568 Phalloidin (1:250 dilution in PBS) (Thermo Fisher Scientific, Runcorn, UK) and Hoechst 33342 (1:5000 dilution in PBS) (Thermo Fisher Scientific, Runcorn, UK) for 20 minutes at room temperature in the dark. Cells were further washed with PBS-T for 10 minutes and then with PBS for another 10 minutes. Finally, cells were mounted using ProLong Gold Antifade Mountant reagent (Thermo Fisher Scientific, Runcorn, UK) which was placed on glass slides, and coverslips were mounted onto glass slides, sealed and left to set

prior to visualisation in a Zeiss Axio Observer Z.1 microscope (Zeiss, Oberkochen, Germany).

5.2.9. Estimation of adiponectin by ELISA

The ELISA kit used in this study was the mouse Adiponectin ELISA Kit by Invitrogen (Thermo Fisher Scientific, Runcorn, UK). Manufacturer's instructions were followed. A total of 100 µL of standards were added in duplicate and the diluted samples (1:100) were added in triplicate to antibody-coated 96-wells. The plate was sealed and incubated for 1 hour at 37 ºC. After incubation with the primary antibody, the contents of the wells were discarded and the wells were washed 3 times with 1xWash buffer. A total of 100 µL of detection antibody solution was added into all wells and the plate was covered and incubated for 1 hour at 37 ºC. The contents of the wells were discarded and the wells were washed 3 times with 1xWash buffer. A total of 100 µL of 1XHRP (horseradish peroxidase) solution was added into each well and the plate was covered and incubated for 1 hour at 37 ºC. The contents of the wells were discarded and the wells were washed 5 times with 1xWash buffer. A total of 100 µL of TMB (3,3',5,5'-tetramethylbenzidine) substrate solution was added to each well, and the plate was incubated for 20 minutes at room temperature in the dark. After incubation, 100 µL of stop solution was added to each well, and the plate was gently mixed and absorbance was read at 450 nm. Adiponectin concentration was calculated as per manufacturer's instructions by a standard curve. Supernatants were taken on day 1, 4, 6and day 10 to measure adiponectin, but in this chapter only used day 10 supernatants were used, as optimisation revealed that on day

10 of adipogenesis, adiponectin reaches concentration levels detectable by the ELISA kit.

5.2.10. Statistical analysis

Statistical analysis of western blot densitometry values was performed as described in section 4.2.7 of Chapter 4. Unpaired two-tailed T-tests were applied for the comparison of two groups after performing an F-test to ensure equal variances. All experiments were done in triplicate to ensure reproducibility. A p-value of <0.05 was considered significant.

5.3. RESULTS

5.3.1. Expression of NCAM during adipogenesis

The antibody used in this study could only detect the NCAM-140 isoform. Expression of NCAM at different time points during adipogenesis (Figure 5.1) was assessed by western blotting. NCAM was found to increase significantly from day 0 to day 12 of adipogenesis.

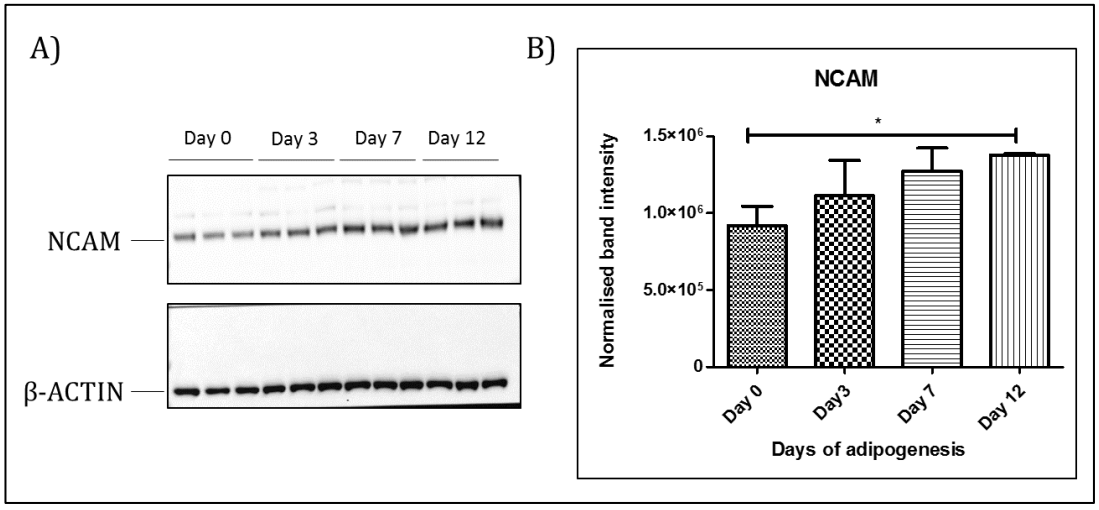

Figure 5.1: Expression of NCAM during adipogenesis. A) Expression of NCAM on days 0, 3, 7 and 12 of adipogenesis. A total of 10 µg of protein loaded/well and β-actin was used as a loading control for normalisation. B) Band densitometry analysis of NCAM protein expression performed in Image Lab. Data are presented as mean ± SD, n=3. * P <0.05 (One-way ANOVA followed by Tukey's Multiple Comparison Test).

5.3.2. Knockdown of NCAM

The role of NCAM as a key regulator of adipogenesis has previously been reported in the 3T3-L1 preadipocyte cell line (Yang *et al.*, 2011). The same method was used in differentiating 3T3-F442A cells to investigate if similar results would be obtained. Effective knockdown of NCAM was observed by western blotting (Figure 5.2). Effective knockdown was achieved on day 4 with a slight recovery in expression observed on day 10.

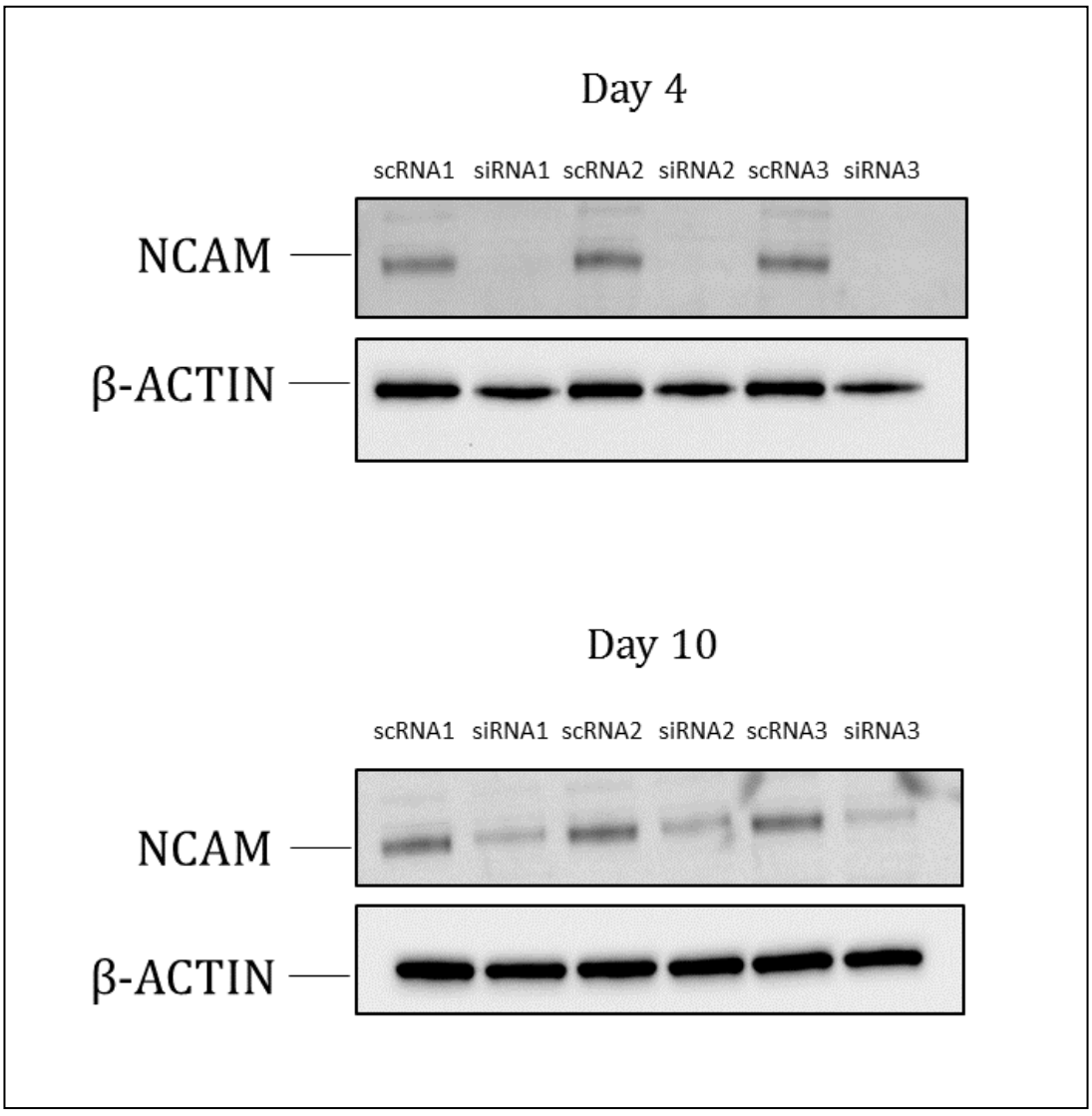

Figure 5.2: Efficient knockdown of NCAM in 3T3-F442A adipocytes. Adipogenesis was initiated on day 0 in the presence of insulin and knockdown of NCAM was carried out in suspended adipocytes on day 1. 3T3-F442A adipocytes were transfected using

Lipofectamine RNIMAX containing a scRNA targeting a scrambled sequence or a siRNA targeting NCAM. NCAM expression was observed on days 4 and 10 of adipogenesis by western blotting. Reduction in NCAM expression was observed in the knockdown condition (siRNA) compared to the control (scRNA). Partial recovery was observed from day 4 until day 10 of adipogenesis. A total of 10 µg of protein loaded/well and β-actin was used as a loading control for normalisation.

5.3.3. Effect of NCAM knockdown on adipocyte lipid accumulation

3T3-F442A differentiating adipocytes were transfected on day 1 of adipogenesis. Cells were in suspension for transfection, but they adhere again to the well after a few hours. Cells were differentiated for 10 days in the presence of insulin. On day 4, western blot was performed to test the efficiency of NCAM knockdown. On day 10 of adipogenesis, intracellular lipid droplet accumulation was visualised; as previously reported by Yang *et al.*, (2011), NCAM knockdown reduced lipid accumulation (Figure 5.3).

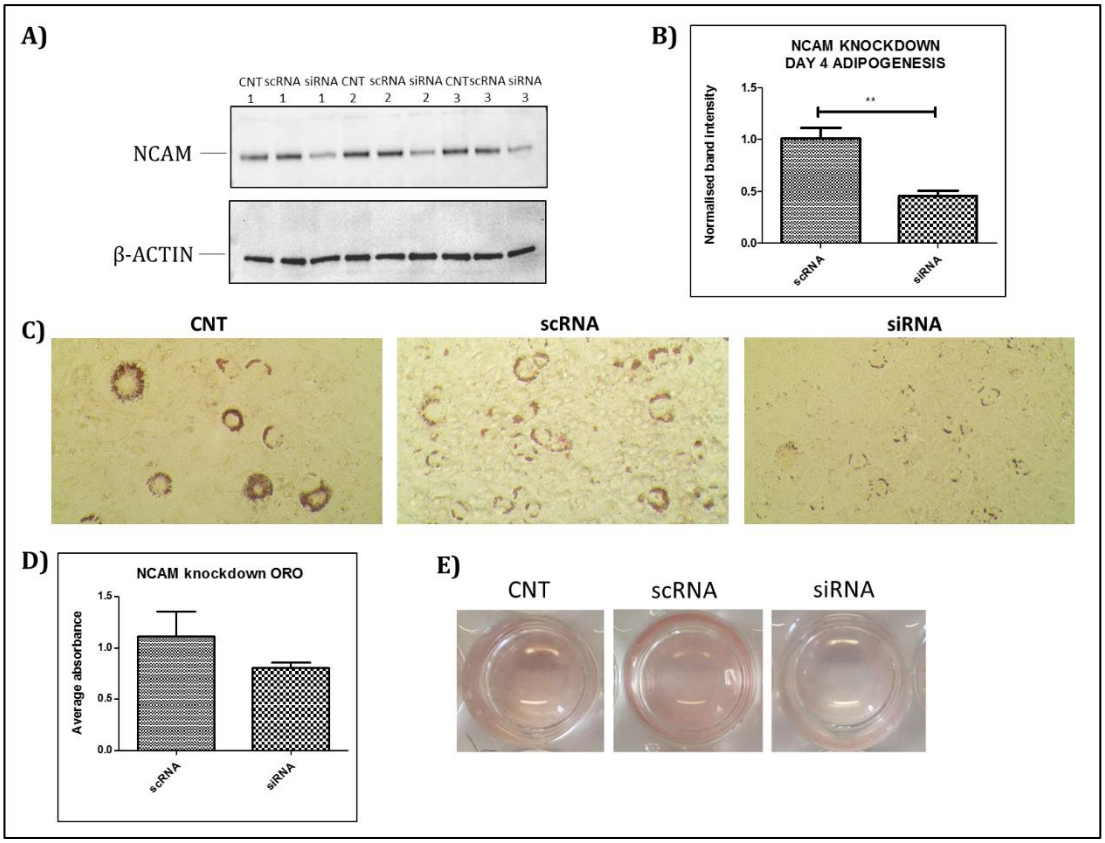

Figure 5.3: NCAM knockdown interfered with adipogenesis of 3T3-F442A cells reducing lipid droplet accumulation. A) Western blot showing effective knockdown

of NCAM (siRNA) compared to scRNA and CNT (untreated cells used as a normalisation control) on day 4 of adipogenesis; B) Band densitometry was performed in Image Lab to observe the difference in protein expression between the siRNA and the scRNA conditions on day 4 of adipogenesis. A total of 10 µg of protein was loaded per well and β-actin was used as a loading control for normalisation; C) Photomicrographs (20x magnification) showing lipid accumulation of mature adipocytes (day 10) in the controls (scRNA and CNT) and NCAM knockdown (siRNA) condition on day 10 of differentiation; D) Absorbance of extracted lipid-bound Oil Red O within the adipocytes in both knockdown and control conditions was measured at 450 nm on day 10 of differentiation; E) mature differentiated adipocytes cultured in 24-well plates after Oil red O staining. B) and D) were analysed using an unpaired T-test and each value is normalised by its respective control (CNT). Data represents the means ± SD of three independent experiments (n=3); ** P <0.01.

5.3.4. Effect of NCAM knockdown on basal GLUT4 expression

The important role of GLUT4 in glucose homeostasis is explained in section 1.4.3 of the general introduction. The impact of NCAM knockdown on GLUT4 expression in adipocytes has not been previously studied. GLUT4 protein expression following knockdown of *NCAM* was assessed by western blotting. A significant but marginal increase (17% increase) in GLUT4 expression was found in NCAM knockdown mature adipocytes (siRNA) (day 10 of adipogenesis) compared to control adipocytes (scRNA) (Figure 5.4). All values were normalised to control untreated adipocytes (CNT). It should be noted that this study only looked at basal GLUT4 expression rather than after insulin stimulation.

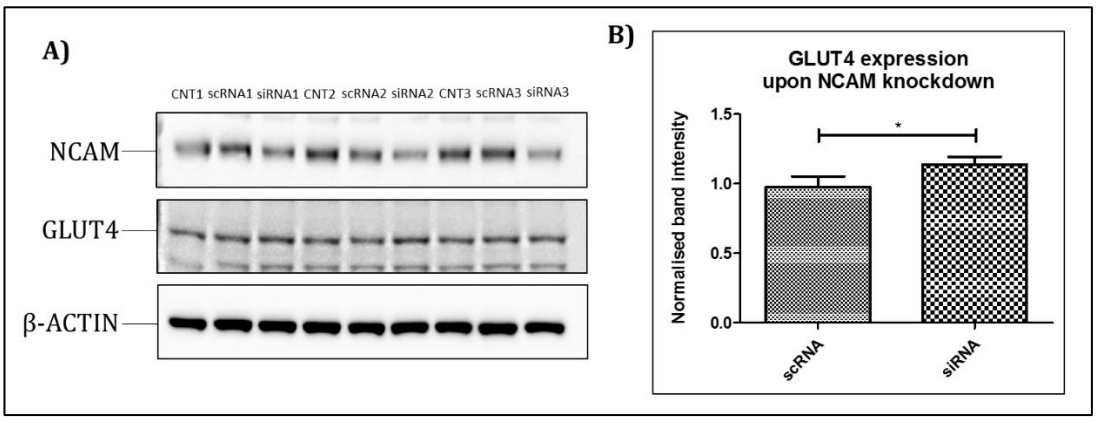

Figure 5.4: Effect of NCAM knockdown on basal GLUT4 expression of 3T3-F442A mature adipocytes. A) GLUT4 expression of NCAM knockdown adipocytes was observed by western blotting and compared to controls (scRNA-treated adipocytes) on day 10 of adipogenesis. CNT: untreated cells used for normalisation. A total of 10 µg of

protein were loaded per well. B) Band densitometry was performed in Image Lab and β-actin was used as a loading control for normalisation. Each value is normalised by its respective control (CNT) and analysed using an unpaired T-test. Data represents the means ± SD of three independent experiments (n=3);* P <0.05.

5.3.5. Effect of NCAM knockdown on adiponectin secretion

Adiponectin is an insulin-sensitising adipokine and its role is explained in section 1.4.4.2 of the general introduction. The effect of NCAM knockdown on adiponectin secretion was investigated. To the best of our knowledge, this had not been previously investigated. Adiponectin levels showed an increase following NCAM knockdown, however this was not statistically significant due to the high variability between biological replicates (Figure 5.5).

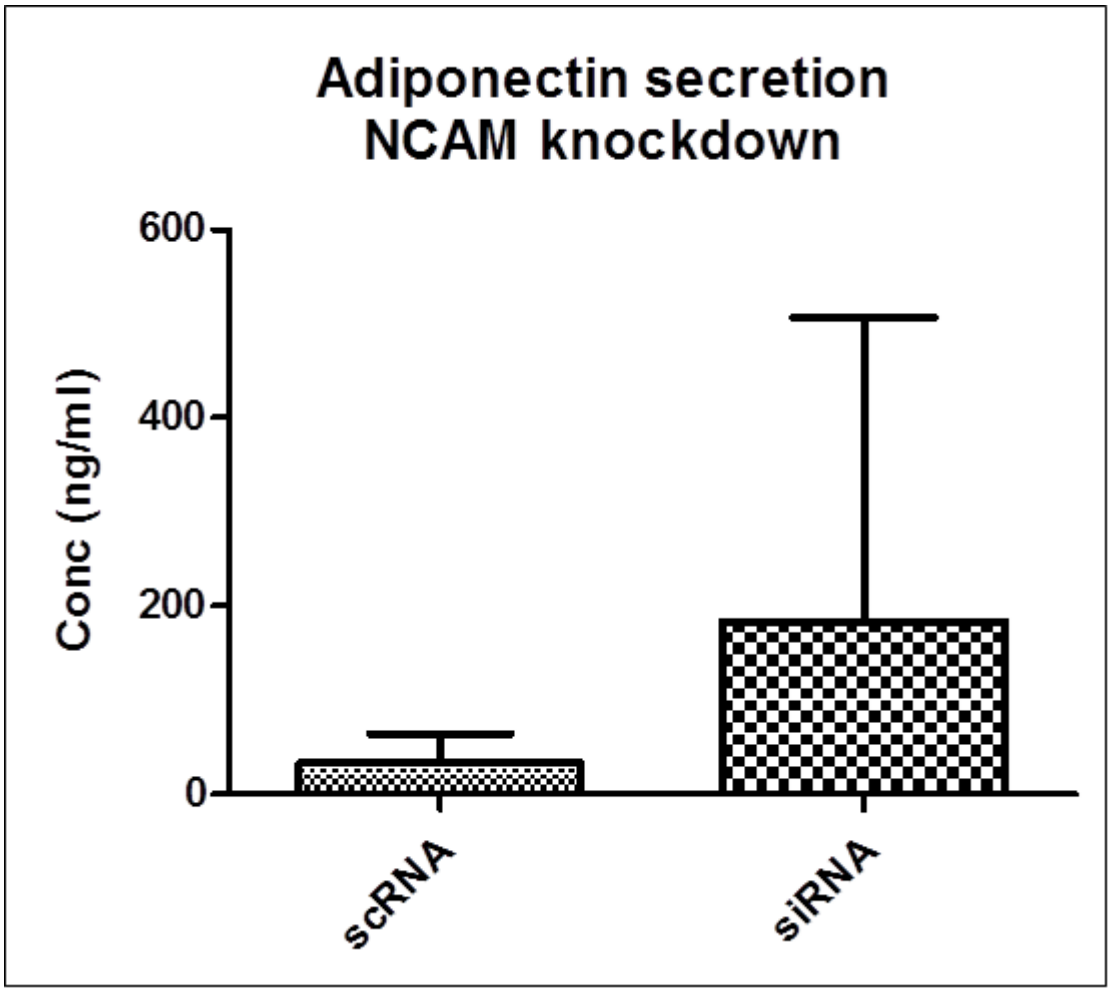

Figure 5.5: Effect of NCAM knockdown on adiponectin secretion by mature 3T3-F442A adipocytes. On day 1 of adipogenesis, adipocytes were transfected using

Lipofectamine RNAIMAX containing a scRNA targeting a scrambled sequence or a siRNA targeting NKCC1. Supernatants were collected on day 10 and adiponectin secretion was measured using ELISA (enzyme-linked immunosorbent assay). All experiments were done in triplicate and each condition (scRNA and siRNA) was normalised by its respective control (untreated cells). Data was analysed using an unpaired T-test. Data represents the means ± SD of three independent experiments (n=3).

5.3.6. Expression of NKCC1 during adipogenesis

Expression of NKCC1 at different time points during adipogenesis (Figure 5.6) was observed by western blotting. NKCC1 expression remained stable in the ealier stages of adipogenesis but it decreased significantly after day 3.

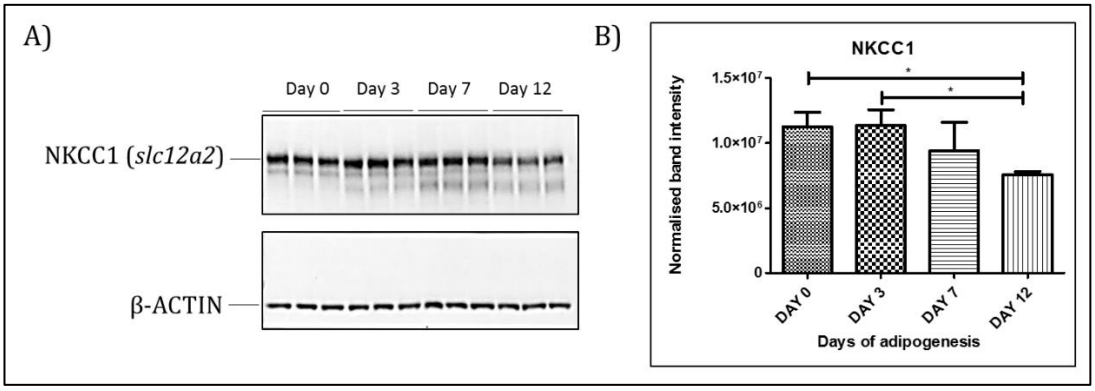

Figure 5.6: Expression of NKCC1 during adipogenesis. A) Expression of NKCC1 on days 0, 3, 7 and 12 of adipogenesis. A total of 10 µg of protein loaded/well and β-actin was used as a loading control for normalisation. B) Band densitometry analysis of NCAM protein expression performed in Image Lab. Data are presented as mean ± SD, n=3. * P <0.05 (One-way ANOVA followed by Tukey's Multiple Comparison Test).

5.3.7. Knockdown of NKCC1

The same protocol was applied to study the effect of NKCC1 on adipogenesis and lipid accumulation. The knockdown of NKCC1 was confirmed by western blotting (Figure 5.7). NKCC1 expression was distinctly depleted in the siRNA-treated adipocytes as compared to scRNA-treated controls on day 4 of adipogenesis. Recovery of NKCC1 expression was observed on day 7 and day 10 but expression was still reduced compared to controls.

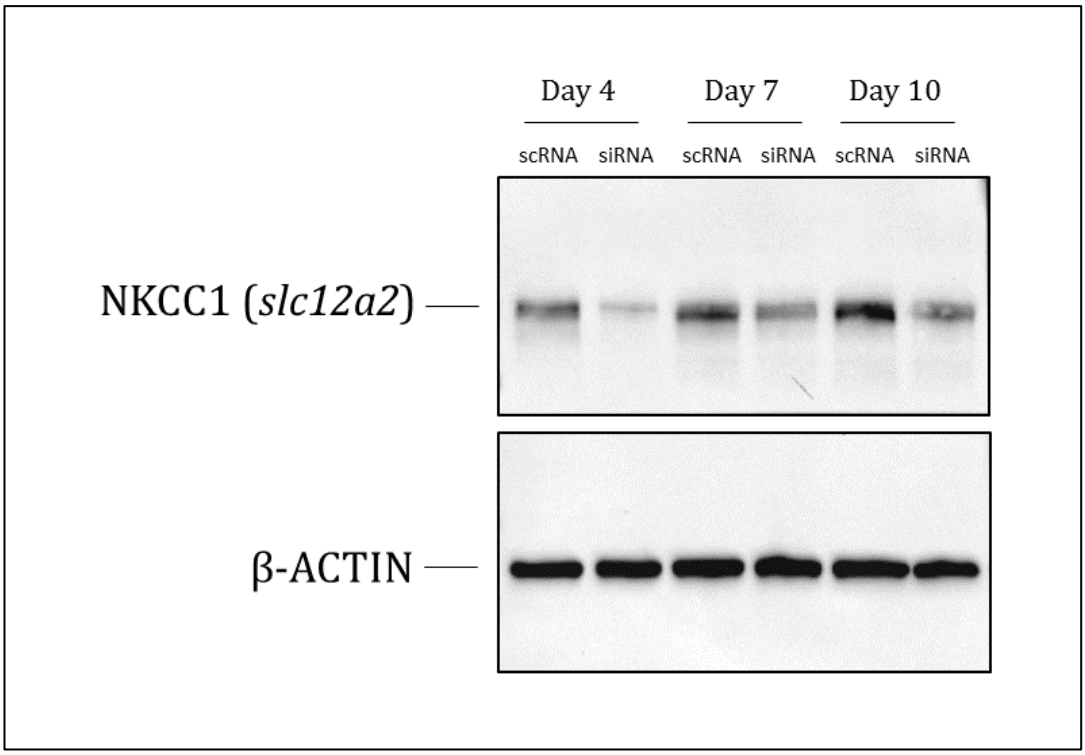

Figure 5.7: Efficient knockdown of NKCC1 in 3T3-F442A adipocytes. Adipogenesis was initiated on day 0 in the presence of insulin and knockdown of NKCC1 was carried out in suspended adipocytes on day 1. 3T3-F442A adipocytes were transfected using Lipofectamine RNAIMAX containing a scRNA targeting a scrambled sequence or a siRNA targeting NKCC1. A total of 10 µg of protein was loaded per well and β-actin was used as a loading control for normalisation.

5.3.8. Knockdown of NKCC1 did not affect lipid droplet accumulation during adipogenesis of 3T3-F442A adipocytes

Mature adipocytes accumulating fully formed lipid droplets in the cytoplasm were observed in both the siRNA-transfected cells and in the controls. Absorbance measurements revealed that there was no difference in lipid accumulation between the siRNA-transfected cells and controls (Figure 5.8).

It was concluded that knockdown of NKCC1 did not affect lipid accumulation during adipogenesis of 3T3-F442A adipocytes.

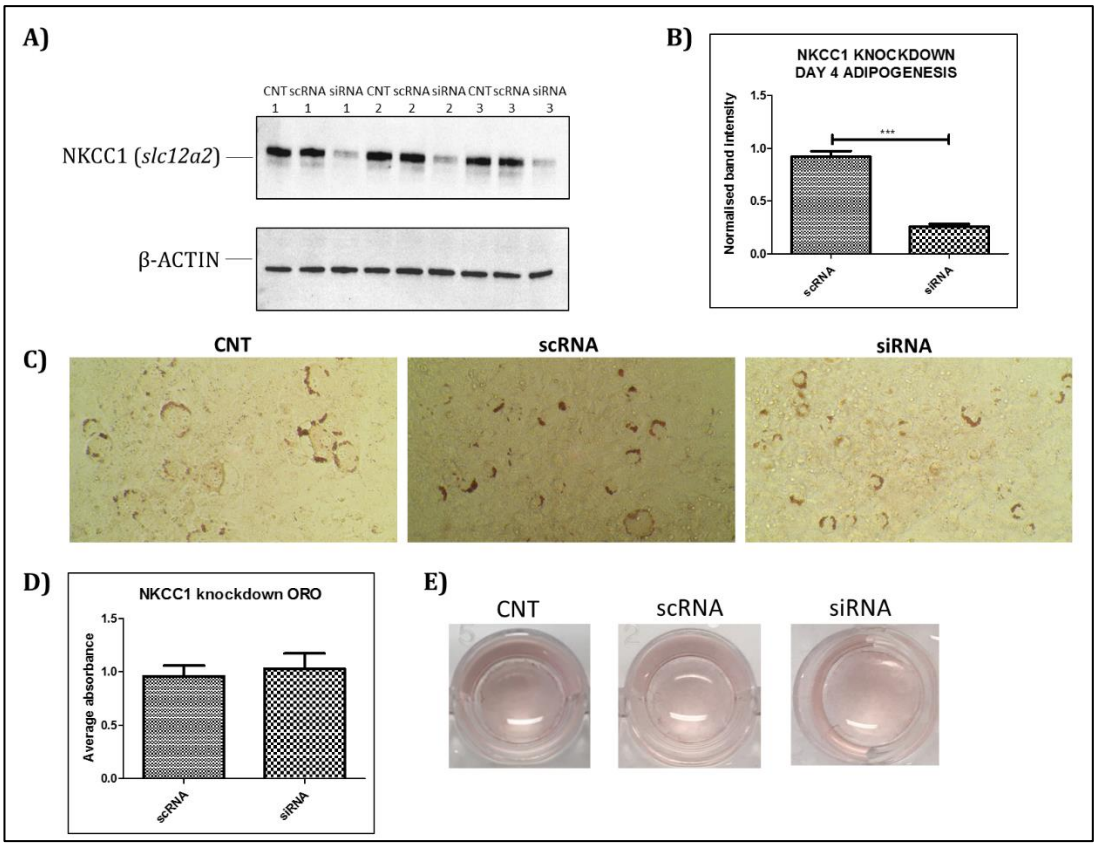

Figure 5.8: Role of NKCC1 on lipid accumulation in differentiating 3T3-F442A adipocytes. A) Western blot showing effective knockdown of NKCC1 (siRNA) compared to scRNA and CNT (untreated cells used as a normalisation control) on day 4 of adipogenesis; B) Band densitometry was performed in Image Lab to observe the difference in protein expression between the siRNA and the scRNA conditions on day 4 of adipogenesis. A total of 10 µg of protein was loaded per well and β-actin was used as a loading control for normalisation. C) Photomicrographs (20x magnification) showing lipid accumulation of mature adipocytes (day 10) in the controls (scRNA and CNT) and NKCC1 knockdown (siRNA) condition on day 10 of differentiation; D) Absorbance of extracted lipid-bound Oil Red O within the adipocytes in both knockdown and control conditions was measured at 450 nm on day 10 of differentiation; E) mature differentiated adipocytes cultured in 24-well plates after Oil red O staining. B) and D) were analysed using an unpaired T-test and each value is normalised by its respective control (CNT). Data represents the means ± SD of three independent experiments (n=3); *** $P < 0.001$.

5.3.9. Effect of acute insulin stimulation on NKCC1 and NKCC2

Next, the expression of NKCC1 following acute insulin stimulation (200 nM insulin) of mature adipocytes was investigated. For this, the expression of both NKCC1 and NKCC2 in the PM-enriched fraction (enriched by colloidal silica bead isolation) obtained from mature adipocytes stimulated by insulin (presented in

chapter 3) was monitored by western blotting, and compared to control adipocytes (unstimulated). No difference was found in the expression of NKCC1 in the adipocyte PM following acute insulin stimulation; however, there was a significant decrease in NKCC2 expression in the PM of insulin-stimulated adipocytes compared to controls (Figure 5.9).

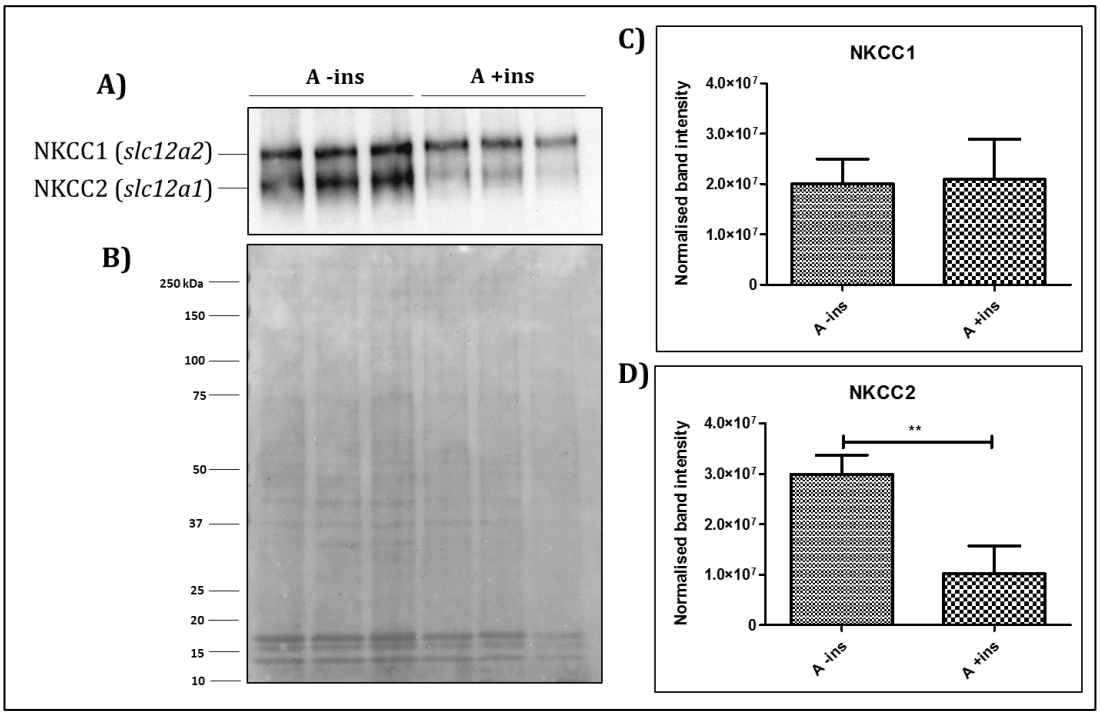

Figure 5.9: Expression of NKCC1 and NKCC2 in the PM fraction of 3T3-F442A adipocytes following acute insulin stimulation. Mature adipocytes were stimulated with insulin (200 nM for 20 minutes) after overnight serum starvation, and the PM fraction was separated by colloidal silica bead isolation. A) Expression of NKCC1 and NKCC2 in the adipocyte PM of insulin stimulated adipocytes ("+ins") was observed by western blotting and compared to unstimulated (control) adipocytes ("-ins"). B) A total of 10 µg was loaded per well and a Ponceau Red stain was used as a loading control to normalise the PM fraction. C) Band densitometry was performed in Image Lab for NKCC1 and D) NKCC2. Data are presented as means ± SD of three independent experiments (n=3) and analysed using an unpaired T-test; ** P <0.01.

5.3.10. Localisation of NKCC1 and NKCC2 in the plasma membrane of 3T3-F442A adipocytes

Given both NKCC1 and NKCC2 were detected in the PM of mature adipocytes by western blot, with NKCC2 showing a reduction in expression when cells were

stimulated with insulin (Figure 5.9), there was a need to identify the location of these two transporters in the adipocyte using immunofluorescence.

However, the antibody used in this thesis was not specific for each isoform, and targetted both transporters. Immunofluorescence images of both insulin-stimulated (100 nM) (Figure 5.11) and unstimulated mature adipocytes (Figure 5.10) located NKCC1 and NKCC2 in the PM as well as in vesicles. In basal conditions, NKCC2 is localised in recycling endosomes but it also translocates to the PM under hyperosmotic stress (Singh *et al.*, 2016).

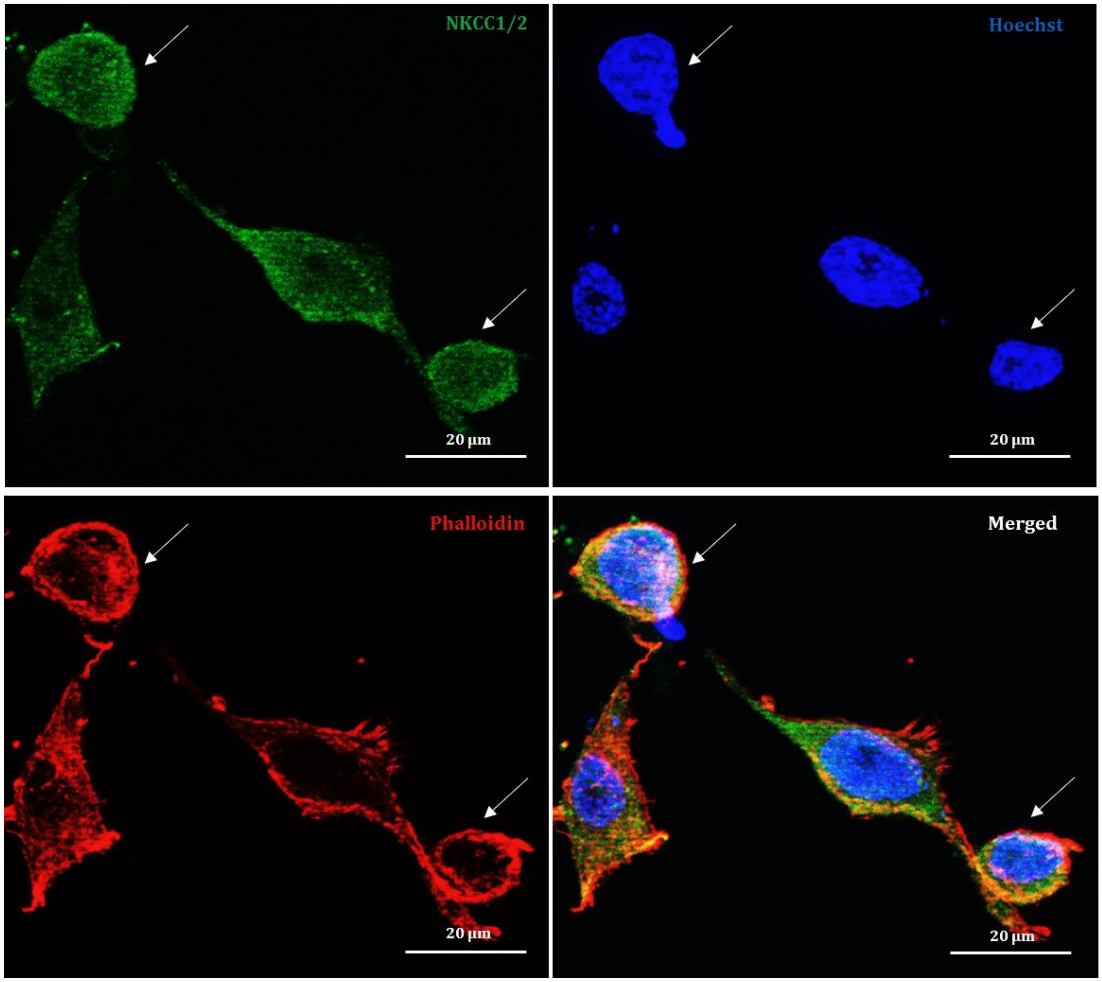

Figure 5.10: Localisation of NKCC1 and NKCC2 in the plasma membrane of 3T3-F442A adipocytes under basal conditions (control). Immunofluorescence microscopy images of 3T3-F442A adipocytes (indicated by arrows), showing expression of NKCC1 and NKCC2 in the PM. Cell nuclei were stained using Hoechst (blue) and the actin cytoskeleton was stained using phalloidin (red). Scale bars represent 20 µm.

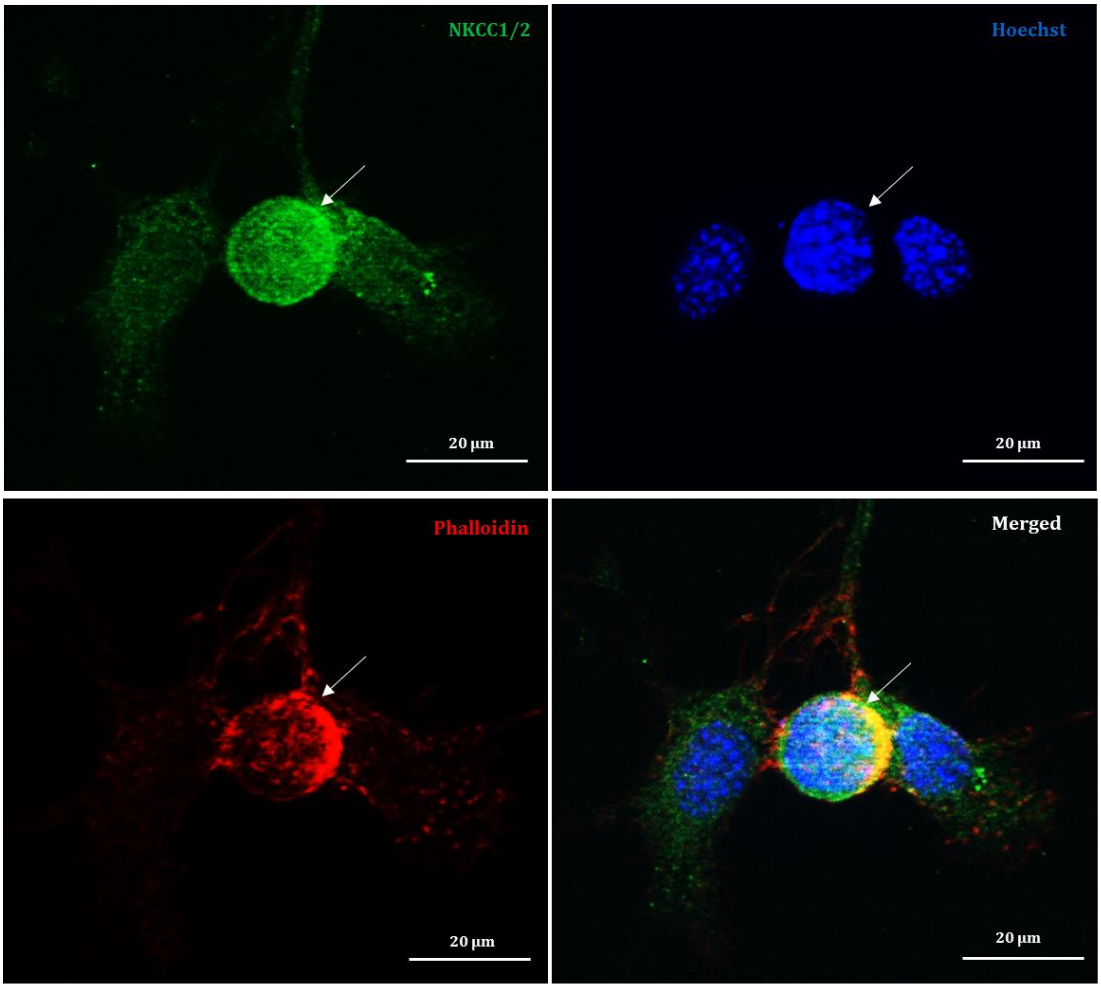

Figure 5.11: Localisation of NKCC1 and NKCC2 in the plasma membrane of 3T3-F442A adipocytes after acute insulin stimulation. Immunofluorescence microscopy images of 3T3-F442A adipocytes (indicated by arrows), showing expression of NKCC1 and NKCC2 in the PM. Cell nuclei were stained using Hoechst (blue) and the actin cytoskeleton was stained using phalloidin (red). Scale bars represent 20 µm.

5.3.11. Effect of NKCC1 knockdown on basal GLUT4 expression

Western blotting analysis revealed no significant difference in GLUT4 protein expression with NKCC1 knockdown in mature adipocytes (day 10 of adipogenesis) compared to controls (Figure 5.12). All values were normalised to control untreated adipocytes (CNT).

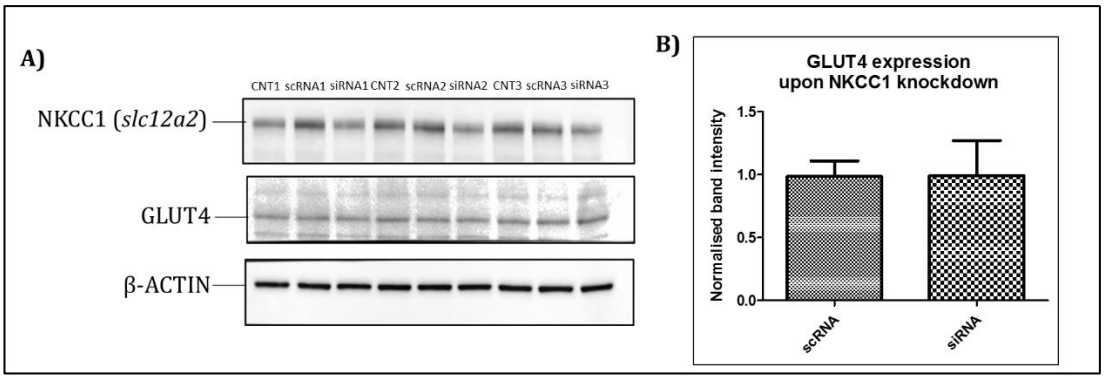

Figure 5.12: Effect of NKCC1 knockdown on GLUT4 expression of 3T3-F442A mature adipocytes. A) GLUT4 expression of NKCC1 knockdown adipocytes was observed by western blotting and compared to controls (scRNA-treated adipocytes) on day 10 of adipogenesis. CNT: untreated cells used for normalisation. A total of 10 µg of protein were loaded per well. B) Band densitometry was performed in Image Lab and β-actin was used as a loading control for normalisation. Each value is normalised by its respective control (CNT) and analysed using an unpaired T-test. Data represents the means ± SD of three independent experiments (n=3).

5.3.12. Effect of NKCC1 knockdown on adiponectin secretion

Adiponectin secretion by adipocytes after NKCC1 knockdown was monitored using ELISA; to the best of our knowledge, this has not been previously studied. Adiponectin levels showed an increase following NKCC1 knockdown, however this was not statistically significant (Figure 5.13).

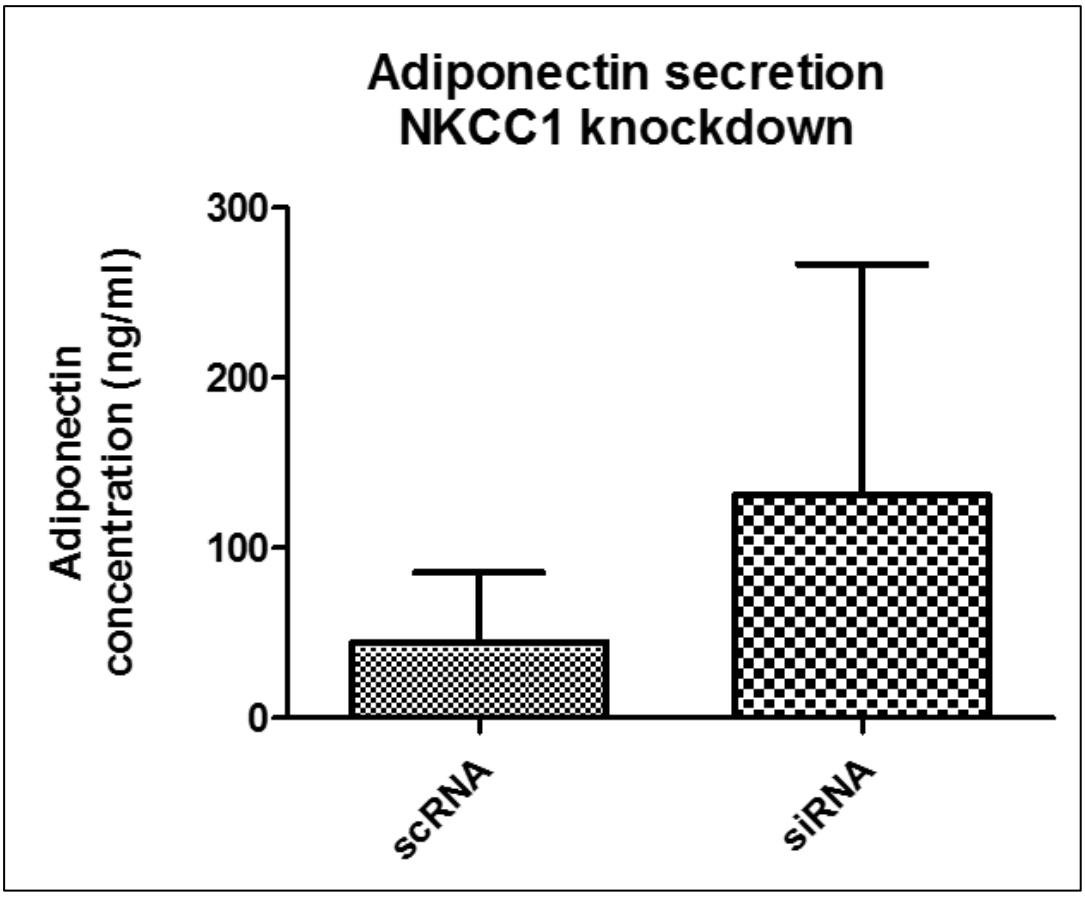

Figure 5.13: Effect of NKCC1 knockdown on adiponectin secretion by mature 3T3-F442A adipocytes. On day 1 of adipogenesis, adipocytes were transfected using Lipofectamine RNAIMAX containing a scRNA targeting a scrambled sequence or a siRNA targeting NKCC1. Supernatants were collected on day 10 and adiponectin secretion was measured using ELISA (enzyme-linked immunosorbent assay). All experiments were done in triplicate and each condition (scRNA and siRNA) was normalised by its respective control (untreated cells). Data was analysed using an unpaired T-test. Data represents the means ± SD of three independent experiments (n=3).

5.4. DISCUSSION

NCAM, a known key regulator of adipogenesis and insulin signalling, was examined using functional assays in this chapter; this study built on existing data on the effect of this protein in adipogenesis but also previously unreported investigations were performed on this protein. An increase in NCAM protein expression was observed as adipogenesis progressed. An increased expression of NCAM was also previously observed in mesenchymal stem cells (MSCs) cultured

for up to three weeks, compared to freshly isolated MSCs (Yang *et al.*, 2011); however, this is the first report on NCAM expression during adipogenesis in a 3T3-F442A cell line.

The results presented in this study revealed that knockdown of NCAM led to a markedly reduced lipid accumulation similar to what has been observed with 3T3-L1 adipocytes (Yang *et al.*, 2011). The mechanism behind adipogenesis regulation by NCAM may involve modulation of adipogenic factors, and actin cytoskeleton remodelling. In *Ncam*$^{-/-}$ MSCs, the expression of the adipocyte inducers PPARγ and αP2 was reduced, and cells also presented faulty F-actin cytoskeleton remodelling (Yang *et al.*, 2011). In 3T3-L1 adipocytes, NCAM knockdown was shown to induce expression of TNFα, an adipogenesis inhibitor (Cawthorn *et al.*, 2007) and a contributor to insulin resistance (Hotamisligil, 1999; Zhang *et al.*, 2009).

Furthermore, NCAM deficiency reduced activation of the IR, disrupting insulin signaling in 3T3-L1 adipocytes (Yang *et al.*, 2011). These findings show NCAM as a protein involved in insulin signaling. It was observed that knockdown of NCAMled to reduced lipid accumulation in the 3T3-F442A adipocytes. The role of NCAM in GLUT4 expression and adiponectin secretion was also investigated in this chapter. NCAM knockdown induced a slight increase in basal GLUT4 expression. Although NCAM knockdown resulted in increased secretion of adiponectin, given the variability observed with thetechnical replicates, there is a need to further clarify the effect on adiponectin in NCAM-knockdown adipocytes.

The findings on GLUT4 expression presented in this study were not consistent with the previously published effect of NCAM knockdown on 3T3-L1 adipocytes, which reduced the activation of the IR, a necessary trigger for the translocation of GLUT4 to the PM (Yang *et al.*, 2011). Nevertheless, it is important to consider that this study has looked at the basal expression of GLUT4 and not its expression following insulin stimulation. Also, the western blots presented in Figure 5.4 and Figure 5.12 show expression of GLUT4 on whole cell lysates and, due to the fact that GLUT4 translocates to the PM inside vesicles following insulin stimulation, the results of the current study do not present the expression of GLUT4 in the PM specifically. Previous studies have used enrichment techniques for the isolation of GSVs (Potthoff *et al.*, 2010; Prior *et al.*, 2011) and the application of GLUT4 vesicle isolation techniques may provide a more accurate representation of the effect of both NKCC1 and NCAM on GLUT4 expression.

Overall, NCAM protein levels were found to increase during adipogenesis. NCAM knockdown was found to reduce lipid accumulation in 3T3-F442A adipocytes, and to marginally increase basal GLUT4 expression. Further investigation is needed on the role of NCAM in GLUT4 translocation, and this may involve isolation of GSVs or glucose uptake assays.

Variability between technical replicates did not allow for a conclusion on the effect of NCAM knockdown on adipocyte secretion. It was observed that adiponectin levels decreased with increasing passage numbers. It was previously reported that preadipocyte cell lines lose differentiation capacity with increasing number of passage (Ali *et al.*, 2013), therefore adiponectin secretion would also be affected. This may have happened with the cells used in this study and

increasing passages may have resulted in a reduction of differentiation efficiency of the cells.

The transporter NKCC1 was one of the proteins found to be significantly differentially regulated following exposure to PIs as presented in the previous chapter. However, the role of NKCC1 on adipocyte metabolic toxicity remains to be clarified and hence this studyattempted to do this by using functional studies.

The expression of NKCC1 was found to remain stable initially during adipogenesis and then decrease after day 3. However, knockdown of NKCC1 did not affect adipocyte lipid accumulation. This may suggest a limited role for NKCC1 at least in the latter stages of adipogenesis. The influence of acute insulin stimulation on NKCC1 expression in the adipocyte PM was investigated. NKCC1 expression did not appear to be altered by acute insulin stimulation; however, a 2.9-fold reduction in the expression of the isoform NKCC2 (Figure 5.9) in the adipocyte PM of insulin-stimulated adipocytes compared to controls was observed.

NKCC1 and NKCC2 are both activated in response to cell shrinkage induced by hyperosmotic stress. Regulatory Volume Increase (RVI), the compensatory cell response to shrinkage, is carried out by the activation of NKCC1 (by its active co-transport of water into the cell) (Hoffmann *et al.*, 2009; Hamann *et al.*, 2010). In fact, stable silencing (shRNA) of *Nkcc1* in COS7cells has been shown to result in cell shrinkage (Singh *et al.*, 2016). As a response to NKCC1 inhibition, NKCC2 has been shown to be up-regulated, and to translocate from the ER to the PM via endosomes of COS7 and β-cells under hyperosmotic conditions (cell shrinkage) (Alshahrani *et al.*, 2015; Singh *et al.*, 2016).

The effect of cell volume alterations on insulin signalling is well established (Schliess *et al.*, 2000; Eduardsen *et al.*, 2011). Hyperosmotic cell shrinkage is thought to contribute to insulin resistance, and insulin is known to induce cell swelling by activation of NKCC1 (Mager *et al.*, 2000; Schliess *et al.*, 2000; Eduardsen *et al.*, 2011). No change was found regarding NKCC1 expression following insulin stimulation. But an increase in NKCC1 following chronic treatment with lopinavir was observed. Whilst it is difficult to suggest the role of NKCC1 in adipocyte metabolic toxicity, the increase observed in NKCC1 with lopinavir may actually be a compensatory increase in its expression (protein estimation was done after 10 days of drug treatment) to restore the cell volume and thereby potentially, insulin signalling.

Alshahrani *et al.*, (2015) observed a translocation of NKCC2 to the PM of β-cells in response to cell shrinkage induced by inhibition of NKCC1. Reduced NKCC2 expression in the PM of adipocytes following insulin stimulation was observed; this may suggest translocation of NKCC2 back into cytoplasmic vesicles following insulin stimulation. As insulin induces cell swelling by activation of NKCC1, and cell shrinking induces translocation of NKCC2 to the PM, this suggests that the results presented in the current study may be linked to cell volume regulation by insulin.

It is important to mention that the compensatory mechanism behind NKCC1 and NKCC2 is not well understood, as these transporters are functionally different. NKCC2 does not transport water and it was found unable to revert the effects of NKCC1 inhibition in cell shape in COS7 cells (Singh *et al.*, 2016); however when *Nkcc1* was knocked out in mice, NKCC2 was suggested to promote insulin

secretion by pancreatic β-cells and to improve glucose tolerance on its own, suggesting a compensatory effect on insulin secretion (Alshahrani *et al.*, 2012).

In 3T3-L1 adipocytes, osmotic-induced cell shrinkage was observed to inhibit phosphorylation of the IR in a transient manner, but cell swelling did not impact phosphorylation of IR (Eduardsen *et al.*, 2011). This study did not investigate insulin signalling; hence it is not clear what the effect of NKCC1 knockdown is on adipocyte IR or insulin signalling molecules. Additional experiments targeting the expression of IR following inhibition or knockdown of NKCC1 and expression of key mediators of insulin signalling may help clarify the effect of this transporter on insulin signalling.

Immunofluorescence located both NKCC1 and NKCC2 in the PM and vesicles of adipocytes. To get a deeper understanding, each isoform would need to be targeted by specific antibodies that would allow to differentially localise them through different immunofluorescence channels. This may allow observation of any translocation of NKCC2 to the PM upon insulin stimulation. A challenge when performing immunofluorescence in adipocytes was the inability of these cells to adhere to glass slides. Different coatings (matrigel, gelatin and collagen) were attempted, but effective attachment was not achieved.

Knockdown of NKCC1 did not seem to influence GLUT4 expression. Unless a detailed investigation of NKCC1 and its effect on insulin signalling has been conducted, it is difficult to suggest a role of this transporter in insulin signalling and metabolic homeostatsis at least from an adipocyte perspective.

Finally, there was a need to investigate the effect of NKCC1 knockdown on adiponectin secretion. For this, ELISA Adiponectin assays were employedto

measure the adiponectin content in the medium in which both the knockdown and the control cells were maintained. There was a high variability in adiponectin secretion between biological replicates, and therefore it was concluded that there was not enough evidence of a change in adiponectin secretion by adipocytes following knockdown of NKCC1. Overall, NKCC1 knockdown did not affect adipocyte lipid accumulation, GLUT4 expression and adiponectin secretion; this might suggest NKCC1 to be of less important in the maintenance of metabolic homeostasis by the adipocyte. However, its increased expression when incubated chronically with PIs, and the reduction in NKCC2, a closely related isoform of NKCC1 during acute insulin stimulation, warrants further investigation to clarify their roles in PI-induced adipocyte effects.

In conclusion, this chapter investigated the role of NKCC1 and NCAM in cellular events that are important in metabolic homeostasis: adipogenesis, lipid accumulation, insulin stimulation, GLUT4 expression, and adiponectin secretion. Although the results presented in the current study suggest that NKCC1 did not have an effect on lipid accumulation, GLUT4 expression and adiponectin secretion, there was an interesting observation in the expression of NKCC2 following acute insulin stimulation. The maintenance in NKCC1 expression levels and the downregulation of NKCC2 after acute exposure of adipocytes to insulin, may point towards a compensatory action between the two isoforms, consistent with the results of Chapter 4 and with previous publications (Alshahrani *et al.*, 2015; Singh *et al.*, 2016). Further investigation of the compensatory effect between NKCC1 and NKCC2, and of NKCC2 translocation to the PM of adipocytes needs to be performed.

CHAPTER 6
FINAL DISCUSSION

6.1. Thesis Overview

Antiretroviral therapy has transformed HIV infection into a manageable chronic condition, considerably increasing the life expectancy of HIV patients (World Health Organization, 2016; Panel on Antiretroviral Guidelines for Adults and Adolescents, 2018). However, aging HIV patients who have been exposed to ART for most of their lifetime have developed an increased susceptibility to metabolic syndrome when compared to age matched cohorts not receiving ART (Wand *et al.*, 2007; Magkos *et al.*, 2011). Metabolic syndrome dramatically increases the risk of cardiovascular disease (CVD) in an already high-risk population with the risk of CVD in HIV patients known to be almost double that of the general population (Triant, 2013).

The adipose tissue is a key regulator of metabolic homeostasis and it exerts an endocrine action by secreting adipokines (Musi *et al.*, 2014). Disruptions in the adipocyte metabolic homeostasis may lead to metabolic toxicity and consequently result in insulin resistance, T2DM, and dyslipidaemias, and eventually lead to CVD (Laclaustra *et al.*, 2007; Rezaee *et al.*, 2013).

The metabolic adverse effects of antiretrovirals on adipose tissue have been thoroughly investigated and first-generation PIs like lopinavir have been shown to be particularly harmful (Bernal *et al.*, 2007; Martin *et al.*, 2013; Zha *et al.*, 2013), whereas certain other antiretrovirals are considered to be metabolically safer (e.g. atazanavir) (Minami *et al.*, 2011). A variety molecular mechanisms by which antiretroviral drugs cause metabolic toxicity have been proposed: these include adipogenesis disruption, dysregulation of adipokine secretion, disturbances in the insulin signalling pathway, inhibition of GLUT4 translocation to the PM,

interference in mitochondrial function, disturbances in lipid metabolism, pro-inflammatory cytokines, enhanced release of ROS, and disruption of PPARγ expression (Anuurad *et al.*, 2010; Feeney *et al.*, 2011; Minami *et al.*, 2011; Kitazawa *et al.*, 2014). However, little is known about how antiretroviral drugs get into the adipocyte and what effects they cause on the adipocyte PM.

The PM is a key target for proteomics research because it comprises a vast amount of drug targets, transporters, and biomarkers of disease. It is also the location of several important proteins involved in insulin signalling and glucose homeostasis, such as the IR and GLUT4 (Cordwell *et al.*, 2010; Prior *et al.*, 2011; Lai, 2013; Hörmann *et al.*, 2016). However, PM proteomics is a challenging area of research due to the relatively low abundance of PM proteins when compared to the cytosolic proteins in the cell. Detection of PM proteins is also rendered challenging by their poor solubility and post-translational modifications these proteins undergo (Tan *et al.*, 2008; Cordwell *et al.*, 2010; Barrera *et al.*, 2011; Renes *et al.*, 2013).

The principal aim of this thesis was to investigate changes in the adipocyte PM proteome following exposure to HIV PIs in order to gain insight into the mechanisms behind antiretroviral-induced metabolic toxicity and to understand if adipocyte PM proteins contributed to the development of this important toxicity. For this, there was first a needto optimise and validate a methodology that can enrich PM proteins in the adipocyte cell lysate so that they can be better detected using downstream techniques such as LC-MS/MS.

This study developed and optimised a protocol for the enrichment and isolation of the adipocyte PM in 3T3-F442A adipocytes. Enrichment was carried out using colloidal silica bead isolation.

Theaim of this study was to enrich the cell lysate with PM proteins so that they are not masked by the highly abundant cytoplasmic proteins. A total of 419 (35%) PM proteins were identified following silica bead isolation enrichment; this was higher than the number of PM proteins identified in human adipocytes various other research groups (Xie *et al.*, 2010). The results of the current study concluded that the developed protocol was efficient for the analysis of the adipocyte PM proteome (chapter 2).

Once the experimental methodology was optimised, this study proceeded to examine the changes in the adipocyte PM proteome during adipogenesis, and following acute insulin stimulation (chapter 3), as these are key processes in adipocyte biology. The PM proteome of undifferentiated preadipocytes and mature adipocytes both in basal conditions and under acute stimulation with insulin were analysed using LC-MS/MS. Label-free relative protein quantitation was carried out using Progenesis QI. A number of differentially regulated PM proteins known to be involved in adipogenesis were identified, such as RACK1 (Kong *et al.*, 2016) and Ezrin (Titushkin *et al.*, 2013), but also proteins with no previous link to adipocyte differentiation (Zinc transporter ZIP10 (Slc39a10), Disks large-associated protein 1 and Podoplanin, amongst others) were identified. Furthermore, this study found PM proteins associated with metabolic syndrome, such as Perilipin-2, a protein associated with obesity, and adipose tissue inflammation (McManaman *et al.*, 2013; Takahashi *et al.*, 2016) and

Prohibitin-2, whose overexpression has been associated to obesity and alterations in glucose homeostasis (Ande *et al.*, 2014).

After classifying the detected PM proteins based on GO "Molecular Function" annotations, this studyound that hydrolase activity was the major functional component for these proteins. The findings of the current study were consistent with the study by Prior *et al.*, (2011) in which hydrolases were also found to be a big component of the adipocyte PM proteome; hydrolases have also been proposed to play a role in ECM modulation (Renes *et al.*, 2013). Bioinformatic analysis found pathways consistent with adipogenic events, such as extracellular matrix organisation, MAPK family signalling cascades, collagen-formation related pathways, transport and vesicle translocation-related pathways. The ECM has a role in providing mechanical support to the adipocyte. During adipogenesis, the cells undergo abrupt changes in shape and ECM modulates adipocyte differentiation, changing from a fibrillar to a laminar structure (Ali *et al.*, 2013). Collagen, elastin and fibronectin are components of the ECM. A recent study revealed that the expression of type I and type III collagens occurs in early adipogenesis, and types IV, V and VI of collagens are produced in the middle stage of adipogenesis (Ojima *et al.*, 2016). Differential expression of collagens during adipogenesis is explained by changes in the ECM conformation to accommodate for the shape changes in adipocytes. Data from the current study showed upregulation of collagen VI in the PM proteome of mature adipocytes compared to that of preadipocytes, consistent with findings reported by Renes *et al.* (2013), and Prior *et al.*, (2011); the latter found differential regulation of collagens in response to insulin stimulation. Collagen VI has been shown to regulate insulin sensitivity and Akt signalling (Khan *et al.*, 2009). Changes in the ECM have been

linked to metabolic toxicity; in obesity, adipocytes become hypertrophic and the ECM is unable to maintain its stability (Mariman *et al.*, 2010).

The effect of HIV PIs (chapter 4) on the adipocyte PM proteome was investigated. For this, lopinavir was used as an example of a metabolically toxic drug and atazanavir as a comparator with a more favourable metabolic profile. The anti-hypertensive telmisartan was used to investigate any protection against the effects of lopinavir toxicity at the protein level. This drug has been shown to revert the metabolic adverse effects of lopinavir *in vitro* (Pushpakom *et al.*, 2018). The PM proteome of mature adipocytes after chronic exposure with lopinavir and atazanavir (both alone and also in combination with telmisartan) was analysed. The doses used were therapeutically relevant doses and were established in our research group (Pushpakom *et al*., 2018) in a chronic drug toxicity model. A total of 96 significantly differentially regulated PM proteins were identified.

Using label-free relative protein quantitation analysis and bioinformatics, two target proteins were selected for validation: the transporter protein NKCC1 and the cell adhesion protein NCAM. Western blot analysis detected not only differential regulation of NKCC1 following exposure to PIs, but also detected the isoform of this transporter, NKCC2 in the adipocyte PM. To our knowledge, NKCC2 has not been previously detected in the PM of adipocytes.

A number of Progenesis predictions were validated by western blotting: significant up-regulation of NKCC1 after exposure to lopinavir combined with telmisartan compared to controls (Figure 4.14), and significant up-regulation of NKCC1 after lopinavir exposure compared to atazanavir (Figure 4.15).

Lopinavir was found to up-regulate NKCC1 in the adipocyte PM. An opposite trend for NKCC2 was observed. The fact that NKCC2 translocates to the PM as a compensatory effect for NKCC1 inhibition was already reported (Alshahrani *et al.*, 2012); this may explain the current study´s observation and suggests that a compensatory effect between these two transporters may be taking place in the adipocytes.

Telmisartan was also observed to reverse the lopinavir-induced upregulation of NKCC1 expression in adipocytes. A similar reversal with telmisartan was also observed for NKCC2. Telmisartan was reported to reverse the toxic effects of lopinavir on adipocytes, such as reversion of lopinavir-induced dowregulation of *PPARγ* AND *LPIN1* and downregulation of adiponectin secretion (Pushpakom *et al.*, 2018). This may explain the current study´s observations and suggests that telmisartan may be reversing the effect of lopinavir on NKCC1 expression in the adipocyte PM.

To gain more insight into the role of the selected targets in adipocyte biology, functional characterisation assays were applied to the selected targets NKCC1 and NCAM (chapter 5). Firstly, knockdown assays were used to characterise the effects of downregulation of these target proteins on adipogenesis and other aspects of glucose homeostasis. An increasing expression of NCAM during adipogenesis was observed, whereas the expression of NKCC1 decreased during adipogenesis. To our knowledge, expression of NKCC1 during adipogenesis has not been previously investigated.

An experimental protocol for functional characterisation of target proteins was optimised, and it comprised knockdown of protein expression, ORO staining,

western blot and ELISA adiponectin assays. NCAM was used as a model protein for optimisation since it was previously reported that knockdown of NCAM disrupted adipogenesis and decreased lipid accumulation in the 3T3-L1 cell line (Yang *et al.*, 2011); this publication's protocol was adapted for 3T3-F442A adipocytes in this thesis and a reduction in lipid accumulation in NCAM-knockdown adipocytes compared to controls was observed, and this was consistent with the results observed by (Yang *et al.*, 2011).

The effect of knockdown of NKCC1 on lipid accumulation during adipogenesis was investigated; it was observed that knockdown of this transporter did not affect lipid accumulation. To investigate the effect of acute insulin stimulation on NKCC1 expression,the expression of NKCC1 in control and insulin-stimulated adipocytes was measured by western blotting and found no differential expression of NKCC1 following acute insulin stimulation; however, NKCC2 was observed to be downregulated in the adipocyte PM of insulin-stimulated adipocytes compared to controls.

Interestingly, detectable levels of NKCC2 were only observed by western blotting in the PM-enriched fraction, but not in whole lysate samples; the expression of NKCC2 in the PM fraction could be a consequence of enrichment, as vesicles containing NKCC2 closely positioned to the PM may be also isolated by the silica beads; but it may also be a compensatory response to NKCC1 down-regulation. Under basal conditions, NKCC2 is barely detectable in the PM, and is mainly localised in cytoplasmic vesicles (Alshahrani *et al.*, 2015; Singh *et al.*, 2016).

While the role of NKCC1 in adipocyte metabolic toxicity has not been previously studied and it is therefore difficult to elucidate, the difference in expression of

both NKCC1 and NKCC2 following drug treatments (up-regulation of NKCC1 and downregulation of NKCC2 following lopinavir treatment) and following insulin stimulation (downregulation of NKCC2 following acute insulin stimulation) observed in this thesis may point towards a compensatory mechanism based on translocation of NKCC2 to the PM.

Furthermore, western blots show a higher expression of NKCC2 compared to NKCC1 in the PM fraction of control mature adipocytes (for both drug treatments and insulin stimulation experiments). The expression of NKCC1 during adipogenesis was observed to decrease in the last stages of adipogenesis by western blot in whole-cell lysates (Figure 5.6). This down-regulation of NKCC1 may lead to translocation of NKCC2 to the PM as a compensatory mechanism, as already reported by (Alshahrani *et al.*, 2015) in β-cells, and this may explain the higher expression of NKCC2 compared to NKCC1 in the PM of mature control adipocytes (observed in Figure 4.14, Figure 4.15 and Figure 5.9).

6.2. Perspectives for future work

Despite increasing attention towards PM proteomics research, no previous studies have focused on the metabolic effects of antiretrovirals on the adipocyte PM. This study identified two potential targets for PIs, which may play a role in the metabolically toxic effects of lopinavir. Further investigation of the association between NKCC1/2 and antiretrovirals needs to be performed. Transport assays would need to be applied to investigate whether these transporters participate in antiretroviral uptake in adipocytes; other transporters of the SLC family have been shown to transport lopinavir (Hartkoorn *et al.*, 2010; Kis *et al.*, 2010).

To further clarify if there is a compensatory effect between NKCC1 and NKCC2 in adipocytes, translocation of NKCC2 to the PM following blocking of NKCC1 could be investigated by immunofluorescence. Immunofluorescence would also help to observe if there is a translocation of NKCC2 between the adipocyte PM and cytoplasmic vesicles following insulin stimulation, but the use of specific antibodies for each isoform will be required to differentiate their location. In addition, the effect of NKCC1/2 and NCAM knockdown on the expression of key proteins for adipocyte metabolic homeostasis like PPARγ and the IR remains to be investigated.

To improve the investigation of the effect of knockdown of NCAM, NKCC1 and NKCC2 on GLUT4 expression, immunoadsorption of GLUT4 vesicles should be performed (as previously done by Prior *et al.*, (2011)); this may provide with a more in-depth picture of GLUT4 expression, as it travels between the PM and GSVs. Glucose uptake assays could also be applied to NKCC1/2 and NCAM-knockdown adipocytes to observe the effect of these proteins on glucose uptake by adipocytes.

The application of label-free proteomics for relative protein quantitation is commonly applied for the analysis of complex mixtures; other studies may apply labelling methods such as iTRAQ and SILAC. Overall, label-free approaches provide a bigger coverage of the proteome, whereas labelling approaches provide with a more accurate and precise quantification (F. Xie *et al.*, 2011). However, a number of studies showed better accuracy and detection of higher numbers of differentially expressed proteins when label-free proteomics was employed (Trinh *et al.*, 2013; Latosinska *et al.*, 2015). This study applied label-free

proteomics because it is cost-effective and provides a broader proteome coverage. Relative protein quantitation based on peptide intensities was performed using the software Progenesis QI. The FDR was set at 5%, consistently with previous proteomic studies (Catherman, Durbin, *et al.*, 2013; Catherman, Li, *et al.*, 2013), and the minimum number of unique peptides per protein was set to one. A more restrictive approach for protein identification would be to apply a FDR of 1% and to only include proteins with at least two or three unique peptides in the analysis. However, due to the small abundance of PM proteins and the difficulty in their detection, this study set for less restrictive parameters and aimed for a bigger proteome coverage to avoid missing important PM proteins. To ensure that the predictions generated by Progenesis were accurate, they were validated by western blotting.

However, modifications could be applied to improve the accuracy of the experimental design of the work conducted in this thesis. When performing LC-MS/MS, an additional sample should be included, and this sample should contain a mixture of all the different conditions of the analysis. This sample would be used as a reference for alignment of ion intensity maps in Progenesis QI and would make the differences in protein abundance detected between samples more accurate, as well as help identify proteins exclusive of each condition.

Another approach to increase the number of detected PM proteins would be to decrease the dilution of the resuspended samples into formic acid before injection into the mass spectrometer; the amount of proteins detected under a 1:10 sample dilution in 0.1% formic acid applied in chapters 2 and 3 was observed to be a lot lower than the amount detected in the undiluted samples in

chapter 4. When possible, it may be also recommended to increase the amount of protein that is digested for mass spectrometry analysis (100 μg of total protein lysate per sample were used), as well as increasing the number of replicates. The cytosolic fraction obtained by applying the methodology developed in the current study could also be subjected to LC-MS/MS to get full coverage of the adipocyte proteome. Finally, this analysis would need to be replicated in human adipocytes for further investigation.

6.3. Conclusions

This thesis provides a comprehensive proteomic analysis of the adipocyte PM regarding two important processes for metabolic homeostasis: adipogenesis and insulin signalling. More importantly, this study presents an analysis on the changes induced by the PIs lopinavir and atazanavir on the adipocyte PM proteome. In this study, a protocol for enrichment and analysis of the adipocyte PM was developed, combining enrichment, mass spectrometry, label-free relative protein quantitation, bioinformatic analysis, target validation and functional assays.

The list of differentially regulated PM proteins detected in this study offers a large number of potential candidates for further investigation. This study not only identified previously unreported proteins for the processes of adipogenesis and insulin signalling, but also revealed differential regulation of PM proteins following exposure to PIs. Of relevance was the differential regulation of the transporter isoforms NKCC1 and NKCC2 following lopinavir exposure, which has not been previously investigated.

Data presented in the current study suggests NKCC1 and NKCC2 could be potential targets for PIs, with a possible implication in drug-induced metabolic toxicity. However, their role in antiretroviral-induced metabolic syndrome requires further investigation.

Although challenging, PM proteomics research is key for the identification of novel therapeutic targets and biomarkers of disease, and its application to the study of adipocyte biology may shed light on the mechanisms behind metabolic toxicity. Understanding the mechanisms by which antiretrovirals cause metabolic toxicity in the adipocyte and identifying their protein targets in the plasma membrane may help to modulate with these mechanisms and targets or to combine antiretrovirals with additional drugs that would prevent toxicity (e.g. Telmisartan). This may help minimise antiretroviral-induced metabolic toxicity in patients.

7. APPENDICES

APPENDICES CHAPTER 2

Appendix 1. List of adipocyte proteins detected by ProteinPilot-no sonication method. This Appendix can be found in the accompanying USB flash drive within the chapter 2 folder as "Appendix 1 Chapter 2".

Appendix 2. List of adipocyte plasma membrane proteins-no sonication method. This Appendix can be found in the accompanying USB flash drive within the chapter 2 folder as "Appendix 2 Chapter 2".

Appendix 3. List of adipocyte proteins detected by ProteinPilot-probe sonication method. This Appendix can be found in the accompanying USB flash drive within the chapter 2 folder as "Appendix 3 Chapter 2".

Appendix 4. List of adipocyte plasma membrane proteins-probe sonication method. This Appendix can be found in the accompanying USB flash drive within the chapter 2 folder as "Appendix 4 Chapter 2".

Appendix 5. Comparison total protein yield obtained by optimised colloidal silica bead isolation to Prior *et al.*, (2011). This Appendix can be found in the accompanying USB flash drive within the chapter 2 folder as "Appendix 5 Chapter 2".

APPENDICES CHAPTER 3

Appendix 1. List of proteins detected during adipogenesis. This Appendix can be found in the accompanying USB flash drive within the chapter 3 folder as "Appendix 1 Chapter 3".

Appendix 2. List of plasma membrane proteins detected during adipogenesis. This Appendix can be found in the accompanying USB flash drive within the chapter 3 folder as "Appendix 2 Chapter 3".

Appendix 3. List of significantly differentially regulated plasma membrane proteins detected during adipogenesis. This Appendix can be found in the accompanying USB flash drive within the chapter 3 folder as "Appendix 3 Chapter 3".

Appendix 4. Progenesis QI report of proteins detected during adipogenesis. This Appendix can be found in the accompanying USB flash drive within the chapter 3 folder as "Appendix 4 Chapter 3".

Appendix 5. List of proteins detected following insulin stimulation. This Appendix can be found in the accompanying USB flash drive within the chapter 3 folder as "Appendix 5 Chapter 3".

Appendix 6. List of plasma membrane proteins detected following insulin stimulation. This Appendix can be found in the accompanying USB flash drive within the chapter 3 folder as "Appendix 6 Chapter 3".

Appendix 7. Progenesis QI report of proteins detected following insulin stimulation. This Appendix can be found in the accompanying USB flash drive within the chapter 3 folder as "Appendix 7 Chapter 3".

Appendix 8. Pathway analysis for significantly differentially regulated PM proteins detected during adipogenesis. This Appendix can be found in the accompanying USB flash drive within the chapter 3 folder as "Appendix 8 Chapter 3".

Appendix 9. Pathway analysis for significantly differentially regulated PM proteins detected following insulin stimulation. This Appendix can be found in the accompanying USB flash drive within the chapter 3 folder as "Appendix 9 Chapter 3".

Appendix 10. Comparison of proteins detected following insulin stimulation to Prior *et al.*, (2011). This Appendix can be found in the accompanying USB flash drive within the chapter 3 folder as "Appendix 10 Chapter 3".

APPENDICES CHAPTER 4

Appendix 1. List of proteins detected following drug treatments. This Appendix can be found in the accompanying USB flash drive within the chapter 4 folder as "Appendix 1 Chapter 4".

Appendix 2. List of plasma membrane proteins detected following drug treatments. This Appendix can be found in the accompanying USB flash drive within the chapter 4 folder as "Appendix 2 Chapter 4".

Appendix 3. Tukey's post hoc corrected p-values for pair-wise comparisons. This Appendix can be found in the accompanying USB flash drive within the chapter 4 folder as "Appendix 3 Chapter 4".

Appendix 4. Plasma membrane proteins after Tukey's post hoc corrected p-values for pair-wise comparisons. This Appendix can be found in the accompanying USB flash drive within the chapter 4 folder as "Appendix 4 Chapter 4".

Appendix 5. Plasma membrane proteins significantly differentially regulated following drug treatments. This Appendix can be found in the accompanying USB flash drive within the chapter 4 folder as "Appendix 5 Chapter 4.

Appendix 6. Ranking of significantly differentially regulated PM proteins following drug treatments. This appendix includes the significantly differentially regulated PM proteins from both the ANOVA performed by Progenesis and the ANOVA with Tukey´s post hoc correction test for pairwise comparisons perfomed in RStudio. This appendix can be found in the accompanying USB flash drive within the chapter 4 folder as "Appendix 6 Chapter 4".

Appendix 7. Progenesis QI report of proteins detected following drug treatments. This Appendix can be found in the accompanying USB flash drive within the chapter 4 folder as "Appendix 7 Chapter 4".

Appendix 8. Pathway analysis for significantly differentially regulated PM proteins detected following drug treatments.

Appendix 9. Expression of GLUT4 in the plasma membrane fraction of adipocytes following drug treatments.

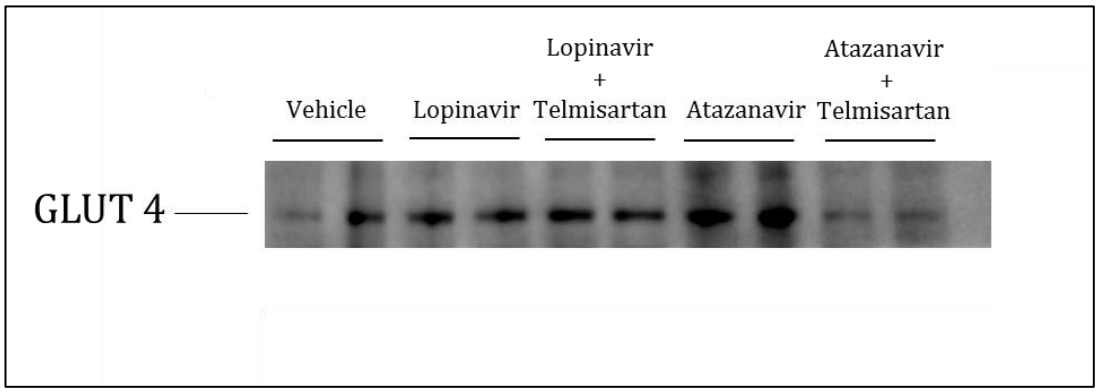

8. REFERENCES

ABERG, JUDITH A., TEBAS, PABLO, OVERTON, EDGAR TURNER, GUPTA, SAMIR K., SAX, PAUL E., LANDAY, ALAN, FALCON, RON, RYAN, ROBERT AND DE LA ROSA, GUY (2012) 'Metabolic effects of darunavir/ritonavir versus atazanavir/ritonavir in treatment-naive, HIV type 1-infected subjects over 48 weeks.', *AIDS research and human retroviruses*, 28, pp. 1184–95.

ABOULAICH, N., VAINONEN, J. P., STRALFORS, P. AND VENER, A. V (2004) 'Vectorial proteomics reveal targeting, phosphorylation and specific fragmentation of polymerase I and transcript release factor (PTRF) at the surface of caveolae in human adipocytes', *Biochem J*, 383, pp. 237–248.

ACHARI, ARUNKUMAR E. AND JAIN, SUSHIL K. (2017) 'Adiponectin, a Therapeutic Target for Obesity, Diabetes, and Endothelial Dysfunction.', *International journal of molecular sciences*, 18, p. 1321.

ADACHI, J., KUMAR, C., ZHANG, Y. AND MANN, M. (2007) 'In-depth analysis of the

adipocyte proteome by mass spectrometry and bioinformatics', *Mol Cell Proteomics*, 6, pp. 1257–1273.

AEBERSOLD, R. AND MANN, M. (2003) 'Mass spectrometry-based proteomics.', *Nature*, 422, pp. 198–207.

AGGARWAL, SURUCHI AND YADAV, AMIT KUMAR (2016) 'False Discovery Rate Estimation in Proteomics', in *Statistical Analysis in Proteomics*, pp. 119–128.

ALBRECHT, IMKE, BIERI, RAPHAEL, LEU, ANGELA, GRANACHER, PHILIPP, HAGMANN, JÖRG, KILIMANN, MANFRED W. AND CHRISTOFORI, GERHARD (2013) 'Paralemmin-1 is expressed in lymphatic endothelial cells and modulates cell migration, cell maturation and tumor lymphangiogenesis', *Angiogenesis*, 16, pp. 795–807.

ALBREKTSEN, T., RICHTER, H. E., CLAUSEN, J. T. AND FLECKNER, J. (2001) 'Identification of a novel integral plasma membrane protein induced during adipocyte differentiation', *Biochem J*, 359, pp. 393–402.

ALFADDA, ASSIM A., MASOOD, AFSHAN, AL-NAAMI, MOHAMMED Y. AND CHAURAND, PIERRE (2017) 'A Proteomics Based Approach Reveals Differential Regulation of Visceral Adipose Tissue Proteins between Metabolically Healthy and Unhealthy Obese Patients', *Molecules and Cells*, 40, pp. 685–695.

ALGHADIR, AHMAD H., GABR, SAMI A. AND AL-EISA, EINAS (2016) 'Cellular fibronectin response to supervised moderate aerobic training in patients with type 2 diabetes.', *Journal of physical therapy science*, 28, pp. 1092–9.

ALI, AUS TARIQ, HOCHFELD, WARREN E., MYBURGH, RENIER AND PEPPER, MICHAEL S. (2013) 'Adipocyte and adipogenesis', *European Journal of Cell Biology*, 92, pp. 229–236.

ALSHAHRANI, SAEED, ALMUTAIRI, MOHAMMED MASHARI, KURSAN, SHAMS, DIAS-JUNIOR, EDUARDO, ALMIAHUOB, MOHAMED MAHMOUD, AGUILAR-BRYAN, LYDIA AND DI FULVIO, MAURICIO (2015) 'Increased Slc12a1 expression in β-cells and improved glucose disposal in Slc12a2 heterozygous mice.', *The Journal of endocrinology*, 227, pp. 153–65.

ALSHAHRANI, SAEED AND DI FULVIO, MAURICIO (2012) 'Enhanced insulin secretion and improved glucose tolerance in mice with homozygous inactivation of the

Na(+)K(+)2Cl(-) co-transporter 1.', *The Journal of endocrinology*, 215, pp. 59–70.

ANDE, SUDHARSANA R., NGUYEN, K. HOA, PADILLA-MEIER, G. PAULINE, WAHIDA, WAHIDA, NYOMBA, B. L. GRÉGOIRE AND MISHRA, SURESH (2014) 'Prohibitin overexpression in adipocytes induces mitochondrial biogenesis, leads to obesity development, and affects glucose homeostasis in a sex-specific manner.', *Diabetes*, 63, pp. 3734–41.

ANUURAD, ERDEMBILEG, BREMER, ANDREW AND BERGLUND, LARS (2010) 'HIV protease inhibitors and obesity.', *Current opinion in endocrinology, diabetes, and obesity*, 17, pp. 478–85.

ARAUJO, SUSANA, BAÑÓN, SARA, MACHUCA, ISABEL, MORENO, ANA, PÉREZ-ELÍAS, MARÍA J. AND CASADO, JOSÉ L. (2014) 'Prevalence of insulin resistance and risk of diabetes mellitus in HIV-infected patients receiving current antiretroviral drugs', *European Journal of Endocrinology*, 171, pp. 545–554.

ARNER, P. (2005) 'Resistin: yet another adipokine tells us that men are not mice', *Diabetologia*, 48, pp. 2203–2205.

ARPADI, S., SHIAU, S., STREHLAU, R., MARTENS, L., PATEL, F., COOVADIA, A., ABRAMS, E. J. AND KUHN, L. (2013) 'Metabolic abnormalities and body composition of HIV-infected children on Lopinavir or Nevirapine-based antiretroviral therapy', *Archives of Disease in Childhood*, 98, pp. 258–264.

ARROYO, JUAN PABLO, KAHLE, KRISTOPHER T. AND GAMBA, GERARDO (2013) 'The SLC12 family of electroneutral cation-coupled chloride cotransporters', *Molecular Aspects of Medicine*, 34, pp. 288–298.

BARBARO, GIUSEPPE AND BARBARINI, GIORGIO (2006) 'Highly active antiretroviral therapy-associated metabolic syndrome and cardiovascular risk.', *Chemotherapy*, 52, pp. 161–5.

BARRÉ-SINOUSSI, FRANÇOISE (1996) 'HIV as the cause of AIDS', *The Lancet*, 348, pp. 31–35.

BARRÉ-SINOUSSI, FRANÇOISE, ROSS, ANNA LAURA AND DELFRAISSY, JEAN-FRANÇOIS (2013) 'Past, present and future: 30 years of HIV research', *Nature Reviews Microbiology*, 11, pp. 877–883.

BARRERA, NELSON P. AND ROBINSON, CAROL V (2011) 'Advances in the mass spectrometry of membrane proteins: from individual proteins to intact complexes.', *Annual review of biochemistry*, 80, pp. 247–71.

BASTARD, J. P., COUFFIGNAL, C., FELLAHI, S., BARD, J. M., MENTRE, F., SALMON, D., KATLAMA, C., RAFFI, F., LEPORT, C. AND CAPEAU, J. (2019) 'Diabetes and dyslipidaemia are associated with oxidative stress independently of inflammation in long-term antiretroviral-treated HIV-infected patients', *Diabetes & Metabolism*.

BAUER, SABRINA, WEIGERT, JOHANNA, NEUMEIER, MARKUS, WANNINGER, JOSEF, SCHÄFFLER, ANDREAS, LUCHNER, ANDREAS, SCHNITZBAUER, ANDREAS A., ASLANIDIS, CHARALAMPOS AND BUECHLER, CHRISTA (2010) 'Low-abundant adiponectin receptors in visceral adipose tissue of humans and rats are further reduced in diabetic animals.', *Archives of medical research*, 41, pp. 75–82.

BAVINGER, CLAY, BENDAVID, ERAN, NIEHAUS, KATHERINE, OLSHEN, RICHARD A., OLKIN, INGRAM, SUNDARAM, VANDANA, WEIN, NICOLE, HOLODNIY, MARK, HOU, NANJIANG, OWENS, DOUGLAS K. AND DESAI, MANISHA (2013) 'Risk of Cardiovascular Disease from Antiretroviral Therapy for HIV: A Systematic Review', *PLoS ONE*, 8, p. e59551.

BENABDELKAMEL, HICHAM, MASOOD, AFSHAN, ALMIDANI, GHAITH M., ALSADHAN, ABDULMAJEED A., BASSAS, ABDULELAH F., DUNCAN, MARK W. AND ALFADDA, ASSIM A. (2015) 'Mature adipocyte proteome reveals differentially altered protein abundances between lean, overweight and morbidly obese human subjects', *Molecular and Cellular Endocrinology*, 401, pp. 142–154.

BERNAL, ENRIQUE, MASIÁ, MAR, PADILLA, SERGIO, RAMOS, J. MANUEL, MARTÍN-HIDALGO, ALBERTO AND GUTIÉRREZ, FÉLIX (2007) 'Insulin resistance in HIV-infected patients receiving long-term therapy with efavirenz, lopinavir/ritonavir and atazanavir.', *Medicina clinica*, 129, pp. 252–4.

BI, XINYAN, LOO, YI TING AND HENRY, CHRISTIANI JEYAKUMAR (2019) 'Does circulating leptin play a role in energy expenditure?', *Nutrition*, 60, pp. 6–10.

BI, ZHEN, MERL-PHAM, JULIANE, UEHLEIN, NORBERT, ZIMMER, INA, MÜHLHANS, STEFANIE, AICHLER, MICHAELA, WALCH, AXEL KARL, KALDENHOFF, RALF, PALME, KLAUS, SCHNITZLER, JÖRG PETER AND BLOCK, KATJA (2015) 'RNAi-mediated downregulation of poplar

plasma membrane intrinsic proteins (PIPs) changes plasma membrane proteome composition and affects leaf physiology', *Journal of Proteomics*, 128, pp. 321–332.

BJØRNDAL, BODIL, BURRI, LENA, STAALESEN, VIDAR, SKORVE, JON AND BERGE, ROLF K. (2011) 'Different adipose depots: their role in the development of metabolic syndrome and mitochondrial response to hypolipidemic agents.', *Journal of obesity*, 2011, p. 490650.

BLÜMER, REGJE ME, VAN VONDEREN, MARIT GA, SUTINEN, JUSSI, HASSINK, ELLY, ACKERMANS, MARIETTE, VAN AGTMAEL, MICHIEL A., YKI-JARVINEN, HANNELE, DANNER, SVEN A., REISS, PETER AND SAUERWEIN, HANS P. (2008) 'Zidovudine/lamivudine contributes to insulin resistance within 3 months of starting combination antiretroviral therapy.', *AIDS*, 22, pp. 227–36.

BOGNER-STRAUSS, JULIANE G., PROKESCH, ANDREAS, SANCHEZ-CABO, FATIMA, RIEDER, DIETMAR, HACKL, HUBERT, DUSZKA, KALINA, KROGSDAM, ANNE, DI CAMILLO, BARBARA, WALENTA, EVELYN, KLATZER, ARIANE, LASS, ACHIM, PINENT, MONTSERRAT, WONG, WING CHEONG, EISENHABER, FRANK AND TRAJANOSKI, ZLATKO (2010) 'Reconstruction of gene association network reveals a transmembrane protein required for adipogenesis and targeted by PPARγ', *Cellular and Molecular Life Sciences*, 67, pp. 4049–4064.

BORKOWSKI, KAMIL, WRZESINSKI, KRZYSZTOW, ROGOWSKA-WRZESINSKA, ADELINA, AUDOUZE, KARINE, BAKKE, JESSE, PETERSEN, RASMUS KOEFOED, HAJ, FAWAZ G., MADSEN, LISE AND KRISTIANSEN, KARSTEN (2014) 'Proteomic analysis of cAMP-mediated signaling during differentiation of 3 T3-L1 preadipocytes', *Biochimica et Biophysica Acta (BBA) - Proteins and Proteomics*, 1844, pp. 2096–2107.

BOST, F., AOUADI, M., CARON, L. AND BINÉTRUY, B. (2005) 'The role of MAPKs in adipocyte differentiation and obesity', *Biochimie*, 87, pp. 51–56.

BRAMBILLA, ANNA MARIA, NOVATI, ROBERTO, CALORI, GILIOLA, MENEGHINI, ELENA, VACCHINI, DANIELA, LUZI, LIVIO, CASTAGNA, ANTONELLA AND LAZZARIN, ADRIANO (2003) 'Stavudine or indinavir-containing regimens are associated with an increased risk of diabetes mellitus in HIV-infected individuals.', *AIDS*, 17, pp. 1993–5.

BRASAEMLE, D. L., BARBER, T., WOLINS, N. E., SERRERO, G., BLANCHETTE-MACKIE, E. J. AND LONDOS, C. (1997) 'Adipose differentiation-related protein is an ubiquitously

expressed lipid storage droplet-associated protein.', *Journal of lipid research*, 38, pp. 2249–63.

BROCKMAN, DAVID AND CHEN, XIAOLI (2012) 'Proteomics in the characterization of adipose dysfunction in obesity', *Adipocyte*, 1, pp. 25–37.

CALZA, LEONARDO, COLANGELI, VINCENZO, MANFREDI, ROBERTO, BON, ISABELLA, RE, MARIA CARLA AND VIALE, PIERLUIGI (2016) 'Clinical management of dyslipidaemia associated with combination antiretroviral therapy in HIV-infected patients', *Journal of Antimicrobial Chemotherapy*, 71, pp. 1451–1465.

CANGERI DI NASO, FÁBIO, ROSA PORTO, ROSSANA, SARUBBI FILLMANN, HENRIQUE, MAGGIONI, LUCAS, VONTOBEL PADOIN, ALEXANDRE, JACQUES RAMOS, RAFAEL, CORÁ MOTTIN, CLAUDIO, BITTENCOURT, ALINE, ANAIR POSSA MARRONI, NORMA AND IVO HOMEM DE BITTENCOURT, PAULO (2015) 'Obesity depresses the anti-inflammatory HSP70 pathway, contributing to NAFLD progression', *Obesity*, 23, pp. 120–129.

CAO, RUI, LI, XUANWEN, LIU, ZHEN, PENG, XIA, HU, WEIJUN, WANG, XIANCHUN, CHEN, PING, XIE, JINGYUN AND LIANG, SONGPING (2006) 'Integration of a Two-Phase Partition Method into Proteomics Research on Rat Liver Plasma Membrane Proteins', *Journal of Proteome Research*, 5, pp. 634–642.

CARPENTER, CHARLES C. J., FISCHL, MARGARET A., HAMMER, SCOTT M., HIRSCH, MARTIN S., JACOBSEN, DONNA M., KATZENSTEIN, DAVID A., MONTANER, JULIO S. G., RICHMAN, DOUGLAS D., SAAG, MICHAEL S., SCHOOLEY, ROBERT T., THOMPSON, MELANIE A., VELLA, STEFANO, YENI, PATRICK G. AND VOLBERDING, PAUL A. (1996) 'Antiretroviral Therapy for HIV Infection in 1996', *JAMA*, 276, pp. 78–86.

CARSWELL, KIRSTIN A., LEE, MI-JEONG AND FRIED, SUSAN K. (2012) 'Culture of Isolated Human Adipocytes and Isolated Adipose Tissue', *Methods in molecular biology*, 806, pp. 203–214.

CATHERMAN, A. D., DURBIN, K. R., AHLF, D. R., EARLY, B. P., FELLERS, R. T., TRAN, J. C., THOMAS, P. M. AND KELLEHER, N. L. (2013) 'Large-scale top-down proteomics of the human proteome: membrane proteins, mitochondria, and senescence', *Mol Cell Proteomics*, 12, pp. 3465–3473.

CATHERMAN, A. D., LI, M., TRAN, J. C., DURBIN, K. R., COMPTON, P. D., EARLY, B. P., THOMAS,

P. M. AND KELLEHER, N. L. (2013) 'Top down proteomics of human membrane proteins from enriched mitochondrial fractions', *Anal Chem*, 85, pp. 1880–1888.

CAWTHORN, W. P., HEYD, F., HEGYI, K. AND SETHI, J. K. (2007) 'Tumour necrosis factor-α inhibits adipogenesis via a β-catenin/TCF4(TCF7L2)-dependent pathway', *Cell Death & Differentiation*, 14, pp. 1361–1373.

CENTERS FOR DISEASE CONTROL AND PREVENTION (CDC) (2019) *About HIV/AIDS*. Available at: https://www.cdc.gov/hiv/basics/whatishiv.html (Accessed: 18 June 2019).

CHAMBERLAIN, L. H., GRAHAM, M. E., KANE, S., JACKSON, J. L., MAIER, V. H., BURGOYNE, R. D. AND GOULD, G. W. (2001) 'The synaptic vesicle protein, cysteine-string protein, is associated with the plasma membrane in 3T3-L1 adipocytes and interacts with syntaxin 4', *Journal of Cell Science*, 114, pp. 445–455.

CHANDWANI, ASHISH AND SHUTER, JONATHAN (2008) 'Lopinavir/ritonavir in the treatment of HIV-1 infection: a review.', *Therapeutics and clinical risk management*, 4, pp. 1023–33.

CHANEY, L. K. AND JACOBSON, B. S. (1983) 'Coating cells with colloidal silica for high yield isolation of plasma membrane sheets and identification of transmembrane proteins.', *The Journal of biological chemistry*, 258, pp. 10062–10072.

CHIU, TIM TING, PATEL, NISH, SHAW, ALISA E., BAMBURG, JAMES R. AND KLIP, AMIRA (2010) 'Arp2/3- and cofilin-coordinated actin dynamics is required for insulin-mediated GLUT4 translocation to the surface of muscle cells.', *Molecular biology of the cell*, 21, pp. 3529–39.

CHOI, K. L., WANG, Y., TSE, C. A., LAM, K. S. L., COOPER, G. J. S. AND XU, A. M. (2004) 'Proteomic analysis of adipocyte differentiation: Evidence that alpha 2 macroglobulin is involved in the adipose conversion of 3T3 L1 preadipocytes', *Proteomics*, 4, pp. 1840–1848.

DE CLERCQ, ERIK (2010) 'Antiretroviral drugs', *Current Opinion in Pharmacology*, 10, pp. 507–515.

COELHO, MARISA, OLIVEIRA, TERESA AND FERNANDES, RUBEN (2013) 'Biochemistry of adipose tissue: An endocrine organ', *Archives of Medical Science*, 9, pp. 191–200.

CORDWELL, STUART J. AND THINGHOLM, TINE E. (2010) 'Technologies for plasma membrane proteomics', *PROTEOMICS*, 10, pp. 611–627.

CORTON, M., BOTELLA-CARRETERO, J. I., LOPEZ, J. A., CAMAFEITA, E., SAN MILLAN, J. L., ESCOBAR-MORREALE, H. F. AND PERAL, B. (2008) 'Proteomic analysis of human omental adipose tissue in the polycystic ovary syndrome using two-dimensional difference gel electrophoresis and mass spectrometry', *Hum Reprod*, 23, pp. 651–661.

CRANE, HEIDI M., GRUNFELD, CARL, WILLIG, JAMES H., MUGAVERO, MICHAEL J., VAN ROMPAEY, STEPHEN, MOORE, RICHARD, RODRIGUEZ, BENIGNO, FELDMAN, BETSY J., LEDERMAN, MICHAEL M., SAAG, MICHAEL S. AND KITAHATA, MARI M. (2011) 'Impact of NRTIs on lipid levels among a large HIV-infected cohort initiating antiretroviral therapy in clinical care', *AIDS*, 25, pp. 185–195.

CROFT, DAVID, MUNDO, ANTONIO FABREGAT, HAW, ROBIN, MILACIC, MARIJA, WEISER, JOEL, WU, GUANMING, CAUDY, MICHAEL, GARAPATI, PHANI, GILLESPIE, MARC, KAMDAR, MAULIK R., JASSAL, BIJAY, JUPE, STEVEN, MATTHEWS, LISA, MAY, BRUCE, PALATNIK, STANISLAV, ROTHFELS, KAREN, SHAMOVSKY, VERONICA, SONG, HEEYEON, WILLIAMS, MARK, BIRNEY, EWAN, HERMJAKOB, HENNING, STEIN, LINCOLN AND D'EUSTACHIO, PETER (2014) 'The Reactome pathway knowledgebase', *Nucleic Acids Research*, 42, pp. D472–D477.

CROOM, KATHERINE F., DHILLON, SOHITA AND KEAM, SUSAN J. (2009) 'Atazanavir', *Drugs*, 69, pp. 1107–1140.

CROXFORD, S, KITCHING MFPH, A., DESAI, S, KALL, M, EDELSTEIN MFPH, M., SKINGSLEY MRCP, A., BROWN, A E, CROXFORD, SARA, KITCHING, AILEEN, DESAI, SARIKA, KALL, MEAGHAN, EDELSTEIN, MICHAEL, SKINGSLEY, ANDREW, BURNS, FIONA, COPAS, ANDREW, BROWN, ALISON E, SULLIVAN, ANN K. AND DELPECH, VALERIE (2017) 'Mortality and causes of death in people diagnosed with HIV in the era of highly active antiretroviral therapy compared with the general population: an analysis of a national observational cohort', *The Lancet Public Health*, 2, pp. e35–e46.

CUENI, LEAH N. AND DETMAR, MICHAEL (2009) 'Galectin-8 interacts with podoplanin and modulates lymphatic endothelial cell functions', *Experimental Cell Research*, 315, pp. 1715–1723.

CURTIS, J. R., WESTFALL, A. O., ALLISON, J., BIJLSMA, J. W., FREEMAN, A., GEORGE, V., KOVAC, S. H., SPETTELL, C. M. AND SAAG, K. G. (2006) 'Population-based assessment of adverse events associated with long-term glucocorticoid use', *Arthritis Rheum*, 55, pp. 420–426.

D'SOUZA, ANNA M., NEUMANN, URSULA H., GLAVAS, MARIA M. AND KIEFFER, TIMOTHY J. (2017) 'The glucoregulatory actions of leptin', *Molecular Metabolism*, 6, pp. 1052–1065.

DAHABIEH, MATTHEW S., BATTIVELLI, EMILIE AND VERDIN, ERIC (2015) 'Understanding HIV Latency: The Road to an HIV Cure', *Annual Review of Medicine*, 66, pp. 407–421.

DANDO, TONI M. AND PERRY, CAROLINE M. (2003) 'Enfuvirtide', *Drugs*, 63, pp. 2755–2766.

DASURI, KALAVATHI, PEPPING, JENNIFER K., FERNANDEZ-KIM, SUN-OK, GUPTA, SUNITA, KELLER, JEFFREY N., SCHERER, PHILIPP E. AND BRUCE-KELLER, ANNADORA J. (2016) 'Elevated adiponectin prevents HIV protease inhibitor toxicity and preserves cerebrovascular homeostasis in mice', *Biochimica et Biophysica Acta (BBA) - Molecular Basis of Disease*, 1862, pp. 1228–1235.

DELANY, J. P., FLOYD, Z. E., ZVONIC, S., SMITH, A., GRAVOIS, A., REINERS, E., WU, X., KILROY, G., LEFEVRE, M. AND GIMBLE, J. M. (2005) 'Proteomic analysis of primary cultures of human adipose-derived stem cells: modulation by Adipogenesis', *Mol Cell Proteomics*, 4, pp. 731–740.

DELFRAISSY, JEAN-FRANÇOIS, FLANDRE, PHILIPPE, DELAUGERRE, CONSTANCE, GHOSN, JADE, HORBAN, ANDRZEJ, GIRARD, PIERRE-MARIE, NORTON, MICHAEL, ROUZIOUX, CHRISTINE, TABURET, ANNE-MARIE, COHEN-CODAR, ISABELLE, VAN, PHILIPPE NGO AND CHAUVIN, JEAN-PIERRE (2008) 'Lopinavir/ritonavir monotherapy or plus zidovudine and lamivudine in antiretroviral-naive HIV-infected patients', *AIDS*, 22, pp. 385–393.

DÍAZ-DELFÍN, JULIETA, DOMINGO, PERE, GIRALT, MARTA AND VILLARROYA, FRANCESC (2013) 'Maraviroc reduces cytokine expression and secretion in human adipose cells without altering adipogenic differentiation', *Cytokine*, 61, pp. 808–815.

DÍAZ-DELFÍN, JULIETA, DEL MAR GUTIÉRREZ, M., GALLEGO-ESCUREDO, JOSÉ M., DOMINGO,

JOAN C., GRACIA MATEO, M., VILLARROYA, FRANCESC, DOMINGO, PERE AND GIRALT, MARTA (2011) 'Effects of nevirapine and efavirenz on human adipocyte differentiation, gene expression, and release of adipokines and cytokines.', *Antiviral research*, 91, pp. 112–9.

DUGANI, CHANDRASAGAR B. AND KLIP, AMIRA (2005) 'Glucose transporter 4: cycling, compartments and controversies.', *EMBO reports*, 6, pp. 1137–42.

ECKEL, ROBERT H., GRUNDY, SCOTT M. AND ZIMMET, PAUL Z. (2005) 'The metabolic syndrome', *The Lancet*, 365, pp. 1415–1428.

EDUARDSEN, KATHRINE, LARSEN, SUSANNE L., NOVAK, IVANA, LAMBERT, IAN H., HOFFMANN, ELSE K. AND PEDERSEN, STINE F. (2011) 'Cell volume regulation and signaling in 3T3-L1 pre-adipocytes and adipocytes: on the possible roles of caveolae, insulin receptors, FAK and ERK1/2.', *Cellular physiology and biochemistry : international journal of experimental cellular physiology, biochemistry, and pharmacology*, 28, pp. 1231–46.

FANG, L, GUO, F., ZHOU, L., STAHL, R. AND GRAMS, J. (2015) 'The cell size and distribution of adipocytes from subcutaneous and visceral fat is associated with type 2 diabetes mellitus in humans', *Adipocyte*, 4, pp. 273–279.

FANG, LINGLING, KOJIMA, KYOKO, ZHOU, LIHUA, CROSSMAN, DAVID K., MOBLEY, JAMES A. AND GRAMS, JAYLEEN (2015) 'Analysis of the Human Proteome in Subcutaneous and Visceral Fat Depots in Diabetic and Non-diabetic Patients with Morbid Obesity.', *Journal of proteomics & bioinformatics*, 8, pp. 133–141.

FEARON, MARGARET (2005) 'The laboratory diagnosis of HIV infections.', *The Canadian journal of infectious diseases & medical microbiology = Journal canadien des maladies infectieuses et de la microbiologie medicale*, 16, pp. 26–30.

FEENEY, E. R. AND MALLON, P. W. G. (2011) 'Insulin resistance in treated HIV infection', *Best Practice & Research Clinical Endocrinology & Metabolism*, 25, pp. 443–458.

FISCHL, M. A., RICHMAN, D. D., GRIECO, M. H., GOTTLIEB, M. S., VOLBERDING, P. A., LASKIN, O. L., LEEDOM, J. M., GROOPMAN, J. E., MILDVAN, D. AND SCHOOLEY, R. T. (1987) 'The efficacy of azidothymidine (AZT) in the treatment of patients with AIDS and AIDS-

related complex. A double-blind, placebo-controlled trial.', *The New England journal of medicine*, 317, pp. 185–91.

FISMAN, ENRIQUE Z. AND TENENBAUM, ALEXANDER (2014) 'Adiponectin: a manifold therapeutic target for metabolic syndrome, diabetes, and coronary disease?', *Cardiovascular Diabetology*, 13, p. 103.

FLEXNER, CHARLES (2019) 'Modern HIV Therapy: Progress and Prospects', *Clinical Pharmacology & Therapeutics*, 105, pp. 61–70.

FOOD AND DRUG ADMINISTRATION (FDA) (2017) *Highlights of prescribing information (Lopinavir and Ritonavir, KALETRA)*. Available at: www.fda.gov/medwatch (Accessed: 29 January 2019).

FOOD AND DRUG ADMINISTRATION (FDA) (2018) *Highlights of prescribing information (Atazanavir, REYATAZ)*. Available at: www.fda.gov/medwatch. (Accessed: 29 January 2019).

FRANCAVILLA, CHIARA, LOEFFLER, SÉBASTIEN, PICCINI, DANIELE, KREN, ANGELIKA, CHRISTOFORI, GERHARD AND CAVALLARO, UGO (2007) 'Neural cell adhesion molecule regulates the cellular response to fibroblast growth factor.', *Journal of cell science*, 120, pp. 4388–94.

FRANKEL, D. S., VASAN, R. S., D'AGOSTINO SR., R. B., BENJAMIN, E. J., LEVY, D., WANG, T. J. AND MEIGS, J. B. (2009) 'Resistin, adiponectin, and risk of heart failure the Framingham offspring study', *J Am Coll Cardiol*, 53, pp. 754–762.

FRASER, SCOTT A, GIMENEZ, IGNACIO, COOK, NATASHA, JENNINGS, IAN, KATERELOS, MARINA, KATSIS, FROSA, LEVIDIOTIS, VICKI, KEMP, BRUCE E. AND POWER, DAVID A (2015) 'Regulation of the renal-specific Na+-K+-2Cl- co-transporter NKCC2 by AMP-activated protein kinase (AMPK).', *The Biochemical journal*, 405, pp. 85–93.

FRÖJDÖ, SARA, VIDAL, HUBERT AND PIROLA, LUCIANO (2009) 'Alterations of insulin signaling in type 2 diabetes: a review of the current evidence from humans.', *Biochimica et biophysica acta*, 1792, pp. 83–92.

FU, YUCHANG, LUO, NANLAN, KLEIN, RICHARD L. AND GARVEY, W. TIMOTHY (2005) 'Adiponectin promotes adipocyte differentiation, insulin sensitivity, and lipid accumulation.', *Journal of lipid research*, 46, pp. 1369–1379.

FUKUNAKA, AYAKO, FUKADA, TOSHIYUKI, BHIN, JINHYUK, SUZUKI, LUKA, TSUZUKI, TAKAMASA, TAKAMINE, YURI, BIN, BUM-HO, YOSHIHARA, TOSHINORI, ICHINOSEKI-SEKINE, NORIKO, NAITO, HISASHI, MIYATSUKA, TAKESHI, TAKAMIYA, SHINZABURO, SASAKI, TSUTOMU, INAGAKI, TAKESHI, KITAMURA, TADAHIRO, KAJIMURA, SHINGO, WATADA, HIROTAKA AND FUJITANI, YOSHIO (2017) 'Zinc transporter ZIP13 suppresses beige adipocyte biogenesis and energy expenditure by regulating C/EBP-β expression', *PLOS Genetics*, 13, p. e1006950.

GALESCU, OVIDIU, BHANGOO, AMRIT AND TEN, SVETLANA (2013) 'Insulin resistance, lipodystrophy and cardiometabolic syndrome in HIV/AIDS', *Reviews in Endocrine and Metabolic Disorders*, 14, pp. 133–140.

GEHART, HELMUTH, KUMPF, SUSANN, ITTNER, ARNE AND RICCI, ROMEO (2010) 'MAPK signalling in cellular metabolism: stress or wellness?', *EMBO reports*, 11, pp. 834–40.

GENUTH, SAUL M., PRZYBYLSKI, RONALD J., ROSENBERG, DAVID AND M. (1971) 'Insulin Resistance in Genetically Obese, Hyperglycemic Mice', *Endocrinology*, 88, pp. 1230–1238.

GIBSON, TODD M., EHRHARDT, MATTHEW J. AND NESS, KIRSTEN K. (2016) 'Obesity and Metabolic Syndrome Among Adult Survivors of Childhood Leukemia.', *Current treatment options in oncology*, 17, p. 17.

GIMENO, RUTH E. AND KLAMAN, LORI D. (2005) 'Adipose tissue as an active endocrine organ: recent advances', *Current Opinion in Pharmacology*, 5, pp. 122–128.

GIRALT, MARTA, DOMINGO, PERE AND VILLARROYA, FRANCESC (2011) 'Adipose tissue biology and HIV-infection', *Best Practice & Research Clinical Endocrinology & Metabolism*, 25, pp. 487–499.

GLEASON, RUDOLPH L., CAULK, ALEXANDER W., SEIFU, DANIEL, ROSEBUSH, JULIA C., SHAPIRO, ALYSSA M., SCHWARTZ, MATTHEW H., ECKARD, ALLISON ROSS, AMOGNE, WONDWOSSEN AND ABEBE, WORKEABEBA (2016) 'Efavirenz and ritonavir-boosted lopinavir use exhibited elevated markers of atherosclerosis across age groups in people living with HIV in Ethiopia', *Journal of Biomechanics*, 49, pp. 2584–2592.

GRAVES, P. R. AND HAYSTEAD, T. A. J. (2002) 'Molecular biologist's guide to

proteomics', *Microbiology and Molecular Biology Reviews*, 66, pp. 39–63.

GUILHERME, A., EMOTO, M., BUXTON, J. M., BOSE, S., SABINI, R., THEURKAUF, W. E., LESZYK, J. AND CZECH, M. P. (2000) 'Perinuclear localization and insulin responsiveness of GLUT4 requires cytoskeletal integrity in 3T3-L1 adipocytes.', *The Journal of biological chemistry*, 275, pp. 38151–38159.

GUILHERME, A., VIRBASIUS, JV, PURI, V. AND CZECH, MP (2008) 'Adipocyte dysfunctions linking obesity to insulin resistance and type 2 diabetes', *Molecular Cell*, 9, pp. 367–377.

GULICK, R. M., MELLORS, J. W., HAVLIR, D., ERON, J. J., MEIBOHM, A., CONDRA, J. H., VALENTINE, F. T., MCMAHON, D., GONZALEZ, C., JONAS, L., EMINI, E. A., CHODAKEWITZ, J. A., ISAACS, R. AND RICHMAN, D. D. (2000) '3-year suppression of HIV viremia with indinavir, zidovudine, and lamivudine.', *Annals of internal medicine*, 133, pp. 35–39.

GUO, SHAODONG (2014) 'Insulin signaling, resistance, and the metabolic syndrome: insights from mouse models into disease mechanisms.', *The Journal of endocrinology*, 220, pp. T1–T23.

GUSTAFSON, BIRGIT, HAMMARSTEDT, ANN, HEDJAZIFAR, SHAHRAM AND SMITH, ULF (2013) 'Restricted adipogenesis in hypertrophic obesity: The role of WISP2, WNT, and BMP4', *Diabetes*, 62, pp. 2997–3004.

GUSTAFSON, BIRGIT, HEDJAZIFAR, SHAHRAM, GOGG, SILVIA, HAMMARSTEDT, ANN AND SMITH, ULF (2015) 'Insulin resistance and impaired adipogenesis', *Trends in Endocrinology and Metabolism*, pp. 193–200.

GUTIERREZ-CARBONELL, ELAIN, TAKAHASHI, DAISUKE, LÜTHJE, SABINE, GONZÁLEZ-REYES, JOSÉ ANTONIO, MONGRAND, SÉBASTIEN, CONTRERAS-MOREIRA, BRUNO, ABADÍA, ANUNCIACIÓN, UEMURA, MATSUO, ABADÍA, JAVIER AND LÓPEZ-MILLÁN, ANA FLOR (2016) 'A Shotgun Proteomic Approach Reveals That Fe Deficiency Causes Marked Changes in the Protein Profiles of Plasma Membrane and Detergent-Resistant Microdomain Preparations from *Beta vulgaris* Roots', *Journal of Proteome Research*, 15, pp. 2510–2524.

HAERTER, G., MANFRAS, B. .., MUELLER, M., KERN, P. AND TREIN, A. (2004) 'Regression of

lipodystrophy in HIV-infected patients under therapy with the new protease inhibitor atazanavir', *AIDS*, pp. 952–955.

HALBERG, NILS, WERNSTEDT-ASTERHOLM, INGRID AND SCHERER, PHILIPP E. (2008) 'The Adipocyte as an Endocrine Cell', *Endocrinology and Metabolism Clinics of North America*, pp. 753–768.

HAMANN, STEFFEN, HERRERA-PEREZ, JOSÉ J., ZEUTHEN, THOMAS AND ALVAREZ-LEEFMANS, FRANCISCO J. (2010) 'Cotransport of water by the Na+-K+-2Cl(-) cotransporter NKCC1 in mammalian epithelial cells.', *The Journal of physiology*, 588, pp. 4089–4101.

HARTKOORN, RUBEN C., KWAN, WAI SAN, SHALLCROSS, VICTORIA, CHAIKAN, AMMARA, LIPTROTT, NEILL, EGAN, DEIRDRE, SORA, ENRIQUE SALCEDO, JAMES, CHLOË E., GIBBONS, SARA, BRAY, PAT G., BACK, DAVID J., KHOO, SAYE H. AND OWEN, ANDREW (2010) 'HIV protease inhibitors are substrates for OATP1A2, OATP1B1 and OATP1B3 and lopinavir plasma concentrations are influenced by SLCO1B1 polymorphisms.', *Pharmacogenetics and genomics*, 20, pp. 112–120.

HE, WEIMIN, BARAK, YAACOV, HEVENER, ANDREA, OLSON, PETER, LIAO, DEBBIE, LE, JAMIE, NELSON, MICHAEL, ONG, ESTELITA, OLEFSKY, JERROLD M. AND EVANS, RONALD M. (2003) 'Adipose-specific peroxisome proliferator-activated receptor gamma knockout causes insulin resistance in fat and liver but not in muscle.', *Proceedings of the National Academy of Sciences of the United States of America*, 100, pp. 15712–15717.

HEDIGER, MATTHIAS A., CLÉMENÇON, BENJAMIN, BURRIER, ROBERT E. AND BRUFORD, ELSPETH A. (2013) 'The ABCs of membrane transporters in health and disease (SLC series): Introduction', *Molecular Aspects of Medicine*, 34, pp. 95–107.

HEMKENS, L. G. AND BUCHER, H. C. (2014) 'HIV infection and cardiovascular disease', *European Heart Journal*, 35, pp. 1373–1381.

HENEGAR, CORNELIU, TORDJMAN, JOAN, ACHARD, VINCENT, LACASA, DANIÈLE, CREMER, ISABELLE, GUERRE-MILLO, MICHÈLE, POITOU, CHRISTINE, BASDEVANT, ARNAUD, STICH, VLADIMIR, VIGUERIE ¥#, NATHALIE, LANGIN ¥#, DOMINIQUE, BEDOSSA, PIERRE, ZUCKER, JEAN-DANIEL AND CLEMENT, KARINE (2008) 'Adipose tissue transcriptomic signature

highlights the pathological relevance of extracellular matrix in human obesity Background', *Genome Biology Genome Biology*, 9, p. R14.

HOFFMANN, E. K., LAMBERT, I. H. AND PEDERSEN, S. F. (2009) 'Physiology of Cell Volume Regulation in Vertebrates', *Physiological Reviews*, 89, pp. 193–277.

HOLEC, ASHLEY D., MANDAL, SUBHRA, PRATHIPATI, PAVAN KUMAR AND DESTACHE, CHRISTOPHER J. (2017) 'Nucleotide Reverse Transcriptase Inhibitors: A thorough review, present status and future perspective as HIV therapeutics.', *Current HIV Research*, 15, pp. 411–421.

HOLMES, DAVID (2017) 'Diabetes: Plasma membrane key to diet-induced insulin resistance', *Nature Reviews Endocrinology*, 13, p. 2.

HONG, Y. H., HISHIKAWA, D., MIYAHARA, H., TSUZUKI, H., NISHIMURA, Y., GOTOH, C., CHOI, K. C., HOKARI, Y., TAKAGI, Y., LEE, H. G., CHO, K. K., ROH, S. G. AND SASAKI, S. (2005) 'Up-regulation of adipogenin, an adipocyte plasma transmembrane protein, during adipogenesis', *Mol Cell Biochem*, 276, pp. 133–141.

HÖRMANN, KATRIN, STUKALOV, ALEXEY, MÜLLER, ANDRÉ C., HEINZ, LEONHARD X., SUPERTI-FURGA, GIULIO, COLINGE, JACQUES AND BENNETT, KEIRYN L. (2016) 'A Surface Biotinylation Strategy for Reproducible Plasma Membrane Protein Purification and Tracking of Genetic and Drug-Induced Alterations', *Journal of Proteome Research*, 15, pp. 647–658.

HOTAMISLIGIL, G. S. (1999) 'The role of TNFalpha and TNF receptors in obesity and insulin resistance', *J Intern Med*, 245, pp. 621–625.

HRESKO, RICHARD C. AND HRUZ, PAUL W. (2011) 'HIV Protease Inhibitors Act as Competitive Inhibitors of the Cytoplasmic Glucose Binding Site of GLUTs with Differing Affinities for GLUT1 and GLUT4', *PLoS ONE*, 6, p. e25237.

HRUZ, PAUL W., MURATA, HARUHIKO AND MUECKLER, MIKE (2001) 'Adverse metabolic consequences of HIV protease inhibitor therapy: the search for a central mechanism', *American Journal of Physiology-Endocrinology and Metabolism*, 280, pp. E549–E553.

HSU, DENISE C. AND O'CONNELL, ROBERT J. (2017) 'Progress in HIV vaccine development', *Human Vaccines & Immunotherapeutics*, 13, pp. 1018–1030.

HUANG, PAUL L. (2009) 'A comprehensive definition for metabolic syndrome.', *Disease models & mechanisms*, 2, pp. 231–7.

HUANG, QIAOBING (2012) 'Ezrin/Radixin/Moesin Proteins in the Development of Diabetes and its Cardiovascular Complications', *Journal of Diabetes & Metabolism*, S4, p. 005.

HURST, MIRIAM AND FAULDS, DIANA (2000) 'Lopinavir', *Drugs*, 60, pp. 1371–1379.

IBRAHIMI, AZEDDINE, BONINO, FREDERIC, BARDON, SYLVIE, AILHAUD, GÉRARD AND DANI, CHRISTIAN (1992) 'Essential role of collagens for terminal differentiation of preadipocytes', *Biochemical and Biophysical Research Communications*, 187, pp. 1314–1322.

INNES, STEVE, ABDULLAH, KAMEELAH L., HAUBRICH, RICHARD, COTTON, MARK F. AND BROWNE, SARA H. (2016) 'High Prevalence of Dyslipidemia and Insulin Resistance in HIV-infected Prepubertal African Children on Antiretroviral Therapy.', *The Pediatric infectious disease journal*, 35, pp. e1-7.

INSENSER, M., MONTES-NIETO, R., VILARRASA, N., LECUBE, A., SIMO, R., VENDRELL, J. AND ESCOBAR-MORREALE, H. F. (2012) 'A nontargeted proteomic approach to the study of visceral and subcutaneous adipose tissue in human obesity', *Mol Cell Endocrinol*, 363, pp. 10–19.

INTERNATIONAL DIABETES FEDERATION (2006) *The IDF consensus worldwide definition of the metabolic syndrome*.

JAFARI, ATEFEH, KHALILI, HOSSEIN AND DASHTI-KHAVIDAKI, SIMIN (2014) 'Tenofovir-induced nephrotoxicity: incidence, mechanism, risk factors, prognosis and proposed agents for prevention', *European Journal of Clinical Pharmacology*, 70, pp. 1029–1040.

JALDIN-FINCATI, JAVIER R., PAVAROTTI, MARTIN, FRENDO-CUMBO, SCOTT, BILAN, PHILIP J. AND KLIP, AMIRA (2017) 'Update on GLUT4 Vesicle Traffic: A Cornerstone of Insulin Action', *Trends in Endocrinology & Metabolism*, 28, pp. 597–611.

JEDRYCHOWSKI, MARK P., GARTNER, CARLOS A., GYGI, STEVEN P., ZHOU, LI, HERZ, JOACHIM, KANDROR, KONSTANTIN V AND PILCH, PAUL F. (2010) 'Proteomic analysis of GLUT4 storage vesicles reveals LRP1 to be an important vesicle component and target of

insulin signaling.', *The Journal of biological chemistry*, 285, pp. 104–14.

JERICÓ, CARLOS, KNOBEL, HERNANDO, MONTERO, MILAGRO, ORDOÑEZ-LLANOS, JORDI, GUELAR, ANA, GIMENO, JUAN L., SABALLS, PERE, LÓPEZ-COLOMÉS, JOSE L. AND PEDRO-BOTET, JUAN (2005) 'Metabolic syndrome among HIV-infected patients: prevalence, characteristics, and related factors.', *Diabetes care*, 28, pp. 132–7.

JOHNSON, WELKIN E. AND DESROSIERS, RONALD C. (2002) 'Viral Persistence: HIV's Strategies of Immune System Evasion', *Annual Review of Medicine*, 53, pp. 499–518.

JOHNSTON, O., ROSE, C. L., WEBSTER, A. C. AND GILL, J. S. (2008) 'Sirolimus is associated with new-onset diabetes in kidney transplant recipients', *J Am Soc Nephrol*, 19, pp. 1411–1418.

JONES, SIMON P., WAITT, CATRIONA, SUTTON, ROBERT, BACK, DAVID J. AND PIRMOHAMED, MUNIR (2008) 'Effect of atazanavir and ritonavir on the differentiation and adipokine secretion of human subcutaneous and omental preadipocytes', *AIDS*, 22, pp. 1293–1298.

JUNG, NORMA, LEHMANN, CLARA, RUBBERT, ANDREA, KNISPEL, MEIKE, HARTMANN, PIA, VAN LUNZEN, JAN, STELLBRINK, HANS-JUERGEN, FAETKENHEUER, GERD AND TAUBERT, DIRK (2008) 'Relevance of the organic cation transporters 1 and 2 for antiretroviral drug therapy in human immunodeficiency virus infection.', *Drug metabolism and disposition: the biological fate of chemicals*, 36, pp. 1616–23.

KADOWAKI, TAKASHI, YAMAUCHI, TOSHIMASA, KUBOTA, NAOTO, HARA, KAZUO, UEKI, KOHJIRO AND TOBE, KAZUYUKI (2006) 'Adiponectin and adiponectin receptors in insulin resistance, diabetes, and the metabolic syndrome.', *The Journal of clinical investigation*, 116, pp. 1784–92.

KAHN, BARBARA B. (2019) 'Adipose Tissue, Inter-Organ Communication, and the Path to Type 2 Diabetes: The 2016 Banting Medal for Scientific Achievement Lecture', *Diabetes*, 68, pp. 3–14.

KAMAL, A. H., KIM, W. K., CHO, K., PARK, A., MIN, J. K., HAN, B. S., PARK, S. G., LEE, S. C. AND BAE, K. H. (2013) 'Investigation of adipocyte proteome during the differentiation of brown preadipocytes', *J Proteomics*, 94, pp. 327–336.

KAPLAN-LEWIS, EMMA, ABERG, JUDITH A. AND LEE, MIKYUNG (2016) 'Atherosclerotic Cardiovascular Disease and Anti-Retroviral Therapy', *Current HIV/AIDS Reports*, 13, pp. 297–308.

KAPŁON-CIEŚLICKA, AGNIESZKA, TYMIŃSKA, AGATA, ROSIAK, MAREK, OZIERAŃSKI, KRZYSZTOF, PELLER, MICHAŁ, EYILETEN, CEREN, KONDRACKA, AGNIESZKA, PORDZIK, JUSTYNA, MIROWSKA-GUZEL, DAGMARA, OPOLSKI, GRZEGORZ, POSTUŁA, MAREK AND FILIPIAK, KRZYSZTOF J. (2018) 'Resistin is a prognostic factor for death in type 2 diabetes', *Diabetes/Metabolism Research and Reviews*, p. e3098.

KARAMCHAND, SUMANTH, LEISEGANG, RORY, SCHOMAKER, MICHAEL, MAARTENS, GARY, WALTERS, LOURENS, HISLOP, MICHAEL, DAVE, JOEL A., LEVITT, NAOMI S. AND COHEN, KAREN (2016) 'Risk Factors for Incident Diabetes in a Cohort Taking First-Line Nonnucleoside Reverse Transcriptase Inhibitor-Based Antiretroviral Therapy.', *Medicine*, 95, p. e2844.

KARAS, M., BAHR, U., INGENDOH, A., NORDHOFF, E., STAHL, B., STRUPAT, K. AND HILLENKAMP, F. (1990) 'Principles and applications of matrix-assisted UV-laser desorption/ionization mass spectrometry', *Analytica Chimica Acta*, 241, pp. 175–185.

KAWAGUCHI, T., TAMORI, Y., KANDA, H., YOSHIKAWA, M., TATEYA, S., NISHINO, N. AND KASUGA, M. (2010) 'The t-SNAREs syntaxin4 and SNAP23 but not v-SNARE VAMP2 are indispensable to tether GLUT4 vesicles at the plasma membrane in adipocyte', *Biochem Biophys Res Commun*, 391, pp. 1336–1341.

KERSHAW, ERIN E. AND FLIER, JEFFREY S. (2004) 'Adipose tissue as an endocrine organ.', *The Journal of clinical endocrinology and metabolism*, 89, pp. 2548–56.

KHAN, T., MUISE, E. S., IYENGAR, P., WANG, Z. V., CHANDALIA, M., ABATE, N., ZHANG, B. B., BONALDO, P., CHUA, S. AND SCHERER, P. E. (2009) 'Metabolic Dysregulation and Adipose Tissue Fibrosis: Role of Collagen VI', *Molecular and Cellular Biology*, 29, pp. 1575–1591.

KIM, E. Y., KIM, W. K., OH, K. J., HAN, B. S., LEE, S. C. AND BAE, K. H. (2015) 'Recent advances in proteomic studies of adipose tissues and adipocytes', *Int J Mol Sci*, 16, pp. 4581–4599.

KIM, GUN-HWA, PARK, EDMOND CHANGKYUN, YUN, SUNG-HO, HONG, YEONHEE, LEE, DONG-GYU, SHIN, EUN-YOUNG, JUNG, JONGSUN, KIM, YOUNG HWAN, LEE, KYUNG-BOK, JANG, IK-SOON, LEE, ZEE-WON, CHUNG, YOUNG-HO, CHOI, JONG-SOON, CHEONG, CHAEJOON, KIM, SOOHYUN AND KIM, SEUNG IL (2013) 'Proteomic and bioinformatic analysis of membrane proteome in type 2 diabetic mouse liver', *PROTEOMICS*, 13, pp. 1164–1179.

KIM, K. B., KIM, B. W., CHOO, H. J., KWON, Y. C., AHN, B. Y., CHOI, J. S., LEE, J. S. AND KO, Y. G. (2009) 'Proteome analysis of adipocyte lipid rafts reveals that gC1qR plays essential roles in adipogenesis and insulin signal transduction', *Proteomics*, 9, pp. 2373–2382.

KIM, YUNEE, ELSCHENBROICH, SARAH, SHARMA, PARVEEN, SEPIASHVILI, LUSIA, GRAMOLINI, ANTHONY O. AND KISLINGER, THOMAS (2011) 'Use of colloidal silica-beads for the isolation of cell-surface proteins for mass spectrometry-based proteomics', *Methods in Molecular Biology*, 748, pp. 227–241.

KIS, OLENA, ROBILLARD, KEVIN, CHAN, GARY N. Y. AND BENDAYAN, REINA (2010) 'The complexities of antiretroviral drug-drug interactions: role of ABC and SLC transporters', *Trends in Pharmacological Sciences*, pp. 22–35.

KITAZAWA, TAKATOSHI, YOSHINO, YUSUKE, SUZUKI, SATOSHI, KOGA, ICHIRO AND OTA, YASUO (2014) 'Lopinavir inhibits insulin signaling by promoting protein tyrosine phosphatase 1B expression.', *Experimental and therapeutic medicine*, 8, pp. 851–855.

KLEPPE, RUNE, MARTINEZ, AURORA, DØSKELAND, STEIN OVE AND HAAVIK, JAN (2011) 'The 14-3-3 proteins in regulation of cellular metabolism', *Seminars in Cell & Developmental Biology*, 22, pp. 713–719.

KLÖTING, NORA AND BLÜHER, MATTHIAS (2014) 'Adipocyte dysfunction, inflammation and metabolic syndrome', *Reviews in Endocrine and Metabolic Disorders*, 15, pp. 277–287.

KOETHE, JOHN R. (2017) 'Adipose Tissue in HIV Infection.', *Comprehensive Physiology*, 7, pp. 1339–1357.

KONG, QINGHUA, GAO, LAN, NIU, YANFEN, GONGPAN, PIANCHOU, XU, YUHUI, LI, YAN AND

XIONG, WENYONG (2016) 'RACK1 is required for adipogenesis', *American Journal of Physiology - Cell Physiology*, 311, pp. C831–C836.

KOTSIS, VASILIOS, STABOULI, STELLA, PAPAKATSIKA, SOFIA, RIZOS, ZOE AND PARATI, GIANFRANCO (2010) 'Mechanisms of obesity-induced hypertension', *Hypertension Research*, 33, pp. 386–393.

KRATCHMAROVA, I., KALUME, D. E., BLAGOEV, B., SCHERER, P. E., PODTELEJNIKOV, A. V, MOLINA, H., BICKEL, P. E., ANDERSEN, J. S., FERNANDEZ, M. M., BUNKENBORG, J., ROEPSTORFF, P., KRISTIANSEN, K., LODISH, H. F., MANN, M. AND PANDEY, A. (2002) 'A proteomic approach for identification of secreted proteins during the differentiation of 3T3-L1 preadipocytes to adipocytes', *Mol Cell Proteomics*, 1, pp. 213–222.

KRÜGER, MARCUS, KRATCHMAROVA, IRINA, BLAGOEV, BLAGOY, TSENG, YU-HUA, KAHN, C. RONALD AND MANN, MATTHIAS (2008) 'Dissection of the insulin signaling pathway via quantitative phosphoproteomics.', *Proceedings of the National Academy of Sciences of the United States of America*, 105, pp. 2451–2456.

KULBACKA, JULITA, CHOROMAŃSKA, ANNA, ROSSOWSKA, JOANNA, WEŻGOWIEC, JOANNA, SACZKO, JOLANTA AND ROLS, MARIE-PIERRE (2017) 'Cell Membrane Transport Mechanisms: Ion Channels and Electrical Properties of Cell Membranes', in *Transport Across Natural and Modified Biological Membranes and its Implications in Physiology and Therapy*, pp. 39–58.

KUTZLEB, CHRISTIAN, PETRASCH-PARWEZ, ELISABETH AND KILIMANN, MANFRED W. (2006) 'Cellular and subcellular localization of paralemmin-1, a protein involved in cell shape control, in the rat brain, adrenal gland and kidney', *Histochemistry and Cell Biology*, 127, pp. 13–30.

LACLAUSTRA, MARTIN, CORELLA, DOLORES AND ORDOVAS, JOSÉ M. (2007) 'Metabolic syndrome pathophysiology: The role of adipose tissue', *Nutrition, Metabolism and Cardiovascular Diseases*, pp. 125–139.

LAFLEUR, JOANNE, BRESS, ADAM P., ROSENBLATT, LISA, CROOK, JACOB, SAX, PAUL E., MYERS, JOEL AND RITCHINGS, COREY (2017) 'Cardiovascular outcomes among HIV-infected veterans receiving atazanavir', *AIDS*, 31, pp. 2095–2106.

LAI, XIANYIN (2013) 'Reproducible method to enrich membrane proteins with high purity and high yield for an LC-MS/MS approach in quantitative membrane proteomics', *Electrophoresis*, 34, pp. 809–817.

LAKE, JORDAN E., TSENG, CHI HONG AND CURRIER, JUDITH S. (2013) 'A Pilot Study of Telmisartan for Visceral Adiposity in HIV Infection: The Metabolic Abnormalities, Telmisartan, and HIV Infection (MATH) Trial', *PLoS ONE*, 8, p. e58135.

LAMERS, D., FAMULLA, S., WRONKOWITZ, N., HARTWIG, S., LEHR, S., OUWENS, D. M., ECKARDT, K., KAUFMAN, J. M., RYDEN, M., MULLER, S., HANISCH, F. G., RUIGE, J., ARNER, P., SELL, H. AND ECKEL, J. (2011) 'Dipeptidyl peptidase 4 is a novel adipokine potentially linking obesity to the metabolic syndrome', *Diabetes*, 60, pp. 1917–1925.

LANE, C. S. (2005) 'Mass spectrometry-based proteomics in the life sciences', *Cellular and Molecular Life Sciences*, 62, pp. 848–869.

LANGIN, DOMINIQUE AND ARNER, PETER (2006) 'Importance of TNFα and neutral lipases in human adipose tissue lipolysis', *Trends in Endocrinology & Metabolism*, 17, pp. 314–320.

LARIA, ANNA ELISA, MESSINEO, SEBASTIANO, ARCIDIACONO, BIAGIO, VARANO, MARIACONCETTA, CHIEFARI, EUSEBIO, SEMPLE, ROBERT K., ROCHA, NUNO, RUSSO, DIEGO, CUDA, GIOVANNI, GASPARI, MARCO, BRUNETTI, ANTONIO AND FOTI, DANIELA P. (2018) 'Secretome analysis of hypoxia-induced 3T3-L1 adipocytes uncovers novel proteins potentially involved in obesity', *Proteomics*, 18, p. 1700260.

LARSEN, INGRID K., KASPER, CHRISTINA, RASMUSSEN, HANNE, KASTRUP, JETTE S., IKEMIZU, SHINJI, JONES, E. YVONNE, BEREZIN, VLADIMIR AND BOCK, ELISABETH (2000) 'Structural basis of cell–cell adhesion by NCAM', *Nature Structural Biology*, 7, pp. 389–393.

LATOSINSKA, AGNIESZKA, VOUGAS, KONSTANTINOS, MAKRIDAKIS, MANOUSOS, KLEIN, JULIE, MULLEN, WILLIAM, ABBAS, MAHMOUD, STRAVODIMOS, KONSTANTINOS, KATAFIGIOTIS, IOANNIS, MERSEBURGER, AXEL S., ZOIDAKIS, JEROME, MISCHAK, HARALD, VLAHOU, ANTONIA AND JANKOWSKI, VERA (2015) 'Comparative Analysis of Label-Free and 8-Plex iTRAQ Approach for Quantitative Tissue Proteomic Analysis', *PLOS ONE*, 10, p. e0137048.

LAURENCE, JEFFREY, ELHADAD, SONIA AND AHAMED, JASIMUDDIN (2018) 'HIV-associated cardiovascular disease: importance of platelet activation and cardiac fibrosis in the setting of specific antiretroviral therapies.', *Open heart*, 5, p. e000823.

LAVIOLA, LUIGI, PERRINI, SEBASTIO, CIGNARELLI, ANGELO AND GIORGINO, FRANCESCO (2006) 'Insulin signalling in human adipose tissue', *Archives of Physiology and Biochemistry*, 112, pp. 82–88.

LEAL, VIVIANE DE OLIVEIRA AND MAFRA, DENISE (2013) 'Adipokines in obesity', *Clinica Chimica Acta*, pp. 87–94.

LEE, D. E., KEHLENBRINK, S., LEE, H., HAWKINS, M. AND YUDKIN, J. S. (2009) 'Getting the message across: mechanisms of physiological cross talk by adipose tissue', *Am J Physiol Endocrinol Metab*, 296, pp. E1210–E1229.

LEE, H. K., LEE, B. H., PARK, S. A. AND KIM, C. W. (2006) 'The proteomic analysis of an adipocyte differentiated from human mesenchymal stem cells using two-dimensional gel electrophoresis', *Proteomics*, 6, pp. 1223–1229.

LEFTEROVA, MARTINA I. AND LAZAR, MITCHELL A. (2009) 'New developments in adipogenesis', *Trends in Endocrinology & Metabolism*, 20, pp. 107–114.

LEHR, S., HARTWIG, S. AND SELL, H. (2012) 'Adipokines: a treasure trove for the discovery of biomarkers for metabolic disorders', *Proteomics Clin Appl*, 6, pp. 91–101.

LI, BIN, TAKAHASHI, DAISUKE, KAWAMURA, YUKIO AND UEMURA, MATSUO (2012) 'Comparison of plasma membrane proteomic changes of arabidopsis suspension-cultured cells (T87 Line) after cold and ABA treatment in association with freezing tolerance development', *Plant and Cell Physiology*, 53, pp. 543–554.

LI, JING JING, WANG, RUISHAN, LAMA, RATI, WANG, XINJIANG, FLOYD, Z. ELIZABETH, PARK, EDWARDS A. AND LIAO, FRANCESCA-FANG (2016) 'Ubiquitin Ligase NEDD4 Regulates PPARγ Stability and Adipocyte Differentiation in 3T3-L1 Cells', *Scientific Reports*, 6, p. 38550.

LI, QINKAI, HATA, AKIKO, KOSUGI, CHISATO, KATAOKA, NANANKO AND FUNAKI, MAKOTO (2010) 'The density of extracellular matrix proteins regulates inflammation and insulin signaling in adipocytes', *FEBS Letters*, 584, pp. 4145–4150.

LI, QINKAI, HOSAKA, TOSHIO, JAMBALDORJ, BAYASGLAN, NAKAYA, YUTAKA AND FUNAKI, MAKOTO (2009) 'Extracellular matrix with the rigidity of adipose tissue helps 3T3-L1 adipocytes maintain insulin responsiveness', *The Journal of Medical Investigation*, 56, pp. 142–149.

LIHN, A. S., PEDERSEN, S. B. AND RICHELSEN, B. (2005) 'Adiponectin: action, regulation and association to insulin sensitivity', *Obes Rev*, 6, pp. 13–21.

LIM, J. M., WOLLASTON-HAYDEN, E. E., TEO, C. F., HAUSMAN, D. AND WELLS, L. (2014) 'Quantitative secretome and glycome of primary human adipocytes during insulin resistance', *Clin Proteomics*, 11, p. 20.

LIM, YOUNGHYUP, YOO, SOYEON, LEE, SANG AH, CHIN, SANG OUK, HEO, DAHEE, MOON, JAE CHEOL, MOON, SHINHANG, BOO, KIYOUNG, KIM, SEONG TAEG, SEO, HYE MI, JWA, HYEYOUNG AND KOH, GWANPYO (2015) 'Apolipoprotein B Is Related to Metabolic Syndrome Independently of Low Density Lipoprotein Cholesterol in Patients with Type 2 Diabetes.', *Endocrinology and metabolism*, 30, pp. 208–15.

LIU, JIARUI, YANG, XIAONING, YU, SIWANG AND ZHENG, RUIMAO (2018) 'The Leptin Resistance', in *Neural Regulation of Metabolism*, pp. 145–163.

LUO, FUCHENG, TRAN, AMANDA PHUONG, XIN, LI, SANAPALA, CHANDRIKA, LANG, BRADLEY T., SILVER, JERRY AND YANG, YAN (2018) 'Modulation of proteoglycan receptor PTPσ enhances MMP-2 activity to promote recovery from multiple sclerosis', *Nature Communications*, 9, p. 4126.

LUO, LIPING AND LIU, MEILIAN (2016) 'Adipose tissue in control of metabolism', *Journal of Endocrinology*, 231, pp. R77–R99.

MAARTENS, GARY, CELUM, CONNIE AND LEWIN, SHARON R. (2014) 'HIV infection: epidemiology, pathogenesis, treatment, and prevention', *The Lancet*, 384, pp. 258–271.

MACDOUGALD, ORMOND A. AND MANDRUP, SUSANNE (2002) 'Adipogenesis: forces that tip the scales.', *Trends in endocrinology and metabolism: TEM*, 13, pp. 5–11.

MAGER, W. H., DE BOER, A. H., SIDERIUS, M. H. AND VOSS, H. P. (2000) 'Cellular responses to oxidative and osmotic stress.', *Cell stress & chaperones*, 5, pp. 73–5.

MAGGI, PAOLO, DI BIAGIO, ANTONIO, RUSCONI, STEFANO, CICALINI, STEFANIA, D'ABBRACCIO, MAURIZIO, D'ETTORRE, GABRIELLA, MARTINELLI, CANIO, NUNNARI, GIUSEPPE, SIGHINOLFI, LAURA, SPAGNUOLO, VINCENZO AND SQUILLACE, NICOLA (2017) 'Cardiovascular risk and dyslipidemia among persons living with HIV: a review.', *BMC infectious diseases*, 17, p. 551.

MAGKOS, FAIDON AND MANTZOROS, CHRISTOS S. (2011) 'Body fat redistribution and metabolic abnormalities in HIV-infected patients on highly active antiretroviral therapy: novel insights into pathophysiology and emerging opportunities for treatment', *Metabolism*, 60, pp. 749–753.

MANTZOROS, CHRISTOS S. (2012) 'Leptin in relation to the lipodystrophy-associated metabolic syndrome', *Diabetes and Metabolism Journal*, 36, pp. 181–189.

MARCHANT, D., NEIL, STUART J. D. AND MCKNIGHT, ÁINE (2006) 'Human immunodeficiency virus types 1 and 2 have different replication kinetics in human primary macrophage culture', *Journal of General Virology*, 87, pp. 411–418.

MARGOLIS, ASA M., HEVERLING, HARRY, PHAM, PAUL A. AND STOLBACH, ANDREW (2014) 'A review of the toxicity of HIV medications.', *Journal of medical toxicology : official journal of the American College of Medical Toxicology*, 10, pp. 26–39.

MARIMAN, EDWIN C. M. AND WANG, PING (2010) 'Adipocyte extracellular matrix composition, dynamics and role in obesity', *Cellular and Molecular Life Sciences*, 67, pp. 1277–1292.

MARTIN, ALLISON, MOORE, CECILIA L., MALLON, PATRICK W. G., HOY, JENNIFER F., EMERY, SEAN, BELLOSO, WALDO H., PHANUPHAK, PRAPHAN, FERRET, SAMUEL, COOPER, DAVID A., BOYD, MARK A. AND TEAM, ON BEHALF OF THE SECOND-LINE STUDY (2013) 'HIV Lipodystrophy in Participants Randomised to Lopinavir/Ritonavir (LPV/r) +2–3 Nucleoside/Nucleotide Reverse Transcriptase Inhibitors (N(t)RTI) or LPV/r + Raltegravir as Second-Line Antiretroviral Therapy', *PLoS ONE*, 8, p. e77138.

MASSON, OLIVIER, PRÉBOIS, CHRISTINE, DEROCQ, DANIELLE, MEULLE, ALINE, DRAY, CÉDRIC, DAVIAUD, DANIELLE, QUILLIOT, DIDIER, VALET, PHILIPPE, MULLER, CATHERINE AND LIAUDET-COOPMAN, EMMANUELLE (2011) 'Cathepsin-D, a key protease in breast

cancer, is up-regulated in obese mouse and human adipose tissue, and controls adipogenesis.', *PloS one*, 6, p. e16452.

McManaman, James L., Bales, Elise S., Orlicky, David J., Jackman, Matthew, MacLean, Paul S., Cain, Shannon, Crunk, Amanda E., Mansur, Ayla, Graham, Christine E., Bowman, Thomas A. and Greenberg, Andrew S. (2013) 'Perilipin-2-null mice are protected against diet-induced obesity, adipose inflammation, and fatty liver disease', *Journal of Lipid Research*, 54, pp. 1346–1359.

McTernan, C. L., McTernan, P. G., Harte, A. L., Levick, P. L., Barnett, A. H. and Kumar, S. (2002) 'Resistin, central obesity, and type 2 diabetes.', *Lancet*, 359, pp. 46–7.

Menshawy, Amr, Ismail, Ammar, Abushouk, Abdelrahman Ibrahim, Ahmed, Hussien, Menshawy, Esraa, Elmaraezy, Ahmed, Gadelkarim, Mohamed, Abdel-Maboud, Mohamed, Attia, Attia and Negida, Ahmed (2017) 'Efficacy and safety of atazanavir/ritonavir-based antiretroviral therapy for HIV-1 infected subjects: a systematic review and meta-analysis', *Archives of Virology*, 162, pp. 2181–2190.

Mihai, A. D. and Schroder, M. (2015) 'Glucose starvation and hypoxia, but not the saturated fatty acid palmitic acid or cholesterol, activate the unfolded protein response in 3T3-F442A and 3T3-L1 adipocytes', *Adipocyte*, 4, pp. 188–202.

Minami, Rumi, Yamamoto, Masahiro, Soichiro, Takahama, Ando, Hitoshi, Tomoya, Miyamura and Suematsu, Eiichi (2011) 'Comparison of the influence of four classes of HIV antiretrovirals on adipogenic differentiation: the minimal effect of raltegravir and atazanavir', *Journal of Infection and Chemotherapy*, 17, pp. 183–188.

Miranda, Phillippa J., DeFronzo, Ralph A., Califf, Robert M. and Guyton, John R. (2005) 'Metabolic syndrome: Definition, pathophysiology, and mechanisms', in *American Heart Journal*, pp. 33–45.

Mojiminiyi, O. A., Abdella, N. A., Al Arouj, M. and Ben Nakhi, A. (2007) 'Adiponectin, insulin resistance and clinical expression of the metabolic syndrome in patients with Type 2 diabetes', *Int J Obes*, 31, pp. 213–220.

Molina, Henrik, Yang, Yi, Ruch, Travis, Kim, Jae-Woo, Mortensen, Peter, Otto, Tamara, Nalli, Anuradha, Tang, Qi-Qun, Lane, M. Daniel, Chaerkady, Raghothama

AND PANDEY, AKHILESH (2009) 'Temporal Profiling of the Adipocyte Proteome during Differentiation Using a Five-Plex SILAC Based Strategy', *Journal of Proteome Research*, 8, pp. 48–58.

MOURE, RICARDO, DOMINGO, PERE, GALLEGO-ESCUREDO, JOSÉ M., VILLARROYA, JOAN, GUTIERREZ, MARIA DEL MAR, MATEO, MARIA G., DOMINGO, JOAN C., GIRALT, MARTA AND VILLARROYA, FRANCESC (2016) 'Impact of elvitegravir on human adipocytes: Alterations in differentiation, gene expression and release of adipokines and cytokines', *Antiviral Research*, 132, pp. 59–65.

MURRI, M., INSENSER, M., LUQUE, M., TINAHONES, F. J. AND ESCOBAR-MORREALE, H. F. (2014) 'Proteomic analysis of adipose tissue: informing diabetes research', *Expert Rev Proteomics*, 11, pp. 491–502.

MUSI, NICOLAS AND GUARDADO-MENDOZA, RODOLFO (2014) 'Adipose Tissue as an Endocrine Organ', in *Cellular Endocrinology in Health and Disease*, pp. 229–237.

NATURE MEDICINE (2012) *Metabolic Syndrome ePoster*, *Nature Medicine*. Available at: https://www.nature.com/nm/poster/eposter_full.html (Accessed: 30 January 2019).

NDUKA, CHIDOZIE U., STRANGES, SAVERIO, KIMANI, PETER K., SARKI, AHMED M. AND UTHMAN, OLALEKAN A. (2017) 'Is there sufficient evidence for a causal association between antiretroviral therapy and diabetes in HIV-infected patients? A meta-analysis', *Diabetes/Metabolism Research and Reviews*, 33, p. e2902.

NEDERGAARD, JAN, BENGTSSON, TORE AND CANNON, BARBARA (2007) 'Unexpected evidence for active brown adipose tissue in adult humans.', *American journal of physiology. Endocrinology and metabolism*, 293, pp. E444-52.

NHS (2016) *Metabolic syndrome - NHS*. Available at: https://www.nhs.uk/conditions/metabolic-syndrome/ (Accessed: 30 January 2019).

NOOR, MUSTAFA A., PARKER, REX A., O'MARA, EDWARD, GRASELA, DENNIS M., CURRIE, ALEXANDER, HODDER, SALLY L., FIEDOREK, FRED T. AND HAAS, DAVID W. (2004) 'The effects of HIV protease inhibitors atazanavir and lopinavir/ritonavir on insulin sensitivity in HIV-seronegative healthy adults.', *AIDS*, 18, pp. 2137–44.

NOOR, MUSTAFA A, FLINT, OLIVER P., MAA, JEN-FUE AND PARKER, REX A (2006) 'Effects of atazanavir/ritonavir and lopinavir/ritonavir on glucose uptake and insulin sensitivity: demonstrable differences in vitro and clinically.', *AIDS*, 20, pp. 1813–1821.

NORDSTROM, E. A., RYDEN, M., BACKLUND, E. C., DAHLMAN, I., KAAMAN, M., BLOMQVIST, L., CANNON, B., NEDERGAARD, J. AND ARNER, P. (2005) 'A human-specific role of cell death-inducing DFFA (DNA fragmentation factor-alpha)-like effector A (CIDEA) in adipocyte lipolysis and obesity', *Diabetes*, 54, pp. 1726–1734.

NOROUZI, SHAGHAYEGH, ADULCIKAS, JOHN, SOHAL, SUKHWINDER SINGH AND MYERS, STEPHEN (2017) 'Zinc transporters and insulin resistance: therapeutic implications for type 2 diabetes and metabolic disease.', *Journal of biomedical science*, 24, p. 87.

OH, JISUN AND HEGELE, ROBERT A. (2007) 'HIV-associated dyslipidaemia: pathogenesis and treatment', *The Lancet Infectious Diseases*, 7, pp. 787–796.

OJIMA, KOICHI, OE, MIKA, NAKAJIMA, IKUYO, MUROYA, SUSUMU AND NISHIMURA, TAKANORI (2016) 'Dynamics of protein secretion during adipocyte differentiation.', *FEBS open bio*, 6, pp. 816–26.

OKITA, N., HAYASHIDA, Y., KOJIMA, Y., FUKUSHIMA, M., YUGUCHI, K., MIKAMI, K., YAMAUCHI, A., WATANABE, K., NOGUCHI, M., NAKAMURA, M., TODA, T. AND HIGAMI, Y. (2012) 'Differential responses of white adipose tissue and brown adipose tissue to caloric restriction in rats', *Mech Ageing Dev*, 133, pp. 255–266.

OLESEN, J. B., HANSEN, P. R., ABILDSTROM, S. Z., ANDERSSON, C., WEEKE, P., SCHMIEGELOW, M., ERDAL, J., TORP-PEDERSEN, C. AND GISLASON, G. H. (2011) 'Valproate attenuates the risk of myocardial infarction in patients with epilepsy: a nationwide cohort study', *Pharmacoepidemiol Drug Saf*, 20, pp. 146–153.

OLIVEROS, J. C. (2015) *Venny. An interactive tool for comparing lists with Venn's diagrams.* Available at: http://bioinfogp.cnb.csic.es/tools/venny/index.html.

VAN OOSTERHOUT, JOEP J., MALLEWA, JANE, KAUNDA, SYMON, CHAGOMA, NEWTON, NJALALE, YASSIN, KAMPIRA, ELIZABETH, MUKAKA, MAVUTO AND HEYDERMAN, ROBERT S. (2012) 'Stavudine Toxicity in Adult Longer-Term ART Patients in Blantyre, Malawi', *PLoS*

ONE, 7, p. e42029.

ORAL, ELIF ARIOGLU, SIMHA, VINAYA, RUIZ, ELAINE, ANDEWELT, ALEXA, PREMKUMAR, AHALYA, SNELL, PETER, WAGNER, ANTHONY J., DEPAOLI, ALEX M., REITMAN, MARC L., TAYLOR, SIMEON I., GORDEN, PHILLIP AND GARG, ABHIMANYU (2002) 'Leptin-Replacement Therapy for Lipodystrophy', *New England Journal of Medicine*, 346, pp. 570–578.

ORLOV, SERGEI N., KOLTSOVA, SVETLANA V., KAPILEVICH, LEONID V., GUSAKOVA, SVETLANA V. AND DULIN, NICKOLAI O. (2015) 'NKCC1 and NKCC2: The pathogenetic role of cation-chloride cotransporters in hypertension', *Genes and Diseases*.

OTA, A., KOVARY, K. M., WU, O. H., AHRENDS, R., SHEN, W. J., COSTA, M. J., FELDMAN, B. J., KRAEMER, F. B. AND TERUEL, M. N. (2015) 'Using SRM-MS to quantify nuclear protein abundance differences between adipose tissue depots of insulin-resistant mice', *J Lipid Res*, 56, pp. 1068–1078.

PACENTI, MONIA, BARZON, LUISA, FAVARETTO, FRANCESCA, FINCATI, KARINA, ROMANO, SARA, MILAN, GABRIELLA, VETTOR, ROBERTO AND PALÙ, GIORGIO (2006) 'Microarray analysis during adipogenesis identifies new genes altered by antiretroviral drugs', *AIDS*, 20, pp. 1691–1705.

PAE, MUNKYONG AND ROMEO, GIULIO R. (2014) 'The multifaceted role of profilin-1 in adipose tissue inflammation and glucose homeostasis', *Adipocyte*, 3, pp. 69–74.

PALIOS, JOHN, KADOGLOU, NIKOLAOS P. E. AND LAMPROPOULOS, STYLIANOS (2012) 'The pathophysiology of HIV-/HAART-related metabolic syndrome leading to cardiovascular disorders: the emerging role of adipokines.', *Experimental diabetes research*, 2012, p. 103063.

PANEL ON ANTIRETROVIRAL GUIDELINES FOR ADULTS AND ADOLESCENTS (2018) *Guidelines for the Use of Antiretroviral Agents in Adults and Adolescents Living with HIV. U.S. Department of Health and Human Services.* Available at: https://aidsinfo.nih.gov/contentfiles/lvguidelines/adultandadolescentgl.pdf (Accessed: 14 November 2018).

PANET, RIVKA, MARCUS, MIRIAM AND ATLAN, HENRI (2000) 'Overexpression of the Na+/K+/Cl? cotransporter gene induces cell proliferation and phenotypic

transformation in mouse fibroblasts', *Journal of Cellular Physiology*, 182, pp. 109–118.

PAREKH, BHARAT S., OU, CHIN-YIH, FONJUNGO, PETER N., KALOU, MIREILLE B., ROTTINGHAUS, ERIN, PUREN, ADRIAN, ALEXANDER, HEATHER, HURLSTON COX, MACKENZIE AND NKENGASONG, JOHN N. (2019) 'Diagnosis of Human Immunodeficiency Virus Infection.', *Clinical microbiology reviews*, 32, pp. e00064-18.

PATEL, KUNJAL, LINDSEY, JANE, ANGELIDOU, KONSTANTIA, ALDROVANDI, GRACE AND PALUMBO, PAUL (2018) 'Metabolic effects of initiating lopinavir/ritonavir-based regimens among young children: 7-year follow-up of the IMPAACT P1060 trial', *AIDS*, 32, pp. 2327–2336.

PEINADO, J. R., JIMENEZ-GOMEZ, Y., PULIDO, M. R., ORTEGA-BELLIDO, M., DIAZ-LOPEZ, C., PADILLO, F. J., LOPEZ-MIRANDA, J., VAZQUEZ-MARTINEZ, R. AND MALAGON, M. M. (2010) 'The stromal-vascular fraction of adipose tissue contributes to major differences between subcutaneous and visceral fat depots', *Proteomics*, 10, pp. 3356–3366.

PEINADO, J. R., PARDO, M., DE LA ROSA, O. AND MALAGON, M. M. (2012) 'Proteomic characterization of adipose tissue constituents, a necessary step for understanding adipose tissue complexity', *Proteomics*, 12, pp. 607–620.

PEINADO, J. R., QUIROS, P. M., PULIDO, M. R., MARINO, G., MARTINEZ-CHANTAR, M. L., VAZQUEZ-MARTINEZ, R., FREIJE, J. M., LOPEZ-OTIN, C. AND MALAGON, M. M. (2011) 'Proteomic profiling of adipose tissue from Zmpste24-/- mice, a model of lipodystrophy and premature aging, reveals major changes in mitochondrial function and vimentin processing', *Mol Cell Proteomics*, 10, p. M111 008094.

PELÁEZ-GARCÍA, ALBERTO, BARDERAS, RODRIGO, BATLLE, RAQUEL, VIÑAS-CASTELLS, ROSA, BARTOLOMÉ, RUBÉN A., TORRES, SOFÍA, MENDES, MARTA, LOPEZ-LUCENDO, MARÍA, MAZZOLINI, ROCCO, BONILLA, FÉLIX, DE HERREROS, ANTONIO GARCÍA AND CASAL, J. IGNACIO (2015) 'A Proteomic Analysis Reveals That Snail Regulates the Expression of the Nuclear Orphan Receptor Nuclear Receptor Subfamily 2 Group F Member 6 (Nr2f6) and Interleukin 17 (IL-17) to Inhibit Adipocyte Differentiation', *Molecular & Cellular Proteomics*, 14, pp. 303–315.

PEREZ-DIAZ, SERGIO, JOHNSON, LANCE A., DEKROON, ROBERT M., MORENO-NAVARRETE, JOSE

M., ALZATE, OSCAR, FERNANDEZ-REAL, JOSE M., MAEDA, NOBUYO AND ARBONES-MAINAR, JOSE M. (2014) 'Polymerase I and transcript release factor (PTRF) regulates adipocyte differentiation and determines adipose tissue expandability', *FASEB Journal*, 28, pp. 3769–3779.

PÉREZ-MATUTE, PATRICIA, PÉREZ-MARTÍNEZ, LAURA, BLANCO, JOSÉ R. AND OTEO, JOSÉ A. (2011) 'Neutral actions of Raltegravir on adipogenesis, glucose metabolism and lipolysis in 3T3-L1 adipocytes.', *Current HIV research*, 9, pp. 174–9.

PEREZ-PEREZ, R., ORTEGA-DELGADO, F. J., GARCIA-SANTOS, E., LOPEZ, J. A., CAMAFEITA, E., RICART, W., FERNANDEZ-REAL, J. M. AND PERAL, B. (2009) 'Differential proteomics of omental and subcutaneous adipose tissue reflects their unalike biochemical and metabolic properties', *J Proteome Res*, 8, pp. 1682–1693.

PERONA, JAVIER S. (2017) 'Membrane lipid alterations in the metabolic syndrome and the role of dietary oils', *Biochimica et Biophysica Acta - Biomembranes*, 1859, pp. 1690–1703.

PHILIPPE, A., VAIVA, G. AND CASADEBAIG, F. (2005) 'Data on diabetes from the French cohort study in schizophrenia', *Eur Psychiatry*, 20 Suppl 4, pp. S340-4.

POTTHOFF, A., BROCKMEYER, N. H., GELBRICH, G., NEUHAUS, K., ESSER, S., REINSCH, N., HOWER, M., MOSTARDT, S., NEUMANN, A., NEUMANN, T., COMPETENCE CENTER CARDIAC, INSUFFICIENCY AND THE COMPETENCE NETWORK, HIV AIDS (2010) 'Lipodystrophy - a sign for metabolic syndrome in patients of the HIV-HEART study', *J Dtsch Dermatol Ges*, 8, pp. 92–98.

PRIOR, M. J., LARANCE, M., LAWRENCE, R. T., SOUL, J., HUMPHREY, S., BURCHFIELD, J., KISTLER, C., DAVEY, J. R., LA-BORDE, P. J., BUCKLEY, M., KANAZAWA, H., PARTON, R. G., GUILHAUS, M. AND JAMES, D. E. (2011) 'Quantitative proteomic analysis of the adipocyte plasma membrane', *J Proteome Res*, 10, pp. 4970–4982.

PUSHPAKOM, SUDEEP P., ADAIKALAKOTESWARI, ANTONYSUNIL, OWEN, ANDREW, BACK, DAVID J., TRIPATHI, GYANENDRA, KUMAR, SUDHESH, MCTERNAN, PHILIP AND PIRMOHAMED, MUNIR (2018) 'Telmisartan reverses antiretroviral-induced adipocyte toxicity and insulin resistance in vitro.', *Diabetes & vascular disease research*, 15, pp. 233–242.

PUSHPAKOM, SUDEEP P., TAYLOR, CLAIRE, KOLAMUNNAGE-DONA, RUWANTHI, SPOWART, CATHERINE, VORA, JITEN, GARCÍA-FIÑANA, MARTA, KEMP, GRAHAM J., WHITEHEAD, JOHN, JAKI, THOMAS, KHOO, SAYE, WILLIAMSON, PAULA AND PIRMOHAMED, MUNIR (2015) 'Telmisartan and Insulin Resistance in HIV (TAILoR): protocol for a dose-ranging phase II randomised open-labelled trial of telmisartan as a strategy for the reduction of insulin resistance in HIV-positive individuals on combination antiretroviral therapy', *BMJ Open*, 5, p. e009566.

QUERCIA, ROMINA, ROBERTS, JEREMY, MARTIN-CARPENTER, LOUISE AND ZALA, CARLOS (2015) 'Comparative Changes of Lipid Levels in Treatment-Naive, HIV-1-Infected Adults Treated with Dolutegravir vs. Efavirenz, Raltegravir, and Ritonavir-Boosted Darunavir-Based Regimens Over 48 Weeks', *Clinical Drug Investigation*, 35, pp. 211–219.

R CORE TEAM (2017) 'R: A language and environment for statistical computing.', *R Foundation for Statistical Computing, Vienna, Austria.*

RACIL, Z., RAZGA, F., DRAPALOVA, J., BURESOVA, L., ZACKOVA, D., PALACKOVA, M., SEMERAD, L., MALASKOVA, L., HALUZIK, M. AND MAYER, J. (2013) 'Mechanism of impaired glucose metabolism during nilotinib therapy in patients with chronic myelogenous leukemia', *Haematologica*, 98, pp. e124-6.

RANDELL, PAUL A., JACKSON, AKIL G., ZHONG, LIJIE, YALE, KITTY AND MOYLE, GRAEME J. (2010) 'The effect of tenofovir disoproxil fumarate on whole-body insulin sensitivity, lipids and adipokines in healthy volunteers.', *Antiviral therapy*, 15, pp. 227–33.

REED, SAM E., HODGSON, LORNA R., SONG, SHUANG, MAY, MARGARET T., KELLY, EOIN E., MCCAFFREY, MARY W., MASTICK, CYNTHIA C., VERKADE, PAUL AND TAVARÉ, JEREMY M. (2013) 'A role for Rab14 in the endocytic trafficking of GLUT4 in 3T3-L1 adipocytes.', *Journal of cell science*, 126, pp. 1931–1941.

RENES, J. AND MARIMAN, E. (2013) 'Application of proteomics technology in adipocyte biology', *Mol Biosyst*, 9, pp. 1076–1091.

REZAEE AND DASHTY (2013) 'Role of Adipose Tissue in Metabolic System Disorders', *Journal of Diabetes & Metabolism*, 01, pp. 1–9.

RICHMAN, DOUGLAS D., WRIN, TERRI, LITTLE, SUSAN J. AND PETROPOULOS, CHRISTOS J. (2003) 'Rapid evolution of the neutralizing antibody response to HIV type 1 infection.', *Proceedings of the National Academy of Sciences of the United States of America*, 100, pp. 4144–9.

RIEHLE, CHRISTIAN AND ABEL, E. DALE (2016) 'Insulin Signaling and Heart Failure.', *Circulation research*, 118, pp. 1151–69.

ROSEN, EVAN D. AND MACDOUGALD, ORMOND A. (2006) 'Adipocyte differentiation from the inside out', *Nature Reviews Molecular Cell Biology*, 7, pp. 885–896.

ROSEN, EVAN D. AND SPIEGELMAN, BRUCE M. (2006) 'Adipocytes as regulators of energy balance and glucose homeostasis', *Nature*, 444, pp. 847–853.

ROSEN, EVAN, EGUCHI, JUN AND XU, ZHAO (2009) 'Transcriptional targets in adipocyte biology.', *Expert opinion on therapeutic targets*, 13, pp. 975–86.

RUIZ-OJEDA, FRANCISCO JAVIER, RUPÉREZ, AZAHARA IRIS, GOMEZ-LLORENTE, CAROLINA, GIL, ANGEL AND AGUILERA, CONCEPCIÓN MARÍA (2016) 'Cell Models and Their Application for Studying Adipogenic Differentiation in Relation to Obesity: A Review.', *International journal of molecular sciences*, 17, p. E1040.

SADLER, JESSICA B. A., BRYANT, NIA J., GOULD, GWYN W. AND WELBURN, CASSIE R. (2013) 'Posttranslational modifications of GLUT4 affect its subcellular localization and translocation', *International Journal of Molecular Sciences*, pp. 9963–9978.

SAELY, CHRISTOPH H., GEIGER, KATHRIN AND DREXEL, HEINZ (2011) 'Brown versus white adipose tissue: A mini-review', *Gerontology*, pp. 15–23.

SAMARAS, KATHERINE (2009) 'Prevalence and Pathogenesis of Diabetes Mellitus in HIV-1 Infection Treated With Combined Antiretroviral Therapy', *JAIDS Journal of Acquired Immune Deficiency Syndromes*, 50, pp. 499–505.

SANO, HIROYUKI, EGUEZ, LORENA, TERUEL, MARY N., FUKUDA, MITSUNORI, CHUANG, TUAN D., CHAVEZ, JOSE A., LIENHARD, GUSTAV E. AND MCGRAW, TIMOTHY E. (2007) 'Rab10, a Target of the AS160 Rab GAP, Is Required for Insulin-Stimulated Translocation of GLUT4 to the Adipocyte Plasma Membrane', *Cell Metabolism*, 5, pp. 293–303.

SARJEANT, KELESHA AND STEPHENS, JACQUELINE M. (2012) 'Adipogenesis', *Cold Spring*

Harbor perspectives in biology, 4, pp. a008417–a008417.

SAVARYN, JOHN P., TOBY, TIMOTHY K. AND KELLEHER, NEIL L. (2016) 'A researcher's guide to mass spectrometry-based proteomics.', *Proteomics*, 16, pp. 2435–43.

SAVAS, JEFFREY N., STEIN, BENJAMIN D., WU, CHRISTINE C. AND YATES, JOHN R. (2011) 'Mass spectrometry accelerates membrane protein analysis', *Trends in Biochemical Sciences*.

SCHIAPPARELLI, PAULA, GUERRERO-CAZARES, HUGO, MAGAÑA-MALDONADO, ROXANA, HAMILLA, SUSAN M., GANAHA, SARA, GOULIN LIPPI FERNANDES, ERIC, HUANG, CHUAN HSIANG, ARANDA-ESPINOZA, HELIM, DEVREOTES, PETER AND QUINONES-HINOJOSA, ALFREDO (2017) 'NKCC1 Regulates Migration Ability of Glioblastoma Cells by Modulation of Actin Dynamics and Interacting with Cofilin', *EBioMedicine*, 21, pp. 94–103.

SCHINDLER, JENS, LEWANDROWSKI, URS, SICKMANN, ALBERT, FRIAUF, ECKHARD AND GERD NOTHWANG, HANS (2006) 'Proteomic Analysis of Brain Plasma Membranes Isolated by Affinity Two-phase Partitioning', *Molecular & Cellular Proteomics*, 5, pp. 390–400.

SCHLIESS, F. AND HÄUSSINGER, D. (2000) 'Cell hydration and insulin signalling.', *Cellular physiology and biochemistry : international journal of experimental cellular physiology, biochemistry, and pharmacology*, 10, pp. 403–8.

SCHMELZLE, K., KANE, S., GRIDLEY, S., LIENHARD, G. E. AND WHITE, F. M. (2006) 'Temporal dynamics of tyrosine phosphorylation in insulin signaling', *Diabetes*, 55, pp. 2171–2179.

SCHRANK, BENJAMIN R., APARICIO, TOMAS, LI, YINYIN, CHANG, WAKAM, CHAIT, BRIAN T., GUNDERSEN, GREGG G., GOTTESMAN, MAX E. AND GAUTIER, JEAN (2018) 'Nuclear ARP2/3 drives DNA break clustering for homology-directed repair', *Nature*, 559, pp. 61–66.

SCHROVER, ILSE M., VAN DER GRAAF, YOLANDA, SPIERING, WILKO, VISSEREN, FRANK LJ AND SMART STUDY GROUP (2018) 'The relation between body fat distribution, plasma concentrations of adipokines and the metabolic syndrome in patients with clinically manifest vascular disease.', *European journal of preventive cardiology*, 25, pp. 1548–1557.

SCHWARTZ, CHRISTIAN, BOUCHAT, SOPHIE, MARBAN, CÉLINE, GAUTIER, VIRGINIE, VAN LINT, CARINE, ROHR, OLIVIER AND LE DOUCE, VALENTIN (2017) 'On the way to find a cure: Purging latent HIV-1 reservoirs', *Biochemical Pharmacology*, 146, pp. 10–22.

SENSION, MICHAEL AND DECKX, HENRI (2015) 'Lipid metabolism and lipodystrophy in HIV-1-infected patients: the role played by nonnucleoside reverse transcriptase inhibitors.', *AIDS reviews*, 17, pp. 21–36.

SHAH, ANOOP S. V., STELZLE, DOMINIK, LEE, KUAN KEN, BECK, EDUARD J., ALAM, SHIRJEL, CLIFFORD, SARAH, LONGENECKER, CHRIS T., STRACHAN, FIONA, BAGCHI, SHASHWATEE, WHITELEY, WILLIAM, RAJAGOPALAN, SANJAY, KOTTILIL, SHYAMASUNDARAN, NAIR, HARISH, NEWBY, DAVID E., MCALLISTER, DAVID A. AND MILLS, NICHOLAS L. (2018) 'Global Burden of Atherosclerotic Cardiovascular Disease in People Living With HIV', *Circulation*, 138, pp. 1100–1112.

SHARMA, PARVEEN, ABBASI, CYNTHIA, LAZIC, SAVO, TENG, ALLEN C. T., WANG, DINGYAN, DUBOIS, NICOLE, IGNATCHENKO, VLADIMIR, WONG, VICTORIA, LIU, JUN, ARAKI, TOSHIYUKI, TIBURCY, MALTE, ACKERLEY, CAMERON, ZIMMERMANN, WOLFRAM H., HAMILTON, ROBERT, SUN, YU, LIU, PETER P., KELLER, GORDON, STAGLJAR, IGOR, SCOTT, IAN C., KISLINGER, THOMAS AND GRAMOLINI, ANTHONY O. (2015) 'Evolutionarily conserved intercalated disc protein Tmem65 regulates cardiac conduction and connexin 43 function', *Nature Communications*, 6, p. 8391.

SHIMOMURA, I., HAMMER, R. E., IKEMOTO, S., BROWN, M. S. AND GOLDSTEIN, J. L. (1999) 'Leptin reverses insulin resistance and diabetes mellitus in mice with congenital lipodystrophy.', *Nature*, 401, pp. 73–6.

SHLAY, JUDITH C., VISNEGARWALA, FEHMIDA, BARTSCH, GLENN, WANG, JACK, PENG, GRACE, EL-SADR, WAFAA M., GIBERT, CYNTHIA, KOTLER, DONALD, GRUNFELD, CARL, RAGHAVAN, SUBHASREE AND TERRY BEIRN COMMUNITY PROGRAMS FOR CLINICAL RESEARCH ON AIDS (CPCRA) (2005) 'Body composition and metabolic changes in antiretroviral-naive patients randomized to didanosine and stavudine vs. abacavir and lamivudine.', *Journal of acquired immune deficiency syndromes (1999)*, 38, pp. 147–55.

SIDHU, R. S. (1979) 'Two-dimensional electrophoretic analyses of proteins synthesized during differentiation of 3T3-L1 preadipocytes', *J Biol Chem*, 254, pp.

11111–11118.

SIDHU, VISHALDEEP K., HUANG, BILL X., DESAI, ABHISHEK, KEVALA, KARL AND KIM, HEE YONG (2016) 'Role of DHA in aging-related changes in mouse brain synaptic plasma membrane proteome', *Neurobiology of Aging*, 41, pp. 73–85.

SILICIANO, ROBERT F. AND GREENE, WARNER C. (2011) 'HIV latency', *Cold Spring Harbor Perspectives in Medicine*, 1.

SINGH, RICHA, KURSAN, SHAMS, ALMIAHOUB, MOHAMED Y., ALMUTAIRI, MOHAMMED M., GARZÓN-MUVDI, TOMÁS, ALVAREZ-LEEFMANS, FRANCISCO J. AND DI FULVIO, MAURICIO (2016) 'Plasma Membrane Targeting of Endogenous NKCC2 in COS7 Cells Bypasses Functional Golgi Cisternae and Complex N-Glycosylation.', *Frontiers in cell and developmental biology*, 4, p. 150.

SOLOMON, C. G. (1999) 'The epidemiology of polycystic ovary syndrome. Prevalence and associated disease risks', *Endocrinol Metab Clin North Am*, 28, pp. 247–263.

SPAGNUOLO, VINCENZO, GALLI, LAURA, POLI, ANDREA, SALPIETRO, STEFANIA, GIANOTTI, NICOLA, PIATTI, PIERMARCO, COSSARINI, FRANCESCA, VINCI, CONCETTA, CARINI, ELISABETTA, LAZZARIN, ADRIANO AND CASTAGNA, ANTONELLA (2017) 'Associations of statins and antiretroviral drugs with the onset of type 2 diabetes among HIV-1-infected patients.', *BMC infectious diseases*, 17, p. 43.

STANLEY, TAKARA L., JOY, TISHA, HADIGAN, COLLEEN M., LIEBAU, JAMES G., MAKIMURA, HIDEO, CHEN, CINDY Y., THOMAS, BIJOY J., WEISE, STEVEN B., ROBBINS, GREGORY K. AND GRINSPOON, STEVEN K. (2009) 'Effects of switching from lopinavir/ritonavir to atazanavir/ritonavir on muscle glucose uptake and visceral fat in HIV-infected patients', *AIDS*, 23, pp. 1349–1357.

STEPPAN, C. M., BAILEY, S. T., BHAT, S., BROWN, E. J., BANERJEE, R. R., WRIGHT, C. M., PATEL, H. R., AHIMA, R. S. AND LAZAR, M. A. (2001) 'The hormone resistin links obesity to diabetes', *Nature*, 409, pp. 307–312.

STERN, JENNIFER H. AND SCHERER, PHILIPP E. (2015) 'Adipose tissue biology in 2014: Advances in our understanding of adipose tissue homeostasis.', *Nature reviews. Endocrinology*, 11, pp. 71–2.

SZKLARCZYK, DAMIAN, FRANCESCHINI, ANDREA, WYDER, STEFAN, FORSLUND, KRISTOFFER, HELLER, DAVIDE, HUERTA-CEPAS, JAIME, SIMONOVIC, MILAN, ROTH, ALEXANDER, SANTOS, ALBERTO, TSAFOU, KALLIOPI P., KUHN, MICHAEL, BORK, PEER, JENSEN, LARS J. AND VON MERING, CHRISTIAN (2015) 'STRING v10: protein-protein interaction networks, integrated over the tree of life.', *Nucleic acids research*, 43, pp. D447–D452.

SZKLARCZYK, DAMIAN, MORRIS, JOHN H., COOK, HELEN, KUHN, MICHAEL, WYDER, STEFAN, SIMONOVIC, MILAN, SANTOS, ALBERTO, DONCHEVA, NADEZHDA T., ROTH, ALEXANDER, BORK, PEER, JENSEN, LARS J. AND VON MERING, CHRISTIAN (2017) 'The STRING database in 2017: quality-controlled protein–protein association networks, made broadly accessible', *Nucleic Acids Research*, 45, pp. D362–D368.

TABAK, OMUR, SIMSEK, GONUL, ERDENEN, FUSUN, SOZER, VOLKAN, HASOGLU, TUNA, GELISGEN, REMISE, ALTUNOGLU, ESMA, MUDERRISOGLU, CUNEYT, SENYIGIT, ABDULHALIM AND UZUN, HAFIZE (2017) 'The relationship between circulating irisin, retinol binding protein-4, adiponectin and inflammatory mediators in patients with metabolic syndrome', *Archives of Endocrinology and Metabolism*, 61, pp. 515–523.

TAKAHASHI, DAISUKE, KAWAMURA, YUKIO AND UEMURA, MATSUO (2013) 'Changes of detergent-resistant plasma membrane proteins in oat and rye during cold acclimation: Association with differential freezing tolerance', *Journal of Proteome Research*, 12, pp. 4998–5011.

TAKAHASHI, DAISUKE, KAWAMURA, YUKIO, YAMASHITA, TETSURO AND UEMURA, MATSUO (2012) 'Detergent-resistant plasma membrane proteome in oat and rye: Similarities and dissimilarities between two monocotyledonous plants', in *Journal of Proteome Research*, pp. 1654–1665.

TAKAHASHI, YU, SHINODA, AKIHIRO, KAMADA, HARUHIKO, SHIMIZU, MAKOTO, INOUE, JUN AND SATO, RYUICHIRO (2016) 'Perilipin2 plays a positive role in adipocytes during lipolysis by escaping proteasomal degradation', *Scientific Reports*, 6, p. 20975.

TAN, S., TAN, H. T. AND CHUNG, M. C. (2008) 'Membrane proteins and membrane proteomics', *Proteomics*, 8, pp. 3924–3932.

TANAKA, TOMOKAZU, NAKAZAWA, HARUMASA, KURIYAMA, NAOHIDE AND KANEKI, MASAO (2018) 'Farnesyltransferase inhibitors prevent HIV protease inhibitor

(lopinavir/ritonavir)-induced lipodystrophy and metabolic syndrome in mice.', *Experimental and therapeutic medicine*, 15, pp. 1314–1320.

TARAMASSO, LUCIA, RICCI, ELENA, MENZAGHI, BARBARA, OROFINO, GIANCARLO, PASSERINI, SIMONE, MADEDDU, GIORDANO, MARTINELLI, CANIO VITO, DE SOCIO, GIUSEPPE VITTORIO, SQUILLACE, NICOLA, RUSCONI, STEFANO, BONFANTI, PAOLO, DI BIAGIO, ANTONIO AND CISAI STUDY GROUP, CISAI STUDY (2017) 'Weight Gain: A Possible Side Effect of All Antiretrovirals.', *Open forum infectious diseases*, 4, p. ofx239.

TEPAAMORNDECH, SURAPUN, KIRSCHKE, CATHERINE P., PEDERSEN, THERESA L., KEYES, WILLIAM R., NEWMAN, JOHN W. AND HUANG, LIPING (2016) 'Zinc transporter 7 deficiency affects lipid synthesis in adipocytes by inhibiting insulin-dependent Akt activation and glucose uptake', *FEBS Journal*, 283, pp. 378–394.

THE BRITISH HIV ASSOCIATION (2016) *BHIVA guidelines for the treatment of HIV-1-positive adults with antiretroviral therapy 2015 (2016 interim update)*. Available at: https://www.bhiva.org/file/RVYKzFwyxpgiI/treatment-guidelines-2016-interim-update.pdf (Accessed: 29 January 2019).

TITUSHKIN, IGOR, SUN, SHAN, PAUL, AMIT AND CHO, MICHAEL (2013) 'Control of adipogenesis by ezrin, radixin and moesin-dependent biomechanics remodeling', *Journal of Biomechanics*, 46, pp. 521–526.

TOKARZ, VICTORIA L., MACDONALD, PATRICK E. AND KLIP, AMIRA (2018) 'The cell biology of systemic insulin function', *J Cell Biol*, 217, pp. 2273–2289.

TRIANT, VIRGINIA A. (2013) 'Cardiovascular disease and HIV infection', *Current HIV/AIDS Reports*, 10, pp. 199–206.

TRINH, HUNG V, GROSSMANN, JONAS, GEHRIG, PETER, ROSCHITZKI, BERND, SCHLAPBACH, RALPH, GREBER, URS F. AND HEMMI, SILVIO (2013) 'iTRAQ-Based and Label-Free Proteomics Approaches for Studies of Human Adenovirus Infections.', *International journal of proteomics*, 2013, p. 581862.

TSENG, YU-HUA, BUTTE, ATUL J., KOKKOTOU, EFI, YECHOOR, VIJAY K., TANIGUCHI, CULLEN M., KRIAUCIUNAS, KRISTINA M., CYPESS, AARON M., NIINOBE, MICHIO, YOSHIKAWA, KAZUAKI, PATTI, MARY ELIZABETH AND KAHN, C. RONALD (2005) 'Prediction of preadipocyte differentiation by gene expression reveals role of insulin receptor substrates and

necdin', *Nature Cell Biology*, 7, pp. 601–611.

VARATHARAJAN, LAVANYA AND THOMAS, SARAH A. (2009) 'The transport of anti-HIV drugs across blood–CNS interfaces: Summary of current knowledge and recommendations for further research', *Antiviral Research*, 82, pp. A99–A109.

VECCHIET, JACOPO, UCCIFERRI, CLAUDIO, FALASCA, KATIA, MANCINO, PAOLA, DI IORIO, ANGELO AND DE CATERINA, RAFFAELE (2011) 'Antihypertensive and metabolic effects of telmisartan in hypertensive HIV-positive patients', *Antiviral Therapy*, 16, pp. 639–645.

VELLA, STEFANO, SCHWARTLÄNDER, BERNARD, SOW, SALIF PAPA, EHOLIE, SERGE PAUL AND MURPHY, ROBERT L. (2012) 'The history of antiretroviral therapy and of its implementation in resource-limited areas of the world', *Aids*, 26, pp. 1231–1241.

VERROTTI, A., D'EGIDIO, C., MOHN, A., COPPOLA, G. AND CHIARELLI, F. (2011) 'Weight gain following treatment with valproic acid: pathogenetic mechanisms and clinical implications', *Obes Rev*, 12, pp. e32-43.

WAND, HANDAN, CALMY, ALEXANDRA, CAREY, DIANNE L., SAMARAS, KATHERINE, CARR, ANDREW, LAW, MATTHEW G. AND COOPER, DAVID A. (2007) 'Metabolic syndrome, cardiovascular disease and type 2 diabetes mellitus after initiation of antiretroviral therapy in HIV infection', *AIDS*, 21, pp. 2445–2453.

WANG, P., KEIJER, J., BUNSCHOTEN, A., BOUWMAN, F., RENES, J. AND MARIMAN, E. (2006) 'Insulin modulates the secretion of proteins from mature 3T3-L1 adipocytes: a role for transcriptional regulation of processing', *Diabetologia*, 49, pp. 2453–2462.

WANG, QIONG A, TAO, CAROLINE, GUPTA, RANA K. AND SCHERER, PHILIPP E. (2013) 'Tracking adipogenesis during white adipose tissue development, expansion and regeneration.', *Nature medicine*, 19, pp. 1338–44.

WANG, YONG, LV, ZHENGTONG AND CHU, YUAN (2015) 'HIV protease inhibitors: a review of molecular selectivity and toxicity', *HIV/AIDS - Research and Palliative Care*, 7, p. 95.

WEI, XIAOCHAO, SONG, HAOWEI, YIN, LI, RIZZO, MICHAEL G., SIDHU, ROHINI, COVEY, DOUGLAS F., ORY, DANIEL S. AND SEMENKOVICH, CLAY F. (2016) 'Fatty acid synthesis configures

the plasma membrane for inflammation in diabetes', *Nature*, 539, pp. 294–298.

WELSH, GAVIN I., GRIFFITHS, MATTHEW R., WEBSTER, KENNETH J., PAGE, MARTIN J. AND TAVARÉ, JEREMY M. (2004) 'Proteome analysis of adipogenesis', *Proteomics*, 4, pp. 1042–1051.

VAN WIJK, JEROEN P. H. AND CABEZAS, MANUEL CASTRO (2012) 'Hypertriglyceridemia, Metabolic Syndrome, and Cardiovascular Disease in HIV-Infected Patients: Effects of Antiretroviral Therapy and Adipose Tissue Distribution.', *International journal of vascular medicine*, 2012, p. 201027.

WILCOX, GISELA (2005) 'Insulin and insulin resistance.', *The Clinical biochemist. Reviews*, 26, pp. 19–39.

WILKINS, M. R., SANCHEZ, J. C., GOOLEY, A. A., APPEL, R. D., HUMPHERY-SMITH, I., HOCHSTRASSER, D. F. AND WILLIAMS, K. L. (1996) 'Progress with proteome projects: why all proteins expressed by a genome should be identified and how to do it.', *Biotechnology & genetic engineering reviews*, 13, pp. 19–50.

WILLIAMS, ASHLEY S., KANG, LI AND WASSERMAN, DAVID H. (2015) 'The extracellular matrix and insulin resistance.', *Trends in endocrinology and metabolism: TEM*, 26, pp. 357–66.

WOFFORD, MARION R., KING, DEBORAH S. AND HARRELL, T. KRISTOPHER (2006) 'Drug-Induced Metabolic Syndrome', *The Journal of Clinical Hypertension*, 8, pp. 114–119.

WORLD HEALTH ORGANIZATION (2002) *The Importance of Pharmacovigilance - Safety Monitoring of Medicinal Products*. Available at: http://apps.who.int/medicinedocs/en/d/Js4893e/9.html (Accessed: 23 January 2017).

WORLD HEALTH ORGANIZATION (2016) *Global health sector strategy on HIV, 2016-2021*. Available at: https://www.who.int/hiv/strategy2016-2021/ghss-hiv/en/ (Accessed: 18 December 2018).

WORLD HEALTH ORGANIZATION (2018) *WHO HIV/AIDS Fact sheets*. Available at: https://www.who.int/en/news-room/fact-sheets/detail/hiv-aids (Accessed: 18 December 2018).

WORM, S. W., SABIN, C., WEBER, R., REISS, P., EL-SADR, W., DABIS, F., DE WIT, S., LAW, M., MONFORTE, A. D., FRIIS-MOLLER, N., KIRK, O., FONTAS, E., WELLER, I., PHILLIPS, A. AND LUNDGREN, J. (2010) 'Risk of myocardial infarction in patients with HIV infection exposed to specific individual antiretroviral drugs from the 3 major drug classes: the data collection on adverse events of anti-HIV drugs (D:A:D) study', *J Infect Dis*, 201, pp. 318–330.

WU, L. E., SAMOCHA-BONET, D., WHITWORTH, P. T., FAZAKERLEY, D. J., TURNER, N., BIDEN, T. J., JAMES, D. E. AND CANTLEY, J. (2014) 'Identification of fatty acid binding protein 4 as an adipokine that regulates insulin secretion during obesity', *Molecular Metabolism*, 3, pp. 465–473.

XIE, FANG, LIU, TAO, QIAN, WEI-JUN, PETYUK, VLADISLAV A. AND SMITH, RICHARD D. (2011) 'Liquid chromatography-mass spectrometry-based quantitative proteomics.', *The Journal of biological chemistry*, 286, pp. 25443–25449.

XIE, X., YI, Z., BOWEN, B., WOLF, C., FLYNN, C. R., SINHA, S., MANDARINO, L. J. AND MEYER, C. (2010) 'Characterization of the Human Adipocyte Proteome and Reproducibility of Protein Abundance by One-Dimensional Gel Electrophoresis and HPLC-ESI-MS/MS', *J Proteome Res*, 9, pp. 4521–4534.

XIE, XIANGYANG, GONG, ZHENWEI, MANSUY-AUBERT, VIRGINIE, ZHOU, QIONG L., TATULIAN, SUREN A., SEHRT, DANIEL, GNAD, FLORIAN, BRILL, LAURENCE M., MOTAMEDCHABOKI, KHATEREH, CHEN, YU, CZECH, MICHAEL P., MANN, MATTHIAS, KRÜGER, MARCUS AND JIANG, ZHEN Y. (2011) 'C2 domain-containing phosphoprotein CDP138 regulates GLUT4 insertion into the plasma membrane.', *Cell metabolism*, 14, pp. 378–89.

XIE, XITAO, YI, ZHENGPING, SINHA, SANDEEP, MADAN, MEENU, BOWEN, BENJAMIN P., LANGLAIS, PAUL, MA, DANJUN, MANDARINO, LAWRENCE AND MEYER, CHRISTIAN (2016) 'Proteomics analyses of subcutaneous adipocytes reveal novel abnormalities in human insulin resistance.', *Obesity (Silver Spring, Md.)*, 24, pp. 1506–1514.

YANG, HAI JIE, XIA, YIN YAN, WANG, LEI, LIU, RUI, GOH, KIM JEE, JU, PEI JUN AND FENG, ZHI WEI (2011) 'A novel role for neural cell adhesion molecule in modulating insulin signaling and adipocyte differentiation of mouse mesenchymal stem cells.', *Journal of cell science*, 124, pp. 2552–2560.

YOUNG, JIM, WEBER, RAINER, RICKENBACH, MARTIN, FURRER, HANSJAKOB, BERNASCONI, ENOS, HIRSCHEL, BERNARD, TARR, PHILIP E., VERNAZZA, PIETRO, BATTEGAY, MANUEL AND BUCHER, HEINER C. (2005) 'Lipid profiles for antiretroviral-naive patients starting PI- and NNRTI-based therapy in the Swiss HIV cohort study.', *Antiviral therapy*, 10, pp. 585–591.

YOUNG, S. L., TAYLOR, M. AND LAWRIE, S. M. (2015) '"First do no harm." A systematic review of the prevalence and management of antipsychotic adverse effects', *Journal of Psychopharmacology*, 29, pp. 353–362.

ZEMANY, L., KRAUS, B. J., NORSEEN, J., SAITO, T., PERONI, O. D., JOHNSON, R. L. AND KAHN, B. B. (2014) 'Downregulation of STRA6 in adipocytes and adipose stromovascular fraction in obesity and effects of adipocyte-specific STRA6 knockdown in vivo', *Mol Cell Biol*, 34, pp. 1170–1186.

ZHA, BETH S., WAN, XIAOSHAN, ZHANG, XIAOXUAN, ZHA, WEIBIN, ZHOU, JUN, WABITSCH, MARTIN, WANG, GUANGJI, LYALL, VIJAY, HYLEMON, PHILLIP B. AND ZHOU, HUIPING (2013) 'HIV Protease Inhibitors Disrupt Lipid Metabolism by Activating Endoplasmic Reticulum Stress and Inhibiting Autophagy Activity in Adipocytes', *PLoS ONE*. Edited by Hongyuan Yang, 8, p. e59514.

ZHANG, YIYING, PROENCA, RICARDO, MAFFEI, MARGHERITA, BARONE, MARISA, LEOPOLD, LORI AND FRIEDMAN, JEFFREY M. (1994) 'Positional cloning of the mouse obese gene and its human homologue', *Nature*, 372, pp. 425–432.

ZHANG, Z., ZHAO, M., LI, Q., ZHAO, H., WANG, J. AND LI, Y. (2009) 'Acetyl-l-carnitine inhibits TNF-alpha-induced insulin resistance via AMPK pathway in rat skeletal muscle cells', *FEBS Lett*, 583, pp. 470–474.

ZHAO, YINGXIN, ZHANG, WEI, KHO, YOONJUNG AND ZHAO, YINGMING (2004) 'Proteomic Analysis of Integral Plasma Membrane Proteins', *Analytical Chemistry*, 76, pp. 1817–1823.

ZHONG, JUN, KRAWCZYK, SARAH A., CHAERKADY, RAGHOTHAMA, HUANG, HAILIANG, GOEL, RENU, BADER, JOEL S., WONG, G. WILLIAM, CORKEY, BARBARA E. AND PANDEY, AKHILESH (2010) 'Temporal Profiling of the Secretome during Adipogenesis in Humans', *Journal of Proteome Research*, 9, pp. 5228–5238.